

INSECT POLLINATOR DIVERSITY IN CHERRY ORCHARDS OF KASHMIR VALLEY USING MORPHOLOGICAL TOOLS AND DNA BARCODING

Thesis Submitted for the Award of the Degree of

DOCTOR OF PHILOSOPHY

in
Zoology

By
Arjumand John

Registration Number: 12105717

Supervised By

Co-Supervised By

Dr Amaninder Kaur (21097)

**Department of Zoology (Associate Professor)
Lovely Professional University, Punjab**

Dr Sajad A. Ganie

**Division of Entomology (Assistant Professor)
SKUAST-Kashmir, Shalimar, Srinagar, J&K**

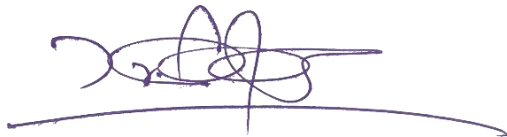


LOVELY PROFESSIONAL UNIVERSITY, PUNJAB

2026

DECLARATION

I, hereby declared that the presented work in the thesis entitled “**INSECT POLLINATOR DIVERSITY IN CHERRY ORCHARDS OF KASHMIR VALLEY USING MORPHOLOGICAL TOOLS AND DNA BARCODING**” in fulfilment of degree of **Doctor of Philosophy (Ph. D.)** is outcome of research work carried out by me under the supervision **Dr. Amaninder Kaur**, working as **Associate Professor**, in the **Department of Zoology of Lovely Professional University**, Punjab, India. In keeping with the general practice of reporting scientific observations, due acknowledgements have been made whenever work described here has been based on findings of other investigators. This work has not been submitted in part or in full to any other University or Institute for the award of any degree.



(Signature of Scholar)

Name of the Scholar: Arjumand John

Registration No.: 12105717

Department/School: Department of Zoology

Lovely Professional University,

Punjab, India

CERTIFICATE

This is to certify that the work reported in the Ph. D. thesis entitled “**INSECT POLLINATOR DIVERSITY IN CHERRY ORCHARDS OF KASHMIR VALLEY USING MORPHOLOGICAL TOOLS AND DNA BARCODING**” submitted in fulfillment of the requirement for the reward of degree of **Doctor of Philosophy (Ph.D.)** in the **Department of Zoology**, is a research work carried out by **Arjumand John, Registration No. 12105717**, is bonafide record of her original work carried out under my supervision and that no part of thesis has been submitted for any other degree, diploma or equivalent course.



(Signature of Supervisor)

Name of supervisor: Dr Amaninder Kaur
Designation: Associate Professor
Department: Zoology
University: Lovely Professional University



(Signature of Co-Supervisor)

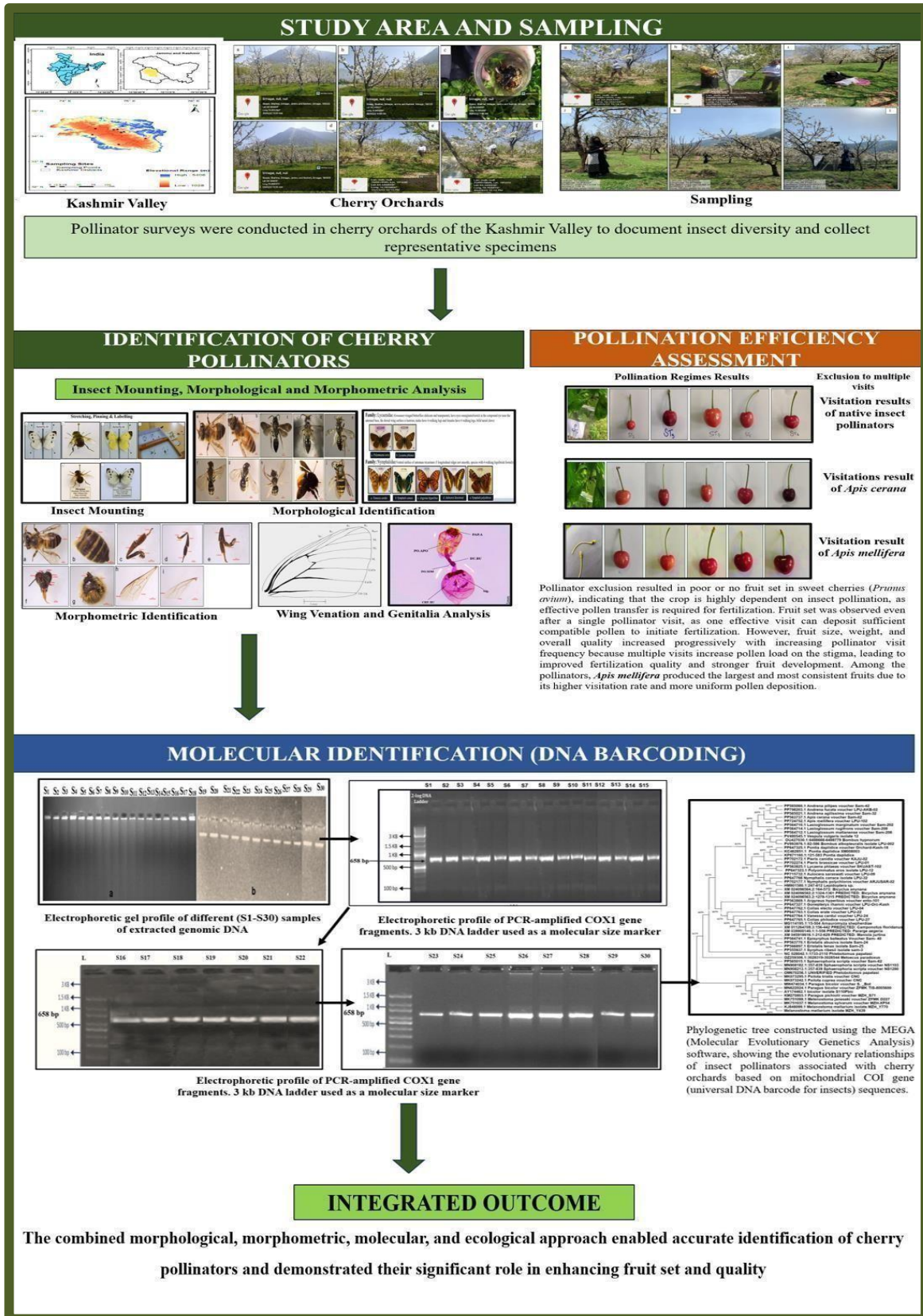
Name of Co-Supervisor: Dr Sajad A. Ganie
Designation: Assistant Professor
Department: Entomology
University: SKUAST-K Shalimar, J&K

Abstract

Insect pollinators are critical to the maintenance of all ecosystem services, crop yield, and biodiversity; however, the diversity, taxonomic structure, and functional performance of insect pollinators in temperate fruit orchards remain poorly understood, especially in the Himalayan region. The current research was conducted to ensure that the research focuses on the diversity, identification, and pollination efficiency of insect pollinators of cherry orchards in the Kashmir Valley. The number of insect pollinator species recorded was 30 in total, and they belonged to three major orders that included Lepidoptera (14 species), Hymenoptera (10 species), and Diptera (6 species) and were of eight families. Lepidoptera was the most diverse family, consisting of the families Nymphalidae, Pieridae and Lycaenidae, followed by Hymenoptera with Apidae, Halictidae, Andrenidae and Vespidae. On the contrary, the Diptera order was represented by a single family, which is the Syrphidae. The work gives the original molecular validation of *Lasioglossum matianense*, *L. marginatum*, *L. rugifrons*, and *Nymphalis canace* in the Kashmir Valley with the mitochondrial cytochrome c oxidase subunit I (COI) gene. High-quality COI sequences have provided a strong taxonomical resolution of these species and also provided useful reference data in world genetic databases. Morphological and morphometric analyses were also done in detail, and they further increased the species discrimination. Genitalia examination in the Lepidoptera order gave important diagnostic characters in distinguishing closely related species. Simultaneously, a comparative wing venation examination identified species-specific features, such as variations, which are represented in the genitalia and wing structures. These features are species-specific, stable, and offer the most dependable diagnostic characteristics for accurately identifying species, particularly in butterflies. The correct and reliable taxonomic understanding of the collected specimens was done by morphological identification of the sampled specimens using standard dichotomous keys. A detailed morphometric study was done on 37 diagnostic characters applied to all species recorded, showing statistically significant interspecific differences in body size and wing measurements. To measure the efficiency of pollination, the plant species used was *Prunus avium* 'Regina', a gametophytic self-incompatible cherry species, which completely depends on insect-mediated cross-pollination to set fruit. The findings have shown that *A. mellifera* had considerably higher rates of visitation, fruit set, fruit weight, and total soluble solids than *A. cerana* and other native pollinators. However, indigenous pollinators were also significant in the complete supportive contribution to the overall pollination services and ecosystem stability. Diversity indices also indicated that there was a steady and well-organised pollinator community at study sites, indicating the ecological stability and functional significance of pollinator assemblage in cherry orchards of Kashmir Valley. On the whole, this research is the first attempt to evaluate pollination diversity, taxonomy, and functional efficiency in cherry orchards in the Kashmir Valley and highlights the significance of intertwining morphological, molecular, and ecological analysis in efficient pollination conservation and

effective control of cherry orchards.

Graphical Abstract



ACKNOWLEDGEMENT

“Allahumma-aslih lee deeni-al-lazi huwa ismatu amri wa asleh lee dunyayallati feeha ma’ashi wa asleh lee aakhiratallati feeha ma’adi waj alil hayata ziyadatal-lee fee kulli khairin waj alil mauta raahatal-lee min kulle sharrin.”

All praise to **Allah**, who bestowed upon me the health and courage to go through this research project. May Allah’s blessings be upon His most revered **Prophet Hazrat Muhammad** (SAW), his family and all his companions.

A successful venture is never the achievement of an individual alone; rather, it is a collective creation shaped with the support, guidance, and goodwill of many eminent persons. Throughout my career and during the course of completing this work, I have experienced both moments of joy and phases of difficulty. Yet, it was the constant inspiration, encouragement, and guidance of my teachers, along with the immense support of my family and friends, that enabled me to transform this effort into reality. Their presence at every stage not only strengthened my determination but also made this journey more meaningful.

*With a profound sense of gratitude, I am highly thankful to my Supervisor, **Dr Amaninder Kaur Rait**, Associate Professor, School of Bioengineering and Biosciences Lovely Professional University, Phagwara, Punjab, for her impeccable and benevolent support, valuable suggestions, constructive criticism, remarkable guidance, enthusiastic discussions and constant encouragement during the entire course of this work, which resulted in its successful completion. The versatile personality of Dr Amaninder Kaur Rait, which stimulates students' thinking, is an underlying factor that will be part of my memory forever. I feel proud to be associated with such a dynamic personality. I am highly indebted to my dear mam for being kind, supportive and giving me ample freedom to carry out my work. I am indeed privileged to have been guided and groomed under a dexterous Biotechnologist of unchallenged repute.*

*I wish to sincerely thank **Dr Ashok Mittal**, Chancellor, and **Ms. Rashmi Mittal**, Pro-Chancellor, for giving me the invaluable opportunity to pursue my research at their esteemed institute (**Lovely Professional University**). Their inspiring vision and constant support have not only provided the platform but also created the right environment where I could explore my ideas, learn with freedom, and grow both academically and personally. It is because of this nurturing atmosphere that I was able to shape my work with confidence and bring my research journey to a meaningful completion.*

*I sincerely acknowledge and extend my heartfelt thanks to **Dr Neeta Raj**, Head of School, and **Dr Joydeep Dutta**, Head of Department, for their invaluable guidance, constructive scholarly criticism, and warm encouragement throughout my research. I am deeply honoured by their gracious permission to conduct part of my work in a different laboratory, which greatly enriched my research experience and contributed significantly to the successful completion of my degree.*

*I want to express my deepest gratitude and heartfelt thanks to my Co-supervisor, **Dr Sajad Ahmad Ganie**, Assistant Professor, Department of Entomology, SKUAST-K Shalimar, for his steadfast guidance and unwavering support throughout my research journey. His expert advice and timely provision of all necessary facilities greatly facilitated the smooth progress of my work. I am also sincerely thankful to all the teaching and non-teaching staff members of the department for their continuous assistance and cooperation at every stage of my research. Their collective support has been invaluable in helping me complete this endeavour.*

*I am truly thankful to **Dr Joydeep Dutta**, **Dr Rahul Sing**, **Dr Najitha Banu**, and **Dr Lovleen**, who were part of my End-Term panel. Their guidance, kind suggestions, and constant support have helped me improve my research and grow with more confidence. Every piece of advice they shared was valuable and easy to apply, and it made my work much stronger. I feel blessed to have such encouraging teachers who not only*

guided my research but also motivated me throughout this journey.

*I take this opportunity to express my heartfelt and profound gratitude to **my husband, Dr Kaisar Ahmad Bhat**, Assistant Professor in the Department of Biotechnology, BGSBU Rajouri, whose unwavering support, dynamic attitude, and inspiring guidance have been the cornerstone of my research journey. His steady encouragement, genuine care, and thoughtful guidance have been invaluable in helping me overcome academic hurdles and build the confidence to keep moving forward. I remain deeply grateful for the patience he has extended, the motivation he has sparked, and the trust he has placed in my abilities. Throughout this journey, his support has been both a source of comfort and a wellspring of intellectual inspiration.*

*I also owe indebtedness to **Prof. Manzoor Ahmed, Parry** Head Division of Entomology and Incharge (RTCPPPM), SKUAST-K Shalimar, whose constant encouragement, support, inspiration and parental affection enriched me both personally and professionally. It was a pleasure working in his lab. I am grateful to him for providing all the facilities I needed.*

*I wish to express a deep sense of gratitude to Incharge RTCPPPM, **Dr Parveena Akhter**, SKUAST Shalimar, for her valuable suggestions, outright cooperation, encouragement and inspiration rendered to me.*

*In particular, I am thankful to **Dr Zakir Khan** and **Dr Saima** for providing me with opportunities to work in their lab and for being highly supportive of me throughout my time there.*

*I am profoundly grateful to **Dr Atif Khursheed Wani**, Department of Biotechnology, Lovely Professional University, Phagwara, Punjab, for his generous guidance and constant encouragement. His selfless assistance in supporting me through the publication of review articles has been invaluable to my academic growth and success.*

*It is truly a privilege for me to acknowledge my sister, **Ms. Birjees John**, Agricultural Extension Officer, Kashmir, as one of the most inspiring and uplifting figures in my life. Her unwavering moral support, sincere encouragement, and warm backing have stood as steadfast pillars throughout my academic journey. In times of doubt and difficulty, her guidance helped me overcome even the most complicated challenges, providing clarity where confusion prevailed. Her faith in my abilities and her steady support gave me the strength and motivation to move forward with confidence. I remain truly thankful for the profound role she has played in shaping not only my academic journey but also my personal growth.*

*I wish to express my deepest gratitude to **Mr. Arooj Shafi Wani, Mr. Saqlain Shafi Wani, Shahzadi Arina, Shah Mahreen, and Shah Ahmad** for their unwavering encouragement and support throughout this journey. Their presence, whether through words of reassurance, timely help, or simply standing as a source of strength, has eased the path and made challenges easier to endure. Without their selfless assistance and faith in me, this endeavour would have been far more difficult. Their kindness and generosity have not only motivated me but also provided comfort and resilience during moments of doubt and fatigue. I feel truly fortunate to have had them by my side, sharing in both the struggles and the triumphs of this academic pursuit.*

*I am sincerely thankful to **Dr Nawaz** and **Er. Athar Abass** for their constant support during the final phase of my PhD journey. Their brotherly care and unwavering help made a profound difference, and I remain deeply grateful to both of them.*

*I am sincerely thankful to my lab mates, **Tamjeeda Nisar, Shweta Kalsi, Samara Sultana, and Firdous Ahmad**, for their constant support, camaraderie, and shared commitment over the years. Their encouragement, thoughtful discussions, and collaborative spirit turned challenging experiments and long hours in the lab into experiences that were not only productive but also enjoyable. The moments we spent together, whether immersed in research or sharing light-hearted conversations, have been a true source of motivation and joy, adding immense value to my academic journey.*

*I express my deep and sincere thanks to **Dr Huraiya Habib** for her empathy, friendship, and great sense of humour. She has been excellent at providing outlets that have allowed me to relax during the often*

frustrating and very isolating process of my PhD.

I extend my heartfelt gratitude to the teaching and non-teaching staff of the School of Bioengineering and Biosciences, Lovely Professional University, Phagwara, Punjab, for their constant support and kindness throughout my Ph.D. journey.

I also find it in place to mention the tremendous help and support received from non-teaching staff, particularly Javid Ahmed of the Research and Training Centre for Pollinators, Pollinizers & Pollination Management, SKUAST -K Shalimar, for always being there to help me and making me feel at home.

*My most heartfelt appreciation goes to the **Shah and Wani families**, whose unwavering love, selfless sacrifices, and constant moral support have been the very foundation upon which this research journey was built. Their encouragement has been my guiding light during moments of doubt, and their faith in my abilities has inspired me to persevere through every challenge. They have not only provided emotional strength but have also made countless personal sacrifices to ensure that I could pursue my academic goals without hesitation. This achievement is as much theirs as it is mine, for without their boundless support, patience, and belief in me, this work would never have come to fruition.*

My biggest Gratitude goes out to Google, Sci Hub, PubMed, and Google Scholar for helping me in discovering literature and other things related to my research.

*Finally, I would like to express my warm veneration to **my loving Parents (Mohammad Shafi Wani and Zareefa Farooqi)**, who are and will always be a source of Love and inspiration for me. Indeed, the words at my command are not adequate to convey my heartfelt thanks and gratitude to my family. I fail to find a suitable word to acknowledge their affection, support and blessings. They have been the source of inspiration all through my life (**I love you, Mami and Abu-G Forever**).*

A venture of this magnitude requires a great deal of help, over a period of time, from a great many people. This number is so big that I am likely to miss many owing to my not-so-perfect memory, the names of at least some of them. To them, I offer my most sincere apologies.

All cannot be mentioned, but none is forgotten.

Arjumand John
PLACE: Lovely Professional University,
Punjab, India

TABLE OF CONTENTS

S. No.	Description	Page No.
1.	Title Page Declaration Certificates	i-iii
2.	Abstract	Iv
3.	Graphical Abstract	V
4.	Acknowledgement	vi-vii
5.	Table of Contents	ix-x
6.	List of Tables	xi-xii
7.	List of Figures	xiii-xxvi
8.	List of Appendices	Xxvii
9.	Chapter 1 Introduction	1-4
10.	Chapter 2 Review of Literature 2.1 Authentication of insect pollinators in cherry orchards through Morphological and DNA barcoding techniques 2.2 Diversity of insect pollinators from cherry orchards of Kashmir Valley-Distribution and Abundance 2.3 Effectiveness of major insect pollinators on fruit set and fruit quality of Cherry.	5-17
11.	Chapter 3 Materials and Methods 3.1 Sampling and collection of insect pollinators 3.2 Insect Mounting	18-42

	<p>3.3 Morphological Studies of Insect Pollinators</p> <p>3.4 Butterfly Genitalia Extraction and Mounting</p> <p>3.5 Statistical Analysis</p> <p>3.6 Authentication of Insect Pollinators Through DNA Barcoding</p> <p>3.7 Diversity of Insect Pollinators from Cherry Orchards of Kashmir</p> <p>3.8 Investigation of Pollinator Effectiveness on Fruit Set and Quality of Cherry</p>	
12.	<p style="text-align: center;">Chapter 4</p> <p style="text-align: center;">Result and Discussion</p> <p>3.9. Mounting and Preservation of Insect Pollinators</p> <p>3.10. Morphometric and Morphological study of Hymenopteran pollinators</p> <p>3.13. Morphometric and Morphological study of Dipteran pollinators</p> <p>3.16. Morphological, Morphometric, and Genitalia Analysis of Lepidopteran Pollinators</p> <p>3.17. Wing Venation in Lepidopteran Taxonomy and Morphological Analysis</p> <p>3.20. DNA barcoding of Insect pollinators</p> <p>3.21. Diversity of Insect Pollinators in Cherry Orchards of Kashmir</p> <p>3.22. Evaluation of Qualitative and Quantitative Parameters of Cherry Fruit</p> <p>3.23. Discussion</p>	43-144
13.	<p>Chapter 5</p> <p>Summary and Conclusion</p>	152-154
14.	Future Scope of the Study	155-156
15.	References	i-xvi

LIST OF TABLES

Table No.	Table Title	Page No.
1.	List of morphometric characters recorded for insect Pollinators	26-27
2.	Components of the PCR reaction mixture for COX-1 markers	35
3.	PCR cyclic conditions using the COX-1 marker	
4.	Experimental treatments to evaluate pollinator impact on cherry yield	40
5.	Insect pollinators from cherry orchards of the Kashmir Valley, India	46
6.	Morphometrics of anterior (cephalic) and thoracic body parts of selected Hymenopteran pollinator species from cherry orchards of the Kashmir Valley (mm)	68
7.	Morphometrics of Cephalic (anterior) structures of selected Hymenopteran pollinator species from cherry orchards of the Kashmir Valley (mm)	69
8.	Morphometrics of Antennal and associated Cephalic structures in selected Hymenopteran pollinator species from cherry orchards of the Kashmir Valley (mm)	70
9.	Morphometrics of Ocellar, Antennal, Clypeal and Labral (cephalic) structures in selected Hymenopteran pollinator species from cherry orchards of the Kashmir Valley (mm)	71
10.	Morphometrics of Cephalic (Antennal and Ocular) and Wing characters in selected Hymenopteran pollinator species from cherry orchards of the Kashmir Valley (mm)	72
11.	Morphometrics of Hindwing, Hind Leg (Basitarsus) and posterior (Abdominal) structures in selected Hymenopteran pollinator species from cherry orchards of the Kashmir Valley (mm)	73
12.	Morphometrics of posterior (Abdominal) and Hind Leg (Tibial) structures in selected Hymenopteran pollinator species from cherry orchards of the Kashmir Valley (mm)	74
13.	Morphometrics of Body, Cephalic, Thoracic and Ocular structures in selected Syrphid pollinator species (Diptera) from cherry orchards of the Kashmir Valley (mm)	87

14.	Morphometrics of Ocular (Compound Eye), Wing (Forewing) and Abdominal structures in selected Syrphid pollinator species (Diptera) from cherry orchards of the Kashmir Valley (mm)	88
15.	Morphometrics of Body, Cephalic, Thoracic and Ocular structures in selected Lepidopteran pollinator species (Butterflies) from cherry orchards of the Kashmir Valley (mm)	124
16.	Morphometrics of wing (Forewing and Hindwing), Antennal and Abdominal structures in selected Lepidopteran pollinator species (Butterflies) from cherry orchards of the Kashmir Valley (mm)	125
17.	NCBI accession numbers of insect pollinator species associated with cherry orchards	129
18.	Diversity Indices of insect pollinator species from different cherry orchards of the Kashmir Valley	133
19.	Quantitative parameters of cherry fruit, viz., Fruit set, fruit weight, fruit size, TSS, and Acidity with Pollination Regimes by Native insect pollinator species	138
20.	Quantitative parameters of cherry fruit, viz., Fruit set, fruit weight, fruit size, TSS, and Acidity with Pollination Regimes by <i>Apis cerana</i>	140
21.	Quantitative parameters of cherry fruit, viz., Fruit set, fruit weight, fruit size, TSS, and Acidity with Pollination Regimes by <i>Apis mellifera</i>	142

LIST OF FIGURES

Figure No.	Figure Description	Page No.
1.	Study area map providing a detailed representation of the Kashmir Valley's cherry orchard geographical layout, with a specific focus on the four districts that play a crucial role in cherry cultivation. These districts are demarcated on the map, allowing for easy identification of the areas where cherry orchards are most concentrated. The map highlights the varying extents of land dedicated to cherry farming in each district, offering insight into the agricultural significance of these regions.	20
2.	Field survey and pollinator sampling conducted in cherry orchards of the Kashmir Valley (a-1). The figure illustrates cherry orchards in full bloom across different sampling locations, with GPS-embedded coordinates marking precise survey sites. It also shows the collection of insect pollinators using Aerial nets and hand collection methods, and temporary storage of specimens in collection jars during fieldwork.	21
3.	Dissection of insect pollinator specimens under a stereo zoom microscope enables the precise visualization of delicate structures, enabling accurate morphometric and taxonomic analysis.	23
4.	Morphometric measurements of insect body parts obtained using MagVision software, showing (a) whole body length, (b) abdomen, (c) antenna, (d) foreleg, (e) hindleg, (f) head, (g) thorax, (h) forewing, and (i) hindwing. Red lines indicate linear measurements recorded in millimetres for quantitative morphological analysis. Scale bar = 1 mm.	24
5.	Morphometric measurements of the butterfly. (a) Adult specimen showing manual measurement of wingspan and body length using a metric scale in centimeters, with values subsequently converted to millimetres (1 cm = 10 mm). (a1) Male genitalia, (a2) compound eye, and (a3) antennae examined under a stereo zoom microscope at 1X magnification. Scale bars: 1 mm.	25
6.	Genitalia extraction and diagnostic features of male and female butterflies. (a-a2) Male: (a) terminal abdominal segments, (a1) dissection and cleaning, (a2) cleared genital capsule showing TG -tegumen, UN-uncus, VAL-valva, CA-costal area, VIN-vinculum, SU- saccus, JX-juxta, AED-aedeagus, DU. EJ-ductus ejaculatorius, TH.APP-thecal appendage. (b-b2) Female: (b) terminal abdominal segments, (b1) dissection and cleaning, (b2) cleared genitalia showing PAP.A-papillae analis, PO.APO-posterior apophyses, DU.BU-ductus bursae,	30

	CRP.BU-carpus bursae, DU.SEM-ductus seminalis, SIG-signum.	
7.	Descaling process of butterfly wings for venation analysis. (a) Wings immersed in sodium hypochlorite solution to loosen scales; (b) descaled forewings post-treatment showing enhanced transparency; (c) detailed venation patterns traced after descaling for use in morphometric and taxonomic studies.	32
8.	Electrophoretic gel profile of different (S1-S30) samples of extracted genomic DNA. The DNA samples were resolved on a 0.8% agarose gel stained with ethidium bromide and visualised under UV light to assess the quality and integrity of the extracted DNA (a, b): clear, high-molecular-weight bands without significant smearing indicate successful extraction of intact genomic DNA suitable for downstream molecular applications such as PCR amplification and sequencing.	34
9.	Electrophoretic profile of PCR-amplified COX1 gene fragments. Lane L represents the 3 kb DNA ladder used as a molecular size marker, while lanes S1 to S15 correspond to different insect pollinator samples, each showing successful amplification of the target mitochondrial COX1 gene region.	36
10.	Electrophoretic profile of COX1 marker following PCR amplification. Lane L represents the 3 kb DNA ladder used as a molecular size reference, and lanes S16 to S22 correspond to different insect pollinator samples, each showing successful amplification of the mitochondrial COX1 gene fragment.	37-38
11.	Electrophoretic profile of COX1 marker after PCR amplification. Lane L shows the 3 kb DNA ladder used as a molecular size standard, while lanes S23 to S30 represent different insect pollinator samples, each displaying successful amplification of the mitochondrial COX1 gene fragment.	
12.	Field Setup and Pollination Assessment in Cherry Orchards of Kashmir. (a) Cherry trees were enclosed in pollination-exclusion bags to regulate insect visitation, with managed bee hives placed nearby for controlled pollination. (b) A honeybee foraging on cherry blossoms during natural bloom. (c) Monitoring of pollination treatments and tagged branches in the orchard. (d-f) Experimental cherry trees under different pollination setups and assessment of fruit set using labeled sampling bags applied to developing fruits after treatment.	40
13.	Measurement of cherry fruit juice pH using a digital pH meter.	42
14.	Estimation of titratable acidity in cherry juice using titration with 0.1 N NaOH and phenolphthalein indicator.	43

15.	Measurement of total soluble solids (TSS) in cherry juice using a digital refractometer.	
16.	Preservation of insect pollinators for morphological and molecular studies. (a) Representative insect pollinator specimens mounted and pinned on entomological boards after drying, used for detailed morphological identification and morphometric analysis. (b) Systematic arrangement and storage of pinned insect collections in insect boxes for long-term reference and taxonomic studies. (c) Insect specimens preserved individually in 95% ethanol, suitable for genomic DNA extraction and DNA barcoding, ensuring minimal DNA degradation while maintaining specimen integrity.	47-48
17.	Representative insect pollinators recorded from cherry orchards (a-j): <i>Apis cerana</i> , <i>Apis mellifera</i> , <i>Andrena agilissima</i> , <i>Andrena fucata</i> , <i>Andrena pilipes</i> , <i>Lasioglossum marginatum</i> , <i>Lasioglossum matianense</i> , <i>Lasioglossum rugifrons</i> , <i>Bombus albopeleralis</i> , and <i>Vespa vulgaris</i> .	49
18.	18a: Dorsal view of <i>Apis cerana</i> adult worker bee showing major external morphological features: compound eye, antenna, fore leg, mid leg, hind leg, thorax, propodeum, fore wing, and abdomen. 18b: Measurement of various morphological characteristics of <i>Apis cerana</i> . (a) Full body, (b) Abdomen, (c) Foreleg, (d) Midleg, (e) Hindleg, (f) Thorax, (g) Hindwing, (h) Forewing, (i) Antenna, and (j) Head.	50-51
19.	19a: Dorsal view of <i>Apis mellifera</i> adult worker bee showing major external morphological features: compound eye, antenna, fore leg, mid leg, hind leg, thorax, propodeum, fore wing, and abdomen. 19b: Measurement of various morphological characteristics of <i>Apis mellifera</i> . (a) Full body, (b) Abdomen, (c) Forewing, (d) Midleg, (e) Hindwing, (f) Hindleg, (g) Thorax, (h) Head, (i) Antenna, and (j) Foreleg.	52-53
20.	Measurement of various morphological characters of <i>Andrena agilissima</i> . (a) Full body, (b) Abdomen, (c) Midleg, (d) Antenna, (e) Foreleg, (f) Hindleg, (g) Hindwing, (h) Forewing, (i) Head, and (j) Thorax.	54
21.	Measurement of various morphological characters of <i>Andrena fucata</i> . (a) Full body, (b) Abdomen, (c) Foreleg, (d) Midleg, (e) Hindleg, (f) Head, (g) Forewing, (h) Hindwing, (i) Thorax, and (j) Antenna.	56

22.	Measurement of various morphological characters of <i>Andrena pilipes</i> . (a) Full body, (b) Foreleg, (c) Head, (d) Midleg, (e) Hindleg, (f) Abdomen, (g) Forewing, (h) Hindwing, (i) Thorax, and (j) Antenna.	58
23.	Measurement of various morphological characteristics of <i>Lasioglossum marginatum</i> . (a) Full body, (b) Abdomen, (c) Hindwing, (d) Forewing, (e) Midleg, (f) Foreleg, (g) Head, (h) Thorax, (i) Hindleg, and (j) Antenna.	59
24.	Measurement of various morphological characteristics of <i>Lasioglossum matianense</i> . (a) Full body, (b) Forewing, (c) Hindwing, (d) Abdomen, (e) Foreleg, (f) Head, (g) Thorax, (h) Midleg, (i) Antenna, and (j) Hindleg.	61
25.	Measurement of various morphological characteristics of <i>Lasioglossum rugifrons</i> . (a) Full body, (b) Abdomen, (c) Forewing, (d) Hindwing, (e) Foreleg, (f) Midleg, (g) Hindleg, (h) Head, (i) Antenna, and (j) Thorax.	63
26.	Measurement of various morphological characteristics of <i>Vespula vulgaris</i> . (a) Full body, (b) Abdomen, (c) Forewing, (d) Hindleg, (e) Hindwing, (f) Midleg, (g) Antenna, (h) Head, (i) Thorax, and (j) Foreleg.	64
27.	Measurement of various morphological characteristics of <i>Bombus albopleuralis</i> . (a) Full body, (b) Abdomen, (c) Head, (d) Midleg, (e) Foreleg, (f) Hindleg, (g) Antenna, (h) Ossicles, (i) Thorax, (j) Hindwing, and (k) Forewing.	66
28.	Hierarchical cluster analysis (HCA) performed on 37 standardized morphometric characters (head, thorax antennal, wings, legs, ocellar, and abdominal traits) using Euclidean distance and Ward's linkage. The resulting dendrogram shows that <i>Bombus albopleuralis</i> and <i>Vespula vulgaris</i> form a distinct high-distance cluster reflecting their unique morphometric profiles among the sampled Hymenoptera. The solitary bees (<i>Andrena</i> and <i>Lasioglossum</i> spp.) group together at low to intermediate distances, indicating strong overlap in proportional traits. The two honeybees, <i>Apis mellifera</i> and <i>A. cerana</i> , form a tight sub-cluster that joins the rest of the taxa only at higher Euclidean distances, confirming their distinct but internally homogeneous morphometric pattern.	75

29.	Principal Component Analysis (PCA) of Hymenopteran Pollinators Based on 37 Morphometric variables representing the head, thorax, abdomen, legs, antennae, and wing structures of ten hymenopteran species. The first two principal components (PC1 and PC2) together capture the major directions of morphological variation. Positive (+) and negative (–) scores on the PCA axes indicate relative differences in trait magnitudes. Species with positive PC1 values possess larger body and wing dimensions, while those with negative PC1 scores tend to be smaller-bodied. Similarly, positive PC2 scores reflect greater variation in head–thorax proportions and antennal traits, while negative PC2 values correspond to smaller or narrower structures. The bumblebee <i>Bombus albopleuralis</i> and the wasp <i>Vespula vulgaris</i> are strongly separated along PC1, reflecting their significantly larger morphologies. Honeybees <i>Apis mellifera</i> and <i>A. cerana</i> cluster closely, indicating high morphometric similarity. <i>Andrena</i> and <i>Lasioglossum</i> species form compact, genus-specific clusters, demonstrating clear taxonomic differentiation. Overall, the PCA highlights size-related and shape-related axes of variation that reliably separate taxa based on multivariate morphometric structure.	76
30.	Wing venation of a syrphid fly, with 13 red-marked landmarks for geometric morphometric analysis (a, b). Conta (C), Subcosta (Sc), Radial (R1-R5), Medial (M1-M2), crossveins (r-m, m-cu), and Anal vein (A1), which are important venal structures. These landmarks support research on evolutionary traits, functional morphology, and species differentiation.	77
31.	Morphologically identified dipteran pollinators (family: Syrphidae) collected from cherry orchards of Kashmir Valley. The specimens include <i>Eristalis tenax</i> , <i>Eristalis arbustorum</i> , <i>Eristalis abusive</i> , <i>Episyrphus balteatus</i> , <i>Sphaerophoria scripta</i> , and <i>Syrphus ribesii</i> , documented under Stereozoom microscopy for taxonomic confirmation and morphometric analysis.	78
32.	Measurement of various morphological characteristics of <i>Eristalis tenax</i> . (a) Body length, (b) Abdomen, (c) Midleg, (d) Foreleg, (e) Hindleg, (f) Head, (g) Forewing, and (h) Thorax.	79
33.	Measurement of various morphological characteristics of <i>Episyrphus balteatus</i> . (a) Body length, (b) Abdomen, (c) Head, (d) Thorax, (e) Hindleg, (f) Foreleg, (g) Midleg, and (h) Wing.	80
34	Measurement of various morphological characteristics of <i>Eristalis abusiva</i> . (a) Body length, (b) Abdomen, (c) Midleg, (d) Head, (e) Hindleg, (f) Thorax, (g) Wing, and (h) Foreleg.	81

35.	Measurement of various morphological characteristics of <i>Eristalis arbustorum</i> . (a) Body length, (b) Abdomen, (c) Midleg, (d) Head, (e) Hindleg, (f) Thorax, (g) Wing, and (h) Foreleg.	83
36.	Measurement of various morphological characteristics of <i>Syrphus ribesii</i> ; a; Body length, b; Abdomen, c; Wing d; Head, e; Hindleg f; Foreleg, g; Thorax, h; Foreleg.	84
37.	Measurement of various morphological characteristics of <i>Sphaerophoria scripta</i> ; a; Full Body, b; Abdomen, c; Wings, d; Thorax, e; Midleg, f; Head, g; Foreleg, h; Hindleg.	85
38.	Hierarchical cluster analysis (HCA) of six syrphid fly species based on 11 standardized morphometric characters (body, head, thorax, compound eye, wing, and abdominal traits), using Euclidean distance and Ward's linkage. The dendrogram reveals two clusters:(i) <i>Eristalis abusive</i> and <i>Eristalis arbustorum</i> , which group tightly at low linkage distances, indicating high morphometric similarity; and (ii) <i>Episyrphus balteatus</i> and <i>Syrphus ribesii</i> , which also cluster closely, reflecting similar body size and wing proportions. <i>Sphaerophoria scripta</i> and <i>Eristalis tenax</i> appear as the most morphometrically distinct species joining the main clusters only at higher Euclidean distances. Overall, the analysis highlights clear separation between large-bodied <i>Eristalis</i> species and the smaller slender hoverflies.	89
39.	Principal Component Analysis (PCA) of six syrphid fly species based on 11 morphometric traits. PC1 represents overall body size (larger species show positive scores; smaller species show negative scores), while PC2 reflects differences in head, eye, and thorax proportions (+/- values indicate higher or lower trait magnitudes). <i>Eristalis tenax</i> is strongly separated on PC1 due to its large body and wing dimensions, whereas <i>Sphaerophoria scripta</i> clusters on the negative side, reflecting its smaller, slender morphology. <i>Episyrphus balteatus</i> and <i>Syrphus ribesii</i> occupy intermediate positions, while <i>Eristalis abusive</i> and <i>Eristalis arbustorum</i> group toward the larger-bodied region. The PCA clearly distinguishes robust <i>Eristalis</i> species from smaller hoverflies.	90
40.	Representation of butterfly species from the family Pieridae observed during the study. Labeled specimens include: (a) <i>Gonepteryx rhamni</i> , (b1) <i>Colias electo</i> ♂, (b2) <i>Colias electo</i> ♀, (c) <i>Colias erate</i> , (d) <i>Colias philodice</i> , (e) <i>Pieris canidia</i> , (f) <i>Pieris brassicae</i> ♂, (f1) <i>Pieris brassicae</i> ♀, and (g) <i>Pontia daplidice</i> . The figure highlights the morphological diversity within the Pieridae family.	92

41.	41a: Dorsal view of a butterfly showing major external morphological features, including head, antenna, thorax, abdomen, forewing, hindwing, and characteristic eyespots.	92
	41b: Dorsal view of <i>Gonepteryx rhamni</i> (a-a1) illustrating the detailed morphology of Antenna, Head and Female genitalia along with associated reproductive structures. Key features are highlighted, showcasing the anatomical adaptations critical for reproductive functions.	93
42.	42a: Dorsal view of <i>Colias electo</i> (a-a1), highlighting the Head, Antenna, female genitalia and associated reproductive structures. The illustration emphasizes key anatomical features, providing insights into their functional morphology.	94-95
	42b: Dorsal view of <i>Colias electo</i> (a-a1) showcasing the detailed morphology of the male genitalia and associated reproductive structures. The figure highlights key anatomical components, including the claspers, aedeagus, and associated sclerites, which play crucial roles in mating and reproductive success.	
43.	Dorsal view of <i>Colias erate</i> (a-a1) male genitalia showing key reproductive structures. Distinguished anatomical components include the claspers, aedeagus, and associated sclerites, which are essential for copulation and species-level identification.	95
44.	Dorsal view of <i>Colias philodice</i> (a-a1) illustrating the male genitalia and associated reproductive structures. The figure highlights critical anatomical features, including the aedeagus, claspers, and supporting sclerites, which are integral to the mating process and reproductive success of the species.	97
45.	45a: Dorsal view of <i>Pieris canidia</i> (a-a1) illustrating the female genitalia and associated reproductive structures. The figure emphasizes key anatomical features such as the ovipositor, accessory glands, and related sclerites, which are critical for understanding the reproductive biology, mating strategies, and species-specific adaptations of <i>P. canidia</i> .	98-99
	45b: Dorsal view of <i>Pieris canidia</i> (a-a1) showcasing the male genitalia and associated reproductive structures. The illustration highlights key features such as the aedeagus, claspers, and supporting sclerites, which are essential for mating and reproductive success.	

46.	46a: Dorsal view of <i>Pieris brassicae</i> (a-a1) illustrating the female genitalia and associated reproductive structures. The figure highlights key anatomical components, including the ovipositor, accessory glands, and reproductive ducts, providing insights into the reproductive morphology and species-specific adaptations of <i>P. brassicae</i> .	100
	46b: Dorsal view of <i>Pieris brassicae</i> (a-a1) illustrating the male genitalia and associated reproductive structures. Key anatomical features, including the aedeagus, claspers, and sclerites, are highlighted, emphasizing their roles in mating and reproductive functions.	
47.	Dorsal view of <i>Pontia daplidice</i> (a-a1), highlighting the male genitalia and reproductive structures, showcasing detailed morphological features critical for species identification and reproductive biology studies.	101
48.	Visual representation of butterfly species from the family Lycaenidae observed during the study. Labelled specimens include: (a) <i>Polyommatus eros</i> and (b) <i>Lycaena phlaeas</i> .	102
49.	Dorsal view of <i>Polyommatus eros</i> (a-a1), highlighting the male genitalia and reproductive structures, illustrating key morphological traits essential for species identification and taxonomic studies.	103
50.	Dorsal view of <i>Lycaena phlaeas</i> (a-a1) male genitalia showing key reproductive structures. The figure highlights critical morphological traits essential for accurate species identification and taxonomic analysis.	104
51.	Visual representation of butterfly species from the family Nymphalidae observed during the study. Labelled specimens include: (a) <i>Vanessa cardui</i> , (b) <i>Nymphalis canace</i> , (c) <i>Argyreus hyperbius</i> , (d) <i>Vanessa cashmirensis</i> , and (e) <i>Aulocera saraswati</i> .	105
52.	Dorsal view of <i>Vanessa cardui</i> male genitalia, highlighting key reproductive structures. The figure illustrates essential morphological traits used for accurate species identification and taxonomic classification.	106
53.	Dorsal view of <i>Nymphalis canace</i> male genitalia, highlighting key reproductive structures. The figure illustrates critical morphological features essential for species identification and taxonomic studies.	107
54.	Dorsal view of <i>Argyreus hyperbius</i> male specimen, highlighting the genitalia and associated reproductive structures. The image illustrates key morphological features, including the shape and sclerotization patterns of the uncus, valvae, and aedeagus, which are essential for accurate species identification and taxonomic studies.	108

55.	Dorsal view of <i>Nymphalis polychloros</i> male specimen, highlighting the genitalia and reproductive structures. The image illustrates key morphological traits, including the shape and structure of the uncus, valvae, and aedeagus, which are essential for accurate species identification and taxonomic studies.	109
56.	Dorsal view of <i>Aulocera saraswati</i> male specimen, highlighting the genitalia and reproductive structures. The image illustrates key morphological features such as the shape of the uncus, valvae, and aedeagus, which are critical for accurate species identification and taxonomic differentiation.	110
57.	Detailed venation patterns of the forewing and hindwing of <i>Colias electo</i> , highlighting key structural veins used in taxonomic identification and morphometric evaluation. a: hindwing with 1A+2A, 3A, Cu1a, Cu1b, M3, M2, M1, Rs, and fused Sc + R1. b: forewing with 1A+2A, Cu1b, Cu1a, M3, M2, M1, radial series (R5–R1), Sc, and Rs.	111
58.	Detailed venation patterns of the Forewing and hindwing of <i>Pieris canidia</i> , displaying detailed venation used for taxonomic differentiation and morphometric analysis. a: forewing with 1A+2A, Cu1b, Cu1a, M3-M1, Rs, radial series (R1-R5), and Sc. b: hindwing with 1A+2A, 3A, Cu1b, Cu1a, M3-M1, Rs, and PV.	112
59.	Forewing and hindwing venation of <i>Nymphalis polychloros</i> , showing key veins for species identification and morphometric analysis. a: forewing with 1A+2A, Cu1b, Cu1a, M3–M1, radial series (R1-R5), Rs, and Sc. b: hindwing with 1A+2A, 3A, Cu1b, Cu1a, M3-M1, Rs, fused Sc+R1, discocellulars (UDC, MDC, LDC), and PV.	113-114
60.	Forewing and hindwing venation of <i>Aulocera saraswati</i> showing key veins for identification within Satyrinae. a: forewing with 1A+2A, Cu1b, Cu1a, M3-M1, R5-R1, Rs, Sc, and DC; marginal parts (A-D) labeled. b: hindwing with 1A+2A, 3A, Cu1b, Cu1a, M3-M1, Rs, Sc+R1, PV, and discocellulars (UDC, MDC, LDC).	
61.	Forewing and hindwing venation of <i>Colias philodice</i> , showing key veins for species identification and morphometric analysis. a: forewing with 1A+2A, Cu1b, Cu1a, M3-M1, Rs+R4, R3-R1, Sc, and R5 near apex. b: hindwing with 1A+2A, 3A, Cu1b, Cu1a, M3-M1, Rs, and fused Sc+R1.	

62.	Forewing and hindwing venation of <i>Pontia daplidice</i> showing key veins for taxonomic and morphometric analysis. a: forewing with 1A+2A, Cu1b, Cu1a, M3-M1, Rs+R4, R3-R1, and Sc. b: hindwing with 1A+2A, 3A, Cu1b, Cu1a, M3-M1, Rs, Sc+R1, and PV.	115
63.	Forewing and hindwing venation of <i>Gonepteryx rhamni</i> showing key veins for species identification and morphometric analysis. a: forewing with 1A+2A, Cu1b, Cu1a, M3-M1, Rs+R4, R3-R1, and Sc. b: hindwing with 1A+2A, 3A, Cu1b, Cu1a, M3-M1, Rs, and Sc+R1.	116-117
64.	Forewing and hindwing of <i>Colias erate</i> showing key venation for species identification within Pieridae. Forewing (a) includes 1A+2A, Cu1b, Cu1a, M3-M1, Rs+R4+5, R3-R1, and Sc; hindwing (b) features 1A+2A, 3A, Cu1b, Cu1a, M3-M1, Rs, and Sc+R1. Tight radial convergence and evenly spaced medians are diagnostic of <i>C. erate</i> .	
65.	Forewing and hindwing of <i>Lycaena phlaeas</i> exhibit venation patterns that are crucial for morphometric study and taxonomic identification within the Lycaenidae. 1A+2A, Cu1b, Cu1a, M3, M2, M1, R5-R3, R1, and Sc are all present in the forewing (a), which has a compact discal region that is characteristic of Lycaenids. (b) 1A+2A, 3A, Cu1b, Cu1a, M3, M2, M1, Rs, Sc+R1, and the discocellulars UDC, MDC, and LDC are seen in the hindwing.	118
66.	Forewing and hindwing of <i>Pieris brassicae</i> showing venation patterns for taxonomic identification and morphometric analysis. The forewing (a) features 1A+2A, Cu1b, Cu1a, M3-M1, Rs+R4+5, R3-R1, and Sc; the hindwing (b) includes 1A+2A, 3A, Cu1b, Cu1a, M3-M1, Rs, Sc+R1, and PV. The spacious radial and median branching, with the arched Sc+R1 and Rs, is characteristic of the species.	119
67.	Venation patterns on the forewing and hindwing of <i>Argynnis hyperbius</i> are crucial for morphometric analysis and species identification within the Nymphalidae. 1A+2A, Cu1b, Cu1a, M3-M1, R5-R1, Rs, and Sc are present in the forewing (a), which also has an elongated discal cell surrounded by crossveins. In the hindwing (b), 1A+2A, 3A, Cu1b, Cu1a, M3-M1, Rs, and fused Sc+R1 are shown. The species is characterised by evenly spaced veins and a broad hindwing shape.	120
68.	Venation patterns on the forewing and hindwing of <i>Nymphalis canace</i> are crucial for morphometric analysis and taxonomic identification. Whereas the hindwing exhibits a compact, rounded layout with converging venation, the forewing has narrow discal cells and closely spaced radial veins.	121

69.	Venation patterns on the forewing and hindwing of <i>Polyommatus eros</i> are crucial for taxonomic identification and morphometric analysis within the Lycaenidae family. Veins 1A+2A, Cu1b, Cu1a, Cula, M3, M2, M1, R5-R1, and Sc are all arranged in a dense network in the forewing (a). Features of the hindwing (b) include fused Sc+R1, M3, M1, Rs, Cu1b, Cu1a, Cula, 1A+2A, and 3A.	122
70.	Forewing (a) and hindwing (b) of <i>Vanessa cardui</i> showing characteristic venation patterns, including major anal, cubital, median, and radial veins, discocellular cross-veins, and precostal spur.	123
71.	Hierarchical Cluster Analysis (HCA) of 14 butterfly species based on 13 standardized morphometric traits (body length, head length and width, thorax length and width, compound eye dimensions, forewing and hindwing length and width, antenna length, and abdomen length). The analysis separates the butterflies into two major morphological groups. Smaller-bodied Lycaenids (<i>Lycaena phlaeas</i> and <i>Polyommatus eros</i>) form a distinct high-distance cluster, indicating their large proportional difference from the rest of the species. <i>Pieris brassicae</i> also joins this cluster at a higher distance because of its exceptionally large wing dimensions. The remaining species cluster more gradually, reflecting intermediate to large body sizes and similar wing and thoracic proportions. Closely related taxa such as <i>Colias erate</i> , <i>C. electo</i> , and <i>C. philodice</i> cluster tightly at low Euclidean distances, demonstrating strong morphometric similarity. Larger-bodied nymphalid species (<i>Nymphalis canace</i> , <i>Nymphalis polychloros</i> , <i>Aulocera saraswati</i>) cluster together, indicating shared structural traits.	126
72.	PCA plot of morphometric traits in 14 butterfly species collected from cherry orchards in the Kashmir Valley. Positive PC1 scores represent species with larger overall body size, broader wings, and longer abdomen (e.g., <i>Pontia daplidice</i> , <i>Colias electo</i>). Negative PC1 values indicate smaller species such as <i>Lycaena phlaeas</i> and <i>Aulocera saraswati</i> . Along PC2, positive values reflect species with proportionally larger head, thorax, and eye dimensions (e.g., <i>Pieris brassicae</i> , <i>Vanessa cardui</i>), while negative PC2 values correspond to compact-bodied nymphalids (e.g., <i>Nymphalis canace</i> , <i>Aulocera saraswati</i>). Clustering patterns show genus-level similarity: the three <i>Colias</i> species cluster closely, whereas <i>Nymphalis</i> and <i>Aulocera</i> form a distinct group on the negative PC1 axis, highlighting clear morphometric divergence.	127

73.	Phylogenetic tree illustrating the intra- and interspecific genetic variation among insect pollinator species collected from cherry orchards. Each branch represents an individual species, highlighting the genetic relationships and divergence patterns based on COX-1 gene sequences. The circular tree depicts three major clades corresponding to Orders- Lepidoptera, Hymenoptera, and Diptera, with Family-level clusters recognised. The tree effectively delineates species-level clustering and evolutionary relatedness, supporting both taxonomic resolution and molecular identification.	131
74.	Abundance of insect pollinators recorded across eight sampling sites in cherry orchards of the Kashmir Valley, categorised by district. The bar graph illustrates the total number of pollinator individuals recorded from eight locations across four districts of Kashmir Valley. Shalimar and Dhara (Srinagar district), Lar and Baba Wayil (Ganderbal district), Tangmarg and Sopore (Baramulla district), and Kullar and Aerhal (Shopian district) show varying pollinator abundances. Shalimar recorded the highest abundance (576 individuals), followed by Baba Wayil (525) and Aerhal (520), while Lar showed the lowest (465). Error bars are not included as the values represent total counts.	133
75.	The line graph represents the dominance index (D) of pollinator assemblages recorded from eight sampling locations. Dominance values remain relatively low across all sites, indicating an even distribution of species. The highest dominance was observed at Baba Wayil ($D \approx 0.0356$), followed by Kullar ($D \approx 0.0350$) and Sopore ($D \approx 0.0348$), whereas the lowest dominance occurred at Tangmarg ($D \approx 0.0340$). These slight variations reflect minor differences in species dominance patterns among the locations.	134
76.	The line graph shows the variation in Simpson's Index (D) for pollinator assemblages across eight sampling locations. Overall, diversity remains high at all sites ($D \approx 0.964-0.966$), indicating a well-balanced pollinator community with low dominance. The highest diversity was recorded at Tangmarg ($D \approx 0.9659$), while Baba Wayil exhibited the lowest value ($D \approx 0.9645$). Minor fluctuations across locations reflect slight differences in species evenness and richness.	134
77.	The line graph illustrates the Shannon-Weiner Index (H') for pollinator assemblages recorded across eight sampling locations. Diversity values remain consistently high ($H' \approx 3.35-3.37$), reflecting a rich and well-distributed pollinator community. The highest diversity was observed at Tangmarg ($H' \approx 3.371$), while Baba Wayil showed the lowest diversity ($H' \approx 3.352$). Variations across sites indicate subtle differences in	135

	species richness and evenness within the pollinator populations.	
78.	The line graph represents the evenness index (E) of pollinator species recorded across eight sampling locations. Evenness values are consistently high ($E \approx 0.985-1.005$), indicating a uniform distribution of species with minimal dominance. Tangmarg exhibited the highest evenness ($E \approx 1.005$), while Baba Wayil recorded the lowest ($E \approx 0.985$). The slight variations across locations reflect minor differences in the proportional distribution of pollinator species.	136-137
79.	Photographs (a-f) from cherry orchards depicting regimes with Native insect pollinators, including pollination exclusion, single visit, two visits, three visits, four visits, and multiple visits, along with the corresponding fruit set and quality.	
80.	Effect of Native insect pollinator visitation on cherry fruit development and quality. Pollination exclusion shows no fruit formation, whereas one to multiple visits depict progressive improvement in fruit set, size, and quality with increasing pollinator visits.	137-139
81.	Photographs (a-f) from cherry orchards depicting regimes with <i>Apis cerana</i> , including pollination exclusion, single visit, two visits, three visits, four visits, and multiple visits, along with the corresponding fruit set and quality.	
82.	Effect of <i>Apis cerana</i> visitation on cherry fruit development and quality. Pollination exclusion shows no fruit formation, whereas one to multiple visits depict progressive improvement in fruit set, size, and quality with increasing pollinator.	139-141
83.	Photographs (a-f) from cherry orchards depicting regimes with <i>Apis mellifera</i> , including pollination exclusion, single visit, two visits, three visits, four visits, and multiple visits, along with the corresponding fruit set and quality.	
84.	Effect of <i>Apis mellifera</i> visitation on cherry fruit development and quality. Pollination exclusion shows no fruit formation, whereas one to multiple visits depict progressive improvement in fruit set, size, and quality with increasing pollinator visits.	141
85.	The line graph shows the variation in fruit size (mm) of cherry fruits under different pollination regimes. Pollinator exclusion resulted in no fruit development, confirming the essential role of pollinators. Fruit size increased markedly from one visit to multiple visits across all pollinator groups. <i>Apis mellifera</i> consistently produced the largest fruits across treatments, followed by <i>A. cerana</i> and wild pollinators. Maximum fruit size was recorded under multiple visits, highlighting the positive	143

	impact of repeated pollinator activity on fruit development.	
86.	The line graph depicts changes in cherry fruit weight (g) under different pollination regimes. Pollinator exclusion resulted in no fruit development, confirming that pollinators are essential for fruit set. Fruit weight increased consistently from one visit to multiple visits for all pollinator groups. <i>Apis mellifera</i> produced the heaviest fruits across all visitation levels, followed by <i>A. cerana</i> and wild pollinators. The maximum fruit weight occurred under multiple visits, demonstrating that repeated pollinator activity significantly enhances fruit development and yield.	143
87.	The line graph shows the variation in TSS (°Brix) of cherry fruits under different pollination regimes. Pollinator exclusion resulted in no fruit formation and, therefore, no measurable TSS. TSS increased sharply from one visit onward for all pollinator groups. <i>Apis mellifera</i> produced fruits with the highest TSS values across all visitation levels, followed by <i>A. cerana</i> and wild pollinators. The maximum TSS was recorded during multiple visits, indicating that repeated pollinator activity enhances fruit sweetness and overall quality.	144
88.	The line graph illustrates changes in fruit acidity (pH) under different pollination regimes. No fruit developed under pollinator exclusion, resulting in no measurable acidity. Acidity increased progressively from one visit to multiple visits for all pollinator groups. Fruits pollinated by <i>Apis mellifera</i> exhibited the highest acidity across all visitation levels, followed by <i>A. cerana</i> and wild pollinators. Maximum acidity occurred under multiple visits, indicating that repeated pollinator activity influences fruit biochemical properties, including acidity.	

LIST OF APPENDICES

Appendix No.	Title / Description	Page No.
1.	Copyright	158
2.	List of Publications	159-162
3.	List of Conferences	163-166

Chapter 1

Introduction

Insect pollinators play a key role in the reproductive success of both wild flora and agriculturally important crops, serving as vital agents in the transfer of pollen and thereby influencing global patterns of biodiversity, food production, and ecological stability (Katumo et al. 2022). Angiosperms require the process of pollination as the transfer of the pollen grains to the female stigma of flowers is a prerequisite to the sexual mode of reproduction (Maggi and Pardo 2024). The given natural process (pollination) not only guarantees the survival of plant species in the process of sexual reproduction but also promotes the productivity of a wide range of crops, forming the foundation of the staple human diet and acting as a primary source of nutrition (Eeraerts et al. 2019). Insects are by far much more dominant and efficient, ecologically speaking, pollinators due to their abundance of species, versatility, and flight abilities, as well as co-evolutionary associations with flowering plants, among other factors, when compared to other biotic pollinating agents (among which include birds, bats and small mammals) (Abrol 2011). The morphological characteristics and behavioural patterns in insects show a high degree of specialization that not only allows them to retrieve the floral resources effectively, but also allows the transfer of pollen. The structure of many insects has been adapted to make them more useful in pollination, with plumose hairs, extended proboscises, or pollen baskets (e.g., in bees) (Krishna and Keasar 2018). The ecological service of insect pollinators is vast in the whole world. It is assumed that more than 75 per cent of flowering plant species are partially reliant on animal-mediated pollination, and about 35 per cent of the world's food crops are directly dependent on pollinators to achieve better yield and quality (Choi and Jung 2015). Fruit crops are one of the horticultural crops that play a very crucial role in terms of nutritional security in that they contain the much needed vitamins, minerals, antioxidants and dietary fibre, which have a significant role to play in maintaining a balanced human diet. Insect-mediated pollination is linked to the successful cultivation and productivity of most fruit crops, which contributes greatly to fruit set, size, shape, and quality (Ahmed et al. 2024). Several fruit varieties of commercial value, including apples, pears, plums, apricots, peaches, and cherries, are strongly reliant on insect pollination, especially bees, butterflies, and hoverflies, to accomplish successful cross-pollination. Among them, cherry (*Prunus*) takes a significant place in the list of the most valued temperate fruit crops grown in Europe and Asia. They are a favourite among consumer as they look striking, are glossy-skinned, moderately sweet, but with their nutritional profile, containing plenty of vitamin A and C, potassium, fibre and antioxidants, their medicinal and health value is significant. Cherries, despite being of high price in the premium market, have remained highly demanded by their flavour, therapeutic value and beauty (Stern et al. 2007).

Cherry is a high-value temperate fruit crop with substantial economic importance at both global and

regional scales. Globally, cherry production has shown a steady increase, reaching approximately 4.3-4.4 million metric tonnes in recent years, with Türkiye, the United States, and Chile emerging as the leading producers, reflecting the strong commercial demand and export-oriented nature of the crop (FAOSTAT 2024; AgriFarming 2024). Economic studies from major producing regions indicate that cherry cultivation is financially viable, despite relatively high establishment and management costs, owing to premium market prices and strong consumer demand (Noor et al. 2020). In India, cherry cultivation is largely concentrated in the north-western Himalayan region, particularly in Jammu and Kashmir, which contributes more than 90% of the country's total cherry production, with annual output estimated at 12,000-16,000 metric tonnes (Bali et al. 2022). Cherry cultivation in the Kashmir Valley is spatially concentrated in a few key districts that together constitute major production hotspots. Among these, Ganderbal accounts for the largest area under cherry cultivation (~350 ha), producing approximately 1,400 metric tonnes annually with an average productivity of 3,627.84 kg ha⁻¹. Srinagar follows with about 180 ha under cherry orchards, yielding nearly 1,250 metric tonnes and exhibiting comparatively higher productivity (8,964.6 kg ha⁻¹). Shopian district covers around 100 ha, producing approximately 1,150 metric tonnes, with a productivity of 5,440.7 kg ha⁻¹. Notably, Baramulla, despite having a relatively smaller cultivated area of only 70 ha, records a high production of about 1,350 metric tonnes, resulting in the highest productivity among the major cherry-growing districts (~17,099 kg ha⁻¹) (AgriFarming 2024; Directorate of Horticulture J&K 2023). These district-level variations indicate that cherry production in the Kashmir Valley is not solely determined by area under cultivation but is strongly influenced by orchard management practices, agro-climatic conditions, and biological inputs such as pollination efficiency. The high productivity observed in districts like Baramulla and Srinagar underscores the significant economic potential of cherry cultivation in the region and highlights its role as a high-value horticultural crop contributing substantially to farm income and regional agricultural economy (FAOSTAT 2024; AgriFarming 2024). A great number of insect pollinators, such as honeybees (*Apis mellifera*, *A. cerana*), solitary bees (e.g., *Andrena* spp., *Xylocopa* spp.), bumblebees (*Bombus* spp.), hoverflies (*Syrphus* spp.), and other dipterans (*Eristalis* spp.), find cherry blossoms appealing (Queiros et al. 2024). The Hymenoptera, Lepidoptera and Diptera are the three dominant orders of insect pollinators that are, in particular, important due to their diversity, floral fidelity, and efficiency. The morphological and behavioural characteristics of these groups of insects are specific and help them be efficient in terms of transferring pollen and foraging of fruit systems in temperate areas (Inouye et al. 2015). Their ecological functions and conservation in cherry orchards should be improved to maintain their pollination services and guarantee the long-term sustainability of cherry production in such areas as the Kashmir Valley (Banyal et al. 2024). Morphological changes in the Hymenopterans, like

branched body hairs, specialised mouthparts and pollen baskets (corbicula) have facilitated pollen collection and transfer. Their foraging and social behaviour on a colony basis enables them to forage a wide range of flowers within a small time interval (John et al. 2025). Examples of the lepidopterans include moths and butterflies, and they are known as being important insect pollinators, particularly in areas where the diversity of flowering plants is large and the flowering period is prolonged (Faraz et al. 2023). Although bees are traditionally viewed as being more efficient than butterflies, bees are more important in pollination due to the fact that they have a proboscis, which gives them the opportunity to access the nectar in tubular flowers. They specifically play an important role in pollinating orchard crops such as apples and cherries in temperate zones such as the Kashmir Valley (Barrios et al. 2016). Agriculturally, abnormally, families like the Nymphalidae, Pieridae and Lycaenidae are widespread visitors to the habitats. The pollination services of dipterans, especially houseflies (Muscidae), bee flies (Bombyliidae), and hoverflies (Syrphidae), are increasingly known. They can be more efficient in pollination compared to bees, although they are not given enough attention, particularly in unfavourable weather conditions when bee activity is reduced (Inouye et al. 2015). Past studies have found several insect species in cherry and other stone fruit orchards in the valley (Faraz et al. 2023; Bihaly et al. 2024). More than 46 insect species of five orders and 20 families have been documented in surveys, with the most common visitors including *Lasioglossum*, *Xylocopa*, *Andrena*, *Syrphus*, and *Musca* (Sharma et al. 2016). Nevertheless, the abundance and diversity of species have been the main focus of most of these studies, with little attention paid to morphometric characterization, functional characteristics, and species-specific pollination functions, especially in Lepidoptera and Diptera (Wang et al. 2024). Besides, the cryptic diversity, morphological similarities and hybridisation of Hymenoptera make identifying the species quite difficult due to its taxonomic complexity. The morphology-based identification, which is conventional, has not been adequate to differentiate closely related taxa, especially in complex systems such as orchards where more than one species coexists (Steiner et al. 2007). Morphometric analysis has been a useful method of measuring interspecific and intraspecific differences between insect pollinators, which provides important data on the efficiency of flight, body size, floral compatibility, and pollination potential. It has, however, been restricted in its use with the temperate fruit systems of Kashmir, especially in dominating pollinator groups (John et al. 2025). Even though the use of Lepidopteran (butterflies) and Dipteran (hoverflies) species as potential pollinators is increasingly recognised, the current body of literature does not show any efforts to use integrated morphological and molecular methods to identify these species. The majority of the studies are performed using visual taxonomic identification, which is ambiguous as it may share morphological characteristics, or just use the occurrence data of the species without evaluation of functional

characteristics, including body size, proboscis length, and other morphometrical properties of pollination biology. Furthermore, the studies that assess the effectiveness of various types of insect taxa, especially in relation to the percentage of fruit set, fruit size, and fruit quality, are not abundant in the Kashmir region. Although other studies do not ignore the effect of insect pollination on the level of crop production, they rarely separate the individual species of pollinators or quantify the relative contribution of different pollinating species to fruit production parameters in cherry orchards. The fact that no quantitative morphometric data and species-level molecular verification of non-*Apis* pollinators exist is extremely limiting in terms of our understanding of pollination ecology in these systems. To close the gap between the two, a combination of morphometric analysis and DNA barcoding (COX-1 gene sequencing) is used in the current study to capture an accurate record of the diversity and identity of the key groups of insect pollinators, which consist of Diptera, Lepidoptera, and Hymenoptera. In this research, the authors examine the influence of insect pollinators on fruit set and key quality characteristics, such as size, shape, and sweetness. This gives a better understanding of their role in cherry orchards and provides useful insights to control and conserve pollinators in temperate agrifood systems.

Chapter 2

Review of Literature

Angiosperm reproductive processes rely on insect pollinators to facilitate pollen movement and enable seed and fruit development (Katumo et al. 2022). Bees, most importantly *Apis*, *Bombus*, *Andrena*, *Xylocopa*, and *Lasioglossum*, are the best insects for pollination because of their body structure and attachment to flowers (Osterman et al. 2021). Orchard crops are also pollinated by butterflies such as *Vanessa cardui*, *Papilio demoleus*, and *Pieris brassicae*, which increases the overall output (Barrios et al. 2016). Dunn et al. (2020) also state that hoverflies (Syrphidae) are used as pollinators and pest regulators. The richness of pollinators depends on the altitude, the density of flowers, landscape planning, and pesticide application (Hederstrom et al. 2025). Although we have scarce research about the topic, and much of it has not been validated on a molecular basis regarding most of the recently discovered insect pollinators (Dar et al. 2018). COX-I sequencing is a DNA barcoding that assists in improving the precision of species representatives (Alam et al. 2024). According to morphometric and molecular studies on cherry orchards, fruit set, size, sugar content, and quality and market value are increased by effective pollination of cherry orchards (Ramzan et al. 2019). This fact testifies the importance of pollinators in terms of cherry productivity, yield, and quality. That is why the current research pays much attention to the capture of pollinator biodiversity, the accuracy of taxonomic identification, and the effectiveness of current pollinators in cherry orchards in Kashmir. This approach also gives a solid scientific basis to long-term pollinator control and conservation measures in temperate agroecosystems, and the study can help improve the comprehension of pollinator services.

2.1. Authentication of insect pollinators in Cherry orchards through Morphological and DNA barcoding techniques

Morphological identification has traditionally been the most important technique used in identifying the various insect pollinators. It was founded on taxonomic keys that provide a sequence of external features like body segmentation, wing venation, structure of the antennae, and colouration in the taxonomic feature, according to the study of Rosas-Ramos et al. (2020). Even though the morphological identification has contributed significantly to the identification of the species, it presents certain weaknesses, especially when the two taxa with similar morphologies and cryptic species are involved (Rommel et al. 2024). The molecular methods, especially DNA barcoding, transformed the method of authentication of species since they were more efficient and precise in identifying insects. DNA barcoding is a technique that entails the sequence of short and standardized genetic markers, like the cytochrome c oxidase subunit I (COX-I) gene, that is located in the mitochondrion and has ample interspecies variation that can be utilised to effectively distinguish between species (Watanabe et al. 2024). DNA barcoding has enhanced the identification of species and overcome the problem of morphological ambiguity in insects (Bell et al. 2022). Research has shown the potential of DNA barcoding to aid in the determination of the cryptic

species of pollinators in cherry orchards, which had been wrongly determined using morphological characteristics. That is why various findings prove the relevance of the combination of traditional and molecular methods to complete a thorough evaluation of pollinator communities (Liu et al. 2023).

2.1.1 Morphological Study

The study by Dhokane and Chavan (2025) is a morphological characterization of insect pollinators on fruit crops in the Maharashtra district of Aurangabad. The morphological features of the major pollinator groups, such as bees, flies, beetles, and butterflies, were recorded in terms of body segmentation, mouthparts, wing venation, and specialisation with special reference to morphological adaptations. Their results showed the importance of these diagnostic characteristics in proper species identification and ecology research, thus emphasizing the importance of morphology in the connection of structural diversity with pollination efficiency and crop production.

The geometric morphometrics was used to analyse wing shape variation among hoverfly species (Family: Syrphidae) in cherry orchards and showed species-specific shapes of wings, enabling the dependable differentiation within this rich group of pollinators. The research showed that geometric morphometrics is useful in morphological identification to be used in groups where conventional methods are challenging (Acanski et al. 2023).

In a study by Khan and Liu (2022), the morphology of the hair of *Apis mellifera* was studied through SEM and offered a new method of measuring hair length on the body parts. They recognized two hair types and five branches of branching, and the thorax had the longest and most branching hairs, with its pollen delivery being underlined. It was found to have a positive correlation with the branching and hairiness, which are one of the primary characteristics of pollination efficiency.

The study of pollinators in cherry orchards was conducted in a comprehensive way, and standard morphological keys were used to determine pollinator species belonging to various families, Apidae, Syrphidae, and Vespidae. The results showed that a combination of morphological characteristics was needed to identify the species accurately, and in particular, the morphology of the legs, the structure of the antennae, and the genitalia could be used with success in cases of minimal morphological difference (Rosas-Ramos et al. 2020).

The study of morphometric differentiation of *Bombus* spp. in the Kashmir Valley used high morphometry to differentiate closely related species that are hard to distinguish on the basis of traditional morphological techniques. The paper has shed light on the diversity of regional bumblebees and emphasised the need to have accurate species identification when analysing pollinator ecology and behaviour (Parey et al. 2024).

The polyphyly and paraphyly have been revealed in *Andrena* by the recognition of seven genera in the

Andreninae, which include *Alocandrena*, *Cubiandrena*, *Megandrena*, and other related groups (subgenera of *Andrena*, and are separate evolutionary groups defined by morphological and molecular studies). Phylogenetic reconstruction also postulated that the MRCA of *Andrena* + *Cubiandrena* spread out of the New World into the Palaearctic, accompanied by several subsequent Neogene dispersal occurrences between the Palaearctic and Nearctic (Pisanty et al. 2022).

In a detailed examination, Dincă et al. (2021) noted that overlap in the wing pattern is common in Palearctic species of butterflies, and external morphology cannot be relied upon to identify species. Their effort also stressed the evolutionary male and female genital structures that are species-specific, which are thus reliable as diagnostic characteristics even in a low molecular divergence. The research supported the need for genital study in the solution of cryptic and sibling species complications.

Huemer et al. (2020), in a thorough revision of a number of groups of Lycaenidae and Nymphalidae, have found that minor variations in male genitalia, including shape of valva, length of aedeagus and uncus form, were essential in straightforward delimitation of species. The experiment stressed that the wing patterns alone might lead to a wrong identification, particularly between species that are situated in the same geographical area.

A study on the genus *Andrena* gave 24 species known to date in 16 subgenera and the description of three new species, *A. (Zonandrena) pantnagarensis* sp. nov., *A. (Z.) dehradunensis* sp. nov., and *A. (Euandrena) indiaensis* sp. nov. (named after their location of discovery and morphological features). Both sex diagnostic keys were aggregated, with new taxonomical features, accompanied by coloured photographs, which boosted identification in the genus (Gautam et al. 2024).

The data on the control of 131 Andrenid bee species in Slovenia was the first to be provided by Gogala (2019). This data was the content of collections, literature, and field observations of the Slovenian Museum of Natural History. Photos of mounted and living specimens that could be found in collections of the Slovenian Museum of Natural History were used to describe each species.

The first study of wing size and shape disparity in *Andrena barbara*, a solitary bee, was conducted in urban landscapes by applying geometric morphometrics. The experiment did not find significant differences in wing morphology, which was also consistent with the past research on urban solitary bees, and indicated that urban environments could have a significant role in the conservation of bees (Beasley et al. 2019).

Santos et al. (2017) researched morphological variation in ichneumonid wasps and established that external structure features, such as wing venation, metasomal segmentation, and body sculpture, are at the heart of species delimitation. They found that genital examination was an additional but not mandatory character in Hymenoptera, whereas it is a mandatory character in Lepidoptera taxonomy.

2.1.2. DNA Barcoding

The COX-I (cytochrome oxidase I) gene DNA barcoding was used to identify pollinator species of the Kashmir Valley cherry orchards, through which the identification of the species was possible, including unknown bees, flies, and beetles. The article emphasized the potential of DNA barcoding to identify cryptic species that shared morphology and proved to be effective in increasing the understanding of pollinator diversity and guaranteeing swift and correct identification of species (Mitra et al. 2025).

Kachhawa (2023) discussed the use of DNA barcoding in the taxonomy of insects and the importance of the cytochrome c oxidase subunit I (COX-I) gene as an effective and precise molecular marker. The intra and interspecific analyses on variation showed that there was low intraspecific divergence, which confirmed the validity of the COX-I gene in species-level identification. The method was especially useful in the recognition of cryptic species, morphologically allied groups, and taxonomic stages like the larva of organisms that are challenging to distinguish using conventional morphology. The significance of building DNA barcode reference libraries was also noted in the study to be used as the basis of novel advances in biodiversity measurements, pest management and conservation measures.

Liu et al. (2023) boiled down ecological surveys and DNA barcoding of the COX-I gene to study pollinator diversity in fruit orchards, such as cherry orchards. They found 40 species of pollinators, of which some were cryptic and could not be distinguished by morphology alone. The combination of both molecular and ecological information offered a more in-depth insight into the topic of diversity among pollinators and the efficiency of DNA barcoding as a research method used to track and control the population of pollinators within fractured environments.

Apple and cherry orchards were studied in the Himalayas to determine the pollinator diversity using DNA barcoding markers COX-I and rRNA gene. The accuracy of species identification improved with this multi-gene approach, taxonomic ambiguity was minimised, and data on biodiversity could be trusted to use in orchard management and conservation planning (Bare et al. 2023).

As the study by Shashank et al. (2022) showed, DNA barcoding is a solid and reliable method of identification of the insect fauna in India. Their work focused on combining molecular methods with conventional morphological methodology in order to have a reliable identification of species. The authors emphasized the value of the mitochondrial COI gene in solving taxonomic uncertainties and suggested its extensive use in biodiversity analysis and ecological surveys, especially when dealing with groups of complex or cryptic morphology.

To determine the usefulness of the molecular taxonomy in the urban ecosystem, Villalta et al. (2021)

developed DNA barcodes of 2,931 bee specimens representing 157 species and 28 genera found in the Loire Valley, France. Automated BIN (Barcode Index Number) grouping detected 172 genetic groups, 137 species (87.26) of which had a one-to-one relationship between morphological species and BINs and so could be easily identified even within similar taxa. Interestingly, 36 species (22.93) were observed in highly urbanised environments, and 14 species (8.92) had deep intraspecific lineages and lacked obvious morphological distinctions, which supports the value of DNA barcoding in the discovery of small hidden diversity and clarifying taxonomic uncertainty.

Kratochwil et al. (2021) researched the *Andrena wollastoni* group (subgenus *Micrandrena*) to examine the colonization or radiation processes of island pollinators at Madeira. Six endemic species and five endemic subspecies make up the archipelago and the Canary Islands. Managerial COX-I sequence studies demonstrated the monophyly of four Canary Island species and two Madeira species, indicating a fairly recent evolutionary past. Their results also found *A. gomerensis* or its evolutionary ancestor to be the primordial inventory on which the rest of the taxa separated.

The DNA barcoding proved the initial collection of the Italian alpine mining bee *Andrena allosa* (Warncke 1975). Also, the COX-I sequence analysis of *A. praecox* (Scopoli 1753) in western Italy showed surprising intraspecific genetic organization, with sequences of the Italian and the western populations showing more differences with the eastern populations by 2.22% (Cornalba et al. 2020).

In this study, Pentinsaari et al. (2019) explored the use of DNA barcoding in the discovery of cryptic diversity within insect taxa. Their results showed that there was a large quantity of hidden species diversity that could not be detected by using only the conventional morphological identification techniques. The research placed a strong argument in favour of applying DNA barcoding as an efficient tool to monitor biodiversity, limit species, and conserve species, especially in areas that are highly diverse in terms of insects with low taxonomic resolution.

A thorough revision of Alpine bee taxa was carried out by Praz et al. (2019) on *Andrena bicolor* (Fabricius 1775), and such taxa as *A. montana* Warncke 1973, and *A. allosa* Warncke 1975, which had long been disputed in terms of taxonomic status. They have also discovered four Alpine species using a combination of mitochondrial and nuclear gene phylogenies, combined with more in-depth morphological studies, including the description of a species, *A. amieti*. Surprisingly, *A. amieti* showed two severely divergent mitochondrial lineages that took place in sympatry. It was also found that *A. allosa*, *A. amieti* and *A. montana* were all polylectic, although they had differing pollen host spectra. Noteworthy, the results showed significant cryptic diversity in the southern European *Andrena* (*EuAndrena*), and *A. croatica* Friese, 1887 came off the list of synonyms and was listed as a subspecies of *A. pileata* Warncke 1875.

Hazir and Bock (2019) tested the efficiency of the DNA extraction of dry pinned specimens of sand bees (*Andrena* spp., Fabricius 1775) and tested the performance of old and new primers. To examine the occurrence of the species among different subgenera and species in distinct bee groups, a total of 256 specimens were analysed (222 dry pinned bees, which represented 37 subgenera and 101 species, and 34 ethanol-preserved specimens, which represented 21 species). The best quality of DNA was obtained in the ethanol-preserved samples. Amongst 31 tested primer sets, 14 were novel, a major improvement in the success of DNA amplification and eventual specification.

Trying to improve the taxonomy of bees in Canada, Sheffield et al. (2017) summarised over 12,500 DNA barcodes of the mitochondrial COX-I, that is, 811 BINs, and found these data reflected 95 per cent of known bee species in Canada. Their analysis showed the effectiveness of DNA barcoding in the description of species diversity, but also showed taxonomic problems with morphologically complicated taxa such as *Andrena* and *Nomada*. Such results highlight the existence of cryptic species and the necessity to integrate molecular data and classical taxonomy.

The first report of *Andrena agilissima* (Scopoli 1770) in India was based on the morphological and molecular markers on the western agro-climatic region of Punjab state (Makkar et al. 2016). With this record, the bee species of mining now numbers more in India. They have also produced DNA barcode sequences of the species and deposited these under Gen Bank, National Centre of Biotechnology Information (NCBI) under accession 'KT960836' and Barcode of Life Data (BOLD) Systems under Barcode Index Number 'BOLD: AAY6909' and Barcode Index Number under Barcode Index Number.

Schmidt et al. (2015) were able to provide almost complete coverage of the German bee fauna using the barcoding of 4,118 bee specimens corresponding to 561 different species, where 503 species had complete COX-I sequences, and 43 had incomplete barcodes. Besides an indispensable molecular landmark in identifying species, this massive undertaking can be used to track biodiversity, ecology and subsequent taxonomic reforms of central European bees.

2.2. Diversity of insect pollinators from Cherry orchards of Kashmir Valley- Distribution and Abundance

Mir et al. (2025) evaluated the impacts of intensive monoculture of cherry on pollinators in the Kashmir Valley. Their results found that orchards with limited floral resources had lower pollinator abundance and diversity as compared to polyculture orchard systems. They suggested introducing intercropping and creating wildflower strips in orchards to increase pollinator benefits to reduce the negative effects.

The study conducted by Ferro et al. (2024) examined the pollinator distribution in cherry orchards of South Asia. Their findings revealed that pollinators were more concentrated in orchard edges and in areas having more varieties of floral resources. The research findings also provided orchard management practices that were recommended to increase floral resource diversity and spatial heterogeneity to increase the number of pollinators on the entire orchard landscape.

The authors Pardo and Borges (2020) studied the abundance of pollinators in cherry orchards of various regions of India. Their results show that the abundance of the pollinators is the highest in the cherry blossom season and is seasonally altered. The analysis proved that in such factors, the abundance of pollinators was strongly dependent on temperature, humidity, and floral availability. The experiment explained the relationship of environmental factors, orchard management and populations of pollinators.

The observations of Weekers et al. (2022) indicated that the cherry orchards are not isolated but are genetically connected with the pollinator population in the surrounding natural habitats. This level of interconnectedness not only increases the robustness of orchard pollinators but also highlights the importance of preserving surrounding ecosystems in ensuring future pollination service and biodiversity in the farm landscapes.

Katumo et al. (2022) studied the pollinators (pollinators and bees) and cherry flowers in the temperate orchards in Northern India. Their study documented the number of visits, foraging activities, and pollen deposition of various insect species with the help of advanced behavioural observation techniques. The paper established that *Apis dorsata* and *Eristalis tenax* are some of the most common visitors, thus highlighting the importance of the hoverfly and bees in pollination.

According to the results of the study conducted by Kline et al. (2022), cherry orchards are biodiversity hotspots because they provide a wide range of floral resources to a wide range of insect pollinators. These orchards also help in maintaining the ecological stability and conservation of biodiversity in the region by facilitating the habitats of bees, butterflies, and hoverflies. These insights emphasise the similarity between the production of cherry orchards as a producer of agriculture and as an ecologically sustainable source.

Osterman et al. (2021) analysed the trends of pollinator abundance in the cherry orchards in China. They discovered that the size of the orchard, the composition of the landscape and the neighbourhood of the orchard to the natural habitat affected the distribution of pollinators. This research highlighted the need to preserve the pollinator distributions of cherry orchards by

preserving habitat connectivity and landscape diversity.

In the meta-analysis study by Bartholomee et al. (2020), it was evident that there is a correlation between orchard management practices and pollinator diversity. The study highlighted the ecological advantages of sustainable farming by showing that the IPM-controlled orchards always had richer communities of pollinators as compared to the conventionally managed orchards. Such results support the increased implementation of IPM activities in the world to balance agricultural production and the protection of biodiversity.

Pardo and Borges (2020) compared pollinator diversity of cherry orchards in Kashmir Valley, the traditional and high-altitude ones. The researchers found out that native pollinators such as *Andrena* spp. and *Bombus Himalayans* were more varied in high-altitude orchards owing to the availability of diverse floral resources and lack of pesticide exposure. Their result showed the effect of high altitudes and microclimate on the community of pollinators.

The conclusions of Rosas-Ramos et al. (2020) placed an emphasis on the fact that sustainable orchard management is beneficial to the community of pollinators. In comparing conventional and organic systems, they found that organic systems favoured an increase in the abundance of pollinators, and this implies that a low level of pesticides used and increased floral diversity can reinforce the ecosystem services and promote successful pollination in cherry orchards. The findings support the idea of incorporating biodiversity-friendly practices into the orchard management strategies.

Eeraerts et al. (2019) examined the pollinator diversity in North American cherry orchards by determining and allocating the key groups of pollinators to the orchards. Their study combined a morphological and molecular technique to list a diverse range of pollinators, such as the native and non-native bee species. The results emphasised the significance of management processes that are sensitive to the diversity of the pollinator community and demonstrated the significance of cherry orchards in preserving both native and invasive pollinator species.

2.3. Effectiveness of major insect pollinators on fruit set and fruit quality of Cherry

The study by Huang et al. (2024) aimed to determine the impact of the timing of pollination on the fruit set and fruit quality in cherry orchards. Their findings emphasized that early morning pollination and especially by the bumblebees, improved fruit set and fruit quality significantly. The researchers attributed these gains to the foraging behaviour of bumblebees that are very active and efficient in the early morning when other pollinators are inactive in the cooler morning. This implies

that the timing of pollinator movement based on favourable microclimatic conditions has an important role to play in the success of pollination and the ultimate yield outcome of cherry orchards.

Osterman et al. (2024) note that one of the possible approaches to ensure a stable fruit set and better fruit quality in organic cherry orchards is the introduction of managed pollinators like solitary bees and bumblebees. Although wild pollinators are also indispensable, in different environmental conditions, it might not be the case that their populations will offer enough services. This paper highlights that by introducing additional pollination to natural pollination, orchard managers can improve their cherry production performance by increasing the stability and productivity of the pollination regime.

Huang et al. (2024) investigated the influence of certain pollinators on the quality of cherry fruit in China. The authors found that bumblebee and hoverfly (Syrphidae) pollination was most beneficial to fruit quality, delivering fruits of greater firmness and taste superiority as compared to fruits that were pollinated predominantly by honeybees. The researchers are of the view that such pollinators can better distribute the pollen among the cherry blossoms, thus increasing the quality of the fruit. The results of the present study are very useful in offering novel information on how various species of pollinators influence cherry fruit quality.

Fliszkiewicz and Giejdasz (2023) also suggested that managed *Osmia* bees introduction to organic cherry orchards would be a feasible remedy to reduce the risks of the decreased population of wild pollinators. Managed solitary bees can be crucial in ensuring a quality yield and also in ensuring economic returns, by ensuring that the fruit size is consistent, and that the seed set is higher. This study underlines the need to consider the implementation of solitary bees managed in the orchard management systems, especially in areas that experience pollinator shortages.

In the study conducted by Osterman et al. (2021), the authors determined the contribution of wild bees to pollination service in cherry orchards in North America. They have shown that wild bees, especially those of the genus *Osmia* and *Andrena*, were important in fruit set. Notably, the study also found that orchards with a diverse population of wild species of bees had a higher fruit set compared to those that depended on one species of pollinator. This highlights the ecological and agricultural importance of conserving pollinator diversity because communities with diverse wild bees are more stable and efficient in the delivery of pollination services. All in all, the paper has established the relevance of maintaining and improving the population of wild bees in order to maintain fruit production sustainability in cherry orchards.

The research evaluated the effectiveness of pollination of South Asian cherry orchards within the

fruits of honeybees, bumblebees, and indigenous solitary bees. Although the honeybees were most effective in increasing the fruit set, bumblebees and solitary bees were more effective in improving the quality of the fruit. A combination of these findings highlights the complementary nature of various pollinator groups and indicates that combining several species is the most likely to achieve the best fruit quality and the total yield (Eeraerts et al. 2020).

The study by Iler and Goodell (2014) aimed at exploring how floral density and pollinator behaviour interact to affect fruit set in Spanish cherry orchards. They found that orchards that had concentrated floral resources provided foraging by pollinators to be more efficient, since the distance between flowers was shortened after foraging, and since flowers were likely to be visited repeatedly. This behaviour changes not only increased the rate of cross-pollination but also led to an increase in overall fruit yields. These results imply that the design and planting arrangement of orchards, especially the investment of floral resources, could contribute to high pollinator efficiency and consequently enhance productive crop yield.

2.4. Research Gap

1. This research was aimed at filling significant gaps in the research on pollination, especially in the temperate fruit orchards of Kashmir, India. Though several studies have been carried out on insect pollinators, most studies have used single methodological approaches, as these do not allow proper identification of species. Although the insect biodiversity in India is large, only 3.7 per cent of all known insect species have been DNA barcoded, which is a huge gap in the molecular documentation. Such significant pollinators as Hymenoptera, Diptera, and Lepidoptera are still under-represented in the genetic databases (Shashank et al. 2022). Therefore, existing information on pollinator diversity, identity and ecological functions in fruit orchards is incomplete. To overcome these shortcomings, the study at hand uses an integrative methodology of morphological, morphometric, and molecular (DNA barcoding) studies. This combined system made species identification accurate, minimised misclassification and gave a complete picture of pollinator diversity. No method can be applied to provide sufficient identification in ecologically complicated groups such as insect pollinators.

2. The fundamental pollination performance of particular groups of pollinators, including *Apis*, *Bombus*, wild bees, hoverflies and butterflies, has hardly been tested internationally and in temperate fruit orchards of India in controlled, visit-based experiments. Specifically, few studies have been done to determine the direct connection between the frequency of pollinator visitation and its impact on fruit set and quality of crops like cherry, apple, and plum. The current research paper covers this gap by assessing the relative importance of various groups of pollinators in the fruit set and quality of cherry orchards.

2.5. Hypothesis

The following main hypotheses will be tested using the integrated morphological, molecular, and ecological evaluation of various insect pollinators in cherry orchards of Kashmir Valley:

1. The taxonomic Resolution Hypothesis

The Kashmir Valley has a morphologically diverse and under-documented taxonomically assemblage of insect pollinators with species representatives of Hymenoptera, Lepidoptera and Diptera, with possible taxonomic novelties and regionally unknown taxa.

2. Hypothesis of Pollinator Diversity and Spatial Distribution.

The abundance and diversity of these insect pollinators vary strongly among the cherry orchard sites in the valley, with greater richness in orchards that are located at mid-elevations and less diversity found in agroecosystems that are highly cultivated or intensively pesticide-treated.

3. Ecological and Functional Hypothesis.

Insect pollinators have varied foraging behaviours and pollination performance, which depends on morphological characteristics of body size and activity patterns, thus impacting quantitative and qualitative parameters of cherry.

4. Molecular Recognition and phylogenetic Hypothesis.

Mitochondrial COX-1 gene sequences can effectively differentiate morphologically cryptic species with DNA barcoding, and phylogenetic analysis will provide distinct genetic divergence between taxa, which confirms morphometric differentiation and ecological functions.

2.6. Objectives of the study

- 1.** To authenticate the identification of insect pollinators in cherry orchards through morphological and DNA barcoding techniques.
- 2.** To study the diversity of insect pollinators from cherry orchards of Kashmir Valley- distribution and abundance.
- 3.** To investigate the effectiveness of major insect pollinators on fruit set and fruit quality of cherry.

Chapter 3

Materials and Methods

The study, entitled “**INSECT POLLINATOR DIVERSITY IN CHERRY ORCHARDS OF KASHMIR VALLEY USING MORPHOLOGICAL TOOLS AND DNA BARCODING**” was carried out between 2022 and 2024 with the primary objective of evaluating the diversity, morphometric variation, and molecular identity of insect pollinators in cherry orchards in the region. Besides taxonomic evaluation, the research also sought to establish the effectiveness of key insect pollinators in pollinating different plants through an examination of their effects on both qualitative (e.g. fruit size, shape, total soluble solids) and quantitative (e.g. fruit set percentage) fruit production parameters. The 03 year time span was chosen in a strategic way to be able to evaluate the inter-annual changes in the abundance of pollinators, the structure of species populations, and environmental parameters, including temperature, rainfall, and access to flowers, which can greatly affect pollinator behaviour and efficiency. This longitudinal study was not only able to generate more ecologically valid and representative data, but it also reinforced the conclusion that could be drawn on the stability, reliability and ecological significance of particular insect pollinators in the cherry orchards of the Kashmir Valley. Combinatory morphological characteristics, morphometric analysis and DNA barcoding further increased the precision of the species identification, particularly of cryptic or morphologically close species, with a strong foundation to further conservation and pollination management plans in temperate fruit agroecosystems.

3.1. Sampling and collection of insect pollinators

An extensive sampling of the insect pollinators was done when the cherry was at the height of the cherry bloom (mid-March to mid-April), the best period when the insect pollinators' activity was at its highest in the Kashmir Valley. A systematic field survey was conducted in 04 major cherry-growing districts, Srinagar, Shopian, Baramulla and Ganderbal, wherein 2 ecologically significant and agriculturally dominant sites were identified in each of the districts: Shalimar and Dhara in Srinagar, Kullar and Aerhal in Shopian, Tangmarg and Sopore in Baramulla and Lar and Baba-Wayil in Ganderbal (**Figure 1**). The sampling was also timed to coincide with the flowering stage of cherry orchards, to maximize pollinator interactions and was conducted only between 9:00 AM and 3:00 PM, as it was reported to be the most active foraging period by prior studies of pollinators (Nyarko 2012). Active and passive sampling methods were used to have a complete coverage of the community of pollinators: active sampling was done using the sweep/aerial nets in order to collect the foraging floral visitors, which is very efficient with

large-bodied pollinators like the bees and butterflies (Potts et al. 2005). All the collected specimens were euthanized using 95% ethyl acetate in airtight glass killing jars to preserve significant morphological characteristics used in conducting precise taxonomic and morphometric analyses (Connor et al. 2019). This standardised integrative sampling framework in the pollination services of temperate cherry orchards in Kashmir provided a good foundation for the documentation of the pollinator diversity and the morphological attributes of pollinators.

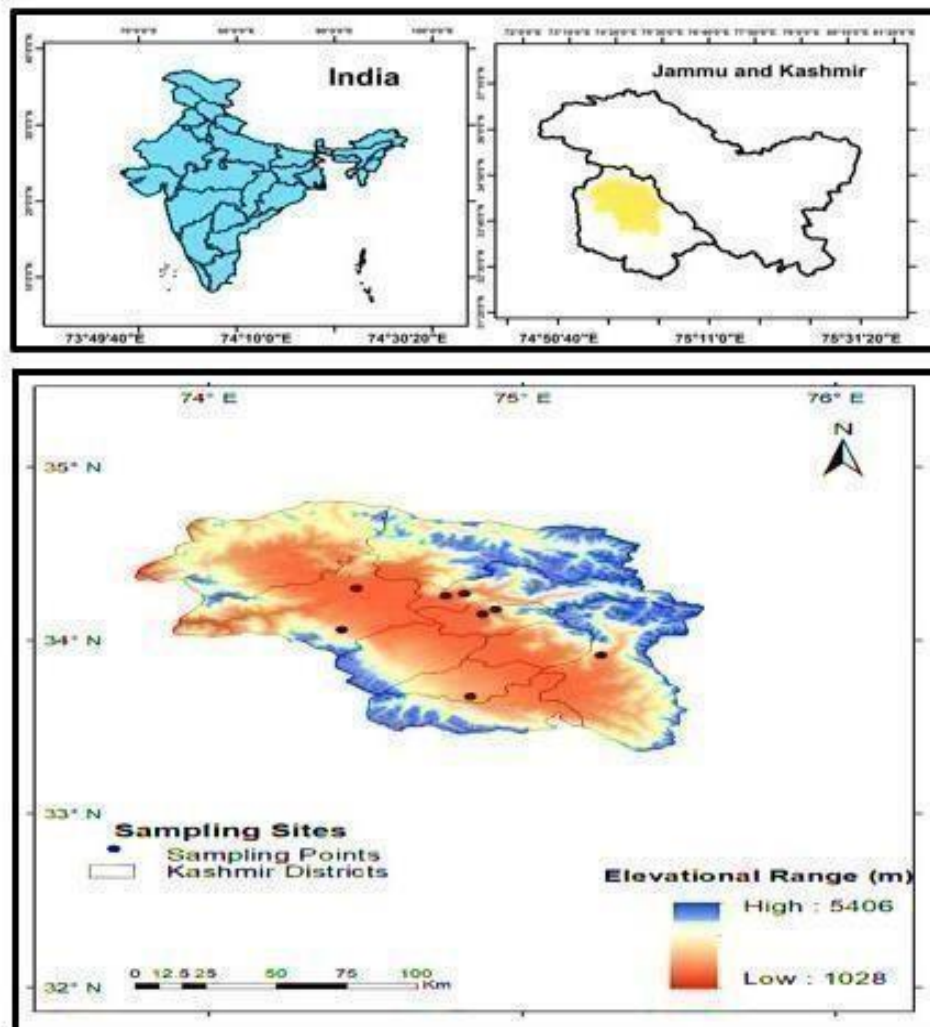


Figure 1: Study area map illustrates a detailed representation of the Kashmir Valley's cherry orchard geographical layout, with a specific focus on the four districts (Srinagar, Ganderbal, Baramulla and Shopian) that play a crucial role in cherry cultivation. These districts are demarcated on the map, allowing for easy identification of the areas where cherry orchards are most concentrated. The map highlights the varying extents of land dedicated to cherry farming in each district, offering insight into the agricultural significance of these regions.

3.1.1. Sampling Sites

The study was conducted across multiple cherry-growing regions of the Kashmir Valley. The geo-location metadata embedded within the images includes latitude, longitude, elevation, and timestamps, ensuring accurate spatial referencing of each collection site (**Figure 2**). This spatial and visual representation underscores the ecological variability and field conditions encountered during the year 2022-2024 survey period, highlighting the systematic approach adopted to capture pollinator diversity across a range of cherry orchard environments.

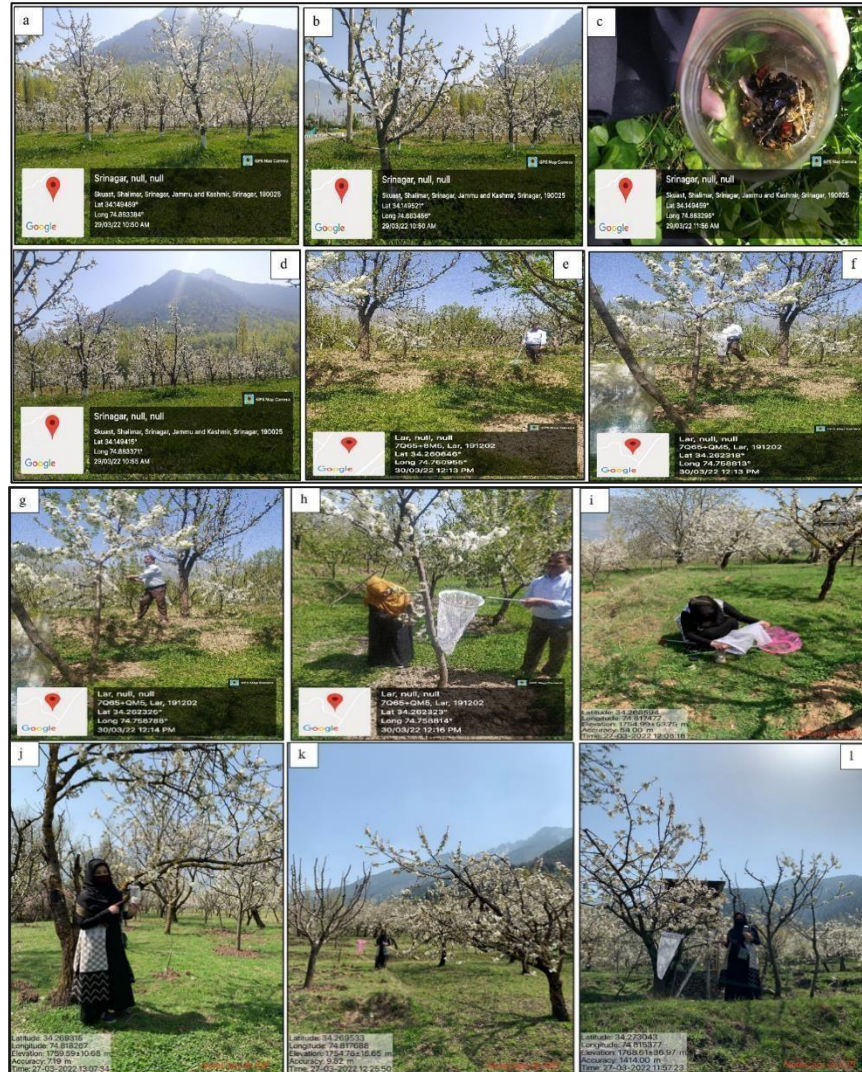


Figure 2: Field survey and pollinator sampling conducted in cherry orchards of the Kashmir Valley (a-l). The figure illustrates cherry orchards in full bloom across different sampling locations, with GPS-embedded coordinates marking precise survey sites. It also shows the collection of insect pollinators using Aerial nets and hand-collection methods, and temporary storage of specimens in collection jars during fieldwork.

3.2. Insect Mounting

Insect mounting was carefully done in the laboratory of the Research and Training Centre

For Pollinators, Pollinizers and Pollination Management (RTCPPM), SKUAST-K, Shalimar, Kashmir, the main aim of the whole procedure was to preserve the collected specimens both morphologically and molecularly. To ascertain the integrity and scientific usefulness, the following standardised entomological protocol was observed. The samples were handled with care, pinned, and techniques of wing positions were applied to limit damage to important taxonomic structures, including wing venation (Sharma et al. 2025). Such methods make sure that the samples are of good quality to be subjected to further morphological and morphometric, and molecular study as reported by Quicke et al. (1999)

3.2.1. Collection and Handling of Specimens

Insect pollinators were sampled in four areas of the Kashmir Valley, Srinagar, Ganderbal, Baramulla, and Shopian, using standard sweep netting in cherry orchards when insect pollinators were highly active. They were put in jars that contained 75% ethyl acetate in order to immobilize the captured specimens rapidly and maintain delicate morphological features that would be required in taxonomic and molecular studies. In order to preserve the specimens during mounting, imaging, morphometric analysis, and DNA extraction, they were handled carefully with fine-tipped entomological forceps to minimise the damage on the wings, antennae and legs (Dar et al. 2018).

3.2.2. Stretching of Wings and Appendages

To ensure proper alignment, morphological study, and long-term preservation, the wings of butterflies and other insects were stretched and positioned using standard entomological spreading boards. To mount the specimens, entomological pins were inserted through the thorax, and delicate brushes or tiny forceps were used to gently spread the wings into their resting position. Tracing paper strips were used to secure the forewings and hindwings in a symmetrical position until they dried, exposing diagnostic features like venation, colouration, and patterning. This approach maintained vital characteristics for morphometric measurements, photography, and comparative analysis while guaranteeing smooth, intact wings (Krogmann and Holstein 2010).

3.2.3. Pinning of Specimens

The insect specimens were put on size 2 entomological pins, depending on the size and durability of the individual specimen. Pins were inserted vertically up through the thorax so that the vital structures would be undamaged, and particularly in larger insects such as bees, wasps and butterflies, just to the right of the midline. To achieve stability, preservation, and ease in manipulation during the morphological and molecular studies, all specimens were pinned at the same height of 10 to 15 mm above the pinhead (Garner et al. 2011).

3.2.4. Labeling of Specimens

All specimens of insects mounted were marked correctly and significant data placed on the cover label, such as date of collection, collector name, elevation of place of collection and the district where the insect was collected. This mark was put right below the insect on the same pin as per the applicable entomological standards (Lopez et al. 2020).

3.2.5. Drying and Preservation

The insect specimens were preserved using the usual entomological methods after morphological analysis. Pinned specimens were dried for three to five days in a drying chamber or at room temperature to stabilise posture and wing position (Cho et al. 2016). They were then transported to Styrofoam or cork-lined insect boxes to keep them safe. To guarantee reliable DNA barcoding and sequencing, molecular analysis samples were immediately put in 95% molecular ethanol, which does not alter structural and chemical properties (Gamboa and Arrivillaga 2009).

3.3. Morphological study of insect pollinators

Morphological examination of insect pollinators was carried out under a stereo zoom binocular microscope, and diagnostic characters were studied using standard entomological keys and relevant taxonomic literature (**Figure 3(a-c)**).

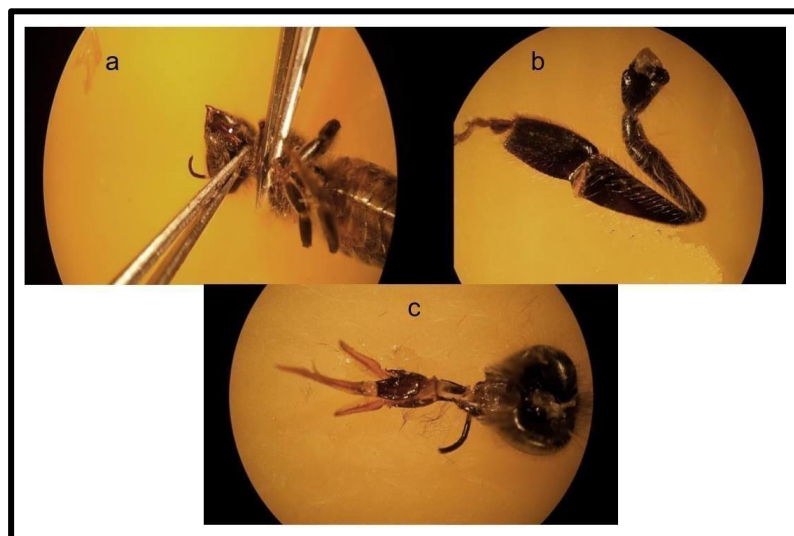


Figure 3(a-c): Dissection of insect pollinator specimens under a stereo zoom microscope enabling the precise visualization of delicate structures, enabling accurate morphometric and taxonomic analysis.

To enhance the visibility of sclerotized morphological structures, particularly those crucial for taxonomic identification, such as genitalia and mouthparts, the dissected body parts were

macerated overnight in a 10% potassium hydroxide (KOH) solution. This tissue-clearing technique, adapted from the protocol by Padial et al. (2014), effectively removed soft tissues and enhanced the microscopic visibility of the chitinous components. After digestion, the samples were carefully rinsed in distilled water to neutralise any leftover KOH and prevent further tissue degradation. The cleared structures were then preserved in 70% ethanol to maintain their morphological integrity. As recommended by Ortego et al. (2021), temporary mounts were created in glycerine for close examination, as it provided a distortion-free medium for clearly observing fine structures.

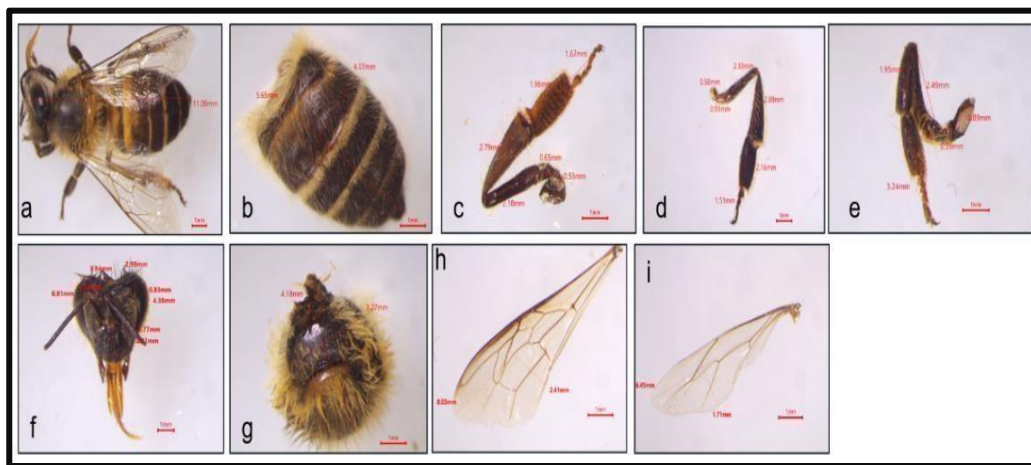


Figure 4: Morphometric measurements of insect body parts obtained using MagVision software, showing (a) whole body length, (b) abdomen, (c) antenna, (d) foreleg, (e) hindleg, (f) head, (g) thorax, (h) forewing, and (i) hindwing. Red lines indicate linear measurements recorded in millimetres for quantitative morphological analysis. Scale bar = 1 mm depicting natural size.

A total of 12 adult specimens per species were selected for dissection and detailed morphometric analysis. This sample size was considered sufficient to capture intraspecific variation and to allow meaningful statistical comparisons among species, in accordance with previous studies on insect morphology and taxonomy (Lanyon and Sanson 2006). All observations and measurements were conducted using a stereo zoom microscope (OLYMPUS SZX16) equipped with a high-resolution digital imaging system (**Figure 4**). Photographs were captured at 1X magnification at different resolutions between 0.7 to 6.25, ensuring that all images represented the structures at their actual size. A calibrated scale bar was applied to each image to maintain measurement accuracy and enable reliable morphometric comparisons across species.

A total of 37 morphometric traits were measured for each species, analysed using Magvision v3.0 software to facilitate a robust assessment of morphological variation among insect pollinators (**Table 1**). All measurements were recorded in millimetres (mm) and aimed to capture interspecific variability across both *Apis* and non-*Apis* taxa, encompassing representatives from Hymenoptera, Lepidoptera, and Diptera. The measured parameters included general body dimensions such as body length, head length, and head width; thoracic features including thorax length and thorax width; and a detailed set of facial metrics such as clypeus length and width, inter-orbital distances (upper, lower, and across antennal sockets), clypeo-antennal distance, and compound eye dimensions. Additionally, antennal features, including scape length, pedicel length, third flagellomere diameter, total flagellum length, and number of flagellomeres, were measured. The ocellar region was examined for parameters such as inter-ocellar distance, ocellocular distance, antennocellar distance, median ocellus diameter, and clypeocular distance. Mouthpart traits, including labrum length and width, along with the maximum diameter of the antennal socket, were also recorded. To assess functional morphology, wing dimensions (forewing and hindwing length and width, Jugovanmal index, and Hemuli number) and leg characteristics such as hind tibia length, basitarsus length, and basitarsus width were also included. This comprehensive morphometric profiling approach is consistent with methodologies used in prior studies by Aytekin et al. (2007). They have applied similar trait-based analyses for taxonomic differentiation and assessments of pollinator diversity.

3.3.1. Morphometric measurement of Butterflies

Butterflies were measured manually using a metric scale because their larger body size did not allow the entire specimen to be clearly visualised under the microscope. Full-body measurements, including wingspan and body length, were therefore recorded manually with the specimen aligned from the zero mark of the scale (**Figure 5**). Similar manual approaches for measuring large lepidopteran specimens have been widely adopted in morphometric and taxonomic studies (Mutanen et al. 2016; Todisco et al. 2022). In contrast, smaller morphological structures such as the compound eyes, antennae, head, thorax, and abdomen were measured under a stereo zoom microscope at 1X magnification, which enabled accurate visualisation and precise measurement of fine diagnostic features (Sourakov & Zakharov 2019; Simonsen et al. 2021).

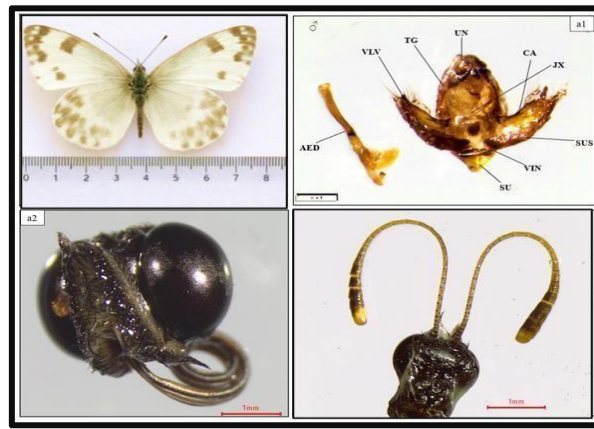


Figure 5: Morphometric measurements of the butterfly. (a) Adult specimen showing manual measurement of wingspan and body length using a metric scale in centimeters, with values subsequently converted to millimetres (1 cm = 10 mm). (a1) Male genitalia, (a2) compound eye, and (a3) antennae examined under a stereo zoom microscope at 1X magnification. Scale bars: 1 mm.

Table 1: List of morphometric characters recorded for insect pollinators

S. No.	Morphological characters
1.	Body length
2.	Head length
3.	Head width
4.	Thorax length
5.	Thorax width
6.	Clypeus length
7.	Clypeus width
8.	Lower inter-orbital distance
9.	Upper inter-orbital distance
10.	Inter-orbital distance
11.	Clypeo-antennal distance
12.	Compound eye length
13.	Scape length
14.	Pediceal length
15.	3 rd Flagellomere diameter
16.	Flagellum length
17.	Distance between antennal sockets
18.	Inter-ocellar distance
19.	Ocellocular distance

20.	Antennocellar distance
21.	Clypeocular distance
22.	Median ocellus diameter
23.	Labrum Length
24.	Labrum width
25.	Antennal socket maximum diameter
26.	Compound eye width
27.	Forewing length
28.	Jugovanmal index
29.	Hemuli number
30.	Hindwing length
31.	Hind basitarsus length
32.	Hind basitarsus width
33.	Number of flagellomeres
34.	Forewing width
35.	Hind tibia length
36.	Labrum Length
37.	Abdomen Length

3.3.2. Identification of Hymenopteran, Lepidopteran and Dipteran pollinators

Different species of Hymenopteran, Lepidopteran, and Dipteran pollinators were identified based on morphological characteristics using standard dichotomous taxonomic keys. These keys, specifically tailored for each insect order, facilitated accurate identification at the species level by sequentially evaluating distinguishing features such as wing venation, antennal segments, body colouration, and genitalia structures (Kaya et al. 2015). The identification process adhered to the diagnostic criteria provided in established entomological manuals and region-specific taxonomic references.

3.3.2.1. Hymenoptera

3.3.2.1.1. Taxonomic key for *Apis* species (Michener 2007; Kitnya et al. 2024)

- 1a. Body size larger (12-14 mm); abdomen with distinct yellow or orange bands; commonly domesticated species..... *Apis mellifera* (Western Honeybee)
- 1b. Body size smaller (less than 12 mm); abdomen with or without distinct bands..... 2
- 2a. Abdomen with distinct yellow bands; smaller in size (7-10 mm); less aggressive behavior
.....*Apis cerana* (Asian Honeybee)

3.3.2.1.2. Taxonomic key for *Andrena* species (Michener 2007; Wood et al. 2021)

- 1a. Hind tibia with long, dense, black hairs (scopa).....2
- 1b. Hind tibia with shorter, less dense, pale hairs (scopa).....3

- 2a. Body size larger (13-15 mm); scutum and scutellum distinctly punctate; facial foveae broad and distinct..... *Andrena agilissima*
- 2b. Body size smaller (8-11 mm); scutum and scutellum with fine punctation; facial foveae narrow *Andrena pilipes*
- 3a. Facial foveae narrow; abdomen with distinct, broad, pale bands... on. the terga..... *Andrena fucata*
- 3b. Facial foveae broad; abdomen without distinct bands..... *Andrena agilissima*

3.3.2.1.3. Taxonomic key for *Lasioglossum* species (Gibbs 2018)

- 1a. Face and front of the head with distinct rugose (wrinkled) texture... *Lasioglossum rugifrons*
- 1b Face and front of the head not distinctly rugose..... 2
- 2a. Body with broad, shiny metallic green or blue sheen..... *Lasioglossum marginatum*
- 2b. Body with less pronounced metallic sheen, generally duller..... *Lasioglossum matianense*

3.3.2.1.4. Taxonomic key for wasp and non-*Apis* bee species (Kitnya et al. 2024)

- 1a. Body covered in fuzzy hairs and generally robust, with a more rounded appearance..... 2
- 1b. Body smooth, not fuzzy, and with a more wasp-like appearance..... 4
- 2a. Body large and robust, with a very fuzzy appearance, and usually black with yellow or orange bands..... *Bombus albopleuralis*
- 3a. Body with relatively smaller yellow or orange patches and shorter legs..... 4
- 4a. Body with a smooth, shiny appearance and a distinctive yellow and black striped pattern..... *Vespula vulgaris*
- 4b. Body with a more uniform colour and less distinct striping or banding..... 5

3.3.2.2. Lepidoptera

3.3.2.2.1. Taxonomic key for regional butterflies (Evans 1932; Talbot 1947; Perveen 2016)

Family: Lycaenidae

- 1a. Body small and delicate; antennal base close to eye margin; eyes emarginated; ♂ forelegs reduced..... 2
- 2a. Dorsal surface bluish; underside finely spotted; tail absent..... *Polyommatus eros*
- 2b. Dorsal surface coppery-orange; dark marginal band present..... *Lycaena phlaeas*

Family: Pieridae

- 1a. Six walking legs present in both sexes; tarsal claws bifid..... 2
- 2a. Forewings leaf-shaped; resting posture leaf-like; greenish-yellow..... *Gonepteryx rhamni*
- 2b. Forewings not leaf-shaped. 3
- 3a. Sexual dimorphism distinct; males brighter..... 4
- 4a. Wings orange-yellow with broad dark borders..... *Colias electo*
- 4b. Wings yellow with narrow margins..... 5
- 5a. Bright yellow; margins narrow and distinct..... *Colias erate*
- 5b. Yellow-greenish; margins diffuse..... *Colias philodice*
- 3b. Sexual dimorphism weak; wings white or creamy..... 6
- 6a. Body large; black apical markings prominent..... *Pieris brassicae*
- 6b. Body smaller; markings reduced..... 7
- 7a. Wings creamy white; body slender..... *Pieris canidia*
- 7b. Wings white with dark venation and greenish mottling..... *Pontia daplidice*

Family: Nymphalidae

- 1a. Forelegs reduced (brush-footed condition); body medium-sized..... 2

- 2a. Wings orange-brown with black spots..... *Vanessa cardui*
- 2b. Colour pattern different..... 3
- 3a. Wings dark brown with bluish marginal lunules..... *Nymphalis canace*
- 3b. Wings without blue lunules..... 4
- 4a. Bright orange wings with black spots; margins scalloped..... *Argyreus hyperbius*
- 4b. Brown wings with yellow transverse bands..... *Aulocera saraswati*
- 4c. Reddish-brown wings with numerous black spots..... *Nymphalis polychloros*

3.3.2.3. Diptera

3.3.2.3.1. Taxonomic key for Syrphid species (Speight et al. 2021)

- 1a. Abdomen with broad yellow bands; thorax with narrow black-bordered yellow transverse band..... *Episyrphus balteatus*
- 1b. Abdomen with narrow yellow bands or distinct markings..... 2
- 2a. Abdomen with distinct dark ring around the middle; thorax with shiny dark markings..... *Sphaerophoria scripta*
- 2b. Abdomen without a dark ring; thorax with more uniform or less shiny markings 3
- 3a. Abdomen with broad yellow bands, often lighter than other species; legs with orange hind femor..... *Eristalis arbustorum*
- 3b. Abdomen with narrow or less prominent yellow bands, or other distinguishing features 4
- 4a. Body hairy with large dark spots on wings; face narrow with few setae..... *Eristalis abusive*
- 4b. Body less hairy, with different wing markings 5
- 5a. Thorax with long black stripe and yellow sides; abdomen with narrow yellow bands..... *Syrphus ribesii*
- 5b. Thorax with little or no stripe, or with other distinctive abdominal markings..... 6
- 6a. Eyes large, covering most of the head; abdomen with four dark bands..... *Eristalis tenax*
- 6b. Eyes not as large, or abdomen with a different pattern..... 7
- 7a. Abdomen with dark bands in a more uniform pattern, less wide than in other species..... *Sphaerophoria scripta*
- 7b. Abdomen with more irregular or wide patterns..... *Episyrphus balteatus*

3.4. Butterfly Genitalia Extraction and Mounting

Adult butterfly specimens selected for genitalia preparation were either freshly collected or taken from dried, curated collections, with only fully sclerotized and intact individuals used to ensure structural integrity (Robinson 1976; Winter 2000). Under a stereomicroscope, the abdomen was detached using fine forceps and a scalpel, ensuring minimal damage to the terminalia. The excised abdomen was placed in 10% aqueous KOH and macerated in 5-7% KOH at room temperature for smaller, delicate taxa, to dissolve internal tissues and clear obscuring fat bodies (Hardwick 1950; Lafontaine 2004). After maceration, the abdomen was rinsed thoroughly in distilled water and immersed in 3-5% acetic acid for 1-2 min to neutralize any residual alkali, followed by additional water rinses (Robinson 1976). Dissection of the cleared abdomen was performed in a watch glass containing water or 70% ethanol, carefully teasing apart the terminal segments to separate the tegumen unicus, valvae, vinculum saccus,

and aedeagus in males, or the papillae analis, apophyses, ductus bursae, corpus bursae, and signum in females; in males, the aedeagus was removed with gentle traction and the vesica everted by applying pressure at the base or by ethanol immersion and air injection through a fine capillary (Klots 1970; Winter 2000).

3.4.1. Dissection and Diagnostic Morphology of Male (♂) and Female (♀) Butterfly Genitalia

The depletion and isolation of the genitalia of butterflies resulted in highly clean, intact and morphologically differentiated structures in both males and females. This allowed clear identification on the species level and morphometric analysis (Robinson 1976; Klots 1970) (**Figure 6**). In the males (a-a2), it was done by excising the terminal segments of the abdomen (a) and then maceration in KOH, and a complete ablation of the internal soft tissues (a1). This operation has shown the entire sclerotised genital capsule, comprising tegumen (TG), uncus (UN), valvae (VAL), vinculum (VIN), saccus (SU), juxta (JX), and costal area (CA) in their natural proportions and points of articulation (Hardwick 1950; Winter 2000). The aedeagus (AED), the ductus ejaculatorius (DU.EJ) and thecal appendages (TH.APP) were removed from the capsule to display internal and external morphology by laying them down on their side (Lafontaine 2004). The terminal abdominal segments (b) of the females (b-b2) were first isolated. These parts were afterwards macerated and washed so that the papillae analis (PAP.A), posterior apophyses (PO.APO), ductus bursae (DU.BU), corpus bursae (CRP.BU) and ductus seminalis (DU.SEM) were revealed. The signum (SIG) was observable in the corpus bursae and had distinct sclerotization patterns that are significant taxonomic clues. The success of the optimised KOH maceration and ethanol dehydration stages was ensured by the maintenance of all the membranous structures without being twisted (Hardwick 1950). The use of selective staining significantly improved the appearance of sclerotised and membranous elements of the sex, and the fine structural details could be studied with ease using stereo-zoom microscopy; surface sculpturing, microtrichia, and junction points, among others, could be seen clearly. The specimens were completely devitalized and free of any residual tissues and scales, making them of high quality with publication-quality results.

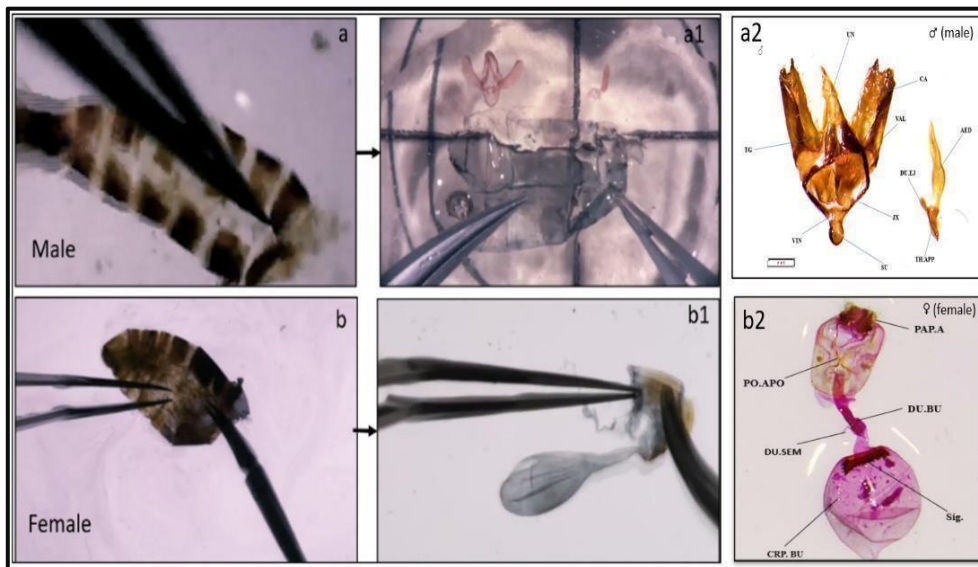


Figure 6: Genitalia extraction and diagnostic features of male and female butterflies. (a-a2) Male: (a) terminal abdominal segments, (a1) dissection and cleaning, (a2) cleared genital capsule showing TG -tegumen, UN-uncus, VAL-valva, CA-costal area, VIN-vinculum, SU-saccus, JX-juxta, AED-aedeagus, DU. EJ-ductus ejaculatorius, TH.APP-thecal appendage. (b-b2) Female: (b) terminal abdominal segments, (b1) dissection and cleaning, (b2) cleared genitalia showing PAP.A-papillae analis, PO.APO-posterior apophyses, DU.BU-ductus bursae, CRP.BU-corpus bursae, DU.SEM-ductus seminalis, SIG-signum.

Where required, the structures were stained with 0.5% Chlorazol Black E in 70% ethanol for 1-3 min to enhance contrast between membranous and sclerotized parts, followed by brief rinsing in ethanol to prevent over-darkening. For permanent mounting, the genitalia were dehydrated through an ethanol series (70%, 95%, absolute) and cleared in clove oil or xylene before arranging them on a clean microscope slide; the male tegumen uncus and valvae were oriented ventrally with the aedeagus parallel, while female structures were positioned to display the bursa and signum. A coverslip was gently lowered to avoid air bubbles, and slides were cured in a dust-free chamber at room temperature. Final preparations were imaged using a compound microscope with a digital camera, with multi-focus image stacking used to capture all structural details, and measurements were taken using calibrated imaging software. All procedures were conducted following standard Lepidoptera dissection protocols (Robinson 1976), with chemical handling performed in a fume hood using gloves and eye protection, and all waste disposed of according to institutional safety guidelines. In Lepidoptera, identifying species only by external appearance is often difficult because wing colour and patterns can change with age,

season, or environmental conditions. Therefore, more reliable characters, such as wing venation and genital structures, are commonly used for accurate identification. Wing venation remains stable and is not easily affected by environmental factors, making it useful for distinguishing species and genera. Similarly, genital structures, especially the male genital parts like the uncus, tegumen, and valvae, are highly specific to each species and remain consistent over time (Müller et al. 2025). Because of this, they are considered one of the most dependable features for identifying closely related or visually similar species.

3.4.2. Wing Descaling for Venation Patterns in Lepidoptera

Freshly collected and relaxed butterfly specimens were used for wing descaling. The forewings and hindwings were carefully detached using fine forceps and placed in a Petri dish. The wings were then immersed in a 5% sodium hypochlorite solution for approximately 30-60 minutes to dissolve the superficial scales without damaging the delicate membranous structure (Scoble 1995; Common 1990). After sufficient clearing, the loosened scales were gently removed under a stereozoom microscope using a fine camel hair brush (Figure 7). The descaled wings were subsequently rinsed several times in 90% ethanol to eliminate residual chemicals and debris. The cleaned wings were then mounted on clean glass slides in 90% ethanol or glycerin, covered with a coverslip, and allowed to settle evenly. The prepared slides were examined and photographed under a stereo microscope for detailed observation of venation patterns and morphometric analysis. This approach provides a clear visualization of venation, which is considered a stable and reliable taxonomic character in Lepidoptera (Kristensen 2003; Mutanen et al. 2010).

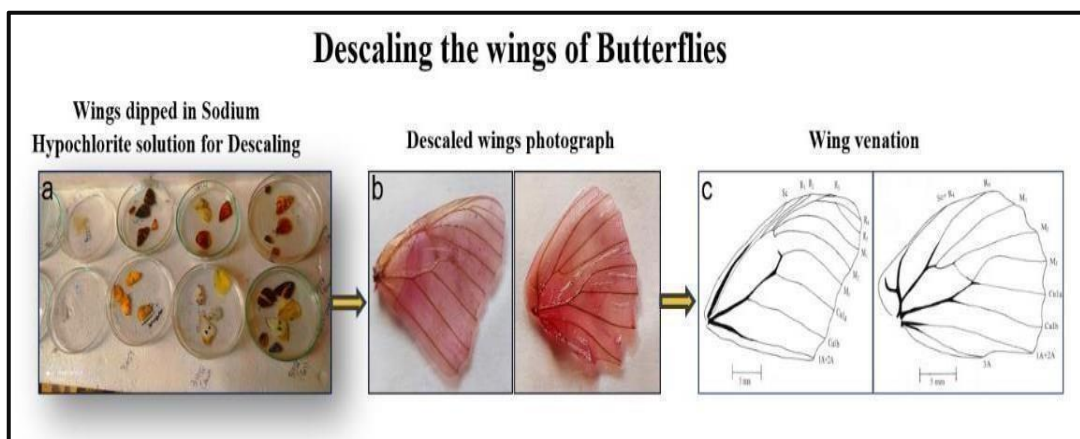


Figure 7: Descaling process of butterfly wings for venation analysis. (a) Wings immersed in sodium hypochlorite solution to loosen scales; (b) descaled forewings post-treatment showing

enhanced transparency; (c) detailed venation patterns traced after descaling for use in morphometric and taxonomic studies.

3.5. Statistical Analysis

Statistical analyses were conducted to evaluate the significance and pattern of differences across measured traits. Using Microsoft Excel (Microsoft Office 2021), a one-way Analysis of Variance (ANOVA) was performed to determine whether the observed differences in morphometric characters, such as body length, head dimensions, thorax size, and wing measurements, were statistically significant among species. In addition to ANOVA, multivariate statistical tools were used to assess species-level clustering based on morphological traits and explore the underlying structure of the data. Principal Component Analysis (PCA) was performed using the PCA package in the Python programming environment (Python v3.11) in order to reduce dimensionality and identify the most informative variables influencing variation. Hierarchical Cluster Analysis (HCA) was also used to visualize natural groupings among species and support interspecific differentiation. These multivariate methods assisted in identifying distinctive morphometric profiles and confirmed the taxonomic dependability of the selected characters (Rohlf 1990).

3.6. Authentication of Insect Pollinators through DNA barcoding

The insect pollinator species were initially identified by morphometric studies and then further characterized using COX-1 markers (Patzold et al. 2020). The collected samples were preserved in 100% ethanol until the DNA was isolated.

3.6.1. Isolation of total genomic DNA

The genomic DNA was extracted using the DNeasy tissue kit (Qiagen) method with slight modifications (Patzold et al. 2020). The following steps were carried out for the extraction of DNA:

1. Before starting, Buffer ATL and Buffer AL were checked for any precipitates, and if found, they were warmed to 56°C for 5 minutes to fully dissolve them. Buffer AW1 and Buffer AW2, which were provided as concentrates, had the appropriate amount of Ethanol (96-100%) was added to each bottle as specified to create working solutions.
2. Buffer AW1 was then mixed thoroughly by inverting the bottle several times. Additionally, an incubator was preheated to 56°C in preparation for use in step 2 (Qiagen, Cat. No: 69504). Up to 25 mg of insect tissue (Hind Leg) was cut into small pieces and placed in a 1.5 ml microcentrifuge tube. Next, 180 µl of Buffer ATL was added, followed by 20 µl of Proteinase K, and the mixture was thoroughly vortexed

before incubating at 56°C until the tissue was fully lysed, with occasional vortexing.

3. The mixture was then vortexed for 15 seconds, followed by adding 200 µl of Buffer AL, which was thoroughly mixed by vortexing. The resulting solution, including any precipitate, was pipetted into a DNeasy Mini spin column, placed in a 2 ml collection tube, centrifuged at 8000 rpm for 1 minute, and the flow-through and collection tube were discarded afterwards. The spin column was then placed in a new 2 ml collection tube, 500 µl of Buffer AW1 was added, and it was centrifuged for another minute at 8000 rpm, again discarding the flow-through and tube.

In the following step, the spin column was placed in a new 02 ml collection tube, 500 µl of Buffer AW2 was added, and it was centrifuged for 03 minutes at 14,000 rpm to dry the DNeasy membrane, discarding the flow-through and tube. Next, the spin column was placed in a clean 1.5 ml microcentrifuge tube, and 200 µl of Buffer AE was pipetted directly onto the membrane, incubated at room temperature for 01 minute, then again centrifuged for 01 minute at 8000 rpm to elute the DNA. For maximum yield, the elution was repeated using either a new tube to prevent dilution or the same tube to combine the eluates (Molin and Menard 2018).

3.6.2. Qualitative and quantitative analysis of genomic DNA

Genomic DNA was extracted from insect pollinator specimens using the DNase tissue kit method, which is optimized to yield high-quality, intact DNA suitable for a range of downstream molecular applications, including PCR amplification and sequencing (Kashyap and Jaiswal 2024). The extraction process was carried out following the manufacturer's protocol to minimise shearing, contamination, thereby ensuring reproducibility and consistency across samples. From each specimen, approximately 5-6 µl of the purified DNA was carefully loaded onto a 0.8% agarose gel prepared with ethidium bromide, a nucleic acid intercalating dye, to facilitate visualisation under UV illumination. Gel electrophoresis was performed under standard voltage and buffer conditions, allowing the DNA fragments to migrate according to size. The electrophoretic profiles, as depicted in **Figure 8**, displayed sharp, distinct, high-molecular-weight DNA bands with negligible smearing or background noise, confirming the absence of significant degradation or RNA contamination. The presence of clear, intact bands indicated that the extraction protocol was effective and the DNA obtained was of sufficient integrity and purity to serve as a reliable template for subsequent molecular analyses such as COX1 gene amplification and DNA barcoding.

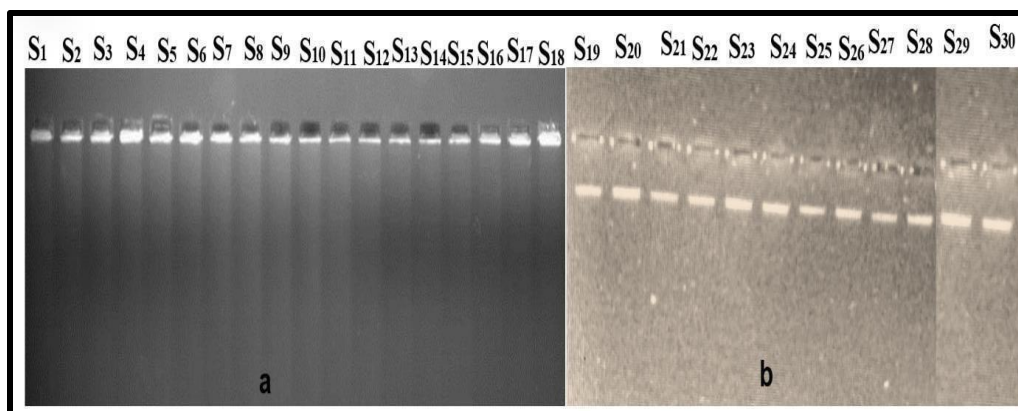


Figure 8: Electrophoretic gel profile of different (S1-S30) samples of extracted genomic DNA. The DNA samples were resolved on a 0.8% agarose gel stained with ethidium bromide and visualised under UV light to assess the quality and integrity of the extracted DNA (a, b): clear, high-molecular-weight bands without significant smearing indicate successful extraction of intact genomic DNA suitable for downstream molecular applications such as PCR amplification and sequencing.

3.6.3. PCR amplification of different species COX-1 markers

The insect pollinator species collected from cherry orchards in the Kashmir Valley, which were morphologically classified into Lepidoptera, Hymenoptera, and Diptera, were further characterised using DNA barcoding with the mitochondrial cytochrome c oxidase subunit I (COX1) gene (658 bp). PCR amplification of the COX1 region produced sharp amplicons of approximately 658 bp, which were visualized on a 1.6% agarose gel. The electrophoretic profiles revealed species-specific variations in band intensity, indicating differences in template DNA quality and quantity. PCR amplification of the COX-1 gene was carried out following a standard protocol. The reaction mixture was prepared in a total volume of 10 μ l, consisting of 5X Taq buffer, template DNA, MgCl₂, dNTPs, forward and reverse primers, Taq DNA polymerase, and nuclease-free water, with concentrations and volumes as detailed in **Table 2**. Amplification was performed in a thermal cycler using 35 cycles, following optimised cycling conditions specific for the COX-1 marker, as summarised in **Table 3**. This protocol ensured efficient and reproducible amplification of the target mitochondrial COX-1 fragment. The molecular data, combined with morphological identification, confirmed the taxonomic placement of these species and revealed a substantial degree of interspecific genetic divergence.

Table 2: Components of PCR reaction mixture for COX-1 markers

Component	Concentration	Volume (μ l)
Taq buffer	5X	2
DNA	25 μ g/ μ l	1
MgCl ₂	25 mM	2
dNTP mix	10 mM	0.6
Forward Primer	10 μ M	1.5
Reverse Primer	10 μ M	1.5
Taq Polymerase	5U/ μ l	0.1
Nuclease-free Water		1.3
Total		10

Table 3: PCR cyclic conditions using COX-1 marker

Step	Temperature ($^{\circ}$ C)	Time
Initial Denaturation	94	4 Min
Denaturation	94	30 Sec
Annealing	55	30 Sec
Extension	72	1 Min
Final extension	72	10 Min

} 35 Cycles

Primers (COX-1) used in the study were specific markers designed for DNA barcoding, targeting the mitochondrial cytochrome oxidase I (COI) gene. Amplification of this conserved region facilitated accurate species identification and differentiation, thereby enhancing taxonomic resolution and validating morphological characterization (Folmer et al. 1994).

Forward - ATTCAACCAATCATAAAGATATTGG

Reverse - TAAACTTCTGGATGTCCAAAAAATCA

3.6.4. Qualitative analysis of PCR products

The amplification of the desired PCR product was verified by agarose gel electrophoresis. A 1.6% agarose gel was prepared in 1X TAE buffer, which provides optimal resolution for fragments in the expected size range of the COX-1 amplicon. The PCR products were loaded into the wells along with a 100 bp DNA ladder, which served as a molecular weight marker to estimate the size of the amplified fragments (**Figure 9-11**). Electrophoresis was carried out under standard conditions, and the gel was subsequently visualised under a UV transilluminator

after staining, allowing confirmation of successful amplification based on the presence of a distinct band of the expected size.

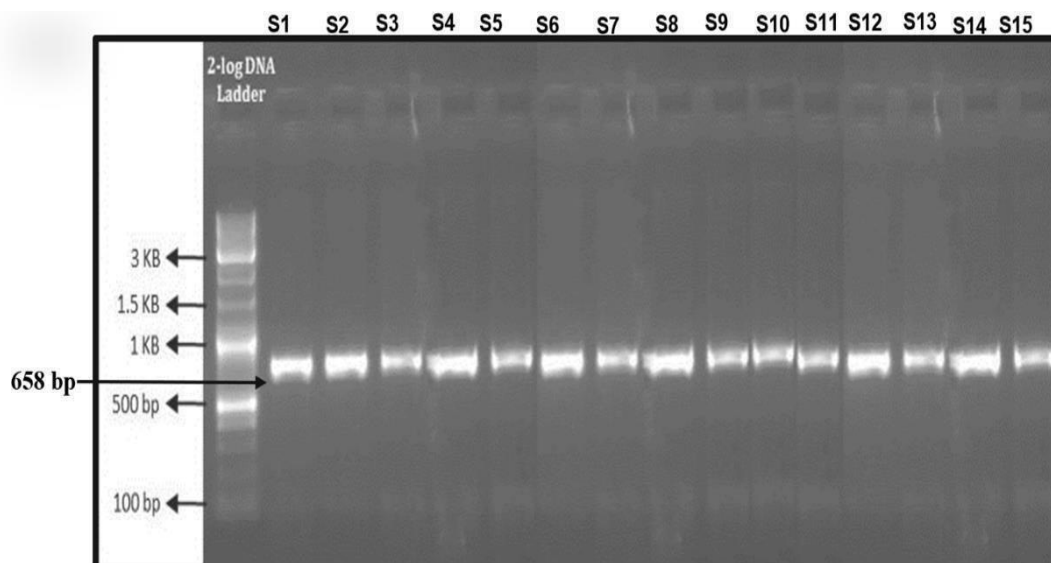


Figure 9: Electrophoretic profile of PCR-amplified COX1 gene fragments. Lane L represents the 3 kb DNA ladder used as a molecular size marker, while lanes S1 to S15 correspond to different insect pollinator samples, each showing successful amplification of the target mitochondrial COX1 gene region.

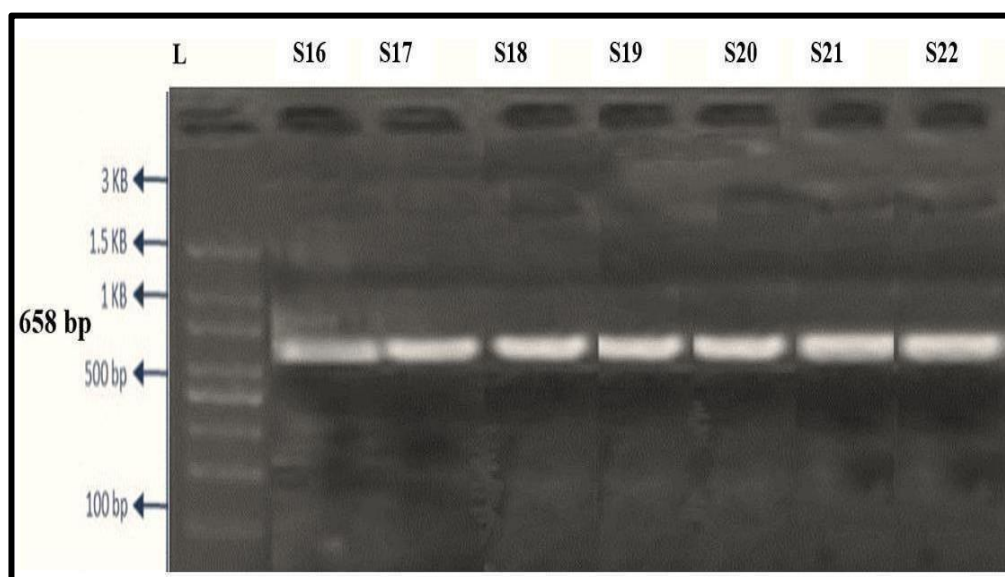


Figure 10: Electrophoretic profile of COX1 marker following PCR amplification. Lane L represents the 3 kb DNA ladder used as a molecular size reference, and lanes S16 to S22

correspond to different insect pollinator samples, each showing successful amplification of the mitochondrial COX1 gene fragment.

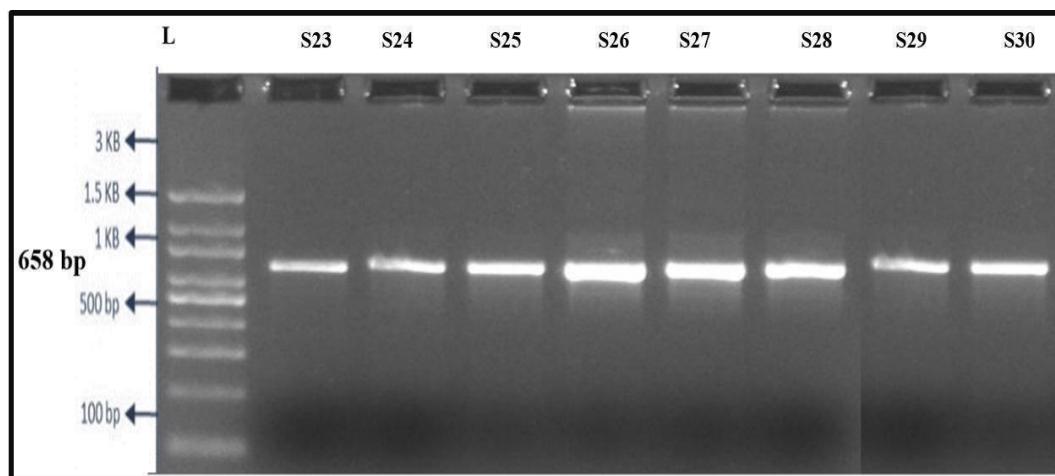


Figure 11: Electrophoretic profile of COX1 marker after PCR amplification. Lane L shows the 3 kb DNA ladder used as a molecular size standard, while lanes S23 to S30 represent different insect pollinator samples, each displaying successful amplification of the mitochondrial COX1 gene fragment.

3.6.4.1. Sequencing of the amplified products and phylogenetic analysis

About 50 μ l PCR product was used for DNA sequencing. The PCR products were sent for sequencing to Agri Genome Labs Pvt. Limited, Kerala (India). In addition to the amplification. Primers, other sequencing primers were used to ensure proper overlapping of fragment products. The sequences obtained were aligned using MEGA and BioEdit software programmes. The BLAST analysis of the sequences was done at NCBI (www.ncbi.nlm.nih.gov) for comparison to other nematode species, and they were later submitted to NCBI, and the accession numbers generated were used for further isolate references. These DNA sequences were later used to construct the phylogenetic trees. The consensus sequences were aligned using BioEdit software. The phylogenetic and evolutionary information was generated by processing the aligned sequences in the MEGA software (Tamura et al. 2013).

3.7. Diversity of Insect pollinators from the cherry orchards of the Kashmir valley

3.7.1. Diversity indices

3.7.1.1. Shannon-Weiner diversity index (H')

The Shannon-Weiner diversity index was calculated by the formula given by Margalef (1957):

$$H = -\sum p_i \ln p_i$$

In the above equation, $p_i = N_i/N$, where N_i = total number of individuals in a species, and N = total number of individuals in all species.

3.7.1.2. Simpson index

The Simpson's Index was calculated using the following formula:

$$D = \sum \left(\frac{n_i(n_i - 1)}{N(N - 1)} \right)$$

- n_i = the total number of individuals in a species
- N = the total number of individuals in all species

This index measures the probability that two individuals randomly selected from a sample will belong to the same species, giving insight into the dominance of certain species within the community. A lower value of **D** indicates higher diversity, while a higher value indicates lower diversity.

3.7.2. Evenness (E)

It is the measure of the relative abundance of each species in its habitat and shall be calculated by using the formula (Pielou 1975):

$$E = H/\ln S$$

In the above equation, **H** is the Shannon index, and **S** is the total number of species present.

3.8. To investigate the effectiveness of major insect pollinators on Fruit Set and Fruit Quality of Cherry.

To investigate the effect of insect pollination on fruit set and fruit quality in cherry (*Prunus avium*), flowers were subjected to different pollination regimes based on controlled levels of insect visitation (**Figure 12**). A pollinator exclusion regime served as the control, while graded visitation regimes involved one to multiple insect visits per flower under natural field conditions (Queirós et al. 2024).



Figure 12: Field Setup and Pollination Assessment in Cherry Orchards of Kashmir. (a) Cherry trees were enclosed in pollination-exclusion bags to regulate insect visitation, with managed bee hives placed nearby for controlled pollination. (b) A honeybee foraging on cherry blossoms during natural bloom. (c) Monitoring of pollination treatments and tagged branches in the orchard. (d-f) Experimental cherry trees under different pollination setups and assessment of fruit set using labeled sampling bags applied to developing fruits after treatment.

In the Randomised Block Design (RBD) experiment, five pollination regimes were included, each statistically validated with three replications. Three cherry trees were randomly selected, and three flowering twigs on each tree were assigned to different pollination regimes (**Table 4**). Varying numbers of pollinator visits, including native wild insect pollinators and *Apis* spp., were evaluated to determine their efficiency in fruit set and development (Montiel et al. 2010). Under carefully monitored conditions, colonies of *A. mellifera* and *A. cerana* were established near selected trees.

Table 4: Pollination regimes based on controlled insect visitation used to evaluate fruit set and fruit quality in cherry

Pollination regimes	Description
PE	Bagging/Pollinator exclusion
PR1	One visit by insect pollinators
PR2	Two visits by insect pollinators
PR3	Three visits by insect pollinators
PR4	Four visits by insect pollinators
PR5	Multiple visits by insect pollinators

Pollination Regimes = 05; Replications= 03

To regulate pollination, cherry buds were bagged before anthesis and assigned to the following pollination regimes: PE (Pollinator exclusion), PR1 (One visit), PR2 (Two visits), PR3 (Three visits), PR4 (Four visits), and PR5 (Multiple visits (5-6)). To prevent repeated visitation, flowers were re-bagged immediately after each designated visit. The bags were removed once the fruit set had occurred to allow normal exposure to sunlight. After tagging, the fruits were left to mature naturally on the tree before being harvested for quality assessment. This experimental design enabled a comprehensive evaluation of the contribution of different pollination regimes to cherry fruit yield and quality.

3.8.1. Fruit Set and Fruit Quality Measurement

To evaluate the impact of insect pollinators on fruit yield and quality in Kashmir Valley cherry orchards, several fruit characteristics were measured using standard protocols:

1. Fruit Set Percentage (%)

Fruit set was calculated as an indicator of successful pollination and fertilisation. The percentage of fruit set was determined using the following formula:

$$\text{Fruit Set (\%)} = (\text{Number of fruits developed} / \text{Total number of flowers}) \times 100$$

A similar approach has been used in studies by Dag and Gazit (2000) and Free (1993) to evaluate pollination success in orchard crops.

2. Acidity Analysis

a. pH Measurement

To determine pH, freshly harvested cherries were crushed to extract juice. A calibrated digital pH meter was used to record the acidity (**Figure 12**). The pH of cherry juice typically ranges between 3.1- 4.5, depending on the cultivar and ripeness stage (Vasco et al. 2009). Lower pH values indicate higher acidity, which tends to decrease during ripening due to sugar accumulation.

b. Titratable Acidity (TA)

Titrateable acidity was estimated following the standard titration method. A known volume of cherry juice was titrated against 0.1 N NaOH using phenolphthalein as an indicator (**Figure 13**). Acidity was expressed as a percentage of malic acid, the dominant organic acid in cherries. The calculation used was:

$$\text{TA (\% malic acid)} = V \times N \times \text{Eq. wt} \times 100$$

- V = Volume of NaOH used (mL)

- N = Normality of NaOH (0.1 N)
- Eq. wt = Equivalent weight of malic acid (67.05 g/mol)
- W = Volume or weight of juice sample (mL or g)

This method aligns with procedures described by Bakshi et al. (2018) and Wrolstad et al. (2005) in evaluating cherry acidity during fruit development.

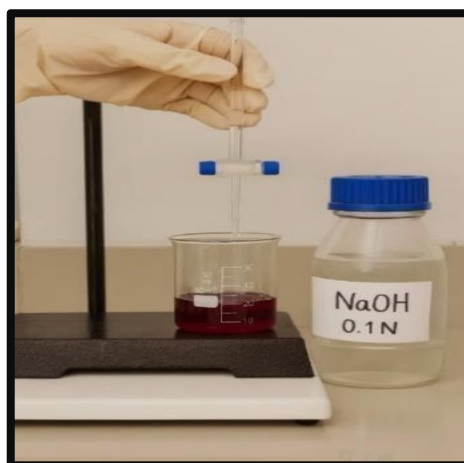


Figure 13: Estimation of titratable acidity in cherry juice using titration with 0.1 N NaOH and phenolphthalein indicator.

3. Total Soluble Solids (°Brix)

TSS was measured using a digital refractometer (°Brix). A drop of extracted juice was placed on the digital refractometer, and readings were recorded (**Figure 14**). TSS values for cherries generally range from 14-20 °Brix, increasing with maturity. This approach follows the standard protocol as used in previous studies by Kassim et al. (2010); Usenik et al. (2008).



Figure 14: Measurement of total soluble solids (TSS) in cherry juice using a digital refractometer.

4. Fruit Size

A Vernier calliper was used to measure each fruit's equatorial diameter to evaluate size variation amongst treatments. Depending on the type and the environment, cherries usually have a diameter of 15 to 30 mm. This method was applied in the morphometric analysis of cherries by Vishwakarma and Singh (2017).

5. Fruit Weight

The fruit's weight was determined using an accurate digital electronic weighing balance. Average weights usually range from 05 to 10 g. This procedure is consistent with methods employed by Vishwakarma and Singh (2017) and Mika et al. (2007) to evaluate fruit development parameters.

Chapter 4

Results

In the Kashmir Valley, a total of 4,057 insect specimens were collected through extensive field surveys conducted in cherry orchards. Four main districts were sampled using conventional methods, such as sweep netting and hand collection. Through an integrated taxonomic approach that included molecular DNA barcoding, genitalia extraction, morphometric and morphological identification, a total of 30 insect pollinator species were documented. These 30 pollinator species were found in eight families and three major insect orders: the Lepidoptera, Hymenoptera, and Diptera (**Table 5**). The community composition was notably dominated by the order Lepidoptera (14 species). These included members of the families Nymphalidae (*Argynnis hyperbius*, *Nymphalis canace*, *N. polychloros*, *Vanessa cardui*, *Aulocera saraswati*), Lycaenidae (*Lycaena phlaeas*, *Polyommatus eros*), and Pieridae (*Pontia daplidice*, *Gonepteryx rhamni*, *Colias erate*, *C. philodice*, *C. electo*, *Pieris canidia*, *P. brassicae*). These species exhibited a wide range of wing patterns and colouration, playing important roles in crop pollination. The Hymenoptera order was represented by 10 species across four families: Apidae (*Apis mellifera*, *A. cerana*, *Bombus albopleuralis*), Halictidae (*Lasioglossum rugifrons*, *L. marginatum*, *L. matianense*), Andrenidae (*Andrena agilissima*, *A. pilipes*, *A. fucata*), and Vespidae (*Vespula vulgaris*). These hymenopteran species, particularly bees and bumblebees, are known for their high pollination efficiency owing to their hairy bodies and pollen-carrying structures. 06 dipteran species were recorded, all from the family Syrphidae (*Eristalis arbustorum*, *Syrphus ribesii*, *E. abusiva*, *E. tenax*, *Episyrphus balteatus*, and *Sphaerophoria scripta*). These hoverflies mimic bees and play a vital role in pollination, particularly in cooler climates where bees are less active. Notably, *L. matianense*, *L. rugifrons*, and *Nymphalis canace* were reported for the first time from the Kashmir Valley. These molecularly validated records not only enrich the regional faunal inventories but also underscore the significance of integrating DNA barcoding with traditional taxonomy to uncover hidden diversity. Such findings highlight the critical need for sustained biodiversity assessments in underexplored Himalayan ecosystems, where unique environmental conditions may harbor unrecorded or cryptic species.

Table 5: Insect Pollinators from Cherry orchards of the Kashmir Valley India

Order	Family	Scientific Name	Common Name
Lepidoptera	Pieridae	<i>Pieris canidia</i>	Indian cabbage white
		<i>Pieris brassicae</i>	Large cabbage white
		<i>Pontia daplidice</i>	Bath white
		<i>Gonepteryx rhamni</i>	Common brimstone
		<i>Colias electo</i>	Clouded emigrant
			African clouded yellow
		<i>Colias erate</i>	Eastern pale Clouded yellows
	<i>Colias philodice</i>	Common Sulphur/ Clouded Sulphur	
	Lycaenidae	<i>Lycaena phlaeas</i>	American copper
		<i>Polymmatos eros</i>	European common blue
	Nymphalidae	<i>Argyreus hyperbius</i>	Brush-footed butterfly
		<i>Nymphalis polychloros</i>	Indian tortoise shell
		<i>Vanessa cardui</i>	Painted lady
		<i>Nymphalis canace</i>	Blue admiral
		<i>Aulocera saraswati</i>	Banded satyrs
Hymenoptera	Apidae	<i>Apis mellifera</i>	Western Honeybee
		<i>Apis cerana</i>	Asian Honeybee
		<i>Bombus albopleuralis</i>	White-ribbed Bumblebee
	Andrenidae	<i>Andrena agillissima</i>	Agile Miner Bee
		<i>Andrena fucata</i>	Fucate Miner Bee
		<i>Andrena pilipes</i>	Hairy-legged Miner Bee
	Halictidae	<i>Lassioglossum marginatum</i>	Margined Sweat Bee
		<i>Lassioglossum matianense</i>	Matian Sweat Bee
		<i>Lassioglossum rugifrons</i>	Rugose-faced Sweat Bee
Vespidae	<i>Vespula vulgaris</i>	Common Wasp	

Diptera	Syrphidae	<i>Episyrphus balteatus</i>	Marmalade Hoverfly
		<i>Sphaerophoria scripta</i>	Long Hoverfly
		<i>Eristalis abusive</i>	Dusky Drone Fly
		<i>Eristalis arbustorum</i>	Short-belted Drone Fly
		<i>Syrphus ribesii</i>	Common Hoverfly
		<i>Eristalis tenax</i>	Common Drone Fly

3.9. Mounting and Preservation of Insect Pollinators

Insect specimens collected from cherry orchards across the Kashmir Valley were processed through stretching, pinning, and labelling for long-term preservation and taxonomic study (**Figure 15**). Each specimen was mounted with proper positioning to retain morphological characters essential for identification, particularly wing venation in butterflies and external features in syrphid flies and bees. Labelling of each specimen included essential collection information such as location, elevation, date, time of collection, and collector's name to ensure traceability, proper documentation, and further reference for taxonomic verification (**Figure 16**). For molecular characterization, representative samples were preserved separately in 95% ethanol in labelled microcentrifuge tubes. This dual approach of morphological mounting and molecular preservation ensured that specimens could be used both for traditional taxonomy and for advanced DNA-based studies.

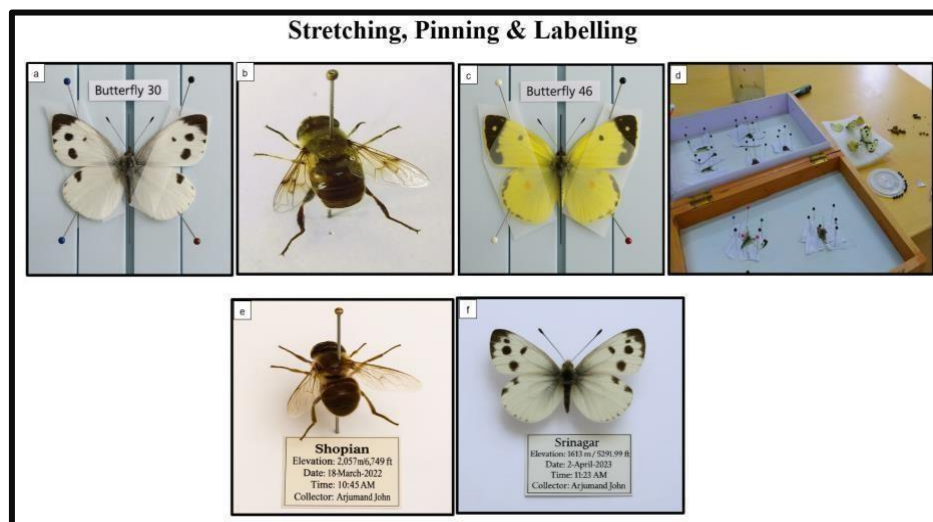


Figure 15: Standardized procedure for mounting and labelling of winged insect pollinators from cherry orchards in the Kashmir Valley. The figure a-d illustrates proper stretching and pinning

of specimens to display wing venation and colour patterns, followed by the use of archival-quality labels containing essential collection information for long-term preservation and taxonomic reference.



Figure 16: Preservation of insect pollinators for morphological and molecular studies. (a) Representative insect pollinator specimens mounted and pinned on entomological boards after drying, used for detailed morphological identification and morphometric analysis. (b) Systematic arrangement and storage of pinned insect collections in insect boxes for long-term reference and taxonomic studies. (c) Insect specimens preserved individually in 95% ethanol, suitable for genomic DNA extraction and DNA barcoding, ensuring minimal DNA degradation while maintaining specimen integrity.

3.10. Morphometric and Morphological study of Hymenopteran pollinators

The order Hymenoptera is one of the largest and most diverse insect orders. Characteristically, hymenopterans possess two pairs of membranous wings (with the hindwings smaller than the forewings), well-developed compound eyes, and chewing or chewing-lapping mouth parts adapted for various feeding behaviours (Papa et al. 2022). A defining feature of many hymenopterans is their narrow waist, or petiole, that separates the thorax and abdomen, especially in bees and wasps. Social behaviour is highly developed in several families, notably Apidae (honey bees and bumblebees), exhibiting complex colony structures and division of labor (Yokoi et al. 2025). In particular, bees (superfamily Apoidea) are among the most important pollinators of both wild and cultivated plants, directly supporting biodiversity and food production. Hymenopterans also include numerous parasitoid species that play a crucial role in regulating pest populations, making them important agents in biological control. Hymenoptera are a major focus of research on biodiversity, pollination biology, and ecosystem functioning because of their ecological adaptability and complex relationships with plants and other insects (Techer et al. 2025).

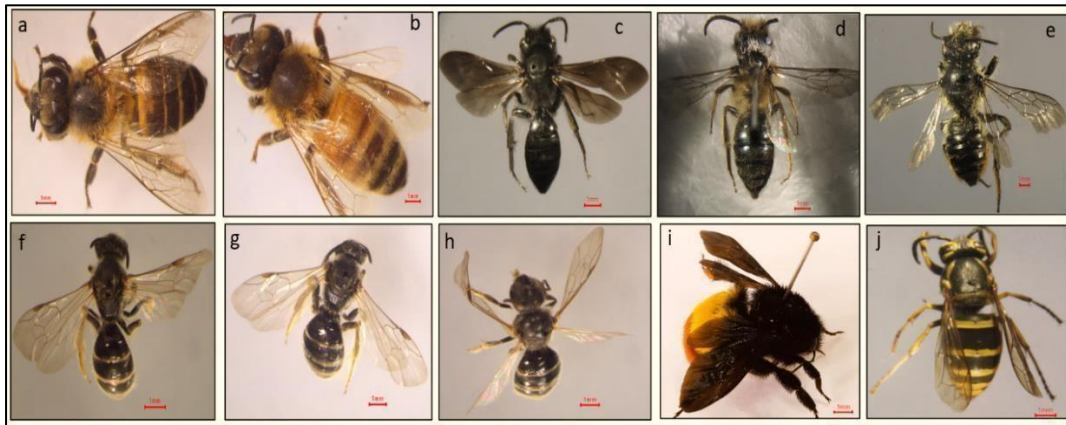


Figure 17: Representative insect pollinators from the order Hymenoptera recorded from cherry orchards (a-j): *Apis cerana*, *A. mellifera*, *Andrena agilissima*, *A. fucata*, *A. pilipes*, *Lasioglossum marginatum*, *L. matianense*, *L. rugifrons*, *Bombus albopeleralis*, and *Vespula vulgaris*.

In this study, morphological analysis of cherry orchards throughout the Kashmir Valley revealed a wide variety of hymenopteran insect pollinators. Important members of the families Apidae, Andrenidae, Halictidae, and Vespidae are among the specimens. Among these, the domesticated honeybee species *Apis cerana* and *A. mellifera* (a-b) are noteworthy because of their high pollination efficiency and were commonly encountered during the height of cherry bloom. There were also reports of other wild bee species, including *Andrena agilissima* and *A. fucata* (d-e), which are solitary ground-nesting bees that are active in the early spring and are essential for pollinating orchards. Three species of small-bodied bees, *Lasioglossum marginatum*, *L. matianense*, and *L. rugifrons* (f-h), which are abundant and frequent visitors to flowers in temperate regions, were used to represent the genus. *Bombus albopeleralis* (i), a large, hairy bumblebee, was observed visiting cherry blossoms frequently and is considered a highly efficient pollinator due to its buzz pollination behavior. *Vespula vulgaris* (j), a social wasp species, was also recorded; while not a primary pollinator, it contributed marginally through incidental visits (**Figure 17**). All specimens were examined under a Stereozoom microscope, measured morphometrically, and preserved for further molecular analysis. This visual representation underscores the richness of hymenopteran pollinator fauna in cherry orchards and supports the integrative approach of combining morphological and molecular tools for accurate identification.

3.10.1. Morphological description of the recorded pollinator species

The Hymenopteran pollinators documented from different cherry orchards of the Kashmir

valley were identified up to the species level based on key morphological characters, including wing venation, body measurements, antennal structure, and abdomen band patterns.

1. *Apis cerana*

A. cerana Fabricius, 1793

A. indica Fabricius, 1798

A. japonica Radoszkowski, 1877

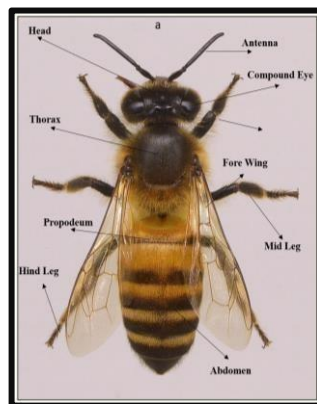


Figure 18a: Dorsal view of *Apis cerana* adult worker bee showing major external morphological features: compound eye, antenna, fore leg, mid leg, hind leg, thorax, propodeum, fore wing, and abdomen.



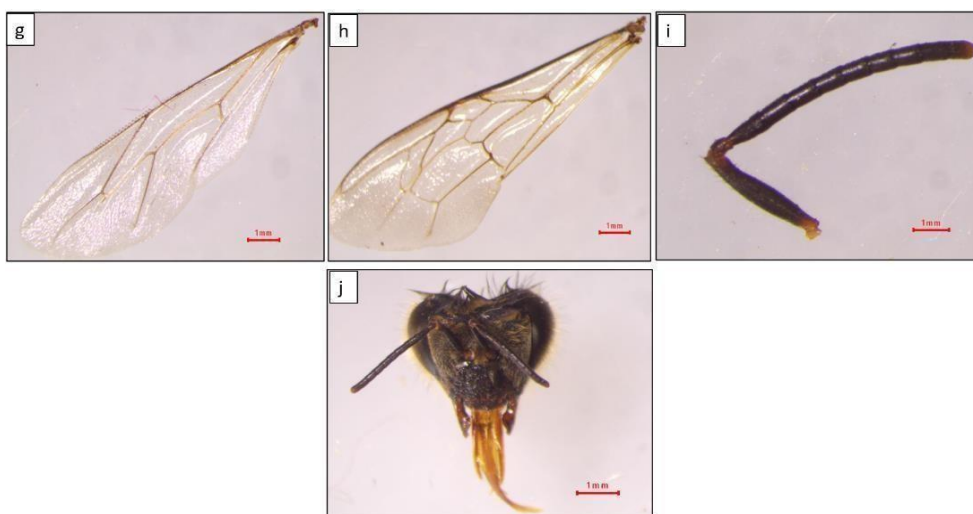


Figure 18b: Measurement of various morphological characteristics of *Apis cerana*. (a) Full body, (b) Abdomen, (c) Foreleg, (d) Midleg, (e) Hindleg, (f) Thorax, (g) Hindwing, (h) Forewing, (i) Antenna, and (j) Head.

3.10.2. Distribution: Native to South and Southeast Asia, including India, China, and Japan.

3.10.2.1. Diagnostic Characters: This species closely resembles *A. cerana* but is smaller, with workers typically measuring 10-13 mm in length. It has a more gracile body, with a darker colouration and more pronounced black bands on the abdomen. The thorax is covered in shorter, finer hairs compared to *A. cerana* (**Figure 18a**). The wings are more translucent and slightly shorter. A key differentiating feature is the presence of a narrower and more pointed abdomen. The hind legs also possess corbiculae, but they appear smaller than those in *A. cerana*. Queens are larger, with a more elongated body, while drones have larger eyes for locating queens during mating flights.

3.10.2.2. Measurements (Mean±SE in mm): *A. cerana* has a body length of 11.15 ± 0.05 mm, a head length of 2.67 ± 0.03 mm, and a head width of 3.31 ± 0.01 mm. The thorax length is 3.35 ± 0.02 mm, while the thorax width is 2.92 ± 0.03 mm. The clypeus length measures 0.88 ± 0.01 mm. Clypeus width of 1.03 ± 0.03 mm, a lower inter-orbital distance of 1.83 ± 0.03 mm, and an upper inter-orbital distance of 1.46 ± 0.03 mm. The inter-orbital distance through antennal sockets is 2.01 ± 0.03 mm, while the clypeo-antennal distance is 0.03 ± 0.01 mm. The compound eye length is 2.04 ± 0.03 mm. Scape length of 1.05 ± 0.02 mm, a pedicel length of 0.21 ± 0.01 mm, and a flagellum length of 2.66 ± 0.08 mm. The 3rd flagellomere diameter is 0.18 ± 0.01 mm, the distance between antennal sockets is 0.22 ± 0.02 mm, and the inter-ocellar distance is 0.31 ± 0.02 mm. Ocellocular distance of 0.31 ± 0.20 mm, an antennocellar distance of 1.79 ± 0.25 mm, and a clypeocular distance of 0.27 ± 0.25 mm (**Table 6-12**). The median ocellus diameter is 0.20 ± 0.30 mm, the labrum length is 0.19 ± 0.30 mm, and the labrum width is 0.84 ± 0.30 mm. Antennal socket maximum diameter of 0.25 ± 0.05 mm and a compound eye width of 0.49 ± 0.07 mm (**Figure 18b**). The forewing length is 7.92 ± 0.40 mm, and the forewing width is 2.64 ± 0.15 mm. The Jugovanmal index is 59.38 ± 1.80 mm, and the species

possesses 17.9 ± 1.30 Hemuli. Hindwing length 5.50 ± 0.40 mm and a hindwing width 3.31 ± 0.15 mm. The hind basitarsus length is recorded at 1.76 ± 0.10 mm, while the hind basitarsus width is 0.89 ± 0.10 mm. This species possesses 10 flagellomeres and has an abdomen length of 5.25 ± 0.30 mm. Abdomen width of 3.64 ± 0.02 mm and a hind tibia length of 2.84 ± 0.01 mm.

2. *Apis mellifera*

A. mellifera Linnaeus, 1758

A. mellifera ligustica Spinola, 1806

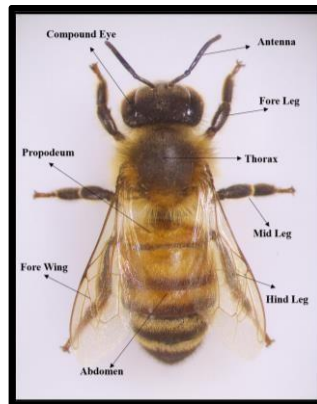
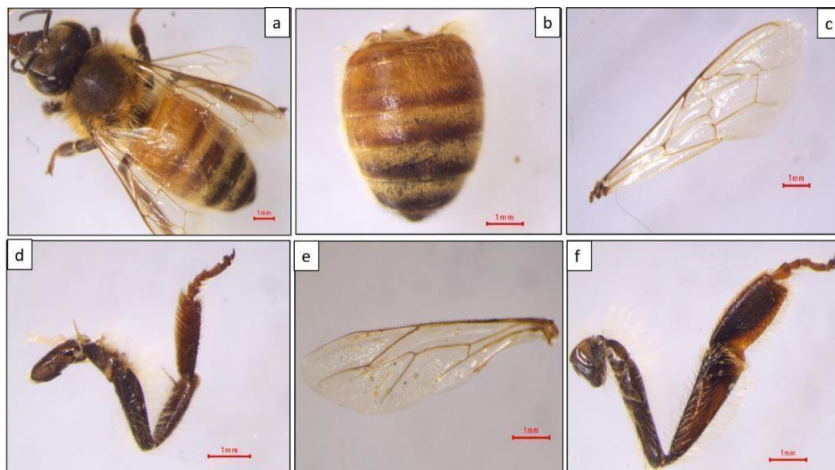


Figure 19a: Dorsal view of *Apis mellifera* adult worker bee showing major external morphological features: compound eye, antenna, fore leg, mid leg, hind leg, thorax, propodeum, fore wing, and abdomen.



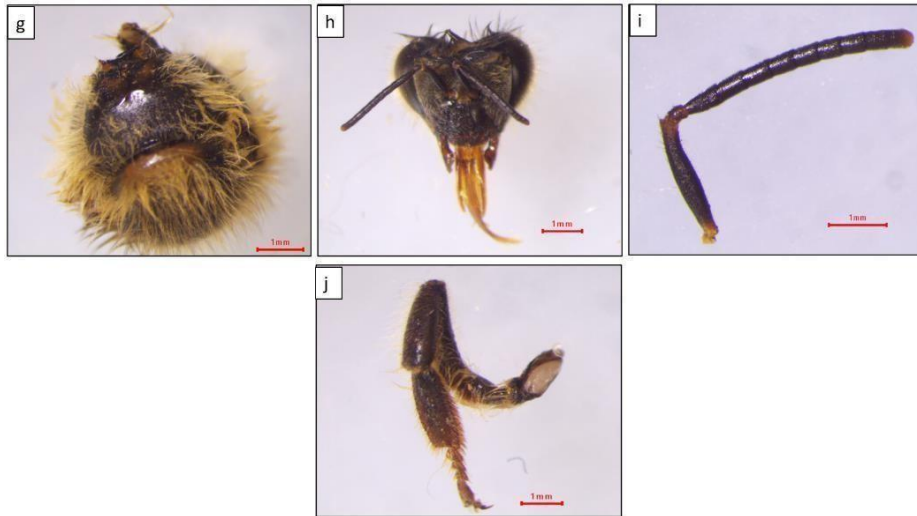


Figure 19b: Measurement of various morphological characteristics of *Apis mellifera*. (a) Full body, (b) Abdomen, (c) Forewing, (d) Midleg, (e) Hindwing, (f) Hindleg, (g) Thorax, (h) Head, (i) Antenna, and (j) Foreleg.

3.10.3 Distribution: Native to Europe, Africa, and the Middle East; introduced worldwide.

3.10.3.1. Diagnostic Characters: *A. mellifera* is a medium-sized honey bee, measuring 12- 15 mm in length. It has a golden-brown body with alternating dark and light brown bands on the abdomen. The thorax is densely covered in short, golden hairs (**Figure 19a**). The wings are translucent with well-defined venation, and they exhibit a slight brownish tint. The head is relatively small, with large, compound eyes and short, curved antennae. The hind legs have well-developed corbiculae for pollen collection. A distinguishing feature is the presence of a hairy depression (pollen press) on the hind tibia. Queens are larger and have a more elongated abdomen compared to workers and drones.

3.10.3.2. Measurements (Mean±SE in mm): *A. mellifera* has a body length of 11.61 ± 0.04 mm, a head length of 2.92 ± 0.03 mm, and a head width of 3.72 ± 0.03 mm. The thorax length is 4.55 ± 0.02 mm, while the thorax width is 3.18 ± 0.02 mm. The clypeus length is 1.09 ± 0.02 mm. Clypeus width of 1.34 ± 0.03 mm, a lower inter-orbital distance of 2.18 ± 0.03 mm, and an upper inter-orbital distance of 1.95 ± 0.03 mm. The inter-orbital distance through antennal sockets is 2.44 ± 0.03 mm, while the clypeo-antennal distance is 0.03 ± 0.01 mm. The compound eye length measures 2.34 ± 0.03 mm. Scape length of 1.26 ± 0.03 mm, a pedicel length of 0.24 ± 0.01 mm, and a flagellum length of 2.70 ± 0.08 mm (**Table 6-12**). The 3rd flagellomere diameter is 0.20 ± 0.01 mm, the distance between antennal sockets is 0.24 ± 0.02 mm, and the inter-ocellar distance is 0.40 ± 0.02 mm. Ocellocular distance of 0.47 ± 0.25 mm, an antennocellar distance of 1.58 ± 0.25 mm, and a clypeocular distance of 0.23 ± 0.30 mm. The median ocellus diameter is 0.25 ± 0.30 mm, the labrum length is 0.24 ± 0.30 mm, and the labrum width is 0.93 ± 0.30 mm. Antennal socket maximum diameter of 0.10 ± 0.02 mm and a compound eye width

of 0.78 ± 0.10 mm (**Figure 19b**). The forewing length measures 8.91 ± 0.45 mm, while the forewing width is 3.08 ± 0.20 mm. The Jugovanmal index is 62.04 ± 1.50 mm, and this species possesses 20.20 ± 1.50 Hemuli. Hindwing length of 6.44 ± 0.40 mm and a hindwing width of 1.64 ± 0.10 mm. The hind basitarsus length is 2.06 ± 0.10 mm, with a hind basitarsus width of 0.10 ± 0.05 mm. This species has 10 flagellomeres and an abdomen length of 5.56 ± 0.30 mm. Abdomen width of 4.26 ± 0.02 mm and a hind tibia length of 3.15 ± 0.01 mm.

3. *Andrena agillissima*

A. agillissima italica -Warncke, 1967.

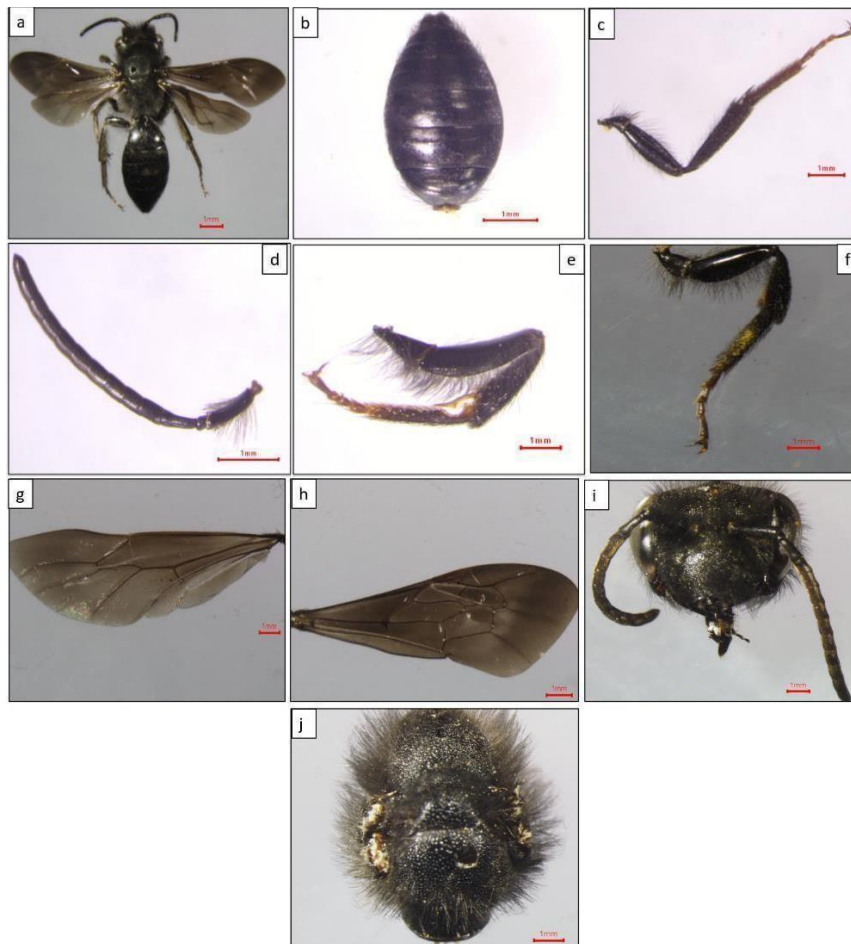


Figure 20: Measurement of various morphological characters of *Andrena agillissima*. (a) Full body, (b) Abdomen, (c) Midleg, (d) Antenna, (e) Foreleg, (f) Hindleg, (g) Hindwing, (h) Forewing, (i) Head, and (j) Thorax.

3.10.4. Distribution: Native to Southern and Central Europe, extending into the Middle East.

3.10.4.1. Diagnostic Characters: This species is relatively large, with females reaching about

12-15 mm in body length. The thorax is covered in dense, shiny black hairs, while the abdomen has a striking metallic blue or bluish-green sheen, which helps distinguish it from other *Andrena* species (**Figure 20**). The legs are predominantly black with dark brown hairs. The face is broad, with a strongly developed clypeus that is slightly punctured. The wings are slightly smoky, with strong venation. The propodeum has a rough, sculptured surface. Males have a slender body, with a less metallic sheen and longer antennae.

3.10.4.2. Measurements (Mean±SE in mm): *A. agillissima* exhibits a body length of 13.29±0.06 mm, with a head length of 2.95±0.02 mm and a head width of 3.21±0.03 mm. The thorax length is 3.53±0.03 mm, and the thorax width is 3.29±0.02 mm. The clypeus length is 1.38±0.02 mm. Clypeus width of 2.37±0.05 mm, a lower inter-orbital distance of 2.62±0.05 mm, and an upper inter-orbital distance of 2.72±0.05 mm. The inter-orbital distance through antennal sockets is 2.86±0.05 mm, while the clypeo-antennal distance is 0.05±0.01 mm. The compound eye length measures 2.32±0.05 mm. Scape length of 1.06±0.02 mm, a pedicel length of 0.19±0.01 mm, and a flagellum length of 3.73±0.09 mm (**Table 6-12**). The 3rd flagellomere diameter is 0.22±0.01 mm, the distance between antennal sockets is 0.49±0.03 mm, and the inter-ocellar distance is 0.38±0.02 mm. Ocellocular distance of 0.87±0.28 mm, an antennocellar distance of 0.77±0.32 mm, and a clypeocular distance of 0.12±0.30 mm. The median ocellus diameter is 0.25±0.30 mm, the labrum length is 0.14±0.30 mm, and the labrum width is 0.30±0.30 mm. Antennal socket maximum diameter of 0.36±0.06 mm and a compound eye width of 0.75±0.09 mm. Its forewing length is 12.74±0.70 mm, and the forewing width is 3.72±0.28 mm. The Jugovanmal index is 65.60±2.10 mm, and the species has 17.00±1.50 Hemuli. Hindwing length of 9.36±0.55 mm and a hindwing width of 2.70±0.12 mm. The hind basitarsus length is recorded at 2.26±0.15 mm, with a hind basitarsus width of 0.38±0.05 mm. This species possesses 10 flagellomeres and has an abdomen length of 6.81±0.30 mm. Abdomen width of 4.29±0.03 mm and a hind tibia length of 3.72±0.02 mm.

4. *Andrena fucata*

A. fucata Smith, 1847

A. clypearis Nylander, 1852

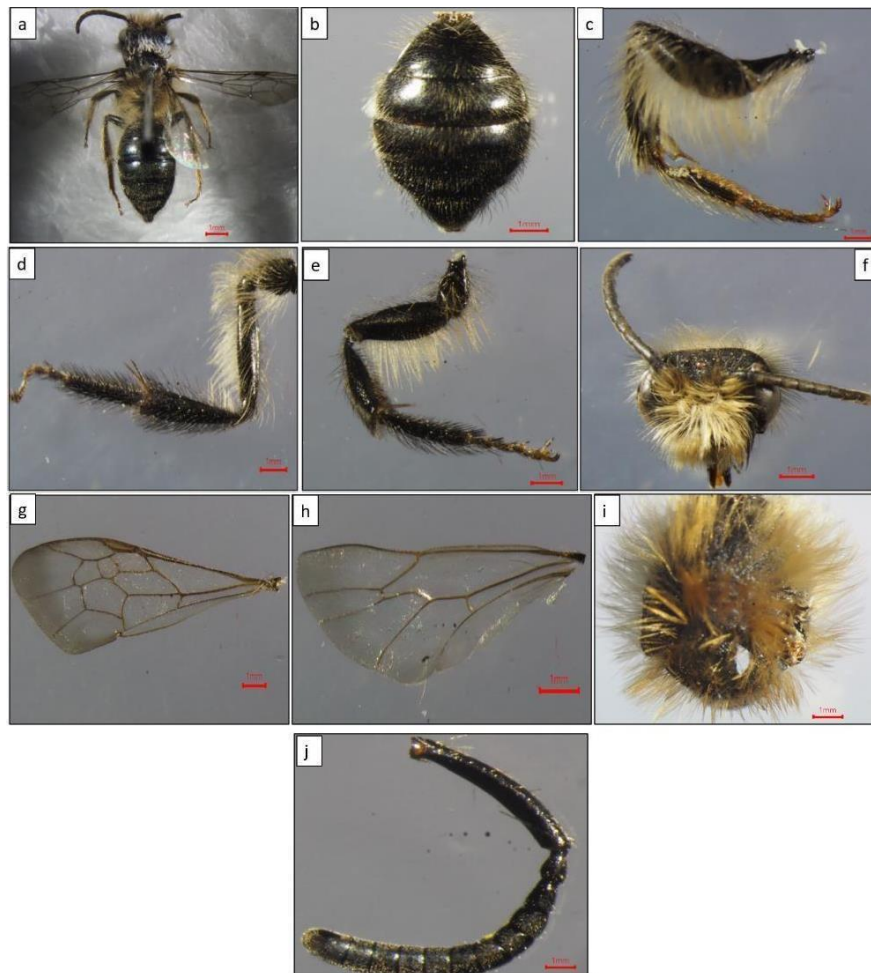


Figure 21: Measurement of various morphological characters of *Andrena fucata*. (a) Full body, (b) Abdomen, (c) Foreleg, (d) Midleg, (e) Hindleg, (f) Head, (g) Forewing, (h) Hindwing, (i) Thorax, and (j) Antenna.

3.10.5. Distribution: Found in Europe and parts of Asia, including temperate regions.

3.10.5.1. Diagnostic Characters: *A. fucata* is a medium-sized mining bee belonging to the family Andrenidae. It exhibits sexual dimorphism, with females typically larger than males. The body length ranges from 10-13 mm (**Figure 21**). It has a predominantly black thorax and abdomen covered with fine, short hairs. A key distinguishing feature is the reddish-brown coloration of the hind tibiae and tarsi in females. The face has dense yellowish-white pubescence, particularly around the clypeus. The wings are translucent with a slightly smoky tint and well-defined venation. The scopa (pollen-collecting hairs) on the hind legs is well-developed and yellowish. Males are slenderer and have longer antennae compared to females.

3.10.5.2. Measurements (Mean±SE in mm): *A. fucata* has a body length of 12.59 ± 0.08 mm, a head length of 2.47 ± 0.03 mm, and a head width of 3.35 ± 0.02 mm. The thorax length is 3.41 ± 0.02 mm, while the thorax width is 2.58 ± 0.03 mm. The clypeus length measures 1.21 ± 0.02 mm. Clypeus width of 2.20 ± 0.04 mm, a lower inter-orbital distance of 2.40 ± 0.04

mm, and an upper inter-orbital distance of 2.13 ± 0.04 mm. The inter-orbital distance through antennal sockets is 2.34 ± 0.04 mm, while the clypeo-antennal distance is 0.06 ± 0.01 mm. The compound eye length measures 2.41 ± 0.04 mm. Scape length of 1.05 ± 0.02 mm, a pedicel length of 0.20 ± 0.01 mm, and a flagellum length of 3.74 ± 0.10 mm. The 3rd flagellomere diameter is 0.24 ± 0.01 mm, the distance between antennal sockets is 0.51 ± 0.03 mm, and the inter-ocellar distance is 0.40 ± 0.02 mm. Ocellocular distance of 0.89 ± 0.15 mm, an antennocellar distance of 0.79 ± 0.15 mm, and a clypeocular distance of 0.15 ± 0.15 mm (**Table 6-12**). The median ocellus diameter is 0.27 ± 0.15 mm, the labrum length is 0.16 ± 0.15 mm, and the labrum width is 0.34 ± 0.15 mm. Antennal socket maximum diameter of 0.37 ± 0.05 mm and a compound eye width of 0.80 ± 0.08 mm. The forewing length measures 12.85 ± 0.75 mm, while the forewing width is 3.83 ± 0.30 mm. The Jugovanmal index for this species is recorded as 78.64 ± 2.00 mm, and it possesses 17.00 ± 1.50 Hemuli. Hindwing length of 9.43 ± 0.50 mm and a hindwing width of 2.89 ± 0.10 mm. The hind basitarsus length is 2.30 ± 0.15 mm, while the hind basitarsus width is 0.40 ± 0.05 mm. This species possesses 10 flagellomeres and has an abdomen length of 6.71 ± 0.30 mm. Abdomen width of 3.30 ± 0.03 mm and a hind tibia length of 2.63 ± 0.02 mm.

5. *Andrena pilipes*

A. pilipes Fabricius, 1781

A. carbonaria Linnaeus, 1767



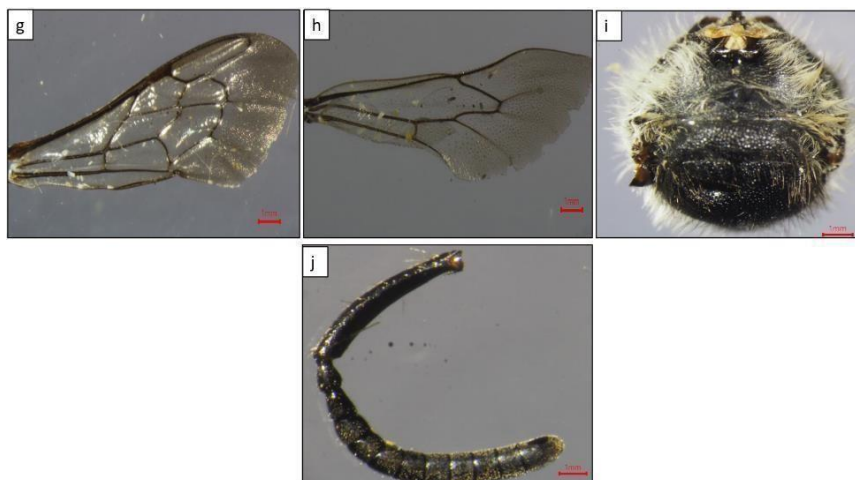


Figure 22: Measurement of various morphological characters of *Andrena pilipes*. (a) Full body, (b) Foreleg, (c) Head, (d) Midleg, (e) Hindleg, (f) Abdomen, (g) Forewing, (h) Hindwing, (i) Thorax, and (j) Antenna.

3.10.6. Distribution: Europe, North Africa, and parts of Asia.

3.10.6.1. Diagnostic Characters: This species is one of the larger *Andrena* bees, with females reaching up to 16 mm in length. It is characterized by its robust black body with dense, dark brown or black hairs on the thorax and abdomen. The hind tibiae and tarsi are entirely black, contrasting with the reddish coloration seen in *A. fucata*. The face has short, dense hair, with a slightly more prominent clypeus (**Figure 22**). The wings are clear with a brownish tinge, and the veins are distinct. A key characteristic is the presence of strong ridges on the propodeum. Males are smaller and have longer, thinner antennae with a more slender body structure.

3.10.6.2. Measurements (Mean±SE in mm): *A. pilipes* has a body length of 9.73 ± 0.05 mm, a head length of 2.68 ± 0.02 mm, and a head width of 3.20 ± 0.03 mm. The thorax length is 3.46 ± 0.02 mm, while the thorax width is 3.23 ± 0.03 mm. The clypeus length is 1.13 ± 0.03 mm. Clypeus width of 1.80 ± 0.03 mm, a lower inter-orbital distance of 1.82 ± 0.03 mm, and an upper inter-orbital distance of 2.06 ± 0.03 mm. The inter-orbital distance through antennal sockets is 0.41 ± 0.03 mm, while the clypeo-antennal distance is 0.02 ± 0.01 mm. The compound eye length is 1.64 ± 0.03 mm. Scape length of 1.02 ± 0.03 mm, a pedicel length of 0.12 ± 0.01 mm, and a flagellum length of 2.12 ± 0.08 mm. The 3rd flagellomere diameter is 0.16 ± 0.01 mm, the distance between antennal sockets is 0.20 ± 0.02 mm, and the inter-ocellar distance is 0.21 ± 0.01 mm. Ocellular distance of 0.41 ± 0.22 mm, an antennocellar distance of 0.67 ± 0.22 mm, and a clypeocular distance of 0.10 ± 0.20 mm (**Table 6-12**). The median ocellus diameter is 0.19 ± 0.30 mm, the labrum length is 0.12 ± 0.30 mm, and the labrum width is 0.20 ± 0.30 mm. Antennal socket maximum diameter of 0.20 ± 0.04 mm and a compound eye width of 0.50 ± 0.07 mm. The forewing length is 11.32 ± 0.60 mm, with a forewing width of 2.79 ± 0.25 mm. The Jugovanmal index is 83.77 ± 0.50 mm, and the species has 13.00 ± 1.00 Hemuli. Hindwing

length of 7.56 ± 0.60 mm and a hindwing width of 2.57 ± 0.15 mm. The hind basitarsus length measures 1.78 ± 0.10 mm, with a hind basitarsus width of 0.28 ± 0.05 mm. This species has 10 flagellomeres and an abdomen length of 3.59 ± 0.25 mm. Abdomen width of 2.81 ± 0.02 mm, with a hind tibia length of 1.21 ± 0.01 mm.

6. *Lasioglossum marginatum*

L. marginatum Brullé, 1832



Figure 23: Measurement of various morphological characteristics of *Lasioglossum marginatum*. (a) Full body, (b) Abdomen, (c) Hindwing, (d) Forewing, (e) Midleg, (f) Foreleg, (g) Head, (h) Thorax, (i) Hind leg, and (j) Antenna.

3.10.7. Distribution: Primarily distributed in South and Southeast Asia.

3.10.7.1. Diagnostic Characters: This is a small sweat bee, generally measuring between 5-7

mm. It has a predominantly dark brown to black body with a subtle metallic sheen on the thorax. The head is slightly broader than in *L. rugifrons*, with fine punctures on the clypeus and frons. The wings are transparent with light brown venation (**Figure 23**). The propodeum has fine striations but lacks the strong rugose sculpturing seen in *L. rugifrons*. The abdomen is smooth, with faint transverse bands of hair. The legs are dark, with short scopal hairs on the hind tibiae. Males are more slender, with longer antennae and less pubescence.

3.10.7.2. Measurements (Mean±SE in mm): *L. marginatum* has a body length of 9.36±0.04 mm, with a head length of 2.63±0.03 mm and a head width of 2.40±0.03 mm. The thorax length is 3.40±0.02 mm, and the thorax width is 2.23±0.03 mm. The clypeus length is 1.15±0.02 mm. Clypeus width of 1.46±0.03 mm, a lower inter-orbital distance of 1.54±0.03 mm, and an upper inter-orbital distance of 1.81±0.03 mm. The inter-orbital distance through antennal sockets is 0.33±0.03 mm, while the clypeo-antennal distance is 0.01±0.01 mm. The compound eye length is 1.55±0.03 mm. Scape length of 1.04±0.02 mm, a pedicel length of 0.11±0.01 mm, and a flagellum length of 2.46±0.09 mm. The 3rd flagellomere diameter is 0.15±0.01 mm, the distance between antennal sockets is 0.20±0.02 mm, and the inter-ocellar distance is 0.19±0.01 mm. Ocellular distance of 0.37±0.20 mm, an antennocellar distance of 0.53±0.16 mm, and a clypeocular distance of 0.12±0.20 mm (**Table 6-12**). The median ocellus diameter is 0.15±0.20 mm, the labrum length is 0.13±0.20 mm, and the labrum width is 0.17±0.20 mm. Antennal socket maximum diameter of 0.19±0.03 mm and a compound eye width of 0.40±0.06 mm. The forewing length measures 11.54±0.55 mm, with a forewing width of 2.90±0.25 mm. The Jugovanmal index is 75.37±1.90 mm, and the species has 16.00±1.00 Hemuli. Hindwing length of 7.58±0.50 mm and a hindwing width of 2.23±0.10 mm. The hind basitarsus length measures 1.59±0.20 mm, while the hind basitarsus width is 0.67±0.10 mm. This species has 10 flagellomeres and an abdomen length of 3.33±0.25 mm. Abdomen width of 2.32±0.01 mm and a hind tibia length of 1.26±0.01 mm.

7. *Lasioglossum matianense*

L. matianense Ebmer, 1978

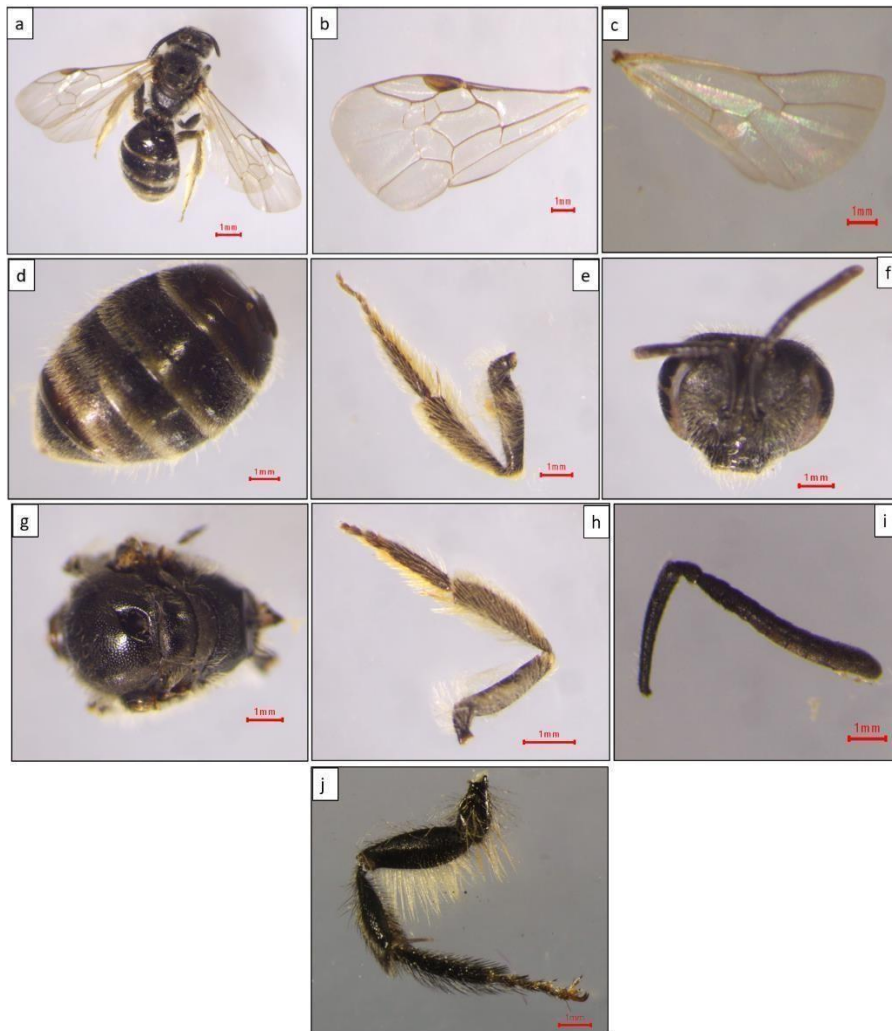


Figure 24: Measurement of various morphological characteristics of *Lasioglossum matianense*. (a) Full body, (b) Forewing, (c) Hindwing, (d) Abdomen, (e) Foreleg, (f) Head, (g) Thorax, (h) Midleg, (i) Antenna, and (j) Hindleg.

3.10.8. Distribution: Widely found across Eurasia, including Europe and parts of Asia.

3.10.8.1. Diagnostic Characters: This species is slightly larger than *L. matianense*, measuring about 7-9 mm in body length. The thorax has a dull metallic green to bluish-green reflection, while the abdomen is primarily black with a faint metallic sheen (**Figure 24**). The face is relatively broad, with a well-defined clypeus. The wings are translucent with brownish veins, and the hind legs have well-developed scopal hairs for pollen collection. A key distinguishing feature is the well-defined, slightly raised margin along the sides of the propodeum. Males are smaller and have longer antennae and a less metallic appearance.

3.10.8.2. Measurements (Mean±SE in mm): *L. matianense* has a body length of 9.08 ± 0.03 mm, a head length of 2.55 ± 0.02 mm, and a head width of 2.35 ± 0.03 mm. The thorax length is 3.32 ± 0.02 mm, while the thorax width is 2.14 ± 0.03 mm. The clypeus length is 1.18 ± 0.02 mm. Clypeus width of 1.32 ± 0.02 mm, a lower inter-orbital distance of 1.48 ± 0.02 mm, and an upper inter-orbital

distance of 1.78 ± 0.02 mm. The inter-orbital distance through antennal sockets is 0.34 ± 0.02 mm, while the clypeo-antennal distance is 0.08 ± 0.01 mm. The compound eye length is 1.67 ± 0.02 mm. Scape length of 1.03 ± 0.02 mm, a pedicel length of 0.14 ± 0.01 mm, and a flagellum length of 2.36 ± 0.10 mm. The 3rd flagellomere diameter is 0.12 ± 0.01 mm, the distance between antennal sockets is 0.13 ± 0.01 mm, and the inter-ocellar distance is 0.24 ± 0.02 mm. Ocellocular distance of 0.47 ± 0.14 mm, an antennocellar distance of 0.58 ± 0.15 mm, and a clypeocular distance of 0.14 ± 0.20 mm (**Table 6-12**). The median ocellus diameter is 0.18 ± 0.20 mm, the labrum length is 0.16 ± 0.20 mm, and the labrum width is 0.19 ± 0.22 mm. Antennal socket maximum diameter of 0.22 ± 0.04 mm and a compound eye width of 0.65 ± 0.09 mm. The forewing length is recorded at 10.89 ± 0.60 mm, while the forewing width is 2.50 ± 0.20 mm. The Jugovanmal index is 65.66 ± 2.00 mm, and the species has 16.00 ± 1.20 Hemuli. Hindwing length of 7.68 ± 0.55 mm and a hindwing width of 2.33 ± 0.12 mm. The hind basitarsus length is 1.66 ± 0.15 mm, and the hind basitarsus width is 0.34 ± 0.05 mm. This species possesses 10 flagellomeres and an abdomen length of 3.21 ± 0.20 mm. The abdomen width of 2.53 ± 0.01 mm, while the hind tibia length measures 1.20 ± 0.01 mm.

8. *Lasioglossum rugifrons*

L. rugifrons (Smith, 1857)

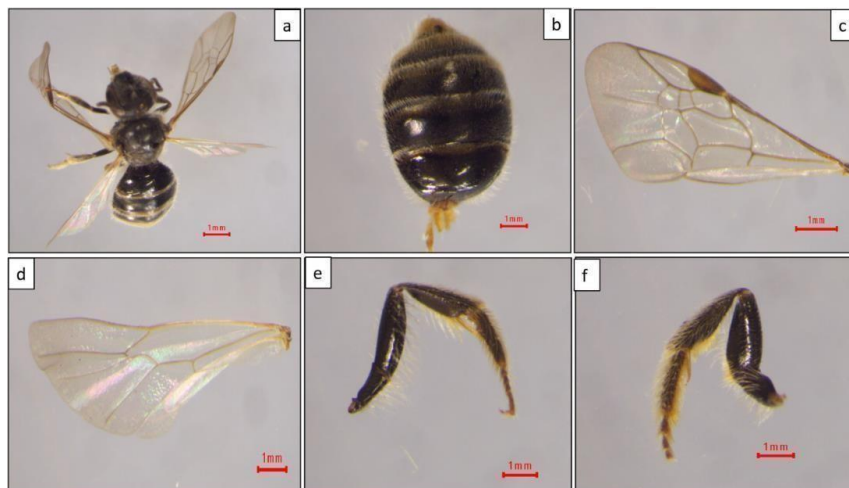




Figure 25: Measurement of various morphological characteristics of *Lasioglossum rugifrons*. (a) Full body, (b) Abdomen, (c) Forewing, (d) Hindwing, (e) Foreleg, (f) Midleg, (g) Hindleg, (h) Head, (i) Antenna, and (j) Thorax.

3.10.9. Distribution: Temperate regions of Europe and parts of North America.

3.10.9.1. Diagnostic Characters: This species is a small to medium-sized sweat bee, generally measuring around 6-8 mm in length. It has a metallic greenish-bronze coloration on the thorax and head, while the abdomen is usually dark brown to black with faint metallic reflections. The face is relatively narrow, with a slightly elongated clypeus (**Figure 25**). A distinguishing feature is the rugose (wrinkled) texture on the frons, which gives the species its name. The wings are translucent, with light brown veins. The legs are dark brown, with the hind tibiae bearing sparse scopal hairs for pollen collection. Males are more slender, with a less metallic sheen and longer antennae.

3.10.9.2. Measurements (Mean±SE in mm): *L. rugifrons* has a body length of 10.23 ± 0.03 mm, with a head length of 2.75 ± 0.04 mm and a head width of 2.43 ± 0.02 mm. The thorax length is 3.61 ± 0.02 mm, and the thorax width is 2.34 ± 0.02 mm. The clypeus length measures 1.14 ± 0.02 mm. Clypeus width of 1.65 ± 0.03 mm, a lower inter-orbital distance of 1.70 ± 0.03 mm, and an upper inter-orbital distance of 1.62 ± 0.03 mm. The inter-orbital distance through antennal sockets is 0.31 ± 0.03 mm, while the clypeo-antennal distance is 0.06 ± 0.01 mm. The compound eye length is 1.44 ± 0.03 mm. Scape length of 1.04 ± 0.02 mm, a pedicel length of 0.13 ± 0.01 mm, and a flagellum length of 2.10 ± 0.08 mm. The 3rd flagellomere diameter is 0.14 ± 0.01 mm, the distance between antennal sockets is 0.19 ± 0.02 mm, and the inter-ocellar distance is 0.20 ± 0.01 mm. Ocellular distance of 0.31 ± 0.15 mm, an antennocellar distance of 0.47 ± 0.12 mm, and a clypeocular distance of 0.19 ± 0.18 mm (**Table 6-12**). The median ocellus diameter is 0.13 ± 0.12 mm, the labrum length is 0.10 ± 0.20 mm, and the labrum width is 0.21 ± 0.25 mm. Antennal socket maximum diameter of 0.23 ± 0.05 mm and a

compound eye width of 0.56 ± 0.08 mm. The forewing length is measured at 11.21 ± 0.65 mm, with a forewing width of 2.65 ± 0.22 mm. The Jugovanmal index is 78.20 ± 1.80 mm, and this species possesses 16.00 ± 1.20 Hemuli. Hindwing length of 7.45 ± 0.50 mm and a hindwing width of 2.45 ± 0.10 mm. The hind basitarsus length measures 1.77 ± 0.12 mm, while the hind basitarsus width is 0.23 ± 0.05 mm. This species has 10 flagellomeres and an abdomen length of 3.87 ± 0.20 mm. Abdomen width of 2.64 ± 0.01 mm and a hind tibia length of 1.23 ± 0.01 mm.

9. *Vespula vulgaris*

V. vulgaris (Linnaeus, 1758)

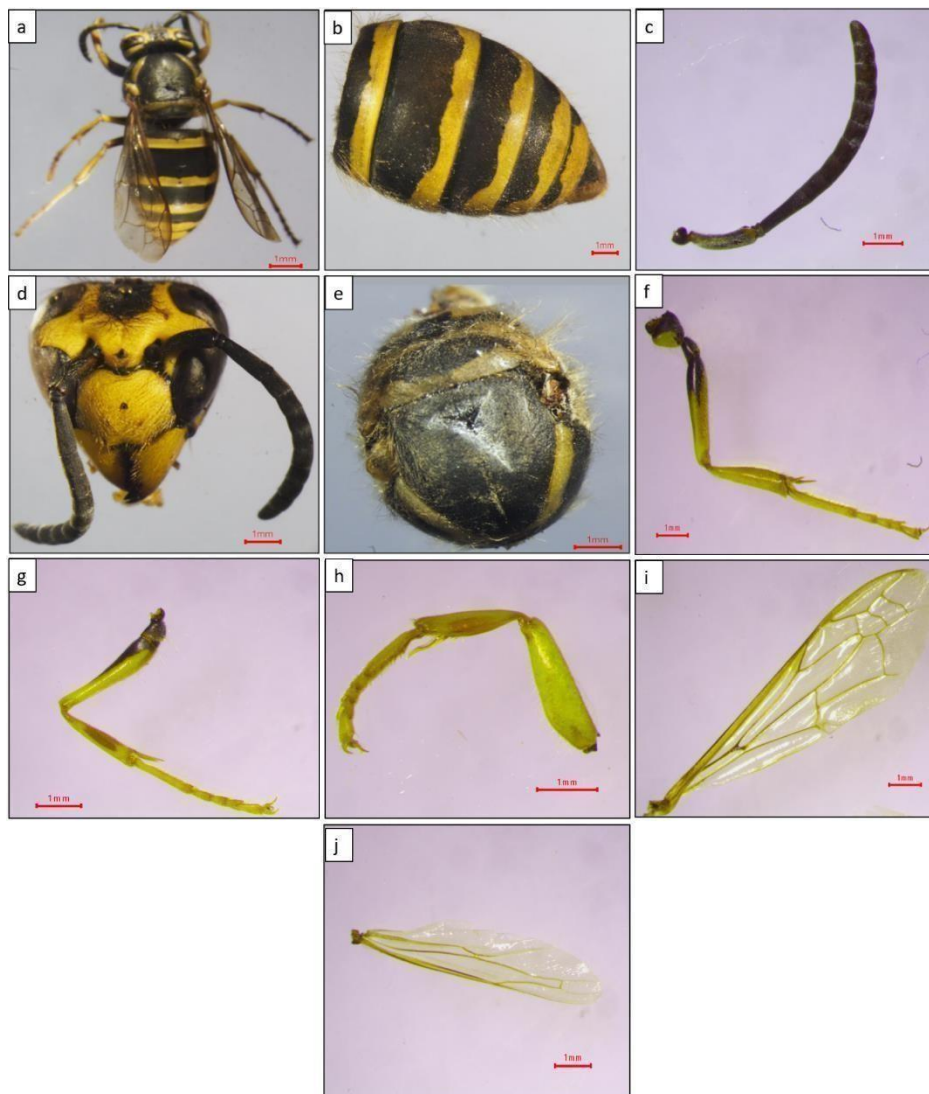


Figure 26: Measurement of various morphological characteristics of *Vespula vulgaris*. (a) Full body, (b) Abdomen, (c) Forewing, (d) Hind leg, (e) Hind wing, (f) Mid leg, (g) Antenna, (h) Head, (i) Thorax, and (j) Foreleg.

3.10.10. Distribution: Native to Europe but also introduced in North America, Australia, and

New Zealand.

3.10.10.1. Diagnostic Characters: This species is a medium to large social wasp, measuring 12-17 mm in length. It has a characteristic black and yellow banded body, with bright yellow markings on the face (**Figure 26**). The thorax is predominantly black with yellow lateral markings. The wings are slightly smoky and fold longitudinally when at rest. A key distinguishing feature is the anchor-shaped black mark on the clypeus. The legs are yellow with black femora. The abdomen has well-defined black bands with a distinctive black arrowhead marking on each tergite. The antennae are black, slightly curved, and shorter in females. Males have longer, more curved antennae.

3.10.10.2. Measurements (Mean±SE in mm): *V. vulgaris* has a body length of 16.02±0.05 mm, a head length of 3.09±0.03 mm, and a head width of 3.46±0.03 mm. The thorax length is 4.43±0.03 mm, while the thorax width is 3.46±0.03 mm. The clypeus length measures 1.45±0.03 mm. Clypeus width of 2.21±0.05 mm, a lower inter-orbital distance of 2.34±0.05 mm, and an upper inter-orbital distance of 2.46±0.05 mm. The inter-orbital distance through antennal sockets is 2.45±0.05 mm, while the clypeo-antennal distance is 0.55±0.02mm. The compound eye length measures 4.18±0.05 mm. Scape length of 1.05±0.02 mm, a pedicel length of 0.19±0.01 mm, and a flagellum length of 4.12±0.10 mm. The 3rd flagellomere diameter is 0.25±0.01 mm, the distance between antennal sockets is 0.56±0.03 mm, and the inter-ocellar distance is 0.52±0.02 mm. Ocellocular distance of 0.23±0.10 mm, an antennocellar distance of 0.32±0.10 mm, and a clypeocular distance of 0.13±0.20 mm (**Table 6-12**). The median ocellus diameter is 0.43±0.30 mm, the labrum length is 0.30±0.30 mm, and the labrum width is 1.45±0.30 mm. Antennal socket maximum diameter of 0.34±0.06 mm and a compound eye width of 1.20±0.15 mm. The forewing length is 14.23±0.80 mm, and the forewing width is 3.64±0.35 mm. The Jugovanmal index is recorded as 79.33±2.20 mm, and this species possesses 19.00±1.80 Hemuli. Hindwing length of 6.56±0.50 mm and a hindwing width of 1.23±0.10 mm. The hind basitarsus length is recorded at 2.67±0.15 mm, with a hind basitarsus width of 0.39±0.05 mm. This species possesses 10 flagellomeres and has an abdomen length of 8.94±0.30 mm. Abdomen width of 5.59±0.02 mm and a hind tibia length of 3.23±0.02 mm.

10. *Bombus albopleuralis*

B. albopleuralis Friese, 1916



Figure 27: Measurement of various morphological characteristics of *Bombus albopleuralis*. (a) Full body, (b) Abdomen, (c) Head, (d) Midleg, (e) Foreleg, (f) Hindleg, (g) Antenna, (h) Ossicles, (i) Thorax, (j) Hindwing, and (k) Forewing.

3.10.11. Distribution: Found in the Himalayas, including India, Nepal, China, and Bhutan.

3.10.11.1. Diagnostic Characters: This species is a relatively large bumblebee, with workers measuring 12-16 mm and queens reaching up to 20 mm. It has a distinctive white or pale yellow thorax, contrasting with its black abdomen (**Figure 27**). The head is large, with a short and broad clypeus. The wings are semi-transparent with brownish venation. The hind legs are adapted for pollen collection, with a well-developed corbicula (pollen basket) on the hind

tibiae. Males have longer antennae and a more gracile body shape compared to females. The dense hair covering the body is a key feature distinguishing it from other bumblebee species.

3.10.11.2. Measurements (Mean±SE in mm): *B. albopleuralis* is the largest species in the dataset, with a body length of 24.41 ± 0.08 mm, a head length of 4.12 ± 0.03 mm, and a head width of 6.21 ± 0.02 mm. The thorax length is 7.32 ± 0.03 mm, while the thorax width is 8.12 ± 0.03 mm. The clypeus length is 1.43 ± 0.02 mm. Clypeus width of 2.22 ± 0.05 mm, a lower inter-orbital distance of 2.45 ± 0.05 mm, and an upper inter-orbital distance of 2.34 ± 0.05 mm. The inter-orbital distance through antennal sockets is 2.47 ± 0.05 mm, while the clypeo-antennal distance is 0.54 ± 0.02 mm. The compound eye length is 4.20 ± 0.05 mm. Scape length of 2.10 ± 0.04 mm, a pedicel length of 0.18 ± 0.01 mm, and a flagellum length of 4.78 ± 0.12 mm. The 3rd flagellomere diameter is 0.34 ± 0.02 mm, the distance between antennal sockets is 0.65 ± 0.04 mm, and the inter-ocellar distance is 0.68 ± 0.03 mm (**Table 6-12**). Ocellocular distance of 0.30 ± 0.20 mm, an antennocellar distance of 0.47 ± 0.20 mm, and a clypeocular distance of 0.12 ± 0.20 mm. The median ocellus diameter is 0.45 ± 0.25 mm, the labrum length is 0.31 ± 0.30 mm, and the labrum width is 1.56 ± 0.30 mm. Antennal socket maximum diameter of 0.38 ± 0.08 mm and a compound eye width of 1.96 ± 0.25 mm. Its forewing length is 20.21 ± 1.00 mm, with a forewing width of 6.34 ± 0.50 mm (Table 6-12). The Jugovanmal index is 82.52 ± 3.00 mm, and it possesses 35.5 ± 2.50 Hemuli. Hindwing length of 11.34 ± 0.70 mm and a hindwing width of 4.23 ± 0.20 mm. The hind basitarsus length measures 4.56 ± 0.12 mm, while the hind basitarsus width is 0.76 ± 0.10 mm. This species possesses 10 flagellomeres and has an abdomen length of 12.97 ± 0.50 mm. Abdomen width of 9.23 ± 0.02 mm and a hind tibia length of 4.52 ± 0.03 mm.

Table 6: Morphometrics of anterior (cephalic) and thoracic body parts of selected Hymenopteran pollinator species from cherry orchards of the Kashmir Valley (mm)

Species	Body length	Head length	Head width	Thorax length	Thorax width	Clypeus length
<i>Andrena fucata</i>	12.59± 0.08	2.47± 0.03	3.35± 0.02	3.41± 0.02	2.58± 0.03	1.21± 0.02
<i>Andrena pilipes</i>	9.73± 0.05	2.68± 0.02	3.20± 0.03	3.46± 0.02	3.23± 0.03	1.13± 0.03
<i>Andrena agilissima</i>	13.29± 0.06	2.95± 0.02	3.21± 0.03	3.53± 0.03	3.29± 0.02	1.38± 0.02
<i>Lasioglossum rugifrons</i>	10.23± 0.03	2.75± 0.04	2.43± 0.02	3.61± 0.02	2.34± 0.02	1.14± 0.02
<i>Lasioglossum matianense</i>	9.08± 0.03	2.55± 0.02	2.35± 0.03	3.32± 0.02	2.14± 0.03	1.18± 0.02
<i>Lasioglossum marginatum</i>	9.36± 0.04	2.63± 0.03	2.40± 0.03	3.40± 0.02	2.23± 0.03	1.15± 0.02
<i>Vespula vulgaris</i>	16.02± 0.05	3.09± 0.03	3.46± 0.03	4.43± 0.03	3.46± 0.03	1.45± 0.03
<i>Bombus albopilealis</i>	24.41± 0.08	4.12± 0.03	6.21± 0.02	7.32± 0.03	8.12± 0.03	1.43± 0.02
<i>Apis mellifera</i>	11.61± 0.04	2.92± 0.03	3.72± 0.03	4.55± 0.02	3.18± 0.02	1.09± 0.02
<i>Apis cerana</i>	11.15± 0.05	2.67± 0.03	3.31± 0.01	3.35± 0.02	2.92± 0.03	0.88± 0.01
C.D(p≤0.05)	0.256	0.096	0.064	0.064	0.096	0.064
<p>CD: Minimum cut of value (Threshold Value derived from ANOVA at p≤0.05) used to decide whether an observed variation is statistically significant or not. Provides a statistically reliable method to compare body measurements across species. If Mean differences are > CD value, indicating morphometric variations are statistically significant (the variation occurred because of actual biological differences among the species, not by accident). Measurements show interspecific variations that support accurate species differentiation and taxonomic validation.</p>						

Table 7: Morphometrics of Cephalic (anterior) structures of selected Hymenopteran pollinator species from cherry orchards of the Kashmir Valley (mm)

Species	Clypeus width	Lower inter-orbital distance	Upper inter-orbital distance	Inter-orbital distance through antennal sockets	Clypeo-antennal distance	Compound eye length
<i>Andrena Fucata</i>	2.20± 0.04	2.40± 0.04	2.13± 0.04	2.34± 0.04	0.06± 0.01	2.41± 0.04
<i>Andrena pilipes</i>	1.80± 0.03	1.82± 0.03	2.06± 0.03	0.41± 0.03	0.02± 0.01	1.64± 0.03
<i>Andrena Agilissima</i>	2.37± 0.05	2.62± 0.05	2.72± 0.05	2.86± 0.05	0.05± 0.01	2.32± 0.05
<i>Lasioglossum rugifrons</i>	1.65± 0.03	1.70± 0.03	1.62± 0.03	0.31± 0.03	0.06± 0.01	1.44± 0.03
<i>Lasioglossum matianense</i>	1.32± 0.02	1.48± 0.02	1.78± 0.02	0.34± 0.02	0.08± 0.01	1.67± 0.02
<i>Lasioglossum marginatum</i>	1.46± 0.03	1.54± 0.03	1.81± 0.03	0.33± 0.03	0.01± 0.01	1.55± 0.03
<i>Vespula Vulgaris</i>	2.21± 0.05	2.34± 0.05	2.46± 0.05	2.45± 0.05	0.55± 0.02	4.18± 0.05
<i>Bombus albopleuralis</i>	2.22± 0.05	2.45± 0.05	2.34± 0.05	2.47± 0.05	0.54± 0.02	4.20± 0.05
<i>Apis mellifera</i>	1.34± 0.03	2.18± 0.03	1.95± 0.03	2.44± 0.03	0.03± 0.01	2.34± 0.03
<i>Apis cerana</i>	1.03± 0.03	1.83± 0.03	1.46± 0.03	2.01± 0.03	0.03± 0.01	2.04± 0.03
C.D(p≤0.05)	0.043	0.027	0.042	0.032	0.040	0.036

CD: Minimum cut of value (Threshold Value derived from ANOVA at $p \leq 0.05$) used to decide whether an observed variation is statistically significant or not. Provides a statistically reliable method to compare body measurements across species. If Mean differences are $>$ CD value, indicating morphometric variations are statistically significant (the variation occurred because of actual biological differences among the species, not by accident). Measurements show interspecific variations that support accurate species differentiation and taxonomic validation.

Table 8: Morphometrics of Antennal and associated Cephalic structures in selected Hymenopteran pollinator species from cherry orchards of the Kashmir Valley (mm)

Species	Scape length	Pedicel length	Flagellum length	3 rd Flagellomere diameter	Distance between antennal sockets	Inter-ocular distance
<i>Andrena fucata</i>	1.05± 0.02	0.20± 0.01	3.74± 0.10	0.24± 0.01	0.51± 0.03	0.40± 0.02
<i>Andrena pilipes</i>	1.02± 0.03	0.12± 0.01	2.12± 0.08	0.16± 0.01	0.20± 0.02	0.21± 0.01
<i>Andrena agilissima</i>	1.06± 0.02	0.19± 0.01	3.73± 0.09	0.22± 0.01	0.49± 0.03	0.38± 0.02
<i>Lasioglossum rugifrons</i>	1.04± 0.02	0.13± 0.01	2.10± 0.08	0.14± 0.01	0.19± 0.02	0.20± 0.01
<i>Lasioglossum matianense</i>	1.03± 0.02	0.14± 0.01	2.36± 0.10	0.12± 0.01	0.13± 0.01	0.24± 0.02
<i>Lasioglossum marginatum</i>	1.04± 0.02	0.11± 0.01	2.46± 0.09	0.15± 0.01	0.20± 0.02	0.19± 0.01
<i>Vespula vulgaris</i>	1.05± 0.02	0.19± 0.01	4.12± 0.10	0.25± 0.01	0.56± 0.03	0.52± 0.02
<i>Bombus albopleuris</i>	2.10± 0.04	0.18± 0.01	4.78± 0.12	0.34± 0.02	0.65± 0.04	0.68± 0.03
<i>Apis mellifera</i>	1.26± 0.03	0.24± 0.01	2.70± 0.08	0.20± 0.01	0.24± 0.02	0.40± 0.02
<i>Apis cerana</i>	1.05± 0.02	0.21± 0.01	2.66± 0.08	0.18± 0.01	0.22± 0.02	0.31± 0.02
C.D(p≤0.05)	0.064	0.032	0.320	0.032	0.096	0.064

CD: Indicates morphometric variations are statistically significant (the variation occurred because of actual biological differences among the species, not by accident). Measurements show interspecific variations that support accurate species differentiation and taxonomic validation.

Table 9: Morphometrics of Ocellar, Antennal, Clypeal and Labral (cephalic) structures in selected Hymenopteran pollinator species from cherry orchards of the Kashmir Valley (mm)

Species	Ocellular distance	Antennocellar distance	Clypeocellar distance	Median ocellus diameter	Labrum length	Labrum width
<i>Andrena fucata</i>	0.89±0.15	0.79±0.15	0.15±0.15	0.27±0.15	0.16±0.15	0.34±0.15
<i>Andrena Pilipes</i>	0.41±0.22	0.67±0.22	0.10±0.20	0.19±0.30	0.12±0.30	0.20±0.30
<i>Andrena agilissima</i>	0.87±0.28	0.77±0.32	0.12±0.30	0.25±0.30	0.14±0.30	0.30±0.30
<i>Lasioglossum rugifrons</i>	0.31±0.15	0.47±0.12	0.19±0.18	0.13±0.12	0.10±0.20	0.21±0.25
<i>Lasioglossum matianense</i>	0.47±0.14	0.58±0.15	0.14±0.20	0.18±0.20	0.16±0.20	0.19±0.22
<i>Lasioglossum marginatum</i>	0.37±0.20	0.53±0.16	0.12±0.20	0.15±0.20	0.13±0.20	0.17±0.20
<i>Vespula vulgaris</i>	0.23±0.10	0.32±0.10	0.13±0.20	0.43±0.30	0.30±0.30	1.45±0.30
<i>Bombus albopleuralis</i>	0.30±0.20	0.47±0.20	0.12±0.20	0.45±0.25	0.31±0.30	1.56±0.30
<i>Apis mellifera</i>	0.47±0.25	1.58±0.25	0.23±0.30	0.25±0.30	0.24±0.30	0.93±0.30
<i>Apis cerana</i>	0.31±0.20	1.79±0.25	0.27±0.25	0.20±0.30	0.19±0.30	0.84±0.30
C.D(p≤0.05)	0.48	0.48	0.64	0.80	0.96	0.96

CD: Indicates morphometric variations are statistically significant (the variation occurred because of actual biological differences among the species, not by accident). Measurements show interspecific variations that support accurate species differentiation and taxonomic validation.

Table 10: Morphometrics of Cephalic (Antennal and Occular) and Wing characters in selected Hymenopteran pollinator species from cherry orchards of the Kashmir Valley (mm)

Species	Antennal socket max. diameter	Compound eye width	Forewing length	Forewing width	Jugal index	Hemuli number
<i>Andrena fucata</i>	0.37± 0.05	0.80± 0.08	12.85± 0.75	3.83± 0.30	78.64± 2.00	17.00± 1.50
<i>Andrena Pilipes</i>	0.20± 0.04	0.50± 0.07	11.32± 0.60	2.79± 0.25	83.77± 0.50	13.00± 1.00
<i>Andrena agilissima</i>	0.36± 0.06	0.75± 0.09	12.74± 0.70	3.72± 0.28	65.60± 2.10	17.00± 1.50
<i>Lasioglossum rugifrons</i>	0.23± 0.05	0.56± 0.08	11.21± 0.65	2.65± 0.22	78.20± 1.80	16.00± 1.20
<i>Lasioglossum matianense</i>	0.22± 0.04	0.65± 0.09	10.89± 0.60	2.50± 0.20	65.66± 2.00	16.00± 1.20
<i>Lasioglossum marginatum</i>	0.19± 0.03	0.40± 0.06	11.54± 0.55	2.90± 0.25	75.37± 1.90	16.00± 1.00
<i>Vespula vulgaris</i>	0.34± 0.06	1.20± 0.15	14.23± 0.80	3.64± 0.35	79.33± 2.20	19.00± 1.80
<i>Bombus albopleuris</i>	0.38± 0.08	1.96± 0.25	20.21± 1.00	6.34± 0.50	82.52± 3.00	35.5± 2.50
<i>Apis mellifera</i>	0.10± 0.02	0.78± 0.10	8.91± 0.45	3.08± 0.20	62.04± 1.50	20.20± 1.50
<i>Apis cerana</i>	0.25± 0.05	0.49± 0.07	7.92± 0.40	2.64± 0.15	59.38± 1.80	17.9± 1.30
C.D(p≤0.05)	0.065	0.152	0.857	0.365	2.519	1.931

CD: Indicates morphometric variations are statistically significant (the variation occurred because of actual biological differences among the species, not by accident). Measurements show interspecific variations that support accurate species differentiation and taxonomic validation.

Table 11: Morphometrics of Hindwing, Hind Leg (Basitarsus) and posterior (Abdominal) structures in selected Hymenopteran pollinator species from cherry orchards of the Kashmir Valley (mm)

Species	Hindwing length	Hind wing width	Hind basitarsus length	Hind basitarsus width	Number of flagellomeres	Abdomen length
<i>Andrena fucata</i>	9.43± 0.50	2.89± 0.10	2.30± 0.15	0.40± 0.05	10± 0	6.71± 0.30
<i>Andrena pilipes</i>	7.56± 0.60	2.57± 0.15	1.78± 0.10	0.28± 0.05	10± 0	3.59± 0.25
<i>Andrena agilissima</i>	9.36± 0.55	2.70± 0.12	2.26± 0.15	0.38± 0.05	10± 0	6.81± 0.30
<i>Lasioglossum rugifrons</i>	7.45± 0.50	2.45± 0.10	1.77± 0.12	0.23± 0.05	10± 0	3.87± 0.20
<i>Lasioglossum matianense</i>	7.68± 0.55	2.33± 0.12	1.66± 0.15	0.34± 0.05	10± 0	3.21± 0.20
<i>Lasioglossum marginatum</i>	7.58± 0.50	2.23± 0.10	1.59± 0.20	0.67± 0.10	10± 0	3.33± 0.25
<i>Vespula vulgaris</i>	6.56± 0.50	1.23± 0.10	2.67± 0.15	0.39± 0.05	10± 0	8.94± 0.30
<i>Bombus albopleuralis</i>	11.34± 0.70	4.23± 0.20	4.56± 0.12	0.76± 0.10	10± 0	12.97± 0.50
<i>Apis mellifera</i>	6.44± 0.40	1.64± 0.10	2.06± 0.10	0.10± 0.05	10± 0	5.56± 0.30
<i>Apis cerana</i>	5.50± 0.40	3.31± 0.15	1.76± 0.10	0.89± 0.10	10± 0	5.25± 0.30
C.D(p≤0.05)	0.90	0.22	0.23	0.11	0.00	0.51

CD: Indicates morphometric variations are statistically significant (the variation occurred because of actual biological differences among the species, not by accident). Measurements show interspecific variations that support accurate species differentiation and taxonomic validation.

Table 12. Morphometrics of posterior (Abdominal) and Hind Leg (Tibial) structures in selected Hymenopteran pollinator species from cherry orchards of the Kashmir Valley (mm)

Species	Abdomen width	Hind tibia length
<i>Andrena fucata</i>	3.30± 0.03	2.63± 0.02
<i>Andrena pilipes</i>	2.81± 0.02	1.21± 0.01
<i>Andrena agilissima</i>	4.29± 0.03	3.72± 0.02
<i>Lasioglossum rugifrons</i>	2.64± 0.01	1.23± 0.01
<i>Lasioglossum matianense</i>	2.53± 0.01	1.20± 0.01
<i>Lasioglossum marginatum</i>	2.32± 0.01	1.26± 0.01
<i>Vespula vulgaris</i>	5.59± 0.02	3.23± 0.02
<i>Bombus albopleuralis</i>	9.23± 0.02	4.52± 0.03
<i>Apis mellifera</i>	4.26± 0.02	3.15± 0.01
<i>Apis cerana</i>	3.64± 0.02	2.84± 0.01
C.D(p≤0.05)	0.082	0.056

CD Value: Indicates morphometric variations are statistically significant (the variation occurred because of actual biological differences among the species, not by accident). Measurements show interspecific variations that support accurate species differentiation and taxonomic validation.

3.11. Hierarchical Cluster Analysis

Different patterns of morphological similarity and divergence among species are revealed by Hierarchical Cluster Analysis (HCA) of hymenopteran pollinators based on standardized morphometric traits. The close clustering of *Apis mellifera* and *A. cerana* suggests a high degree of morphological similarity, most likely as a result of their similar ecological roles and taxonomic lineage. The tight grouping of *Lasioglossum* species, such as *L. rugifrons*, *L. marginatum*, and *L. matianense*, reflects intra-genus consistency in body structure (**Figure 28**). On the other hand, species like *Vespula vulgaris* and *Bombus albopleuralis* are situated on different branches, indicating significant variations in body size and structure. Moderate similarity within the genus is suggested by the distinct cluster formed by *Andrena* species such as *A. agilissima* and *A. fucata*. The morphometric diversity between *Apis* and non-*Apis* pollinators is highlighted by these grouping patterns, which also shed light on their possible ecological differentiation and specialization in pollination dynamics.

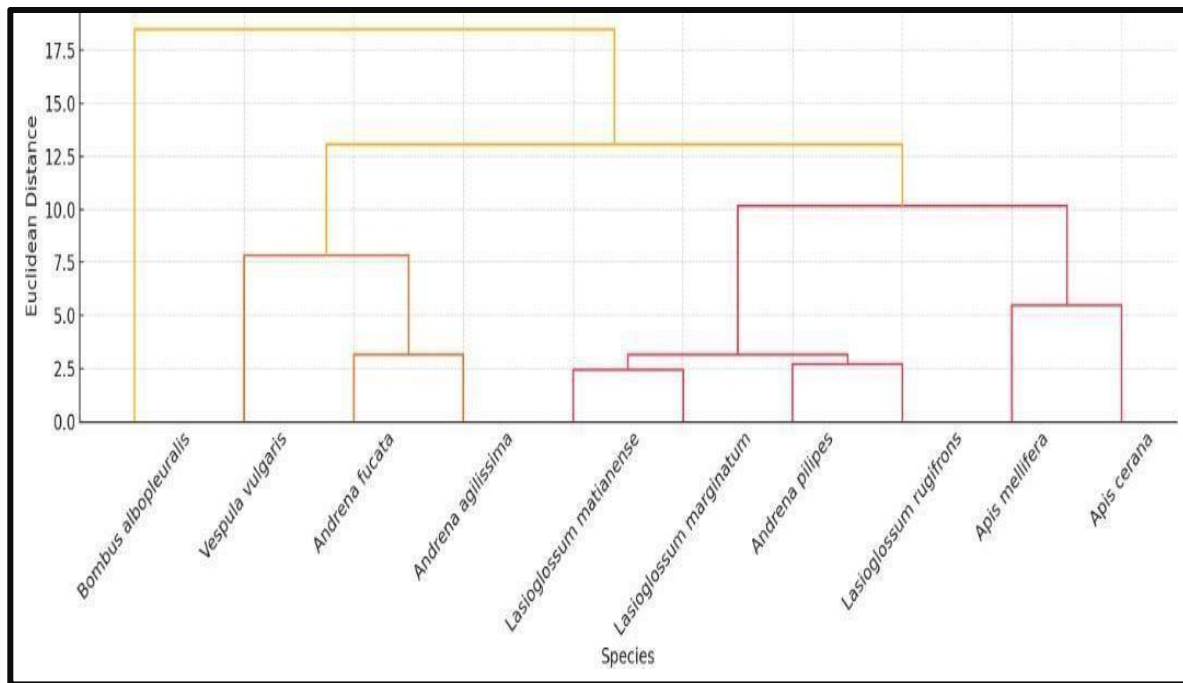


Figure 28: Hierarchical cluster analysis (HCA) performed on 37 standardized morphometric characters (head, thorax, antennae, wings, legs, ocellar, and abdominal traits) using Euclidean distance and Ward’s linkage. The resulting dendrogram shows that *Bombus albopleuralis* and *Vespula vulgaris* form a distinct high-distance cluster, reflecting their unique morphometric profiles among the sampled Hymenoptera. The solitary bees (*Andrena* and *Lasioglossum* spp.) group together at low to intermediate distances, indicating strong overlap in proportional traits. The two honeybees, *Apis mellifera* and *A. cerana*, form a tight sub-cluster that joins the rest of the taxa only at higher Euclidean distances, confirming their distinct but internally homogeneous morphometric pattern.

3.12. Principal Component Analysis (PCA)

Principal Component Analysis (PCA) based on standardised morphometric characters of hymenopteran pollinators reveals clear patterns of species separation along the first two principal components (**Figure 29**). The first two principal components (PC1 and PC2) together capture the major directions of morphological variation. Positive (+) and negative (–) scores on the PCA axes indicate relative differences in trait magnitudes. Species with positive PC1 values possess larger body and wing dimensions, while those with negative PC1 scores tend to be smaller-bodied. Similarly, positive PC2 scores reflect greater variation in head–thorax proportions and antennal traits, while negative PC2 values correspond to smaller or narrower structures.

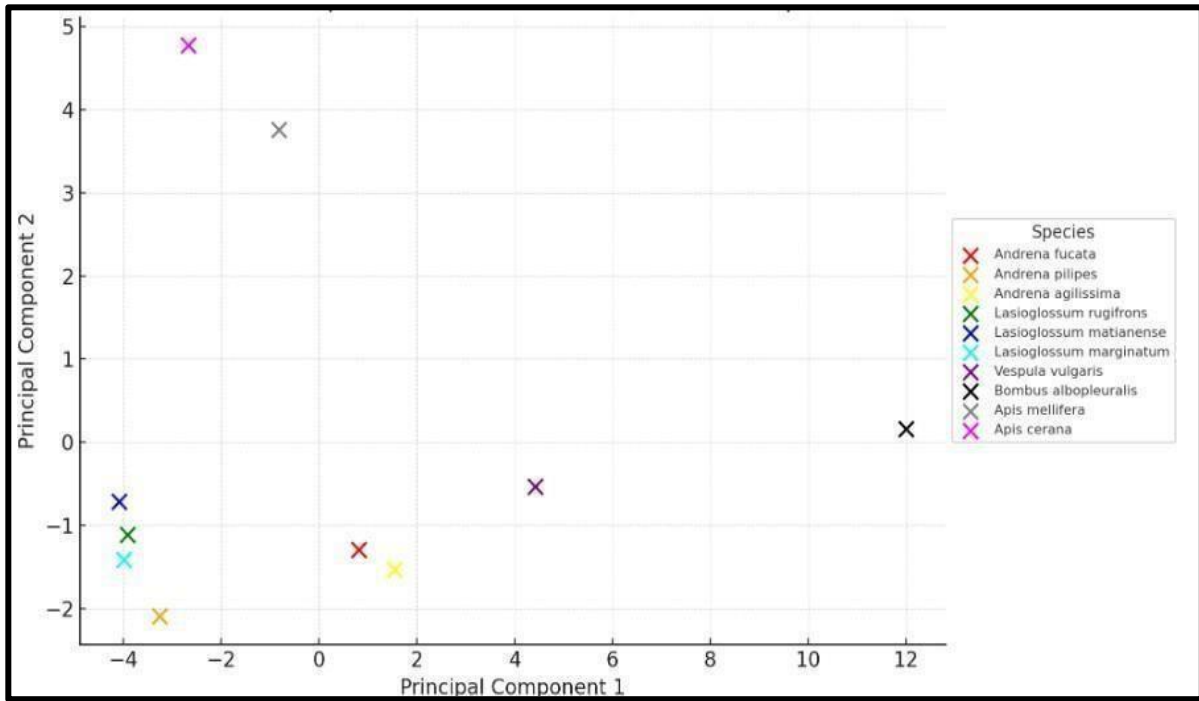


Figure 29: Principal Component Analysis (PCA) of Hymenopteran Pollinators Based on 37 Morphometric variables representing the head, thorax, abdomen, legs, antennae, and wing structures of ten hymenopteran species. The bumblebee *Bombus albopleuralis* and the wasp *Vespula vulgaris* are strongly separated along PC1, reflecting their significantly larger morphologies. Honeybees *Apis mellifera* and *A. cerana* cluster closely, indicating high morphometric similarity. *Andrena* and *Lasioglossum* species form compact, genus-specific clusters, demonstrating clear taxonomic differentiation. Overall, the PCA highlights size-related and shape-related axes of variation that reliably separate taxa based on multivariate morphometric structure.

3.13. Morphometric and Morphological study of Dipteran pollinators

The order Diptera, encompassing true flies, includes a remarkable diversity of species, among which syrphid flies (Family: Syrphidae), also known as hoverflies or flower flies, hold significant ecological importance. These flies are easily recognised by their characteristic hovering flight and often striking mimicry of bees or wasps, a form of Batesian mimicry that offers protection from predators. Syrphid flies are among the most efficient and abundant pollinators, frequently visiting flowers for nectar and pollen, thus playing a critical role in the pollination of both wild and cultivated plants. Unlike bees, many syrphid species do not possess specialised pollen-carrying structures, yet their frequent and diverse floral visits contribute substantially to pollination services. Syrphid flies are essential to agroecosystems and natural

biodiversity in the larger context of the Diptera order, as evidenced by the growing scientific interest in their role in integrated pest and pollinator management.

3.13.1. Family: Syrphidae

3.13.1.1. Wing geometric morphometrics

The characteristic wing venation patterns of syrphid flies (family Syrphidae), also referred to as hoverflies, are essential for species identification and evolutionary research. The vena spuria, a false vein that lies between the radial and medial veins and has no connection to any other vein, but is a distinguishing characteristic of syrphid wings, is characteristic of the family. The Costa (C) and Subcosta (Sc) are the main veins that support the structure; the Anal vein (A1) delineates the wing's posterior margin; the Radial veins (R1-R5) and Medial veins (M1-M2) improve wing rigidity and movement. Moreover, crossveins like m-cu (medial-cubital) and r-m (radial-medial) define distinctive wing cells that are crucial for taxonomic classification (**Figure 30**). The R5 cell is a prominent characteristic of the Syrphidae family. It can be either closed or open, providing a crucial characteristic for species differentiation. Wings were photographed with an OLYMPUS Stereozoom microscope and examined using **IdentiFly Pro** software to identify the species. A total of 13 landmarks were manually digitised on each wing image following the geometric morphometric protocol described by Mielczarek and Tofilski (2018). These landmarks allowed for the quantitative evaluation of shape variation by capturing important venation intersections and cell boundaries. The findings demonstrated the great efficacy of geometric morphometric analysis of wing venation in differentiating between closely related syrphid species. Crucially, the technique only requires a scanner or digital camera that is connected to a computer, making it affordable and widely available. A strong morphometric dataset can be produced by manually positioning landmarks in IdentiFly software after a wing image has been acquired.

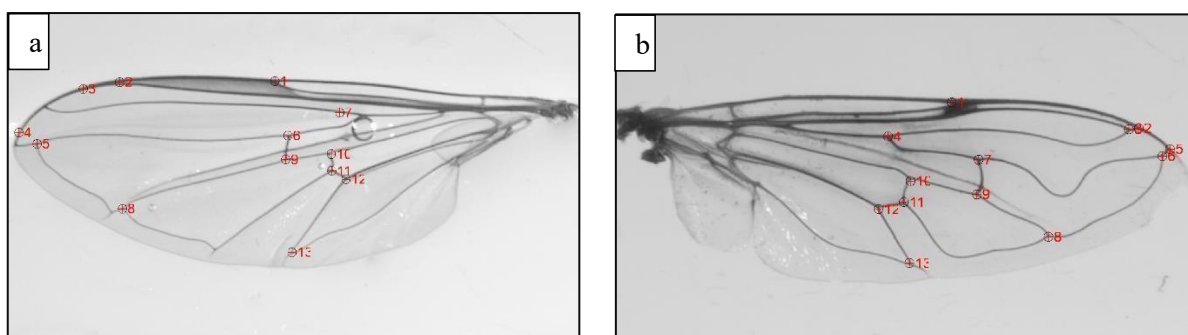


Figure 30: Wing venation of a syrphid fly, with 13 red-marked landmarks for geometric

morphometric analysis (a, b). Conta (C), Subcosta (Sc), Radial (R1-R5), Medial (M1-M2), crossveins (r-m, m-cu), and Anal vein (A1), which are important venal structures. These landmarks support research on evolutionary traits, functional morphology, and species differentiation.

3.13.1.2. Morphological Identification of Dipteran Pollinators

During the 2022–2024 flowering seasons, dipteran pollinators, also known as hoverflies, from cherry orchards throughout the Kashmir Valley were gathered. These species were identified through detailed examination of external morphological features under Stereozoom microscopy using standard taxonomic keys. The hoverfly assemblage included species from multiple genera, with notable examples such as *Eristalis tenax* (a), *E. arbustorum* (d), and *E. abusive* (c), all of which are bee-mimicking syrphids known for their strong flight ability and frequent visitation to cherry blossoms. *Episyrphus balteatus* (b), a widely distributed and highly effective pollinator, was also recorded in high numbers and is distinguished by its yellow-black abdominal pattern and elongated wings. *Syrphus ribesii* (e) and *Sphaerophoria scripta* (f) were also frequently encountered, both of which are known for their role in pollination as well as their predatory larval stages that contribute to aphid control (**Figure 31**). The specimens were documented with precise scale bars, and several showed key diagnostic traits such as wing venation patterns, body coloration, and antennal structure, which facilitated accurate species-level identification. These syrphid flies, although often underrepresented in pollination studies, were found to be regular floral visitors during cherry bloom and are therefore considered important supplementary pollinators in the region’s orchard ecosystems.

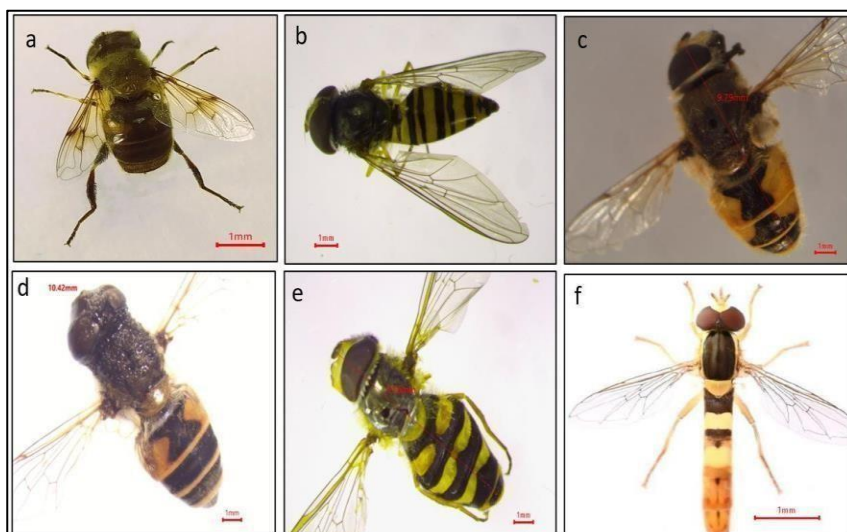


Figure 31: Morphologically identified dipteran pollinators (Family: Syrphidae) collected from cherry orchards of Kashmir Valley. The specimens (a-f) include *Eristalis tenax*, *Episyrphus*

balteatus, *E. abusive*, *E. arbustorum*, *Syrphus ribesii*, and *Sphaerophoria scripta*, documented under stereozoom microscopy for taxonomic confirmation and morphometric analysis.

1. *Eristalis tenax*

E. tenax (Linnaeus, 1758)

E. alpina Strobl, 1893

E. campestris Meigen, 1822

E. claripes Santos Abreu, 1924



Figure 32: Measurement of various morphological characteristics of *Eristalis tenax*. (a) Body length, (b) Abdomen, (c) Midleg, (d) Foreleg, (e) Hindleg, (f) Head, (g) Forewing, and (h) Thorax.

3.13.2. Distribution: Europe, Asia, North America, Australia, New Zealand, and parts of Africa, thriving in urban and rural habitats with abundant floral resources.

3.13.2.1. Diagnostic Characters: *E. tenax* can be identified by several rare diagnostic characters that set it apart from other hoverfly species. One of the most notable features is its relatively large size, with a body length ranging from 8 to 14 mm (**Figure 32**). The species can be easily identified by its characteristic abdominal coloration, which consists of broad yellow-orange bands surrounded by dark brown or black. Males' large, dark eyes, which are nearly fused at the top of the head, are another distinguishing characteristic; females' eyes are more widely spaced. To further differentiate itself, *Eristalis tenax* has clear wings with a characteristic dark mark at the tip of the forewing. Moreover, it has a distinctive hovering flight pattern close to flowers, hovering for prolonged periods of time, in contrast to many other species that land more frequently.

3.13.2.2. Measurements (Mean±SE in mm): Full Body length: 14.55 ± 0.25 mm. The head is 4.55 ± 0.09 mm wide and 4.11 ± 0.08 mm long. **Table 13 & 14** show that the thorax measures 4.78 ± 0.10 mm in length and 3.33 ± 0.07 mm in width. The compound eye is 2.85 ± 0.06 mm long and 1.24 ± 0.07 mm wide. The forewings measure 8.57 ± 0.25 mm in length and 2.78 ± 0.14 mm in width. Lastly, the abdomen measures 5.66 ± 0.18 mm in length and 4.78 ± 0.12 mm in width.

2. *Episyrphus balteatus*

E. balteatus (De Geer, 1776)

E. balteatus persica Hurkmans, 1985

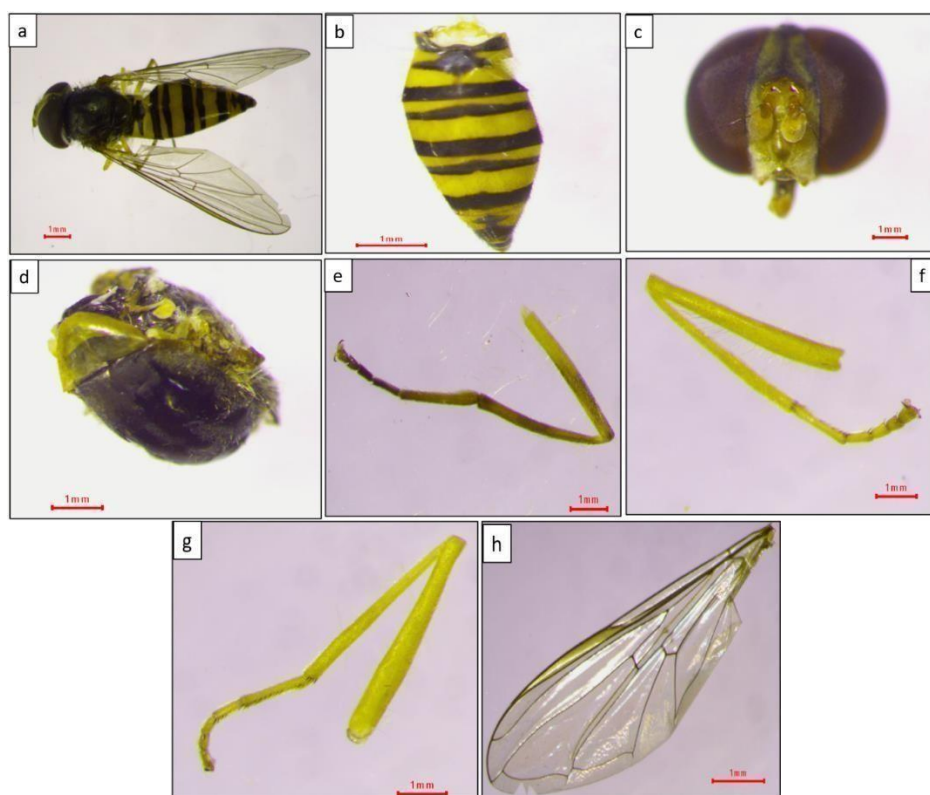


Figure 33: Measurement of various morphological characteristics of *Episyrphus balteatus*. (a) Body length, (b) Abdomen, (c) Head, (d) Thorax, (e) Hindleg, (f) Foreleg, (g) Midleg, and (h) Wing.

3.11.3. Distribution: Europe, Asia, North America, and parts of North Africa, thriving in various habitats such as gardens, agricultural fields, and meadows.

3.11.3.1. Diagnostic Characters: *E. balteatus*, commonly known as the stripe-tailed hoverfly, can be identified by several distinctive diagnostic characters. It has a striking yellow and black striped pattern on its abdomen, which is the most prominent feature, resembling a wasp, with a black "belt" across the middle of its abdomen (**Figure 33**). The thorax is also marked with black and yellow markings, and the legs are mostly yellow with black markings. The head of

E. balteatus is large with dark eyes, and it has a characteristic wing pattern with a dark tip on the forewings. The wings are clear with a distinct dark mark near the top, which helps differentiate it from other similar species. Additionally, the species has a relatively small size, with a body length ranging from 6 to 8 mm, and a fast, agile flight pattern, often hovering near flowers or flying rapidly from one bloom to another. These features are key in distinguishing *E. balteatus* from other hoverfly species.

3.13.3.2. Measurements (Mean±SE in mm): Full body length measuring 8.02 ± 0.15 mm. The head length is 2.03 ± 0.05 mm with a width of 2.24 ± 0.06 mm (**Table 13 & 14**). The thorax length is 1.91 ± 0.05 mm, and its width is 1.42 ± 0.03 mm. The compound eye of this species has a length of 0.57 ± 0.02 mm and a width of 0.65 ± 0.05 mm. The forewing length is 6.66 ± 0.15 mm, with a width of 2.14 ± 0.10 mm. Finally, the abdomen measures 4.08 ± 0.12 mm in length and 1.84 ± 0.08 mm in width.

3. *Eristalis abusiva*

E. abusiva Collin, 1931

E. germanica Sack, 1935

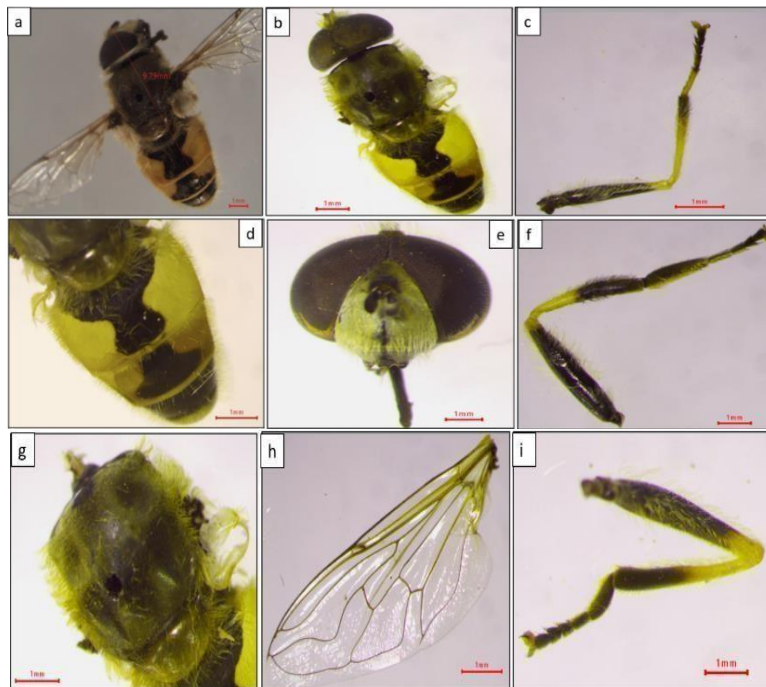


Figure 34: Measurement of various morphological characteristics of *Eristalis abusiva*. (a) Body length, (b) Abdomen, (c) Midleg, (d) Head, (e) Hindleg, (f) Thorax, (g) Wing, and (h) Foreleg.

3.11.4. Distribution: Europe, Asia, North America, and parts of North Africa, inhabiting gardens, agricultural fields, and meadows.

3.11.4.1. Diagnostic Characters: *E. abusiva* exhibits several rare diagnostic characters that help distinguish it from other hoverfly species. Its remarkable wasp-like yellow and black striped pattern on the abdomen, with a noticeable black "belt" around the center, is one of its most distinguishing characteristics. Additionally, the thorax is characterized by bands of yellow and black, which give it a unique look (**Figure 34**). It can be identified by its distinctive dark mark near the top of the forewings, which is present on its clear wings. Its distinctive color pattern is enhanced by the legs' black markings and predominant yellow color. The species is also rather small, usually measuring between 6 and 8 mm in length, and its big, dark eyes are another important characteristic. The hoverfly is distinguished from other similar species by its agile flight, which is typified by quick, darting movements and hovering behavior close to flowers.

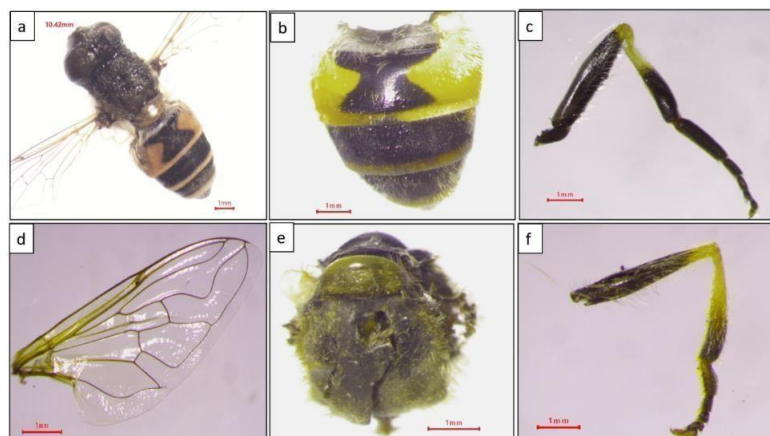
3.13.4.2. Measurements (Mean±SE in mm): Full Body length of 10.67 ± 0.20 mm. The dimensions of the head are 3.29 ± 0.07 mm in width and 2.91 ± 0.06 mm in length. As shown in **Table 13 & 14**, the thorax measures 4.07 ± 0.08 mm in length and 3.07 ± 0.05 mm in width. The compound eye measures 2.39 ± 0.05 mm in length and 1.07 ± 0.06 mm in width. The forewing's width is 2.46 ± 0.12 mm, and its length is 7.09 ± 0.20 mm. At last, the abdomen measures 3.69 ± 0.15 mm in length and 3.25 ± 0.10 mm in width.

4. *Eristalis arbustorum*

E. arbustorum (Linnaeus, 1758)

E. punctulatus Macquart, 1834

E. cinctellus Zetterstedt, 1843



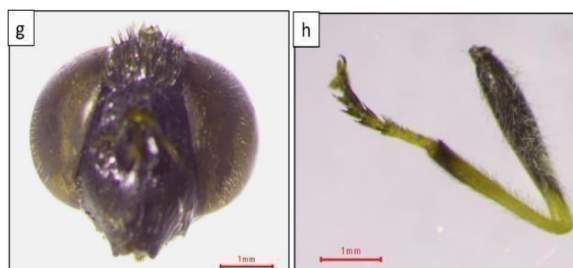


Figure 35: Measurement of various morphological characteristics of *Eristalis arbustorum*. (a) Body length, (b) Abdomen, (c) Midleg, (d) Head, (e) Hindleg, (f) Thorax, (g) Wing, and (h) Foreleg.

3.13.5. Distribution: Europe, Asia, and parts of North America, commonly found in woodland edges, gardens, and meadows.

3.13.5.1. Diagnostic Characters: *E. arbustorum* can be distinguished from other species by several rare diagnostic characters. It has a distinctive yellow and black pattern on its abdomen, with a unique arrangement of black markings that resemble a series of interrupted bands. The thorax is marked with prominent black and yellow stripes, and the legs are largely yellow with some black markings, particularly on the femora. One of the most notable features is its relatively large size, with a body length of 9 to 11 mm (**Figure 35**). The eyes are large and slightly separated in females, while males have closer-set eyes. Additionally, *E. arbustorum* has a characteristic wing pattern, with dark marks on the forewings, particularly near the tip. These features, combined with its hovering flight behavior near flowers, help distinguish it from similar species in the *Eristalis* genus.

3.13.5.2. Measurements (Mean±SE in mm): Full Body length: 9.18 ± 0.18 mm. Its head is 2.39 ± 0.05 mm long and 2.75 ± 0.06 mm wide (**Table 13 & 14**). The thorax measures 3.46 ± 0.07 mm in length and 2.96 ± 0.04 mm in width. The compound eye measures 1.75 ± 0.03 mm in length and 0.76 ± 0.05 mm in width. The forewings measure 2.46 ± 0.10 mm in width and 6.54 ± 0.15 mm in length. Last but not least, the abdomen measures 3.83 ± 0.12 mm in length and 3.29 ± 0.08 mm in width.

5. *Syrphus ribesii*

S. ribesii (Linnaeus, 1758)

S. vitripennis Meigen, 1822

S. flavitibia Macquart, 1829

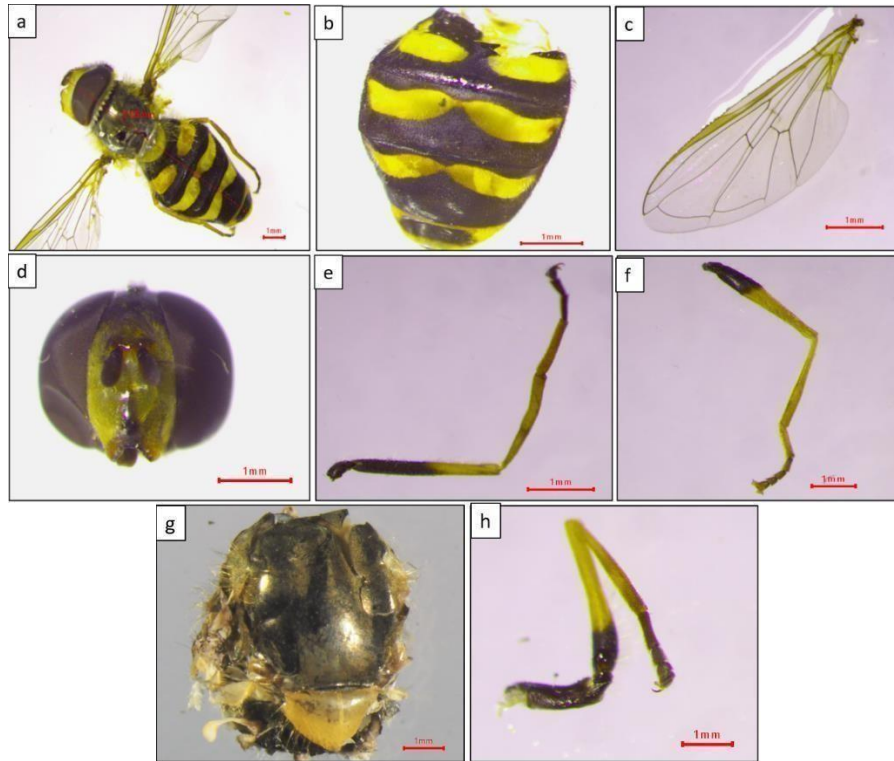


Figure 36: Measurement of various morphological characteristics of *Syrphus ribesii*; a; Body length, b; Abdomen, c; Wing d; Head, e; Hindleg f; Foreleg, g; Thorax, h; Foreleg.

3.13.6. Distribution: Europe, Asia, and parts of North America, commonly found in gardens, orchards, and agricultural fields.

3.13.6.1. Diagnostic Characters: Despite not being extremely uncommon, *S. ribesii* can be challenging to identify because of its similarities to other hoverfly species. This species can be identified by its characteristic yellow and black pattern on the abdomen and thorax, with the latter showing narrow black stripes (**Figure 36**). Additionally, the adult has big, dark eyes that can turn red in certain lighting situations. The legs are mostly black with yellow markings, and the wings are clear with dark veins. The face is pale with a slight darkening around the eyes, and the antennae are rather short. These distinguishing characteristics aid in the identification of *S. ribesii*, as does its unusual flight pattern.

3.13.6.2. Measurements (Mean±SE in mm): Full Body length: 8.49 ± 0.12 mm. According to Tables 14 and 15, the head is 2.61 ± 0.04 mm long and 2.10 ± 0.05 mm wide. The dimensions of the thorax are 1.46 ± 0.03 mm in width and 1.92 ± 0.03 mm in length. The compound eye is 2.05 ± 0.06 mm long and 0.63 ± 0.04 mm wide (**Table 13 & 14**). The forewings measure 2.63 ± 0.11 mm in width and 7.47 ± 0.18 mm in length. Last but not least, the abdomen measures 4.41 ± 0.14 mm in length and 3.15 ± 0.09 mm in width.

6. *Sphaerophoria scripta*

S. scripta (Linnaeus, 1758)

S. flavipes Fabricius, 1794

S. abbreviata Zetterstedt, 1843

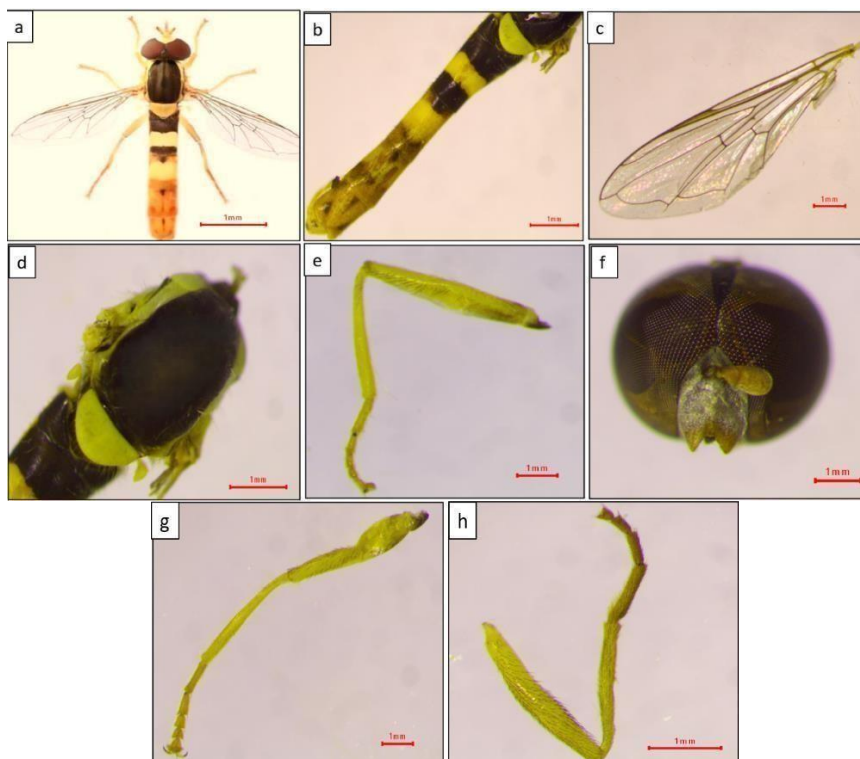


Figure 37: Measurement of various morphological characteristics of *Sphaerophoria scripta*; a; Full Body, b; Abdomen, c; Wings, d; Thorax, e; Midleg, f; Head, g; Foreleg, h; Hindleg.

3.13.7. Distribution: Europe, Asia, and North America, commonly found in grasslands, meadows, and agricultural areas.

3.13.7.1. Diagnostic Characters: Despite the possibility of being mistaken for similar species, *S. scripta* can be distinguished by several unique characteristics. Its distinctive features include a long, lean body and a narrow, segmented abdomen with a noticeable black and yellow banding pattern (**Figure 37**). The face is pale with a thin black line running down the center, and the thorax is typically yellow with black markings. Its long, narrow wings with a dark wing venation and a noticeable black line running the length of the wing are among its most distinctive features. Its antennae are also rather long and simple, and its legs are black with yellow markings. These characteristics help to identify this species, as does its distinctive hovering behavior.

3.13.7.2. Measurements (Mean±SE in mm): Full Body length: 5.33 ± 0.10 mm. Its head is

1.67 ± 0.04 mm long and 0.76 ± 0.03 mm wide (**Table 13 & 14**). The thorax measures 1.32 ± 0.04 mm in length and 0.45 ± 0.02 mm in width. The compound eye is 0.98 ± 0.03 mm long and 0.54 ± 0.04 mm wide. The forewings measure 4.66 ± 0.10 mm in length and 1.48 ± 0.08 mm in width. In conclusion, the abdomen measures 2.34 ± 0.10 mm in length and 1.36 ± 0.07 mm in width. The measurements of several morphological traits of syrphid flies are shown in

Table 13, which also highlights the insects' adaptability to their ecological roles and reveals notable species-specific variations. With a body length of 14.55 ± 0.25 mm, *E. tenax* was the largest of the species examined, while *S. scripta* was the smallest, measuring only 5.33 ± 0.10 mm. These variations in body size imply that larger syrphid flies, such as *E. tenax*, might need more substantial body structures for pollination tasks or be adapted for more effective long-distance flight. Smaller species like *S. scripta*, on the other hand, might be better adapted to more nimble flying techniques. With the largest head length (4.11 ± 0.08 mm) and width (4.55 ± 0.09 mm), *E. tenax* may have evolved a specialized adaptation for feeding on a range of flowers, where larger head structures allow for more noticeable mouthparts. Given its smaller head size, *S. scripta* might have distinct feeding habits or inclinations. These patterns were also seen in thoracic measurements, where *S. scripta* had the shortest thorax (1.32 ± 0.04 mm) and *E. abusive* had the longest thorax (4.07 ± 0.08 mm), indicating the need for a more potent flight mechanism. *E. tenax* had the largest compound eye length (2.85 ± 0.06 mm), which is essential for visual processing and may help it recognize flowers and navigate challenging environments. *S. scripta*, on the other hand, had smaller eyes (0.98 ± 0.03 mm), which might have affected its visual acuity. While smaller species are probably adapted to different ecological niches, larger syrphid species like *E. tenax* and *E. abusive* seem to have morphological traits that support efficient flight and extensive pollination roles (**Table 14**). The measurements' significant statistical differences (**C.D. p ≤ 0.05**) further highlight the fact that these morphological variations are not coincidental but rather represent particular adaptations to their respective roles in flight dynamics and pollination. These results highlight the variety of syrphid fly species and the unique characteristics that affect their ecological roles.

Table 13: Morphometrics of Body, Cephalic, Thoracic and Ocular structures in selected Syrphid pollinator species (Diptera) from cherry orchards of the Kashmir Valley (mm)

Species	Body length	Head length	Head width	Thorax length	Thorax width	Compound eye Length
<i>Episyrphus balteatus</i>	8.02± 0.15	2.03± 0.05	2.24± 0.06	1.91± 0.05	1.42± 0.03	0.57± 0.02
<i>Sphaerophoria scripta</i>	5.33± 0.10	1.67± 0.04	0.76± 0.03	1.32± 0.04	0.45± 0.02	0.98± 0.03
<i>Eristalis abusive</i>	10.67± 0.20	2.91± 0.06	3.29± 0.07	4.07± 0.08	3.07± 0.05	2.39± 0.05
<i>Eristalis arbustorum</i>	9.18± 0.18	2.39± 0.05	2.75± 0.06	3.46± 0.07	2.96± 0.04	1.75± 0.03
<i>Syrphus ribesii</i>	8.49± 0.12	2.61± 0.04	2.10± 0.05	1.92± 0.03	1.46± 0.03	2.05± 0.06
<i>Eristalis tenax</i>	14.55± 0.25	4.11± 0.08	4.55± 0.09	4.78± 0.10	3.33± 0.07	2.85± 0.06
C.D(p≤0.05)	0.42	0.14	0.17	0.14	0.07	0.05

CD: Indicates morphometric variations are statistically significant (the variation occurred due to actual biological differences among species). Measurements show interspecific variations that support accurate species differentiation and taxonomic validation.

A comparison of several morphological characteristics in syrphid fly species, such as compound eye width, forewing length, forewing width, abdomen length, and abdomen width, is given in **Table 14**. The following species are examined: *S. ribesii*, *E. tenax*, *E. abusive*, *E. arbustorum*, *S. scripta*, and *E. balteatus*. With *S. scripta* having the smallest compound eye width (0.54 mm) and *E. tenax* having the largest (1.24 mm), there was a noticeable difference between the species, as indicated by the C.D. of 0.14 mm. This variation most likely has to do with the species' visual abilities, which affect how well they forage and how they pollinate. The C.D. for forewing length is 0.21 mm, indicating notable variations in wing morphology. *E. tenax* had the longest forewing (8.57 mm), while *S. scripta* had the shortest (4.66 mm). Larger forewings, especially in species like *E. tenax*, may improve foraging range and flight stability. Forewing width also differed between species, with *S. scripta* having the narrowest forewings (1.48 mm) and *E. tenax* having the widest (2.78 mm), with a C.D. of 0.16 mm, suggesting functional differences in flight dynamics and maneuverability.

Table 14: Morphometrics of Ocular (Compound Eye), Wing (Forewing) and Abdominal structures in selected Syrphid pollinator species (Diptera) from cherry orchards of the Kashmir Valley (mm)

Species	Compound eye width	Forewing length	Forewing width	Abdomen length	Abdomen width
<i>Episyrphus balteatus</i>	0.65± 0.05	6.66± 0.15	2.14± 0.10	4.08± 0.12	1.84± 0.08
<i>Sphaerophoria scripta</i>	0.54± 0.04	4.66± 0.10	1.48± 0.08	2.34± 0.10	1.36± 0.07
<i>Eristalis abusive</i>	1.07± 0.06	7.09± 0.20	2.46± 0.12	3.69± 0.15	3.25± 0.10
<i>Eristalis arbustorum</i>	0.76± 0.05	6.54± 0.15	2.46± 0.10	3.83± 0.12	3.29± 0.08
<i>Syrphus ribesii</i>	0.63± 0.04	7.47± 0.18	2.63± 0.11	4.41± 0.14	3.15± 0.09
<i>Eristalis tenax</i>	1.24± 0.07	8.57± 0.25	2.78± 0.14	5.66± 0.18	4.78± 0.12
C.D(p≤0.05)	0.14	0.21	0.16	0.17	0.11
<p>CD: Indicates morphometric variations are statistically significant (the variation occurred because of actual biological differences among the species, not by accident). Measurements show interspecific variations that support accurate species differentiation and taxonomic validation.</p>					

With a C.D. of 0.17 mm, the species varying capacities to carry and transport pollen may be reflected in the variation in abdomen length, with *E. tenax* having the longest (5.66 mm) and *S. scripta* the shortest (2.34 mm) (**Table 14**). Last but not least, there was a considerable range in the width of the abdomen, with *Eristalis tenax* having the widest (4.78 mm) and *S. scripta* the narrowest (1.36 mm). The C.D. of 0.11 mm further demonstrates the trait's functional significance in ecological roles specific to a species. Syrphid flies ecological adaptations, such as their capacity for flight, foraging tactics, and pollination efficiency, are strongly linked to the considerable morphological variation that these measurements and the corresponding C.D. values show.

3.14. Hierarchical Cluster Analysis

Using standardised morphometric characters, the Hierarchical Cluster Analysis (HCA) of syrphid fly species identifies clear groupings that emphasise the morphological similarities and

differences between taxa. The close clustering of *E. abusiva* and *E. arbustorum* indicates a strong morphometric resemblance, which may be the result of similar structural adaptations (**Figure 38**). *E. balteatus* and *S. ribesii* also group relatively closely, reflecting a degree of morphological similarity. In contrast, *E. tenax* and *S. scripta* appear on separate and higher branches, indicating notable divergence in body traits. These hierarchical patterns underscore varying degrees of morphological convergence and divergence within the syrphid flies, which may correspond to differences in ecological roles or evolutionary trajectories.

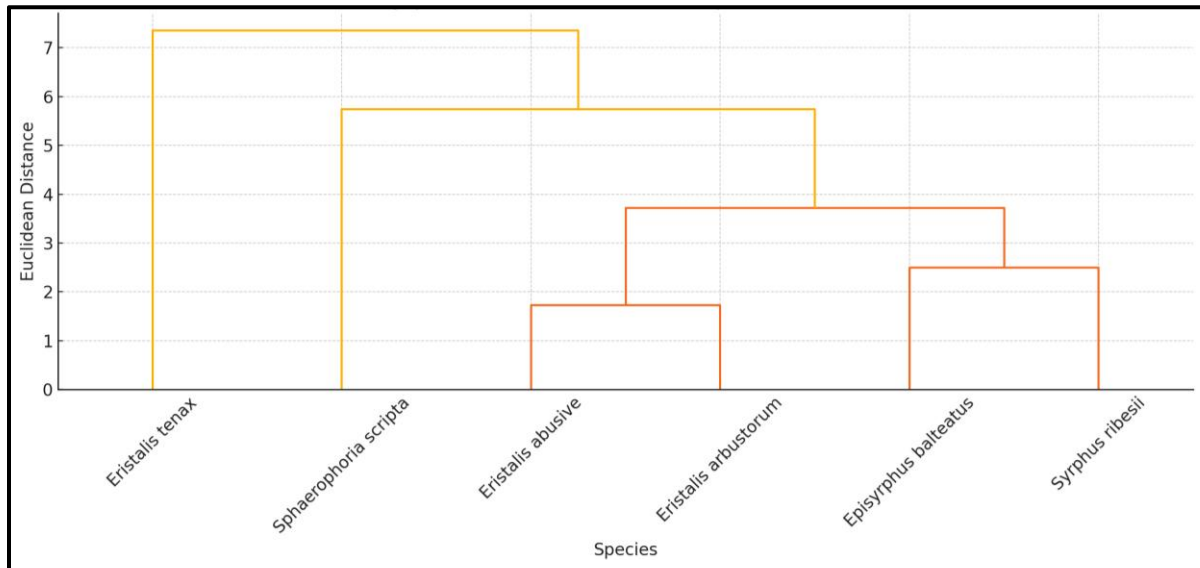


Figure 38: Hierarchical cluster analysis (HCA) of six syrphid fly species based on 11 standardized morphometric characters (body, head, thorax, compound eye, wing, and abdominal traits), using Euclidean distance and Ward’s linkage. The dendrogram reveals two clusters:(i) *E. abusiva* and *E. arbustorum*, which group tightly at low linkage distances, indicating high morphometric similarity; and (ii) *E. balteatus* and *S. ribesii*, which also cluster closely, reflecting similar body size and wing proportions. *S. scripta* and *E. tenax* appear as the most morphometrically distinct species, joining the main clusters only at higher Euclidean distances. Overall, the analysis highlights a clear separation between large-bodied *Eristalis* species and the smaller, slender hoverflies.

3.15. Principal Component Analysis (PCA)

Principal Component Analysis shows the morphometric variation among six syrphid fly species collected from cherry orchards in the Kashmir Valley (**Figure 39**). The analysis is based on 11 standardized morphometric traits, including body length, head length, head width, thorax length, thorax width, compound eye length and width, forewing length and width, and abdomen length and width.

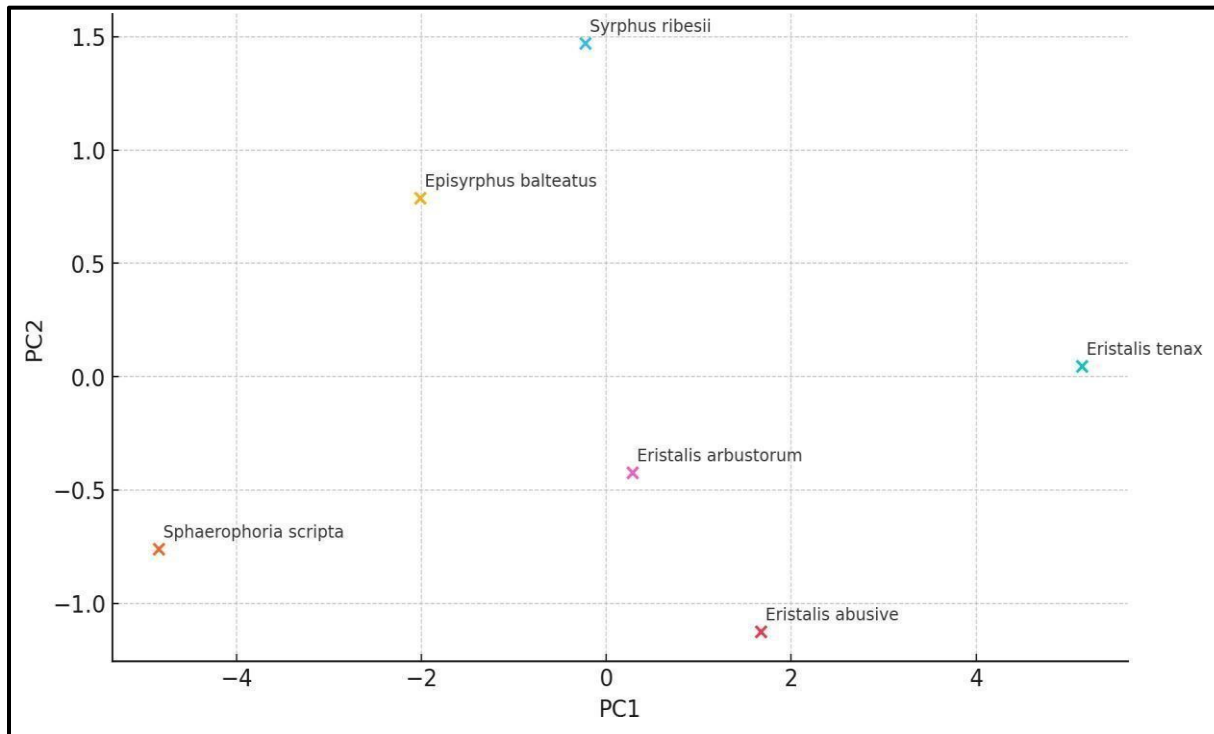


Figure 39: Principal Component Analysis (PCA) of six syrphid fly species based on 11 morphometric traits. PC1 represents overall body size (larger species show positive scores; smaller species show negative scores), while PC2 reflects differences in head, eye, and thorax proportions (+/- values indicate higher or lower trait magnitudes). *E. tenax* is strongly separated on PC1 due to its large body and wing dimensions, whereas *S. scripta* clusters on the negative side, reflecting its smaller, slender morphology. *E. balteatus* and *S. ribesii* occupy intermediate positions, while *E. abusive* and *E. arbustorum* group toward the larger-bodied region. The PCA clearly distinguishes robust *Eristalis* species from smaller hoverflies.

3.16. Morphological and Morphometric Characterization of Lepidopteran Pollinators

The order Lepidoptera, comprising butterflies and moths, represents one of the most diverse and ecologically significant groups of insects. Members of this order are characterised by the presence of scaled wings, complete metamorphosis, and diverse colour patterns that play crucial roles in communication, camouflage, and mate recognition. Among them, families such as Pieridae, Lycaenidae, and Nymphalidae are of particular ecological importance due to their significant contribution to pollination and their sensitivity to environmental changes. Medium-sized butterflies such as *Pieris brassicae* and *Pontia daplidice*, belonging to the family Pieridae, are commonly observed in agricultural landscapes and are considered effective pollinators and herbivores of cruciferous crops. Similarly, small-sized butterflies of the family Lycaenidae, including *Polyommatus eros* and *Lycaena phlaeas*, are notable for their vibrant coloration and

unique ecological interactions, particularly their mutualistic associations with ants. The family Nymphalidae, which includes species such as *Argynnis hyperbius*, *Nymphalis canace*, and *Vanessa cardui*, represents one of the largest and most diverse butterfly families. Members of this family are strong fliers, widely distributed, and highly adaptable, making them important indicators of habitat quality and environmental change. Accurate identification of lepidopteran species often relies heavily on the examination of genitalia, as external morphological characters such as wing colour, pattern, and size can be highly variable due to sexual dimorphism, seasonal polyphenism, and environmental influences. Genitalic structures, particularly male genitalia, are species-specific, evolutionarily conserved, and less influenced by environmental variation, making them reliable diagnostic characters for species delimitation (Klots 1970; Scoble 1995). In contrast to Lepidoptera, insect orders such as Hymenoptera and Diptera often exhibit more distinct external morphological features, such as wing venation, antennal structure, and body segmentation, that allow species-level identification without routine reliance on genital dissections. Therefore, genitalia-based identification is more extensively employed in Lepidoptera to resolve cryptic species complexes and ensure accurate taxonomic classification, especially in groups with high morphological similarity.

3.16.1. Family: Pieridae

The Pieridae family, commonly known as the whites and yellows, represents a diverse group of butterflies characterized by several unique features. One notable characteristic is the presence of bifid tarsal claws, in which the claws at the end of each leg are split into two parts. This adaptation provides a secure grip on various surfaces, thereby facilitating perching and feeding behaviours (**Figure 40**). Additionally, Pieridae butterflies also possess two anal veins in their wings, which are important for maintaining flight stability and flexibility. The wing venation in this family is often triradate, meaning that the veins form three distinct branches, contributing to the structural integrity and flexibility of the wings during flight. Furthermore, members of the Pieridae family are equipped with six walking legs, a common trait of most butterflies. These legs enable them to walk, climb, and interact with their environment throughout their lifecycle, from larval stages to adulthood.

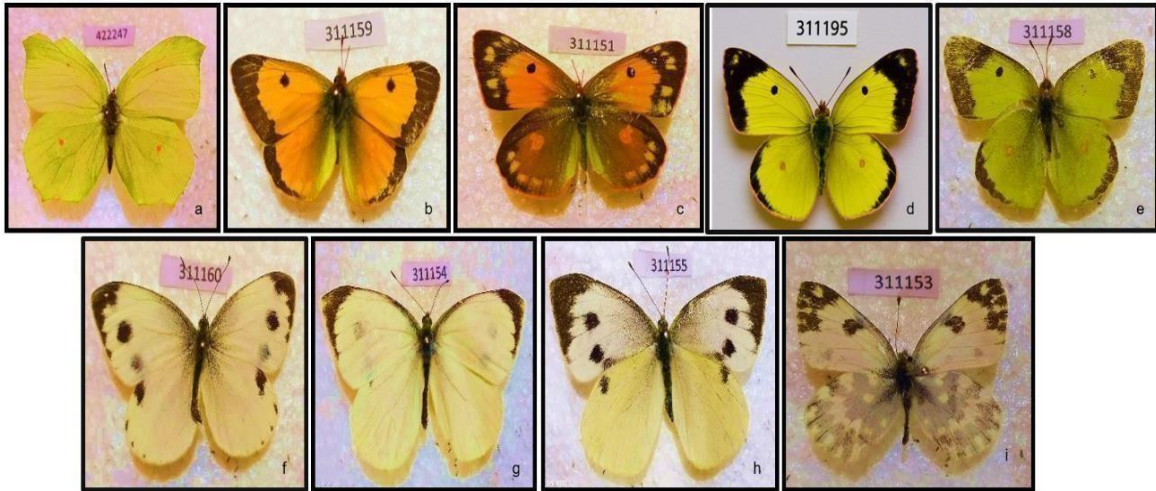


Figure 40: Representation of butterfly species from the family *Pieridae* observed during the study. Labeled specimens include: (a) *Gonepteryx rhamni*, (b1) *Colias electo* ♂, (b2) *C. electo* ♀, (c) *C. erate*, (d) *C. philodice*, (e) *Pieris canidia*, (f) *P. brassicae* ♂, (f1) *P. brassicae* ♀, and (g) *Pontia daplidice*.

1. *Gonepteryx rhamni*

G. rhamni (Linnaeus, 1758)

G. cleobule Fabricius, 1787

G. rhamni provincialis Verity, 1913

G. rhamni is well known for its exceptional leaf mimicry, with angular wing margins and greenish-yellow coloration that closely resemble fresh leaves. It is one of the longest-living butterflies, capable of surviving up to 10-12 months through adult overwintering (**Figure 41a**). The species also shows strong sexual dimorphism, with bright sulphur-yellow males and paler greenish-white females, each bearing a small orange discal spot on the wings.

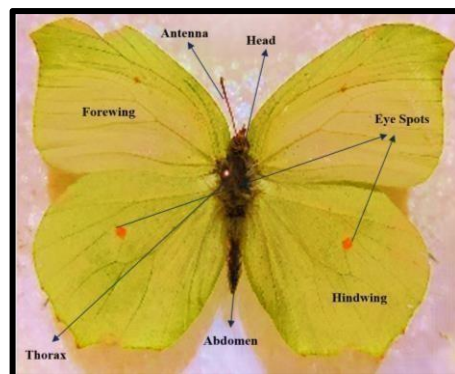


Figure 41a: Dorsal view of a butterfly showing major external morphological features, including head, antenna, thorax, abdomen, forewing, hindwing, and characteristic eyespots.

Material examined: J&K India, Collector: Arjumand John, Crop: Cherry.

Distribution: India, Turkey, Southern England and Austria.

Diagnostic Characters:

Female (♀) Genitalia

The sterigma is small, funnel-like, and strongly sclerotised, formed through the fusion of the lamella antevaginalis and lamella postvaginalis. The ostium bursae is crescent-shaped. The ductus seminalis arises dorsally from about the midpoint of the ductus bursae and is tubular in form. The ductus bursae is relatively short, with a sclerotised proximal region, while the remaining part is membranous, clearly delimited from the beginning of the corpus bursae. The corpus bursae is larger and longer than the ductus bursae, membranous, ovoid with a rounded apex, and curves into an irregular S-shaped configuration. The apophyses anteriores are distinct. The apophyses posteriores are moderately long, narrow, heavily sclerotized, and straight. The papilla analis is oval, with the distal region strongly sclerotised and bearing dense pilosity (**Figure 41b**).



Figure 41b: Dorsal view of *Gonepteryx rhamni* (a-a1) illustrating the detailed morphology of Antenna, Head and Female genitalia along with associated reproductive structures. Key features are highlighted, showcasing the anatomical adaptations critical for reproductive functions.

Measurements (Mean \pm SE, in mm): Body length 12.44 ± 0.30 ; head length 1.67 ± 0.09 , head width 2.56 ± 0.13 ; thorax length 2.56 ± 0.10 , thorax width 2.78 ± 0.09 ; compound eye length 1.98 ± 0.07 , width 2.76 ± 0.06 . Forewing length 28 ± 1.5 , width 15 ± 0.8 ; hindwing length 24 ± 1.2 , width 19 ± 1.0 ; antenna length 5.54 ± 0.22 ; abdomen length 8.21 ± 0.30 (**Table 15 & 16**).

2. *Colias electo*

C. electo (Linnaeus, 1763)

C. electo hecate Butler, 1896

C. electo pseudohecate Berger, 1940

Material examined: J&K India, Collector: Arjumand John, Crop: Cherry.

Distribution: India, Turkey, Southern England and Austria.

Diagnostic Characters:

Female (♀) Genitalia

The tegumen appears dorsally flattened, broad, and almost rectangular. The uncus is straight, forming a Y-shaped outline in dorsal view and exhibiting a tubular form laterally. The gnathos is narrow, strongly sclerotised, and distinctly concave. The saccus is short, thick, tubular, curves slightly upward, and ends in a blunt tip. The vinculum is broad and U-shaped ventrally, extending longer than the tegumen's dorsal projection. The juxta is U-shaped and well-sclerotised. The valvae are comparatively large, extending beyond the tip of the uncus, heavily sclerotised, and clothed with setae. Both the costa and sacculus are simple in structure. The ampulla is sickle-shaped, only moderately curved, with a blunt tip directed downward. The aedeagus has a stout basal portion that narrows sharply into a pointed, sickle-like apex, and is heavily sclerotised (**Figure 42a**).

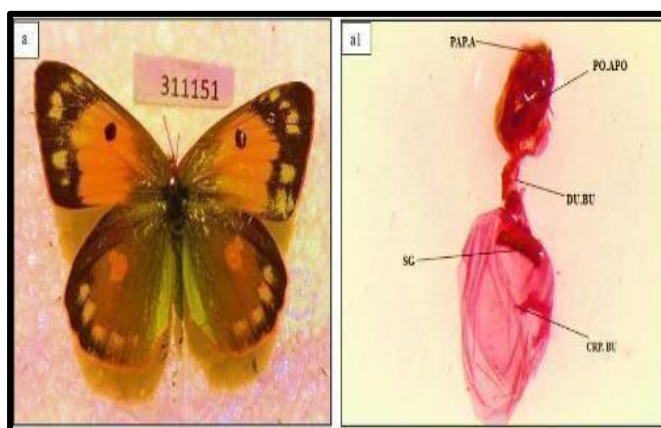


Figure 42a: Dorsal view of *Colias electo*, (a-a1) highlighting the Head, Antenna, female genitalia and associated reproductive structures. The illustration emphasizes key anatomical features, providing insights into their functional morphology.

Male (♂) Genitalia

The tegumen is dorsally broad, flattened, and nearly rectangular in outline. The uncus appears straight, forming a Y-shape in dorsal aspect and tubular in lateral view. The gnathos is narrow, strongly sclerotized, and concave. The saccus is short, thick, and tubular, curving slightly upward with a blunt apex. The vinculum is ventrally broad and U-shaped, extending beyond the projection of the tegumen. The juxta is distinctly U-shaped and heavily sclerotized. The valvae are large, projecting beyond the tip of the uncus, robustly sclerotized, and densely setose. Both the costa and sacculus are simple. The ampulla is sickle-like, only moderately curved, with a blunt tip directed downward. The aedeagus has a stout basal part that narrows abruptly into a pointed, sickle-shaped apex, and is heavily sclerotized (**Figure 42b**).

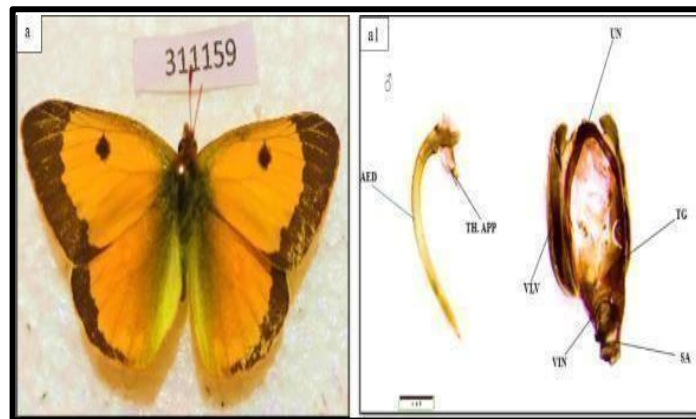


Figure 42b: Dorsal view of *Colias electo* (a-a1) showcasing the detailed morphology of the male genitalia and associated reproductive structures. The illustration highlights key anatomical components, including the claspers, aedeagus, and associated sclerites, which play crucial roles in mating and reproductive success. This detailed depiction provides insights into the structural adaptations and functional relevance of the reproductive anatomy in *C. electo*.

Measurements (Mean \pm SE, in mm): Body length 10.61 ± 0.28 ; head length 1.76 ± 0.09 , head width 2.45 ± 0.10 ; thorax length 2.63 ± 0.08 , thorax width 2.81 ± 0.08 ; compound eye length 1.49 ± 0.06 , width 1.80 ± 0.05 ; forewing length 26 ± 1.5 , width 15 ± 0.7 ; hindwing length 23 ± 1.2 , width 17 ± 0.9 ; antenna length 4.44 ± 0.20 ; abdomen length 6.22 ± 0.20 (**Table 15 & 16**).

3. *Colias erate*

C. erate Esper, 1805

C. edusa erate Esper, 1805

C. poliographus Motschulsky, 1860

C. erate sinensis Grum-Grshimailo, 1891

Material examined: J&K India, Collector: Arjumand John, Crop: Cherry.

Distribution: Central Asia, China, Mongolia, Russia, and Japan.

Diagnostic Characters:

Male (♂) Genitalia

The tegumen is dorsally broad, flattened, and rectangular. The uncus is distinctly shorter than the tegumen. The saccus is short, slender, tubular, well-sclerotised, and directed obliquely upward. The vinculum is broad and U-shaped on the ventral side, extending longer than the tegumen projection. The juxta is heavily sclerotised and U-shaped. The valvae are large, broad, extending beyond the uncus tip, strongly sclerotised, and clothed with setae. Both the costa and sacculus are simple in form. The ampulla is sickle-like, only moderately curved, with a blunt tip directed downward. The harpe is well sclerotised and tapers gradually into a sharp apex. The aedeagus has a stout basal portion, narrowing abruptly after two-thirds of its length into a pointed, sickle-shaped apex that is acutely curved and strongly sclerotised. The vesica is absent. The ductus ejaculatorius enters dorsally (**Figure 43**).

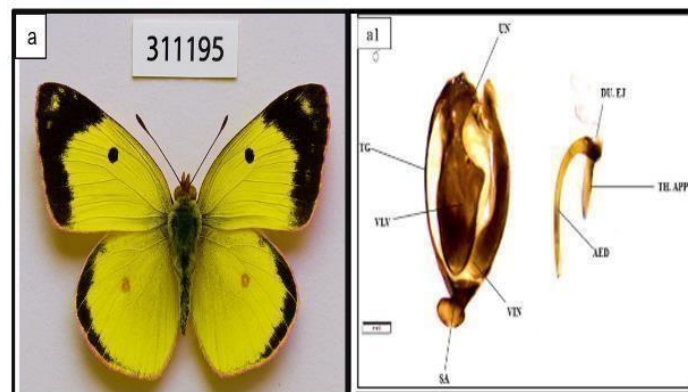


Figure 43: Dorsal view of *Colias erate* (a-a1) male genitalia showing key reproductive structures. Notable anatomical components include the claspers, aedeagus, and associated sclerites, which are essential for copulation and species-level identification.

Measurements (Mean \pm SE, in mm): Body length 10.64 ± 0.27 ; head length 1.67 ± 0.10 , head width 2.38 ± 0.12 ; thorax length 2.76 ± 0.09 , thorax width 2.89 ± 0.08 ; compound eye length 1.44 ± 0.06 , width 1.79 ± 0.05 .; forewing length 28 ± 1.5 , width 18 ± 0.8 ; hindwing length 26 ± 1.2 , width 19 ± 1.0 ; antenna length 4.42 ± 0.22 ; abdomen length 6.21 ± 0.20 (**Table 15 & 16**).

4. *Colias philodice*

C. philodice Godart, 1819

C. chrysotheme philodice Godart, 1819

C. philodice philodice Godart, 1819

C. philodice vitabunda Strecker, 1900

Material examined: J&K India, Collector: Arjumand John, Crop: Cherry.

Distribution: North America, Canada, the United States and Mexico.

Diagnostic Characters:

Male (♂) Genitalia

The saccus is distinctly elongated. The tegumen is rounded and compact in form. The gnathos extends dorsally, projecting beyond the length of the uncus. The uncus itself is elongated, appearing arrowhead-shaped in dorsal aspect. The valvae are long, terminating in a slender, pointed process. The aedeagus is curved and lacks cornuti. The juxta is sclerotized and serves to connect the valvae (**Figure 44**).

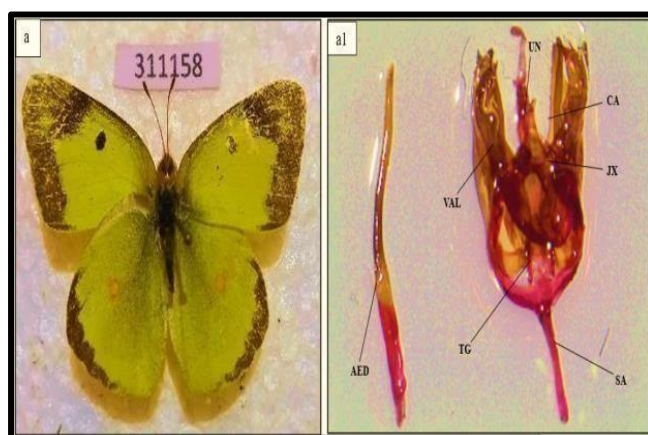


Figure 44: Dorsal view of *Colias philodice* (a-a1) illustrating the male genitalia and associated reproductive structures. The figure highlights critical anatomical features, including the aedeagus, claspers, and supporting sclerites, which are integral to the mating process and reproductive success of the species. This detailed view provides insights into the functional morphology and evolutionary adaptations of *C. philodice*.

Measurements (Mean \pm SE, in mm): Body length 10.98 ± 0.30 ; head length 1.09 ± 0.07 , head width 1.78 ± 0.08 ; thorax length 2.55 ± 0.09 , thorax width 2.78 ± 0.07 ; compound eye length 0.96 ± 0.05 , width 1.50 ± 0.06 ; forewing length 24 ± 1.4 , width 13 ± 0.6 ; hindwing length 21 ± 1.1 , width 15 ± 0.8 ; antenna length 4.58 ± 0.18 ; abdomen length 7.34 ± 0.25 (**Table 15 & 16**).

5. *Pieris canidia*

P. canidia (Sparrman, 1768)

P. canidia canisioides Moore, 1884

P. indica Evans, 1932

P. canidia indica Evans, 1932

Material examined: J&K India, Collector: Arjumand John, Crop: Cherry.

Distribution: India, Turkey, Southern England and Austria.

Diagnostic Characters:

Female (♀) Genitalia

The corpus bursae is large and nearly spherical. The signum is paired, with broad, strongly sclerotized lateral margins bearing spiny structures and a central invagination. The appendix bursae is oval and membranous. The ductus bursae is stout and well developed. The papilla analis is heavily sclerotized and clothed with setae. The posterior apophyses are elongated, slender, slightly curved, and terminate in blunt tips, while the anterior apophyses are comparatively smaller, also ending bluntly (**Figure 45a**).

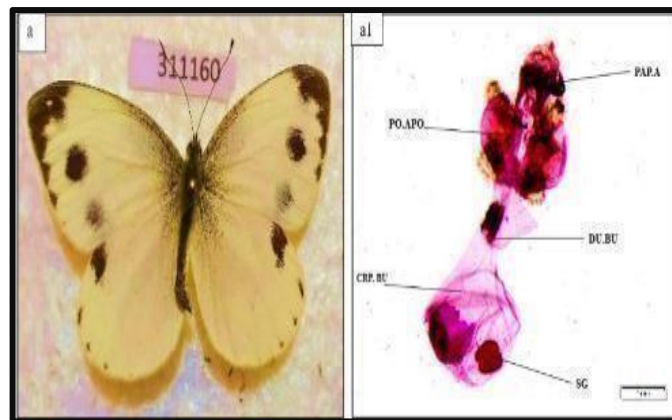


Figure 45a: Dorsal view of *Pieris canidia* (a-a1) illustrating the female genitalia and associated reproductive structures. The figure emphasizes key anatomical features such as the ovipositor, accessory glands, and associated sclerites, which are critical for understanding the reproductive biology, mating strategies, and species-specific adaptations of *P. canidia*.

Male (♂) Genitalia

The uncus is slender, slightly undulating, with a pointed, downward-curved tip, and appears Y-shaped in dorsal view. The tegumen is broad, rectangular in outline dorsally, and exceeds the uncus in length. The vinculum is thin yet strongly sclerotized. The saccus is broad with a rounded distal extremity. The juxta is reduced, cone-like, thin, sclerotized, and bears elongated lateral arms. The valva is broad proximally with sclerotized margins covered in setae, tapering

gradually into a narrow, blunt apex; both the costa and lateral margin are sinuous. The aedeagus is robust, slightly curved, comparatively small, with a sclerotized subzone, a ventral thecal appendage, and the ductus ejaculatorius inserting dorsally (**Figure 45b**).

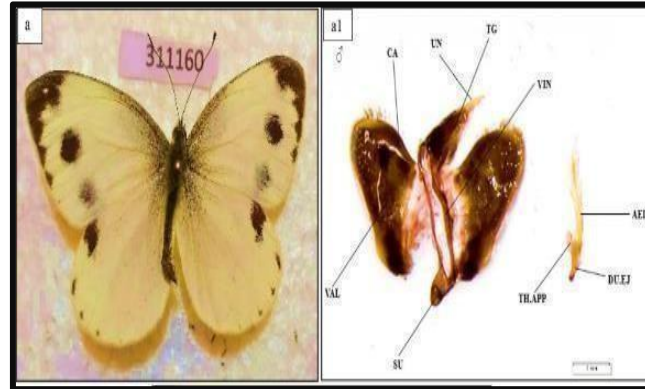


Figure 45b: Dorsal view of *Pieris canidia* (a-a1) showcasing the male genitalia and associated reproductive structures. The illustration highlights key features such as the aedeagus, claspers, and supporting sclerites, which are essential for mating and reproductive success.

Measurements (Mean \pm SE, in mm): Body length 12.85 ± 0.30 ; head length 1.20 ± 0.08 , head width 2.34 ± 0.12 ; thorax length 2.89 ± 0.10 , thorax width 2.90 ± 0.08 ; compound eye length 1.37 ± 0.07 , width 1.75 ± 0.05 ; forewing length 25 ± 1.5 , width 15 ± 0.8 ; hindwing length 20 ± 1.1 , width 16 ± 0.9 ; antenna length 5.84 ± 0.25 ; abdomen length 8.76 ± 0.30 (**Table 15 & 16**).

6. *Pieris brassicae*

P. brassicae (Linnaeus, 1758)

P. brassicae nepalensis Doubleday, 1842

Material examined: J&K India, Collector: Arjumand John, Crop: Cherry.

Distribution: India, Turkey, Southern England and Austria.

Diagnostic Characters:

Female (♀) Genitalia

Posterior Apophysis: Elongated, slender, extends beyond the 8th tergum. Sterigma: Short inner distal lobe-shaped structure, smoothly connected inner basal part. Signum: Cordiform, tapers toward the base, irregularly concave margin (**Figure 46a**).

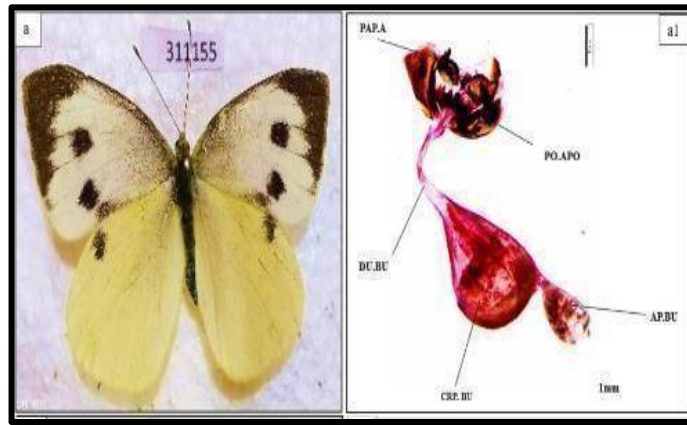


Figure 46a: Dorsal view of *Pieris brassicae* (a-a1) illustrating the female genitalia and associated reproductive structures. The figure highlights key anatomical components, including the ovipositor, accessory glands, and reproductive ducts, providing insights into the reproductive morphology and species-specific adaptations of *P. brassicae*.

Male (♂) Genitalia

The uncus is narrow, slightly curved in lateral view, and V-shaped dorsally. The tegumen is narrow, strongly sclerotised, and also V-shaped in dorsal aspect, with both tegumen and uncus projecting upward. The latero-ventral projections of the tegumen are slender. The vinculum shows sinuous margins. The saccus is sclerotised and curves upward. The appendices angulares are long, heavily sclerotised, broad toward the valva and tapering toward the tegumen. The juxta is conical with sinuous lateral arms. The valva is long, winding, and broad, sparsely clothed with setae, with a concave distal margin and a bifid apex. The aedeagus is relatively short; its subzone is smaller than the suprazone, with a dorsal hump before the midpoint, followed by a constriction and a subsequent swelling that ends in a blunt apex. The thecal appendage is ventral and moderately broad, while the ductus ejaculatorius enters dorsally (Figure 46b).

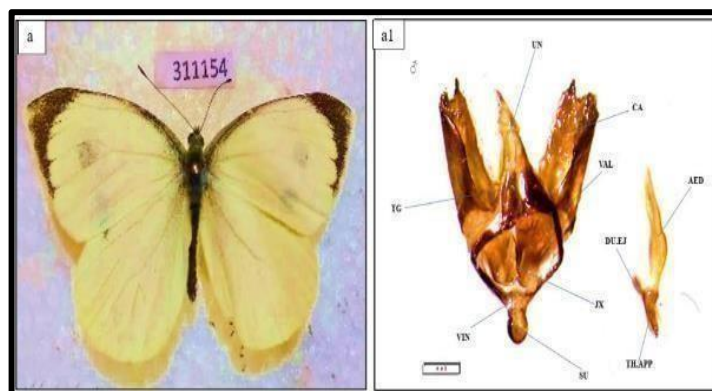


Figure 46b: Dorsal view of *Pieris brassicae* (a-a1) illustrating the male genitalia and associated reproductive structures. The figure highlights key anatomical components, including the uncus, tegumen, vinculum, saccus, appendices angulares, juxta, valva, aedeagus, and thecal appendage, providing insights into the reproductive morphology and species-specific adaptations of *P. brassicae*.

associated reproductive structures. Key anatomical features, including the aedeagus, claspers, and sclerites, are highlighted, emphasizing their roles in mating and reproductive functions.

Measurements (Mean \pm SE, in mm): Body length 12.48 ± 0.28 ; head length 1.35 ± 0.09 , head width 2.08 ± 0.10 ; thorax length 2.90 ± 0.12 , thorax width 3.20 ± 0.08 ; compound eye length 0.91 ± 0.06 , width 2.32 ± 0.07 ; forewing length 40 ± 2.0 , width 28 ± 1.0 ; hindwing length 35 ± 1.5 , width 29 ± 1.2 ; antenna length 6.43 ± 0.30 ; abdomen length 8.23 ± 0.25 (**Table 15 & 16**).

7. *Pontia daplidice*

P. daplidice Linnaeus, 1758

P. daplidice elisa Lucas, 1849

Material examined: J&K India, Collector: Arjumand John, Crop: Cherry.

Distribution: India, Turkey, Southern England and Austria.

Diagnostic Characters:

Male (σ) Genitalia

The tegumen is narrow and elongated posteriorly, appearing oval in dorsal view. The uncus is strongly sclerotised, bifurcated, and Y-shaped dorsally, with a distinct median dilation when observed laterally. The gnathos is slender and only lightly sclerotised. The saccus is moderately long, slightly curved upward, tubular, with a blunt and swollen apex. The vinculum is narrow, longer than the tegumen projections, and convex in outline. The juxta is well developed, elongate, U-shaped, and slit-like. The valvae are broad, obliquely oriented, reaching the tip of the uncus, and terminate in a sickle-shaped pointed hook. The aedeagus is long, somewhat stout, tubular, and blunt at the tip, lacking a vesica, with the ductus ejaculatorius entering dorsally (**Figure 47**).

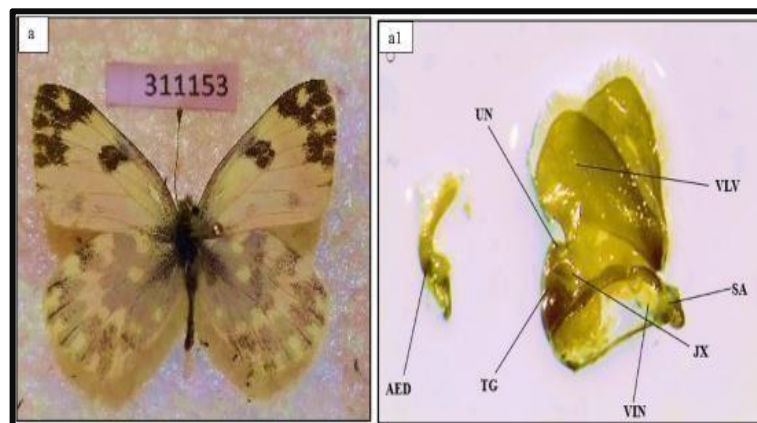


Figure 47: Dorsal view of *Pieris daplidice* (a-a1) highlighting the male genitalia and reproductive structures, showcasing detailed morphological features critical for species

identification and reproductive biology studies.

Measurements (Mean \pm SE, in mm): Body length 8.37 ± 0.25 ; head length 1.05 ± 0.07 , head width 1.42 ± 0.08 ; thorax length 2.14 ± 0.09 , thorax width 2.87 ± 0.07 ; compound eye length 0.87 ± 0.06 , width 1.40 ± 0.05 ; forewing length 25 ± 1.5 , width 14 ± 0.7 ; hindwing length 10 ± 1.0 , width 15 ± 0.8 ; antenna length 5.42 ± 0.25 ; abdomen length 7.32 ± 0.20 (**Table 15 & 16**).

3.16.2. Family: Lycaenidae

The Lycaenidae family, often referred to as gossamer-winged butterflies, is one of the most diverse butterfly families and is characterised by a distinctive array of morphological characters. Their wings are delicate and semi-transparent, lending them an ethereal appearance as they flutter through their habitats. A striking feature is their eyes, which are emarginated close to the antennae. This adaptation enhances visual acuity and aids in navigation (**Figure 48**). The dorsal surface of their wings is lustrous, contributing to their striking appearance. Sexual dimorphism is also evident; males typically possess four walking legs, whereas females have six. This difference influences their mobility and interaction with their environment. Additionally, Lycaenidae butterflies exhibit bifid tarsal claws, providing them with a secure grip on various surfaces and aiding in perching and feeding behaviours. This combination of delicate wings, specialised eyes, lustrous wing surfaces, variable leg count, and bifid tarsal claws exemplifies the remarkable adaptations of the Lycaenidae family to thrive in diverse ecosystems worldwide.

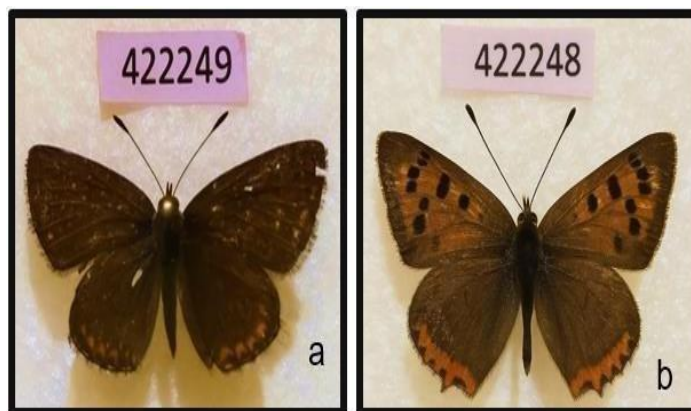


Figure 48: Visual representation of butterfly species from the family Lycaenidae observed during the study. Labeled specimens include: (a) *Polyommatus eros* and (b) *Lycaena phlaeas*.

1. *Polyommatus eros*

P. eros Ochsenheimer, 1808

P. eros eroides (Frivaldszky, 1835)

Material examined: J&K India, Collector: Arjumand John, Crop: Cherry.

Distribution: Europe, Scandinavia to the Mediterranean region.

Diagnostic Characters:

Male (♂) Genitalia

The tegumen is dorsally flattened and projects posteriorly. The uncus is also flattened, longer than the tegumen, Y-shaped in dorsal view, and terminates in a blunt apex. The gnathos is narrow and strongly sclerotised. The saccus is short, slender, obliquely directed, blunt at the tip, and extends backward. The vinculum is narrow, U-shaped ventrally, and longer than the tegumen projection. The juxta is U-shaped and heavily sclerotized. The valvae are large, broad, extend beyond the uncus, and are densely hirsute with long setae. The costa is rounded and broad, while the sacculus is also broad, bearing a basal crest. The aedeagus is long, stout at the base, abruptly narrowing into a pointed, sickle-shaped tip (**Figure 49**).

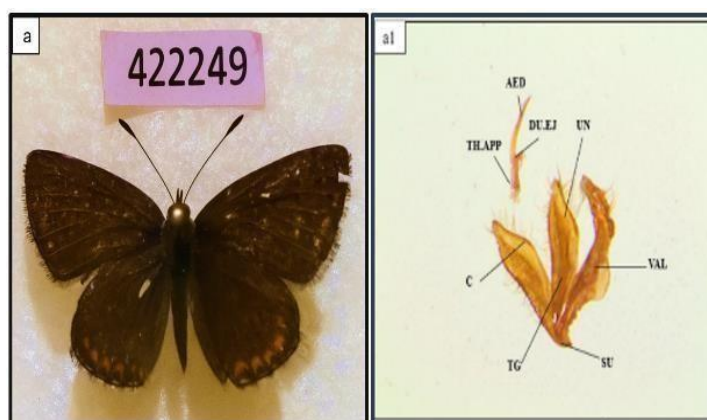


Figure 49: Dorsal view of *Polymmatus eros* (a-a1) highlighting the male genitalia and reproductive structures, illustrating key morphological traits essential for species identification and taxonomic studies.

Measurements (Mean \pm SE, in mm): Body length 6.78 ± 0.20 ; head length 1.73 ± 0.08 , head width 2.34 ± 0.12 ; thorax length 1.79 ± 0.08 , thorax width 2.42 ± 0.07 ; compound eye length 1.48 ± 0.05 , width 1.78 ± 0.06 ; forewing length 18 ± 1.2 , width 10 ± 0.6 ; hindwing length 14 ± 1.0 , width 0.9 ± 0.4 ; antenna length 3.81 ± 0.18 ; abdomen length 2.62 ± 0.12 (**Table 15 & 16**).

2. *Lycaena phlaeas*

L. phlaeas (Linnaeus, 1761)

L. phlaeas americana Edwards, 1861

L. phlaeas hypophlaeas Boisduval, 1852

Material examined: J&K India, Collector: Arjumand John, Crop: Cherry.

Distribution: Europe, Asia, and North Africa.

Diagnostic Characters:

Male (♂) Genitalia

The tegumen is slender, extending posteriorly, and appears oval in dorsal aspect. The uncus is strongly sclerotised, Y-shaped when viewed dorsally, and shows a median dilation in lateral view. The gnathos is narrow and only lightly sclerotised. The saccus is of moderate length, slightly curved upward, tubular, and terminates in a swollen, blunt apex. The vinculum is narrow, convex, and longer than the tegumen projections. The juxta is conspicuous, elongate, U-shaped, and slit-like. The valvae are broad, obliquely oriented, reaching the tip of the uncus, and extend into a heavily sclerotised, sickle-shaped, pointed hook. The aedeagus is long, somewhat stout, tubular, with a blunt apex, lacking a vesica, and with the ductus ejaculatorius inserting dorsally (**Figure 50**).

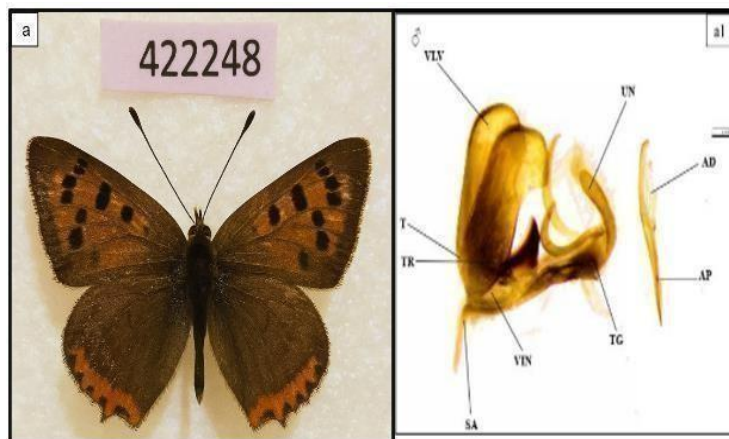


Figure 50: Dorsal view of *Lycaena phlaeas* (a-a1) male genitalia showing key reproductive structures. The illustration highlights critical morphological traits essential for accurate species identification and taxonomic analysis.

Measurements (Mean \pm SE, in mm): Body length 5.50 ± 0.25 ; head length 1.20 ± 0.08 , head width 2.11 ± 0.10 ; thorax length 1.89 ± 0.07 , thorax width 2.34 ± 0.06 ; compound eye length 1.23 ± 0.06 , width 1.87 ± 0.04 ; forewing length 14 ± 1.0 , width 10 ± 0.5 ; hindwing length 13 ± 0.8 , width 10 ± 0.5 ; antenna length 3.56 ± 0.20 ; abdomen length 2.41 ± 0.10 (**Table 15 & 16**).

3.16.3. Family: Nymphalidae

The Nymphalidae family, renowned for its diversity and beauty, presents a fascinating array of features that distinguish it in the butterfly world (**Figure 51**). One characteristic peculiarity is found in their antennae; the ventral surface typically bears tricarinate structures with three longitudinal ridges. These ridges provide structural support and also serve an important sensory

function, assisting in the detection of environmental stimuli and chemical cues. Furthermore, some species in this varied family only have four walking legs. These represent a significant difference from the typical six-legged condition found in insects. Despite this variance, butterflies of the Nymphalidae family are most highly adaptable to their surroundings, using their unique characteristics to move efficiently, feed on diverse floral resources and engage with their surroundings. The Nymphalidae family's ecological success and evolutionary adaptability across a broad range of habitats and geographical regions are reflected in their combination of tricarinate antennae and variable leg count.

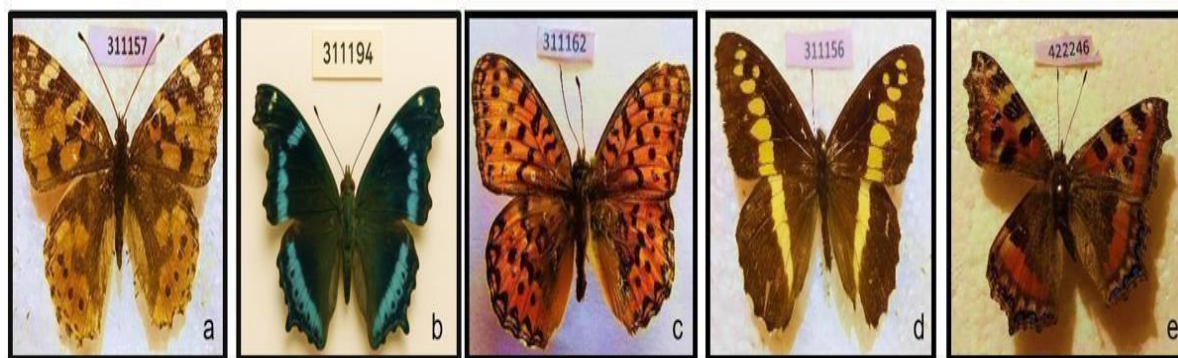


Figure 51: Visual representation of butterfly species from the family Nymphalidae observed during the study. Labeled specimens include: (a) *Vanessa cardui*, (b) *Nymphalis canace*, (c) *Argyreus hyperbius*, (d) *Nymphalis polychloros*, and (e) *Aulocera saraswati*.

1. *Vanessa cardui*

V. cardui (Linnaeus, 1758)

V. cardui kershawi McCoy, 1868

Material examined: J&K India, Collector: Arjumand John, Crop: Cherry.

Distribution: India, Turkey, Southern England and Austria.

Diagnostic Characters:

Male (♂) Genitalia

The tegumen is extended posteriorly, broad, and somewhat rectangular in dorsal view. The uncus is straight, longer than the tegumen, broad at the base, narrowing into a blunt tip, Y-shaped in dorsal aspect, and tubular in lateral view. The gnathos is narrow, strongly sclerotized, and concave. The saccus is short, thin, tubular, well sclerotized, directed obliquely upward, and terminates in a blunt apex. The vinculum is broad, U-shaped ventrally, and much longer than the tegumen projection. The juxta is heavily sclerotized and U-shaped. The valvae are large, broad, extending beyond the uncus, strongly sclerotized, and covered with long setae. Both the

costa and sacculus are simple. The aedeagus is long, stout at the base, abruptly narrowing after two-thirds of its length, ending in a pointed apex, heavily sclerotized, and acutely curved into a sickle-like shape. The vesica is absent, and the ductus ejaculatorius enters dorsally (**Figure 52**).



Figure 52: Dorsal view of *Vanessa cardui* (a-a1) male genitalia, highlighting key reproductive structures. The figure illustrates essential morphological traits used for accurate species identification and taxonomic classification.

Measurements (Mean \pm SE, in mm): Body length 10.72 ± 0.25 ; head length 1.04 ± 0.06 , head width 2.47 ± 0.10 ; thorax length 2.56 ± 0.08 , thorax width 2.76 ± 0.08 ; compound eye length 1.05 ± 0.05 , width 1.40 ± 0.04 ; forewing length 35 ± 1.8 , width 16 ± 0.8 ; hindwing length 26 ± 1.3 , width 21 ± 1.2 ; antenna length 6.94 ± 0.30 ; abdomen length 7.12 ± 0.25 (**Table 15 & 16**).

2. *Nymphalis canace*

N. canace (Linnaeus, 1763)

N. canace drilon Fruhstorfer, 1912

N. canace haronica Moore, 1872

N. canace canacides Fruhstorfer, 1899

Material examined: J&K India, Collector: Arjumand John, Crop: Cherry.

Distribution: North America, Europe, and Asia.

Diagnostic Characters:

Male (σ) Genitalia

The tegumen is heavily sclerotised, convex, and extends posteriorly, appearing wide and rectangular in dorsal view. The uncus is straight, equal in length to the tegumen, broad at the base, tapering to a blunt V-shaped apex dorsally, and tubular in lateral aspect. The gnathos is strongly sclerotised and appears horn-like in dorsal view. The saccus is short, slender, tubular,

well-sclerotised, directed obliquely upward, and terminates in a slightly swollen, blunt tip. The vinculum is moderately broad throughout its length, U-shaped ventrally, and longer than the tegumen projection. The juxta is U-shaped and sclerotised. The valvae are large, broad, not extending beyond the uncus tip, strongly sclerotised, and clothed with long setae. Both the costa and sacculus are simple. The ampulla is simple with a blunt apex. The aedeagus is long, stout at the base, narrowing abruptly beyond two-thirds of its length into a sharp, pointed tip, robust, strongly sclerotised, and deeply curved (**Figure 53**).

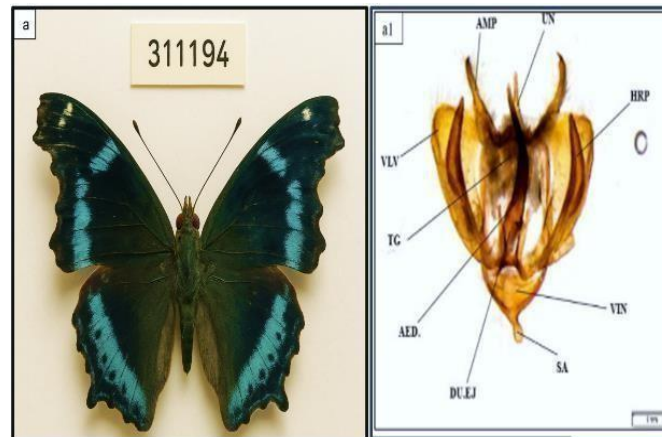


Figure 53: Dorsal view of *Nymphalis canace* (a-a1) male genitalia, highlighting key reproductive structures. The figure illustrates critical morphological features essential for species identification and taxonomic studies.

Measurements (Mean \pm SE, in mm): Body length 12.77 ± 0.28 ; head length 1.76 ± 0.08 , head width 2.87 ± 0.14 ; thorax length 2.67 ± 0.11 , thorax width 2.90 ± 0.07 ; compound eye length 1.89 ± 0.06 , width 2.97 ± 0.05 ; forewing length 29 ± 1.4 , width 17 ± 0.7 ; hindwing length 22 ± 1.1 , width 16 ± 0.9 ; antenna length 5.41 ± 0.20 ; abdomen length 8.34 ± 0.25 (**Table 15 & 16**).

3. *Argyreus hyperbius*

A. hyperbius (Linnaeus, 1763)

A. hyperbius taprobana Moore, 1881

A. hyperbius castetsi Fruhstorfer, 1906

Material examined: J&K India, Collector: Arjumand John, Crop: Cherry.

Distribution: East Asia, Southeast Asia, and the Indian subcontinent.

Diagnostic Characters:

Male (σ) Genitalia

The tegumen is subtriangular in lateral view, strongly sclerotized, dorsally elongated, with a curved angular apex; its anterior arm is nearly equal in length and width. The vinculum is robust in lateral aspect, with only a faintly developed apical process, and is inconspicuous in ventral view. The saccus is nearly straight. The lateral transtilla is triangular with a broad base. The base of the uncus shows a distinct dorsoventral constriction and is fused to the tegumen. The aedeagus bears a thickened distal process, with the posterior portion stout and gradually tapering. The juxta is thin on the ventral side (**Figure 54**).

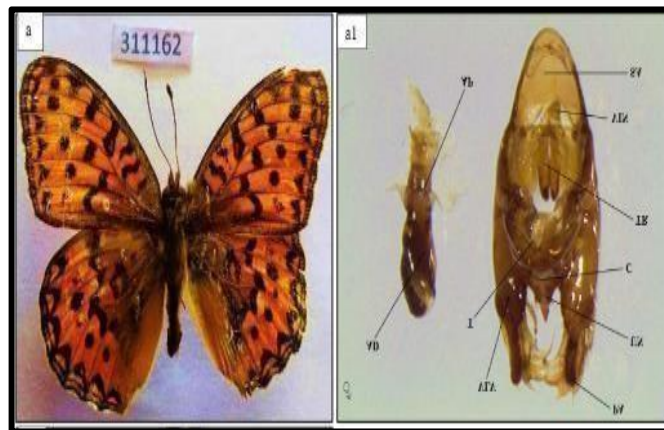


Figure 54: Dorsal view of *Argyreus hyperbius* (a-a1) male specimen highlighting the genitalia and associated reproductive structures. The image illustrates key morphological features, including the shape and sclerotization patterns of the uncus, valvae, and aedeagus, which are essential for accurate species identification and taxonomic studies.

Measurements (Mean \pm SE, in mm): Body length 12.25 ± 0.30 ; head length 1.79 ± 0.10 , head width 2.86 ± 0.15 ; thorax length 2.34 ± 0.12 , thorax width 2.67 ± 0.08 ; compound eye length 1.65 ± 0.07 , width 2.32 ± 0.05 ; forewing length 30 ± 1.5 , width 20 ± 1.0 ; hindwing length 28 ± 1.5 , width 18 ± 1.0 ; antenna length 5.34 ± 2.5 ; abdomen length 8.12 ± 0.30 (**Table 15 & 16**).

4. *Nymphalis polychloros*

N. polychloros (Linnaeus, 1758)

N. polychloros tibetana Riley, 1921

Material examined: J&K India, Collector: Arjumand John, Crop: Cherry.

Distribution: India, Turkey, Southern England and Austria.

Diagnostic Characters:

Male (σ) Genitalia

The saccus is elongated. The tegumen is short and rounded. The gnathos is long, pointed, and

directed upward. The uncus is elongate in dorsal view, with lateral extensions giving it an arrowhead-like appearance. The valvae are long, terminating in a protuberance that extends into a slender, pointed projection. The aedeagus is curved and lacks cornuti. The juxta is sclerotized and functions to connect the valvae (**Figure 55**).

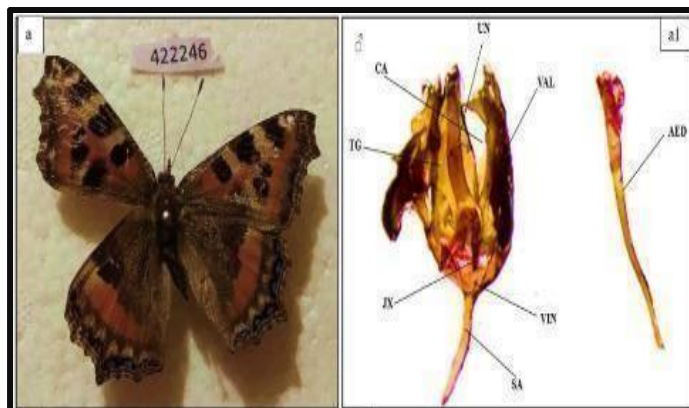


Figure 55: Dorsal view of *Nymphalis polychloros* (a-a1) male specimen highlighting the genitalia and reproductive structures. The image illustrates key morphological traits, including the shape and structure of the uncus, valvae, and aedeagus, which are essential for accurate species identification and taxonomic studies.

Measurements (Mean \pm SE, in mm): Body length 14.19 ± 0.30 ; head length 2.12 ± 0.08 , head width 3.24 ± 0.14 ; thorax length 2.86 ± 0.11 , thorax width 3.21 ± 0.09 ; compound eye length 2.11 ± 0.07 , width 2.87 ± 0.06 ; forewing length 31 ± 1.7 , width 18 ± 0.8 ; hindwing length 25 ± 1.2 , width 20 ± 1.1 ; antenna length 6.31 ± 0.30 ; abdomen length 9.21 ± 0.25 (**Table 15 & 16**).

5. *Aulocera saraswati*

A. saraswati (Kollar, 1844)

A. padma Kollar, 1844

A. saraswati garhwalensis Tytler, 1914

Material examined: J&K India, Collector: Arjumand John, Crop: Cherry.

Distribution: India, Nepal, Bhutan, and parts of Southeast Asia.

Diagnostic Characters:

Male (♂) Genitalia

The uncus is subtriangular. The transtilla is incomplete medially. The juxta is crescentic, resembling a half-moon. The vinculum is rounded ventrally. The valva tapers distally, with a weakly inflated basal costa. The sacculus is inflated, bearing dorsal spinules, with its distal portion carrying a small cluster of dorsal spines at the base. The editum basal pad forms a crest of 8–12 dorsally directed scales, accompanied by a narrow ventral process. The phallus has a

broad apex with three roughly serrated notches, while the vesica bears two slender, spiniform cornuti (Figure 56).



Figure 56: Dorsal view of *Aulocera saraswati* (a-a1) male specimen highlighting the genitalia and reproductive structures. The image illustrates key morphological features such as the shape of the uncus, valvae, and aedeagus, which are critical for accurate species identification and taxonomic differentiation.

Measurements (Mean \pm SE, in mm): Body length 14.65 ± 0.35 ; head length 2.33 ± 0.10 , head width 3.22 ± 0.15 ; thorax length 2.98 ± 0.12 , thorax width 3.30 ± 0.10 ; compound eye length 2.13 ± 0.08 , width 2.90 ± 0.06 ; forewing length 35 ± 1.8 , width 17 ± 0.8 ; hindwing length 26 ± 1.3 , width 21 ± 1.2 ; antenna length 7.64 ± 0.35 ; abdomen length 9.34 ± 0.30 (Table 15 & 16).

3.17. Wing Venation in Lepidopteran Taxonomy and Morphological Analysis

Wing venation is a fundamental morphological feature that plays a crucial role in the taxonomy, phylogenetics, and functional interpretation of Lepidoptera. The arrangement and structure of veins provide stable and diagnostic characters that are widely used to differentiate between families, genera, and species. Typically, butterfly wings possess a characteristic network of longitudinal veins: costa (C), subcosta (Sc), radius (R), media (M), cubitus (Cu), and anal veins (A) interconnected by cross-veins forming closed or open cells, such as the discal cell. Variations in vein number, branching patterns, fusion, and termination points are often species-specific and remain relatively constant across environmental conditions, making them highly reliable for taxonomic identification. Wing venation is particularly valuable in lepidopteran systematics because external wing colouration and patterning are often influenced by seasonal variation, sexual dimorphism, and ecological factors, whereas venational characters remain evolutionarily conserved. Features such as the fusion of veins (e.g., Sc+R₁), branching of the radial sector (Rs), and the configuration of median and cubital veins are widely used to

distinguish closely related taxa and to resolve cryptic species complexes (Kristensen 2003). In addition, venation patterns provide insights into phylogenetic relationships, as they reflect evolutionary modifications associated with flight mechanics and ecological adaptation. The study of wing venation also contributes to understanding functional morphology, as vein arrangement influences wing rigidity, flexibility, and aerodynamic efficiency during flight. Consequently, venation-based analysis is extensively employed in integrative taxonomic studies, often in combination with morphometric and molecular approaches, to achieve robust species delimitation and evolutionary interpretation (Scoble 1995; Mutanen et al. 2010). Thus, wing venation remains a cornerstone in lepidopteran systematics and continues to play a pivotal role in both classical and modern taxonomic research.

1. *Colias electo*

C. electo has distinctive venation patterns on the forewing and hindwing, which are needed to perform morphometric analysis and taxonomic identification. In the hindwing (left panel), the radial sector (Rs) is visible, as is the fused Sc + R1 (subcosta and first radius), the 1A+2A (first anal vein), the 3A (second anal vein), the Cu1a (first cubitus), the Cu1b (second cubitus), the M3, M2 and M1 (third, second, and first median veins respectively). The forewing (right wing) bears a different venation pattern of 1A+2A, Cu1b, Cu1a, M3, M2, M1, accessory radial series of R5, R4, R3, R2, R1, subcosta (Sc) and radial sector (Rs). A scale bar of 5 mm (shown on both wings) eases the reference of dimensionality (**Figure 57**). The accurate definition of these veins ensures the correct species demarcation at the species level in *Colias*, and it also provides good comparative morphometric markers among the entire family of Pieridae.

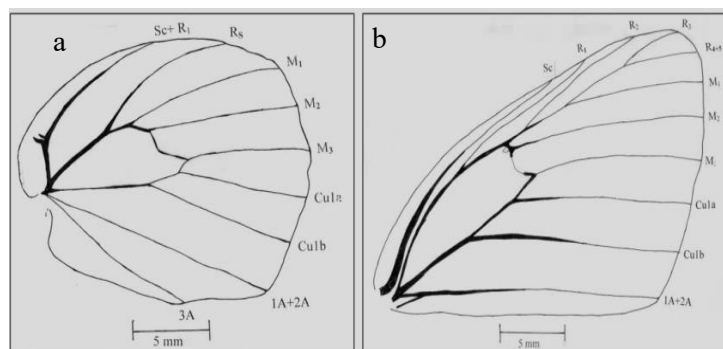


Figure 57: Detailed venation patterns of the forewing and hindwing of *Colias electo*, highlighting key structural veins used in taxonomic identification and morphometric evaluation. a: hindwing with 1A+2A, 3A, Cu1a, Cu1b, M3, M2, M1, Rs, and fused Sc + R1. b: forewing with 1A+2A, Cu1b, Cu1a, M3, M2, M1, radial series (R5-R1), Sc, and Rs.

2. *Pieris canidia*

The forewing and hindwing venation of *P. canidia* also has different structural features that are important to differentiate taxonomically and to use in morphometrical comparisons. In the forewing (on the left), major veins are also distinct, with 1A+2A, first anal, Cu1b, second cubitus, Cu1a, first cubitus, M3, M2, and M1, the radial sector Rs, and the radial series R1-R5, the subcosta Sc (**Figure 58**). There are 1A+2A, 3A (second anal vein), Cu1b, Cu1a, M3, M2, M1, Rs, and an accentuated precostal vein (PV) as shown in the hindwing (right panel). The conspicuous radial branching and characteristic discal cell shapes are good diagnostic features that can be used to differentiate *P. canidia* and closely related species of Pieridae. A 5 mm scale bar is used to depict both wings in the illustration to make morphometric interpretation easy.

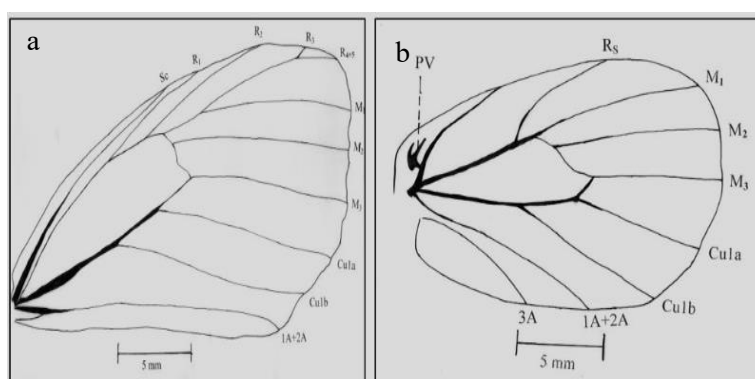


Figure 58: Detailed venation patterns of the forewing and hindwing of *Pieris canidia*, displaying detailed venation used for taxonomic differentiation and morphometric analysis. a: forewing with 1A+2A, Cu1b, Cu1a, M3-M1, Rs, radial series (R1-R5), and Sc. b: hindwing with 1A+2A, 3A, Cu1b, Cu1a, M3-M1, Rs, and PV.

3. *Nymphalis polychloros*

Forewing and hindwing of *N. polychloros* exhibit a complex venation structure that is essential for morphometric evaluation and species-level identification within the Nymphalidae. The radial series (R1-R5), the radial sector (Rs), the subcosta (Sc), the first anal vein (1A+2A), the second cubitus (Cu1b), the first cubitus (Cu1a), the third to first median veins (M3, M2, and M1), and the radial series (R1-R5) form a complex and diagnostically useful venation pattern in the forewing (left panel). In addition to the well-defined upper (UDC), middle (MDC), and lower (LDC) discocellulars and a conspicuous precostal vein (PV), the hindwing (right panel) displays 1A+2A, 3A (second anal vein), Cu1b, Cu1a, M3, M2, M1, Rs, and fused Sc+R1 (**Figure 59**). The distinctive arrangement of discocellular veins combined with the pronounced

radial sector is characteristic of the genus *Nymphalis*. Both wings are illustrated with a 5 mm scale bar to aid in comparative morphometric analysis across Nymphalid taxa.

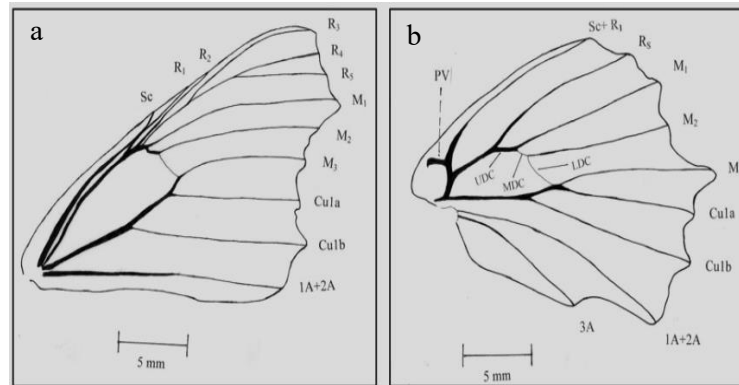


Figure 59: Forewing and hindwing venation of *Nymphalis polychloros*, showing key veins for species identification and morphometric analysis. a: forewing with 1A+2A, Cu1b, Cu1a, M3-M1, radial series (R1-R5), Rs, and Sc. b: hindwing with 1A+2A, 3A, Cu1b, Cu1a, M3-M1, Rs, fused Sc+R1, discocellulars (UDC, MDC, LDC), and PV.

4. *Aulocera saraswati*

The forewing and hindwing of *A. saraswati* have strong venation patterns, which are diagnostic of recognition in the subfamily Satyrinae (family Nymphalidae). The longitudinal veins that are prominent in the forewing (left panel) are: 1A+2A (first anal vein), Cu1b (second cubitus), Cu1a (first cubitus) and M3, M2, and M1 (median veins), R5-R1 (fifth to first radius), radial sector (Rs), the subcosta, (Sc) and a distinct discal cell (DC). The marginal structures are also named (A-D) to help with the orientation of the structures (**Figure 60**), including the costa, termen, tornus, and the inner margin. The hindwing (right panel) shows 1A+2A, 3A (second anal vein), Cu1b, Cu1a, M3, M2, M1, Rs, and fused Sc+R1, precostal vein (PV) and separate discocellulars upper (UDC), middle (MDC) and lower (LDC). The dense, well-developed venation, especially the discocellular pattern, presents stable characters with the ability to distinguish *A. saraswati* from other species of satyrines. The 5 mm scale bars on both wings are used to provide morphometric evaluation.

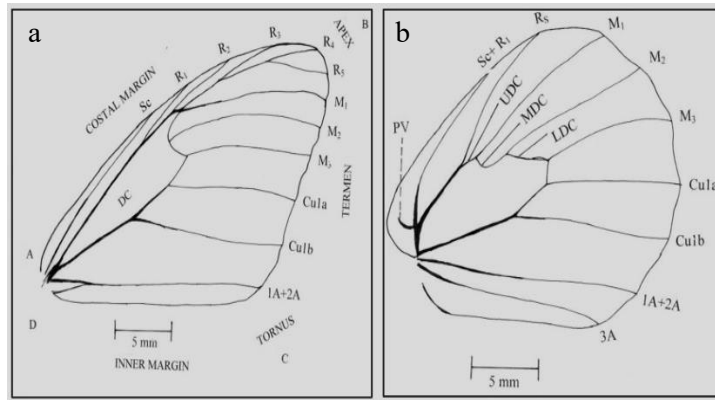


Figure 60: Forewing and hindwing venation of *Aulocera saraswati* showing key veins for identification within Satyrinae. a: forewing with 1A+2A, Cu1b, Cu1a, M3-M1, R5-R1, Rs, Sc, and DC; marginal parts (A-D) labeled. b: hindwing with 1A+2A, 3A, Cu1b, Cu1a, M3-M1, Rs, Sc+R1, PV, and discocellulars (UDC, MDC, LDC).

5. *Colias philodice*

The forewing and hindwing of *C. philodice* display a venation arrangement that is highly diagnostic for species-level identification and comparative morphometric evaluation within the Pieridae. In the forewing (left panel), venation is well defined, comprising 1A+2A (first anal vein), Cu1b (second cubitus), Cu1a (first cubitus), M3, M2, and M1 (median veins), Rs+R4 (radial sector and fourth radius fused), R3, R2, R1, and Sc (subcosta), with R5 positioned near the apex. The hindwing (right panel) bears 1A+2A, 3A (second anal vein), Cu1b, Cu1a, M3, M2, M1, Rs, and fused Sc+R1, radiating from the wing base. The configuration of radial and median veins, particularly the close clustering of Rs and R1 in both wings, is a distinctive feature of *C. philodice*, facilitating its separation from closely related congeners (**Figure 61**). Both wings are illustrated with a 5 mm scale bar to support morphometric comparison and venation-based taxonomic classification.

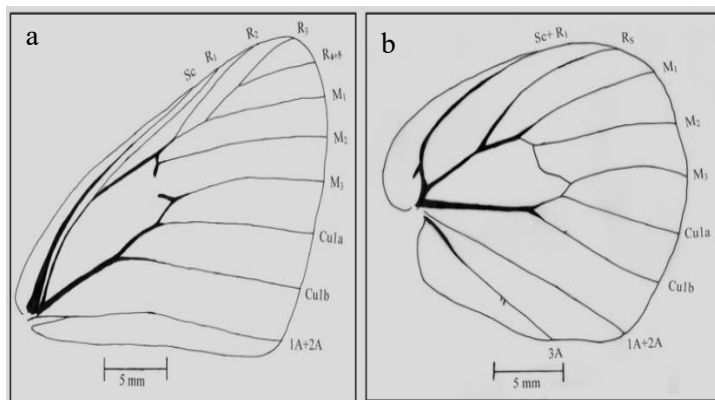


Figure 61: Forewing and hindwing venation of *Colias philodice*, showing key veins for species

identification and morphometric analysis. a: forewing with 1A+2A, Cu1b, Cu1a, M3-M1, Rs+R4, R3-R1, Sc, and R5 near apex. b: hindwing with 1A+2A, 3A, Cu1b, Cu1a, M3-M1, Rs, and fused Sc+R1.

6. *Pontia daplidice*

The forewing and hindwing of *P. daplidice* exhibit distinct venation features that are important for taxonomic identification and morphometric assessment within the family Pieridae. In the forewing (left panel), major veins include 1A+2A (first anal vein), Cu1b (second cubitus), Cu1a (first cubitus), M3, M2, and M1 (median veins), Rs+R4 (radial sector fused with fourth radius), R3, R2, R1, and Sc (subcosta), forming a characteristic pierid radial branching arrangement. The hindwing (right panel) displays 1A+2A, 3A (second anal vein), Cu1b, Cu1a, M3, M2, M1, Rs, and fused Sc+R1, with the precostal vein (PV) visible near the wing base (**Figure 62**). The pronounced development of radial veins, coupled with the alignment of median and cubital branches, provides diagnostic traits for distinguishing *P. daplidice* from closely related congeners. Both wings are illustrated with 5 mm scale bars to support accurate morphometric comparisons in lepidopteran wing studies.

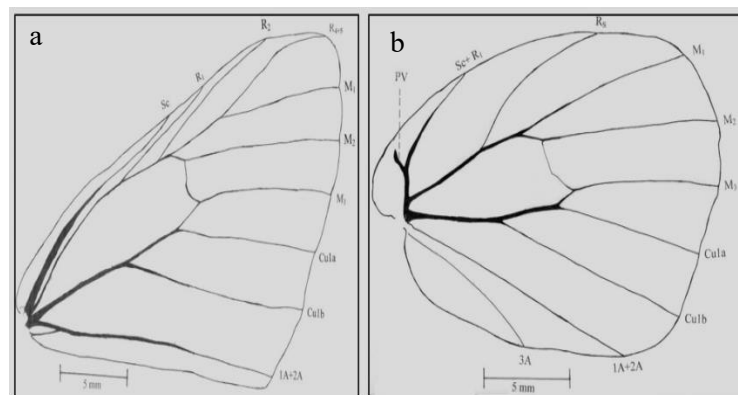


Figure 62: Forewing and hindwing venation of *Pontia daplidice* showing key veins for taxonomic and morphometric analysis. a: forewing with 1A+2A, Cu1b, Cu1a, M3-M1, Rs+R4, R3-R1, and Sc. b: hindwing with 1A+2A, 3A, Cu1b, Cu1a, M3-M1, Rs, Sc+R1, and PV.

7. *Gonepteryx rhamni*

The forewing and hindwing of *G. rhamni* exhibit distinct venation features that are critical for species identification and comparative morphometric analysis within the Pieridae. In the forewing (left panel), key veins include 1A+2A (first anal vein), Cu1b (second cubitus), Cu1a (first cubitus), M3, M2, and M1 (median veins), Rs+R4 (radial sector with fourth radius), R3, R2, R1, and Sc (subcosta). The hindwing (right panel) displays 1A+2A, 3A (second anal vein),

Cu1b, Cu1a, M3, M2, M1, Rs, and fused Sc+R1. Both wings possess well-defined, gently curved venation and slightly angular outer margins, traits that are characteristic of *G. rhamni* and aid in distinguishing it from related species (**Figure 63**). A 5 mm scale bar in each panel provides a reference for precise morphometric comparisons, reinforcing the value of venation as a tool in both taxonomic and ecological assessments.

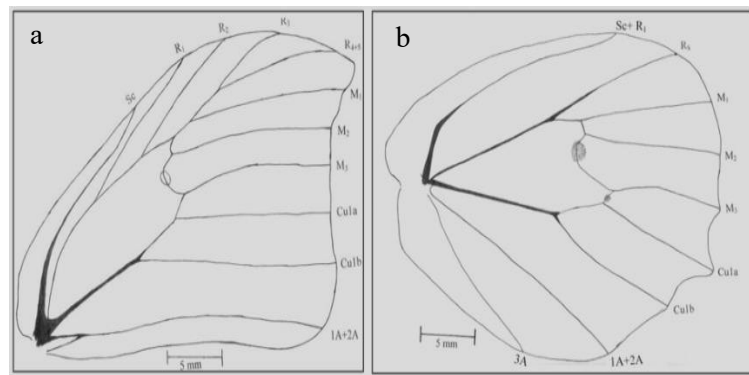


Figure 63: Forewing and hindwing venation of *Gonepteryx rhamni* showing key veins for species identification and morphometric analysis. a: forewing with 1A+2A, Cu1b, Cu1a, M3-M1, Rs+R4, R3-R1, and Sc. b: hindwing with 1A+2A, 3A, Cu1b, Cu1a, M3-M1, Rs, and Sc+R1.

8. *Colias erate*

Forewing and hindwing of *C. erate* with particular venation patterns that are important both in identifying species at the species level and morphometric differentiation in *Colias* (family Pieridae). The forewing (left panel) has a very clear veins that are 1A+2A (1 st Anal Vein), Cu1b (2 nd Cubitus), Cu1a (1 st Cubitus), M3, M2, M1 (Median veins), Rs +R4 +5 (Radial Sector fused with 4 th Radius 5 th Radius), R3, R2, R1, and Sc (Subcosta). The hindwing (right panel) is marked with 1A +2A, 3A (2nd Anal Vein), Cu1b, Cu1a, M3, M2, M1, Rs, and the fused Sc +R1, all emanating clearly out of the wing base (**Figure 64**). *C. erate* has the characteristic tight radial convergence and well-spaced median veins, and it is possible to distinguish between them and their relatives. Each wing has a 5 mm scale bar that allows the accurate evaluation of the morphometrical and taxonomic conditions.

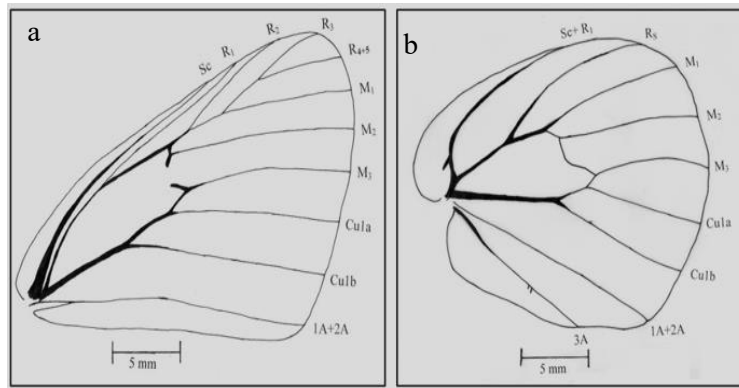


Figure 64: Forewing and hindwing of *Colias erate* showing key venation for species identification within Pieridae. Forewing (a) includes 1A+2A, Cu1b, Cu1a, M3-M1, Rs+R4+5, R3-R1, and Sc; hindwing (b) features 1A+2A, 3A, Cu1b, Cu1a, M3-M1, Rs, and Sc+R1. Tight radial convergence and evenly spaced medians are diagnostic of *C. erate*.

9. *Lycaena phlaeas*

The forewing and hindwing of *L. phlaeas* have a fine venation structure that is critical in the identification of taxa and the morphometric evaluation of the family Lycaenidae. The forewing (1st left panel) has key longitudinal veins that include 1A+2A (1st Anal Vein), Cu1b (2nd cubitus), Cu1a (1st cubitus), M3, M2, M1 (Median veins), R5, R4, R3 (Radial branches), R1, and Sc (Subcosta). The smaller size and shortness of the discal cell and the structure of the radial series embody the property of smaller wings and rapid flight of Lycaenid butterflies. The hindwing (right panel) is also a similarly precise venation pattern, with the three discocellular veins Upper (UDC), Middle (MDC) and Lower (LDC) constituting a typical and diagnostic structural arrangement, 1A+2A, 3A (2nd Anal Vein), Cu1b, Cu1a, M3, M2, M1, Rs (Radial Sector), a fused Sc+R1 (**Figure 65**). The complex structure of the discocellulars and the closely spaced radial branches are credible characteristics that distinguish *L. phlaeas* from other sympatric species of Lycaenids. Each wing has 5 mm scale bars to offer an accurate morphometric comparison and proportional evaluation in lepidopteran studies.

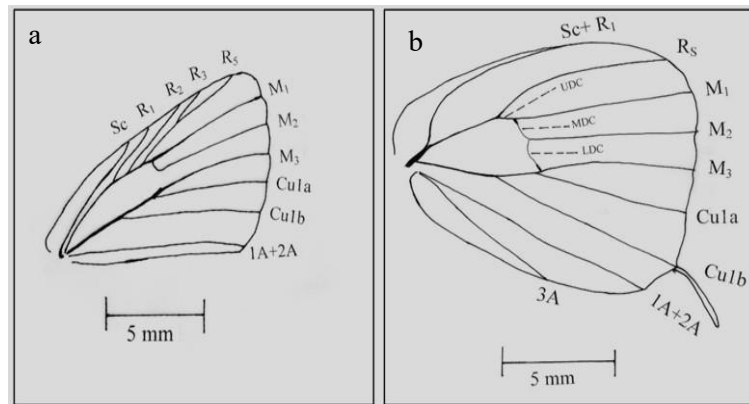


Figure 65: Forewing and hindwing of *Lycaena phlaeas* exhibit venation patterns that are crucial for morphometric study and taxonomic identification within the Lycaenidae. (a); 1A+2A, Cu1b, Cu1a, M3, M2, M1, R5-R3, R1, and Sc are all present in the forewing, which has a compact discal region that is characteristic of Lycaenids. (b); 1A+2A, 3A, Cu1b, Cu1a, M3, M2, M1, Rs, Sc+R1, and the discocellulars UDC, MDC, and LDC are seen in the hindwing.

10. *Pieris brassicae*

Within the Pieridae family, *P. brassicae* forewing and hindwing have a distinct venation architecture that provides a solid foundation for taxonomic identification and in-depth morphometric analysis. The main longitudinal veins in the forewing (left panel) are clearly visible. These include the 1A+2A (1st Anal Vein), Cu1b (2nd Cubitus), Cu1a (1st Cubitus), and the median series M3, M2, and M1. The radial system makes up Rs+R4+5 (Radial Sector fused with the 4th and 5th Radius), R3, R2, R1, and Sc (Subcosta). With uniformly spaced medians and a strong radial alignment, this arrangement creates the distinctive pierid radial branching pattern. In addition to a well-defined PV (Precoastal Vein/spur), the hindwing (right panel) shows 1A+2A, 3A (2nd Anal Vein), Cu1b, Cu1a, M3, M2, M1, Rs, and the fused Sc+R1 (**Figure 66**). One characteristic that sets *P. brassicae* apart is the broad distribution of the radial and median branches, as well as the smooth, arched path of Sc+R1 and Rs. To ensure precise proportional evaluation for comparative morphometric studies and to discern minute interspecific variations within Pieridae, both wings are equipped with 5 mm scale bars.

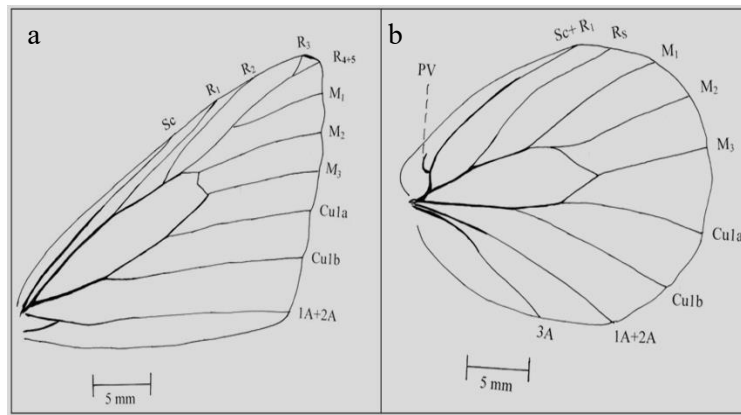


Figure 66: Forewing and hindwing of *Pieris brassicae* showing venation patterns for taxonomic identification and morphometric analysis. The forewing (a) features 1A+2A, Cu1b, Cu1a, M3-M1, Rs+R4+5, R3-R1, and Sc; the hindwing (b) includes 1A+2A, 3A, Cu1b, Cu1a, M3-M1, Rs, Sc+R1, and PV. The spacious radial and median branching, with the arched Sc+R1 and Rs, is characteristic of the species.

11. *Argynnis hyperbius*

The forewing of *A. hyperbius* exhibits a clearly defined venation pattern consisting of 1A+2A (1st Anal Vein), Cu1b (2nd Cubitus), Cu1a (1st Cubitus), M3, M2, M1 (Median veins), and a complete radial series (R5, R4, R3, R2, R1) arising from the Radial Sector (Rs), along with the Subcosta (Sc). The elongated discal cell, bounded by distinct crossveins, is a prominent feature typical of nymphalid butterflies and serves as an important reference in morphometric evaluations. The hindwing displays venation comprising 1A+2A, 3A (2nd Anal Vein), Cu1b, Cu1a, M3, M2, M1, Rs, and the fused Sc+R1, radiating in a balanced arrangement from the wing base (**Figure 67**). Its broad, rounded outline with evenly spaced veins is characteristic of *A. hyperbius*, facilitating distinction from related fritillary species. Both wings are accompanied by 5 mm scale bars to ensure precision in morphometric and taxonomic studies.

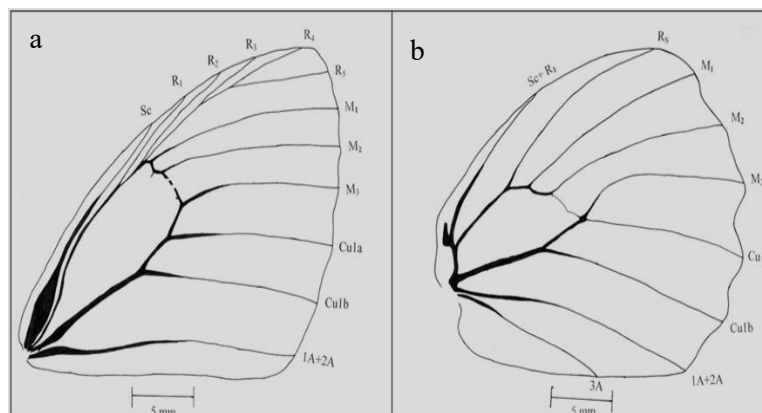


Figure 67: Venation patterns on the forewing and hindwing of *Argynnis hyperbius* are crucial for morphometric analysis and species identification within the Nymphalidae. 1A+2A, Cu1b, Cu1a, M3-M1, R5-R1, Rs, and Sc are present in the forewing (a), which also has an elongated discal cell surrounded by crossveins. In the hindwing (b), 1A+2A, 3A, Cu1b, Cu1a, M3-M1, Rs, and fused Sc+R1 are shown. The species is characterized by evenly spaced veins and a broad hindwing shape.

12. *Nymphalis canace*

It is necessary to identify *N. canace* forewing and hindwing by the unique pattern of venation used to compare morphometric evaluation with precise taxonomical identification of the Nymphalidae family. The forewing is marked by clearly defined longitudinal veins, which include 1A+2A (1st Anal Vein), Cu1b (2nd Cubitus), Cu1a (1st Cubitus), M3, M2, M1 (Median veins), R5, R4, R3, R2, R1 (Radial branches), Rs (Radial Sector) and Sc (Subcosta) in the left panel. These veins form, as is usual with nymphalid butterflies, a rather narrow discal cell, in which the radial series are closely spaced (**Figure 68**). The hindwing in the right panel depicts a rounded venation structure comprising 1A +2A, 3A (2 nd Anal Vein), Cu1b, Cu1a, M3, M2, M1, Rs, and a fused Sc +R1. These smaller dimensions of the hindwing and convergent venation are characteristics of *N. canace* special adaptations to flight, including agility. To do this properly on morphometric comparisons and quantitative analysis between related taxa, both panels have 5 mm scale bars.

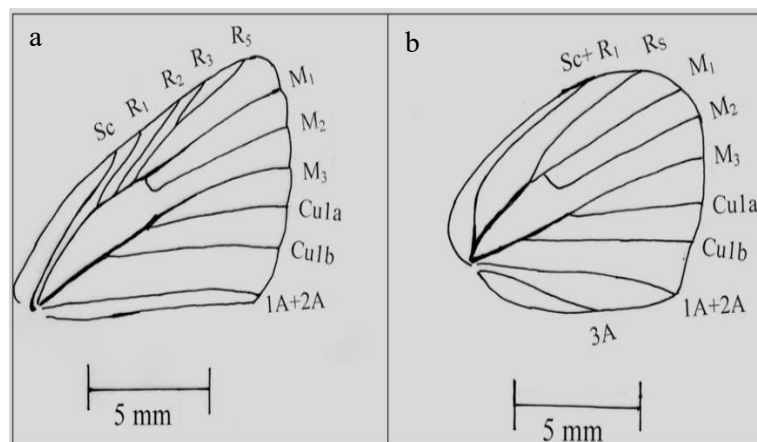


Figure 68: Venation patterns on the forewing and hindwing of *Nymphalis canace* are crucial for morphometric analysis and taxonomic identification. Whereas the hindwing exhibits a compact, rounded layout with converging venation, the forewing has narrow discal cells and closely spaced radial veins.

13. *Polymmatus eros*

P. eros in the Lycaenidae family has distinctive venation patterns in the forewing and hindwing, which are critical to proper taxonomic identification and comprehensive morphometric studies. The forewing is defined by a well arranged web of veins, including 1A+2A (1st Anal Vein), Cu1b (2nd Cubitus), Cu1a (1st Cubitus), Cula, M3, M2, M1 (Median veins), R5, R4, R3, R2, R1 (Radial series), and Sc (Subcosta), visualised in the left panel. This thick, high-density venation is common in small-bodied Lycaenid butterflies and has a structural role in support, as well as a role in aerodynamic efficiency. In 1A+2A, 3A (2nd Anal Vein), Cu1b, Cu1a, Cula, M3, M1, Rs (Radial Sector), and the fused Sc+R1 all in a beautiful radiate at the base of the wing, the hindwing in the right panel (**Figure 69**) has an apterygial form. A single feature that distinguishes *P. eros* among other closely allied taxa is the relatively straight and parallel course of the veins in the hindwing. To be able to make proper morphometric comparisons and assessments of interspecific differences in wing architecture, both wings are shown with 5 mm scale bars.

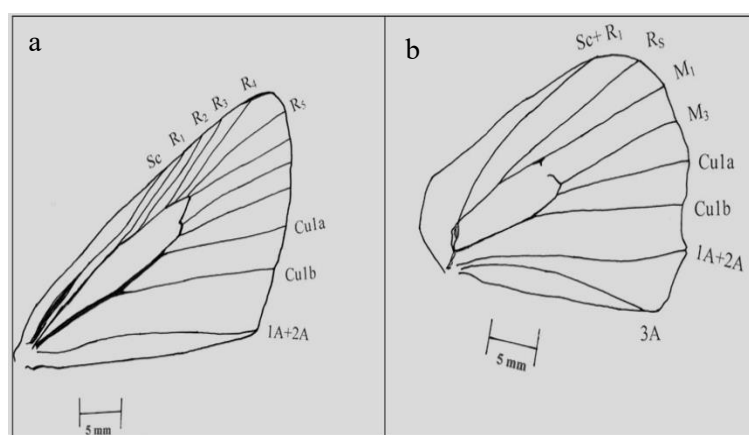


Figure 69: Venation patterns on the forewing and hindwing of *Polymmatus eros* are crucial for taxonomic identification and morphometric analysis within the Lycaenidae family. Veins 1A+2A, Cu1b, Cu1a, Cula, M3, M2, M1, R5-R1, and Sc are all arranged in a dense network in the forewing (a). Features of the hindwing (b) include fused Sc+R1, M3, M1, Rs, Cu1b, Cu1a, Cula, 1A+2A, and 3A.

14. *Vanessa cardui*

The extremely complex venation architecture of *V. cardui* forewing and hindwing provides essential taxonomic markers and morphometric parameters for precise identification within the Nymphalidae family. Major veins including 1A+2A (first anal vein), Cu1b (second cubitus), Cu1a (first cubitus), Cula, M3, M2, M1 (median series), Rs, R5, R4, R3, R2, R1 (radial series),

and Sc (subcosta) are arranged in the forewing (left panel), creating a noticeably elongated discal area that supports species-specific wing patterning and improves aerodynamic efficiency. The hindwing (right panel) has the following features: 1A+2A, 3A (second anal vein), Cu1b, Cu1a, M3, M2, M1, Rs, and the fused Sc+R1. It also has a distinct discocellular system that includes the precostal vein/spur (PV) and the upper (UDC), middle (MDC), and lower (LDC) discocellulars. *V. cardui* is distinguished from morphologically similar nymphalid species by the spatial arrangement and relative complexity of the discocellular cross-veins, as well as the extended and diverging radial branches (**Figure 70**). A 5 mm scale bar is included with both wing images to enable accurate morphometric evaluations, comparative taxonomic research, and interspecific structural analyses.

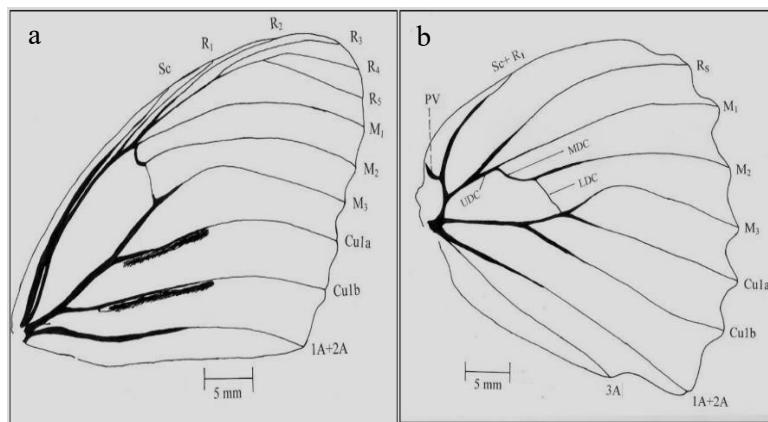


Figure 70: Forewing (a) and hindwing (b) of *Vanessa cardui* showing characteristic venation patterns, including major anal, cubital, median, and radial veins, discocellular cross-veins, and precostal spur.

Table 15: Morphometrics of Body, Cephalic, Thoracic and Ocular structures in selected Lepidopteran pollinator species (Butterflies) from cherry orchards of the Kashmir Valley (mm)

Species	Body length	Head length	Head width	Thorax length	Thorax width	Compound eye Length	Compound eye Width
<i>Argynnis hyperbius</i>	12.25± 0.30	1.79± 0.10	2.86± 0.15	2.34± 0.12	2.67± 0.08	1.65± 0.07	2.32± 0.05
<i>Lycaena phlaeas</i>	5.5± 0.25	1.20± 0.08	2.11± 0.10	1.89± 0.07	2.34± 0.06	1.23± 0.06	1.87± 0.04
<i>Polymmatos eros</i>	6.78± 0.20	1.73± 0.08	2.34± 0.12	1.79± 0.08	2.42± 0.07	1.48± 0.05	1.78± 0.06
<i>Pontia daplidice</i>	8.37± 0.25	1.05± 0.07	1.42± 0.08	2.14± 0.09	2.87± 0.07	0.87± 0.06	1.40± 0.05
<i>Gonepteryx rhamni</i>	12.44± 0.30	1.67± 0.09	2.56± 0.13	2.56± 0.10	2.78± 0.09	1.98± 0.07	2.76± 0.06
<i>Nymphalis canace</i>	12.77± 0.28	1.76± 0.08	2.87± 0.14	2.67± 0.11	2.90± 0.07	1.89± 0.06	2.97± 0.05
<i>Vanessa cardui</i>	10.72± 0.25	1.04± 0.06	2.47± 0.10	2.56± 0.08	2.76± 0.08	1.05± 0.05	1.40± 0.04
<i>Colias erate</i>	10.64± 0.27	1.67± 0.10	2.38± 0.12	2.76± 0.09	2.89± 0.08	1.44± 0.06	1.79± 0.05
<i>Colias philodice</i>	10.98± 0.30	1.09± 0.07	1.78± 0.08	2.55± 0.09	2.78± 0.07	0.96± 0.05	1.50± 0.06
<i>Colias electo</i>	10.61± 0.28	1.76± 0.09	2.45± 0.10	2.63± 0.08	2.81± 0.08	1.49± 0.06	1.80± 0.05
<i>Pieris Canidia</i>	12.85± 0.30	1.20± 0.08	2.34± 0.12	2.89± 0.10	2.90± 0.08	1.37± 0.07	1.75± 0.05
<i>Pieris brassicae</i>	12.48± 0.28	1.35± 0.09	2.08± 0.10	2.90± 0.12	3.20± 0.08	0.91± 0.06	2.32± 0.07
<i>Aulocera Saraswati</i>	14.65± 0.35	2.33± 0.10	3.22± 0.15	2.98± 0.12	3.30± 0.10	2.13± 0.08	2.90± 0.06
<i>Nymphalis polychloros</i>	14.19± 0.30	2.12± 0.08	3.24± 0.14	2.86± 0.11	3.21± 0.09	2.11± 0.07	2.87± 0.06
C.D(p≤0.05)	0.84	0.28	0.42	0.34	0.28	0.19	0.14

Table 16: Morphometric of wing (Forewing and Hindwing), Antennal and Abdominal structures in selected Lepidopteran pollinator species (Butterflies) from cherry orchards of the Kashmir Valley (mm)

Species	Forewing length	Forewing width	Hindwing length	Hindwing width	Antennae length	Abdomen length
<i>Argynnis hyperbius</i>	30±1.5	20±1.0	28±1.5	18±1.0	5.34±2.5	8.12±0.30
<i>Lycaena phlaeas</i>	14±1.0	10±0.5	13±0.8	10±0.5	3.56±0.20	2.41±0.10
<i>Polymmatos eros</i>	18±1.2	10±0.6	14±1.0	0.9±0.4	3.81±0.18	2.62±0.12
<i>Pontia daplidice</i>	25±1.5	14±0.7	10±1.0	15±0.8	5.42±0.25	7.32±0.20
<i>Gonepteryx rhamni</i>	28±1.5	15±0.8	24±1.2	19±1.0	5.54±0.22	8.21±0.30
<i>Nymphalis canace</i>	29±1.4	17±0.7	22±1.1	16±0.9	5.41±0.20	8.34±0.25
<i>Vanessa cardui</i>	35±1.8	16±0.8	26±1.3	21±1.2	6.94±0.30	7.12±0.25
<i>Colias erate</i>	28±1.5	18±0.8	26±1.2	19±1.0	4.42±0.22	6.21±0.20
<i>Colias philodice</i>	24±1.4	13±0.6	21±1.1	15±0.8	4.58±0.18	7.34±0.25
<i>Colias electo</i>	26±1.5	15±0.7	23±1.2	17±0.9	4.44±0.20	6.22±0.20
<i>Pieris Canidia</i>	25±1.5	15±0.8	20±1.1	16±0.9	5.84±0.25	8.76±0.30
<i>Pieris brassicae</i>	40±2.0	28±1.0	35±1.5	29±1.2	6.43±0.30	8.23±0.25
<i>Aulocera Saraswati</i>	35±1.8	17±0.8	26±1.3	21±1.2	7.64±0.35	9.34±0.30
<i>Nymphalis polychloros</i>	31±1.7	18±0.8	25±1.2	20±1.1	6.31±0.30	9.21±0.25
C.D(p≤0.05)	3.0	1.7	2.0	1.5	1.2	0.5

3.18. Hierarchical Cluster Analysis

Hierarchical Cluster Analysis (HCA) of butterfly species based on standardized morphometric traits reveals distinct patterns of morphological similarity and divergence among the studied families (Pieridae, Nymphalidae, Lycaenidae, and others) (**Figure 71**). The dendrogram was

generated using Euclidean distance and Ward's linkage method. The analysis separates the butterflies into two major morphological groups.

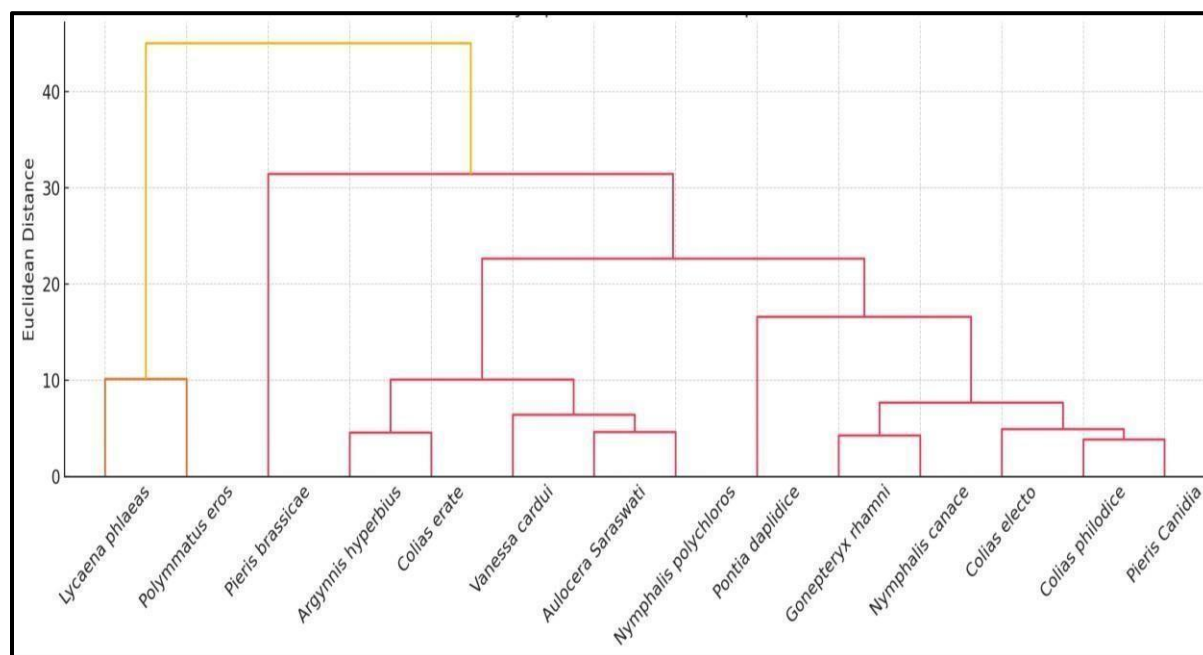


Figure 71: Hierarchical Cluster Analysis (HCA) of 14 butterfly species based on 13 standardized morphometric traits (body length, head length and width, thorax length and width, compound eye dimensions, forewing and hindwing length and width, antenna length, and abdomen length). Smaller-bodied Lycaenids (*Lycaena phlaeas* and *Polymmatius eros*) form a distinct high-distance cluster, indicating their large proportional difference from the rest of the species. *Pieris brassicae* also joins this cluster at a higher distance because of its exceptionally large wing dimensions. The remaining species cluster more gradually, reflecting intermediate to large body sizes and similar wing and thoracic proportions. Closely related taxa such as *Colias erate*, *Colias electo*, and *Colias philodice* cluster tightly at low Euclidean distances, demonstrating strong morphometric similarity. Larger-bodied nymphalid species (*Nymphalis canace*, *Nymphalis polychloros*, *Aulocera saraswati*) cluster together, indicating shared structural traits.

3.19. Principal Component Analysis (PCA)

Principal Component Analysis (PCA) of butterfly morphometric data reveals clear separation of species across the first two principal components, which together accounted for 83.6% of

total variance. PC1 largely represented variation in body size and wing morphology, whereas PC2 reflected differences in thoracic and head dimensions. In the Pieridae family, species such as *Colias philodice*, *Pontia daplidice*, and *Vanessa cardui* occupy upper central positions, suggesting moderate similarity but subtle morphological differences (**Figure 72**). Meanwhile, *Nymphalis polychloros* and *Aulocera Saraswati* clustered near the lower left, showing their shared morphological features and family level resemblance within Nymphalids. This spatial distribution underscores both inter- and intra-family morphometric variation and provides insight into how butterfly structural adaptations correlate with taxonomic identity and ecological strategies.

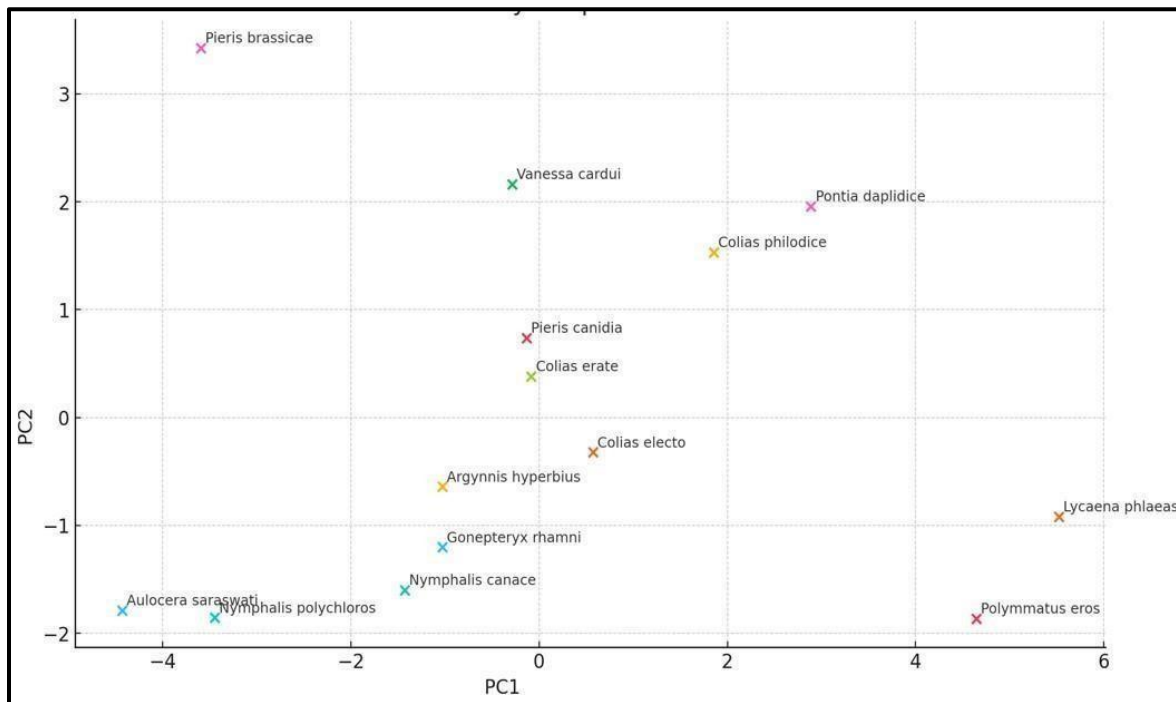


Figure 72: Principal Component Analysis (PCA) of 14 butterfly species based on 13 standardized morphometric traits. Positive PC1 scores represent species with larger overall body size, broader wings, and longer abdomen (e.g., *Pontia daplidice*, *Colias electo*). Negative PC1 values indicate smaller species such as *Lycaena phlaeas* and *Aulocera saraswati*. Along PC2, positive values reflect species with proportionally larger head, thorax, and eye dimensions (e.g., *Pieris brassicae*, *Vanessa cardui*), while negative PC2 values correspond to compact-bodied nymphalids (e.g., *Nymphalis canace*, *Aulocera saraswati*). Clustering patterns show genus-level similarity: the three *Colias* species cluster closely, whereas *Nymphalis* and *Aulocera* form a distinct group on the negative PC1 axis, highlighting clear morphometric divergence.

3.20. DNA barcoding of Insect pollinators

An effective combined molecular strategy was used to precisely define and describe the species of insect pollinators related to cherry orchards. A representative was taken, and genomic DNA was isolated, followed by the amplification of the mitochondrial cytochrome c oxidase subunit I (COX1) gene expression by polymerase chain reaction (PCR). Amplified products were then sequenced, and the resulting nucleotide sequences were corrected and cross-aligned using the BioEdit software to ensure that they were correct and consistent. The obtained sequences were analysed with the help of the BLASTN algorithm in order to verify the species-level identification by comparing them with the reference sequences stored in the National Center of Biotechnology Information (NCBI) database (**Figure 17**). All identified sequences that were successfully identified were given a unique GenBank accession number, thus forming a publicly available molecular repository of pollinator diversity in the Kashmir Valley. These accession numbers are considered permanent genetic identifiers and can be used in future studies in taxonomy, ecology and evolution. The molecular dataset contained 30 species of insect pollinators of the orders Lepidoptera, Diptera and Hymenoptera that were verified by COX1 gene sequencing. Combining molecular data with morphological and morphometric analysis made it possible to delimit the species correctly and reinforce the taxonomic division of pollinator assemblages in the area. This molecular framework as a whole offers a solid framework in the comprehension of diversity in pollinators, in future biodiversity studies, and valuable reference information in pollination ecology and preservation research efforts in the Kashmir Valley.

Table 17: NCBI accession numbers of insect pollinator species associated with cherry orchards

S.NO.	Order	Species	Accession Number	Status
1.	Lepidoptera	<i>Argynnis hyperbius</i>	PP563869	Released
2.		<i>Lycaena phlaeas</i>	PP563825	Released
3.		<i>Polymmatius eros</i>	PP647323	Released
4.		<i>Pontia daplidice</i>	PP647325	Released
5.		<i>Gonepteryx rhamni</i>	PP647327	Released
6.		<i>Nymphalis canace</i>	PP647766	Released
7.		<i>Vanessa cardui</i>	PP647764	Released
8.		<i>Colias erate</i>	PP647763	Released
9.		<i>Colias philodice</i>	PP647765	Released
10.		<i>Colias electo</i>	PP647762	Released
11.		<i>Pieris canidia</i>	PP702274	Released
12.		<i>Pieris brassicae</i>	PP702172	Released
13.		<i>Aulocera saraswati</i>	PP715732	Released
14.		<i>Nymphalis polychloros</i>	PP702177	Released
15.	Diptera	<i>Eristalis arbustorum</i>	PP555892	Released
16.		<i>Syrphus ribesii</i>	PP555937	Released
17.		<i>Eristalis abusiva</i>	PP563770	Released
18.		<i>Eristalis tenax</i>	PP566897	Released
19.		<i>Episyrphus balteatus</i>	PP564741	Released
20.		<i>Sphaerophoria scripta</i>	PP565015	Released
21.	Hymenoptera	<i>Apis mellifera</i>	PP724752	Released
22.		<i>Apis cerana</i>	PP563737	Released
23.		<i>Lasioglossum rugifrons</i>	PP564714	Released
24.		<i>Lasioglossum marginatum</i>	PP564710	Released
25.		<i>Lasioglossum matianense</i>	PP564712	Released
26.		<i>Andrena agillissima</i>	PP565021	Released
27.		<i>Andrena pilipes</i>	PP565060	Released
28.		<i>Andrena fucata</i>	PP798203	Released
29.		<i>Bombus albopleuralis</i>	PP799060	Released
30.		<i>Vespa vulgaris</i>	PV480545	Released

3.20.1. Exploration of Intra and interspecific species variation among collected insect pollinators of cherry by Phylogenetic Analysis

The neighbour-joining tree was inferred from a 658-bp fragment of COX1 from 30 species collected from Jammu and Kashmir. The phylogenetic tree showed that these sequences were well separated and were collected in the group of their conspecifics. In Lepidoptera, species are grouped by Pieridae (e.g., *Pieris canidia*, *P. brassicae*, *Pontia daplidice*, *Gonepteryx rhamni*, *Colias electo*, *C. erate*, *C. philodice*), Lycaenidae (*Lycaena phlaeas*, *Polyommatus eros*), and Nymphalidae (*Argyreus hyperbius*, *Nymphalis polychloros*, *Vanessa cardui*, *N. canace*, *Aulocera saraswati*). Hymenoptera comprises Apidae (*Apis mellifera*, *A. cerana*, *Bombus albopleuralis*), Andrenidae (*Andrena agilissima*, *A. fucata*, *A. pilipes*), Halictidae (*Lasioglossum marginatum*, *L. matianense*, *L. rugifrons*), and Vespidae (*Vespula vulgaris*). Diptera includes Syrphidae (*Episyrphus balteatus*, *Sphaerophoria scripta*, *Eristalis tenax*, *E. arbustorum*, *E. abusiva*, *Syrphus ribesii*). The evolutionary history was inferred using the General Time Reversible model and the Maximum Likelihood approach (**Figure 73**). By employing the Neighbour-Joining method on a matrix of pairwise distances calculated using the Maximum Composite Likelihood (MCL) method, the initial tree(s) for the heuristic search were produced. The evolutionary history of the taxa under consideration is assumed to be represented by the bootstrap consensus tree generated from 1000 replicates. Branches associated with partitions that were replicated in fewer than 50% of bootstrap replicates are collapsed.

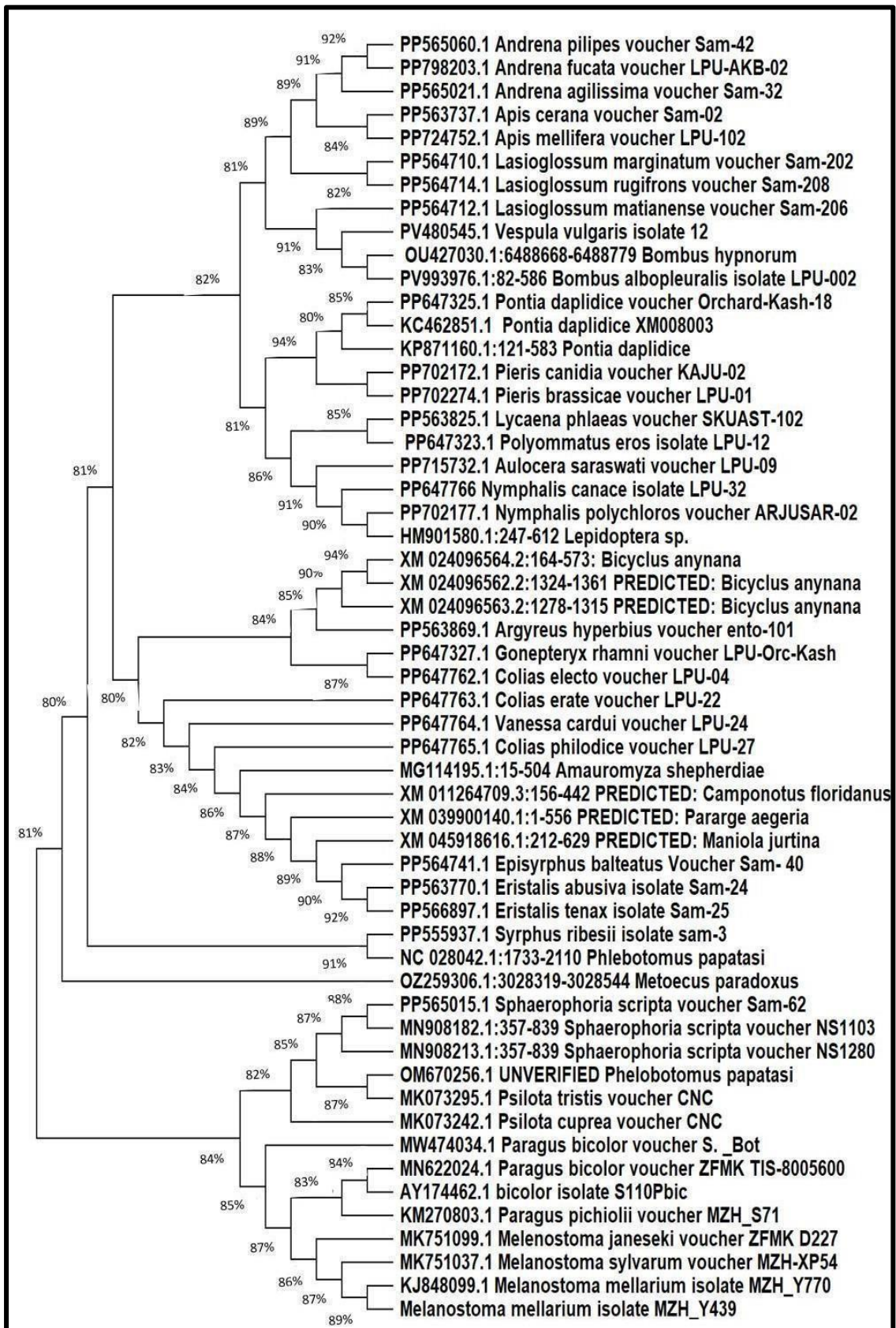


Figure 73: Phylogenetic tree illustrating the intra- and interspecific genetic variation among insect pollinator species collected from cherry orchards. Each branch represents an individual

species, highlighting the genetic relationships and divergence patterns based on COX-1 gene sequences. The circular tree depicts three major clades corresponding to the orders Lepidoptera, Hymenoptera, and Diptera, with Family-level clusters recognised within each Order. The tree effectively delineates species-level clustering and evolutionary relatedness, supporting both taxonomic resolution and molecular identification.

3.21. Diversity of Insect Pollinators in Cherry Orchards of Kashmir

The detailed study of the diversity indices among cherry orchards in the Kashmir Valley, which included the locations in Srinagar, Ganderbal, Baramulla, and Shopian, demonstrated a strong, species-rich, and well-balanced community of insect pollinators. The populations of individual pollinators were high in a number of 465-576 pollinators per site across the eight surveyed sites with Shalimar, Dhara, Lar, Baba Wayil, Tangmarg, Sopore, Kullar and Aerhal (**Figure 74**). The low values of Dominance Index (0.03408-0.03552) are indicative of the lack of one species dominating the pollinator assemblage (**Figure 75**) of which the high values of Simpson Index (D) (exceeds 0.964) and Shannon-Weiner diversity index (H) (between 3.352 and 3.372), are also suggestive of high diversity and even distributions of species (**Figure 76-77**). The values of Evenness (0.9853-1.002) are extraordinarily high, which proves the fair distribution of people among species (**Figure 78**). The abundance patterns were not similar, showing that the highest number of people was recorded in Shalimar (>575), which can probably be explained by the abundance of floral resources and favourable conditions in that habitat (the next two had >520), and Kullar and Tangmarg (both >500). Dhara, Lar, and Sopore, however, were a little less abundant (460- 480) indicating site-specific environmental changes, flora change, and agricultural activities (**Table 18**). These findings signify the spatial differences in pollinator populations and recognize Shalimar, Baba Wayil, and Aerhal as the potential biodiversity hotspots, providing useful objects to the pollinator conservation strategies in the area.

Table 18: Diversity Indices of insect pollinator species from different cherry orchards of the Kashmir Valley

	Srinagar		Ganderbal		Baramulla		Shopian	
	Shalimar	Dhara	Lar	Baba Wayil	Tangmarg	Sopore	Kullar	Aerhal
Individuals/ Abundance	576	480	465	525	507	480	504	520
Dominance	0.0344	0.0344	0.0346	0.0356	0.0340	0.0348	0.0350	0.0346
Simpson Index(D)	0.9656	0.9654	0.9654	0.9645	0.9659	0.9653	0.9652	0.9655
Shannon-Weiner diversity index(H')	3.368	3.368	3.366	3.352	3.372	3.364	3.359	3.365
Evenness(E)	1.001	1.001	0.9984	0.9853	1.005	0.9967	0.9917	0.9981

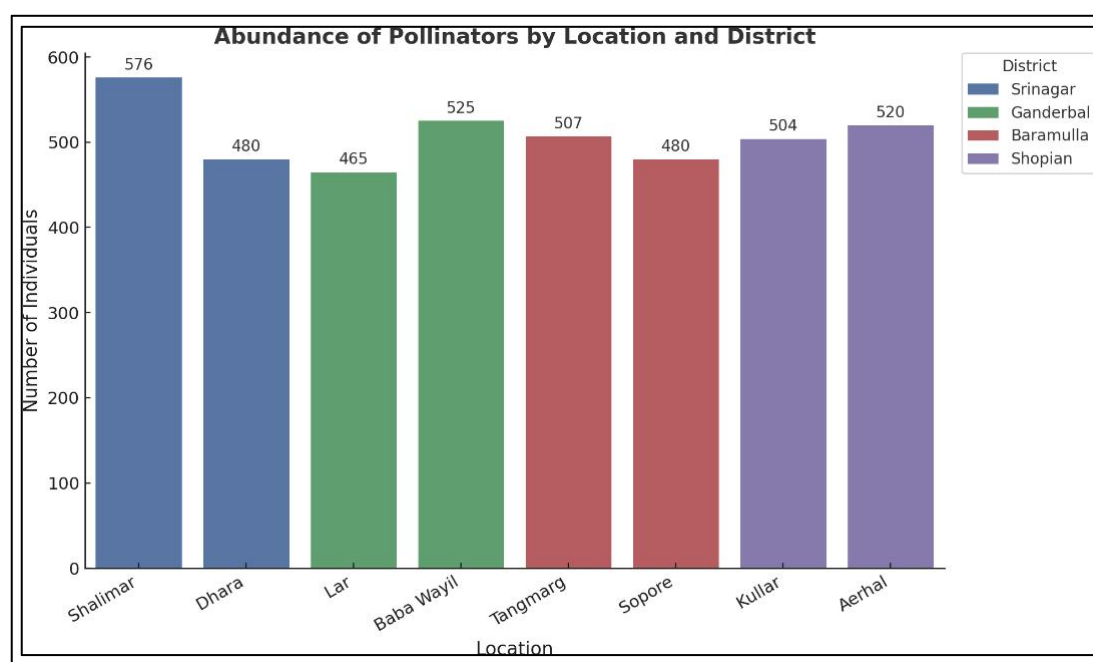


Figure 74: Abundance of insect pollinators recorded across eight sampling sites in cherry orchards of the Kashmir Valley, categorised by district. The bar graph illustrates the total number of pollinator individuals recorded from eight locations across four districts of Kashmir Valley. Shalimar and Dhara (Srinagar district), Lar and Baba Wayil (Ganderbal district),

Tangmarg and Sopore (Baramulla district), and Kullar and Aerhal (Shopian district) show varying pollinator abundances. Shalimar recorded the highest abundance (576 individuals), followed by Baba Wayil (525) and Aerhal (520), while Lar showed the lowest (465). Error bars are not included as the values represent total counts.

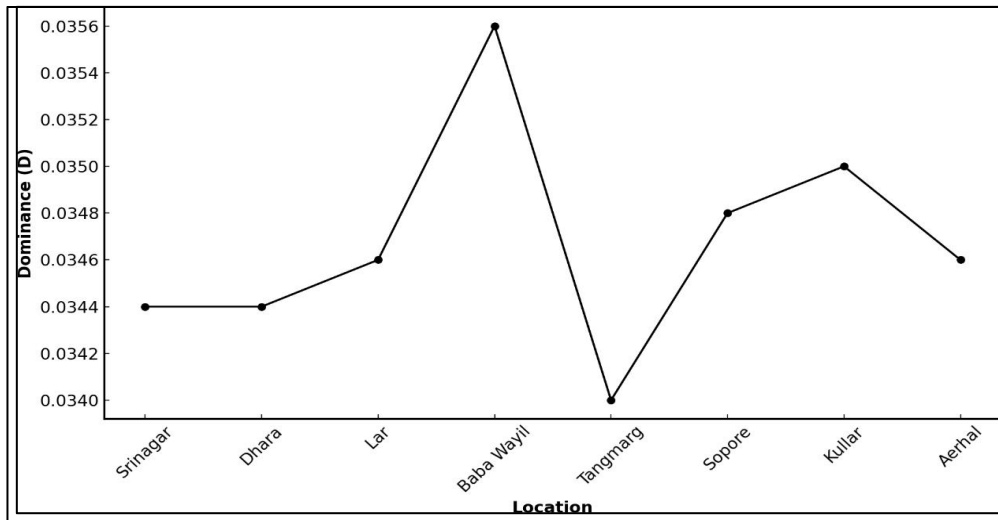


Figure 75: The line graph represents the dominance index (D) of pollinator assemblages recorded from eight sampling locations. Dominance values remain relatively low across all sites, indicating an even distribution of species. The highest dominance was observed at Baba Wayil ($D \approx 0.0356$), followed by Kullar ($D \approx 0.0350$) and Sopore ($D \approx 0.0348$), whereas the lowest dominance occurred at Tangmarg ($D \approx 0.0340$). These slight variations reflect minor differences in species dominance patterns among the locations.

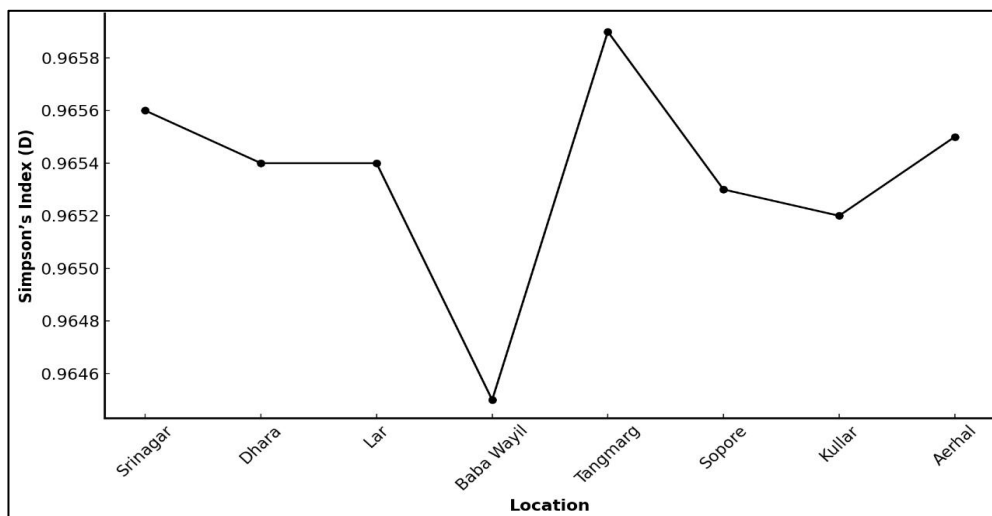


Figure 76: The line graph shows the variation in Simpson's Index (D) for pollinator assemblages across eight sampling locations. Overall, diversity remains high at all sites ($D \approx$

0.964-0.966), indicating a well-balanced pollinator community with low dominance. The highest diversity was recorded at Tangmarg ($D \approx 0.9659$), while Baba Wayil exhibited the lowest value ($D \approx 0.9645$). Minor fluctuations across locations reflect slight differences in species evenness and richness.

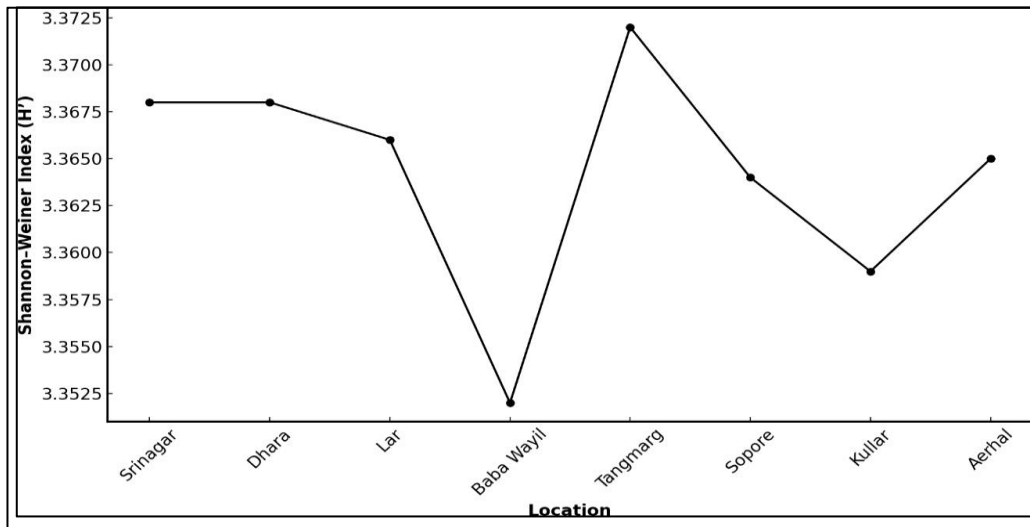


Figure 77: The line graph illustrates the Shannon-Weiner Index (H') for pollinator assemblages recorded across eight sampling locations. Diversity values remain consistently high ($H' \approx 3.35$ - 3.37), reflecting a rich and well-distributed pollinator community. The highest diversity was observed at Tangmarg ($H' \approx 3.371$), while Baba Wayil showed the lowest diversity ($H' \approx 3.352$). Variations across sites indicate subtle differences in species richness and evenness within the pollinator populations.

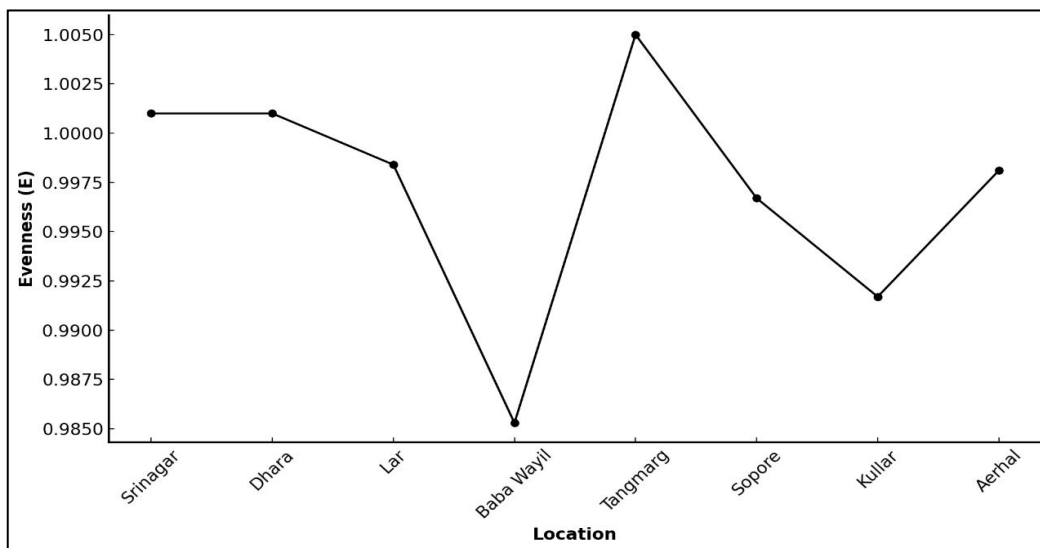


Figure 78: The line graph represents the evenness index (E) of pollinator species recorded across eight sampling locations. Evenness values are consistently high ($E \approx 0.985$ - 1.005), indicating a

uniform distribution of species with minimal dominance. Tangmarg exhibited the highest evenness ($E \approx 1.005$), while Baba Wayil recorded the lowest ($E \approx 0.985$). The slight variations across locations reflect minor differences in the proportional distribution of pollinator species.

3.22. Evaluation of Qualitative and Quantitative Parameters of Cherry Fruit

The results clearly demonstrate the crucial role of insect pollinators in enhancing both fruit set and fruit quality in cherry. With a well-planned Randomised Block Design (RBD) of six pollination regimes and 3 repetition, different parameters of fruit set and quality were found to vary with the type and intensity of pollinator visitation. Native wild insect pollinators (**Figure 79-80**), such as different species of bees and flies, led to slight and inconsistent fruit size, fruit weight and total soluble solids (TSS) enhancement with comparatively increased acidity (**Table 19**). In comparison with *Apis cerana*, control of pollination yielded more consistent fruit size, weight, and sweetness and less acidity (**Figure 81-82**), suggesting (**Table 20**) it was more efficient in pollination. Visits by *A. mellifera* were the most notable (**Figure 83-84**) as several visits caused the largest, heaviest fruits, highest TSS values, and lowest acidity, reflecting the most effective pollination by this managed species (**Table 21**). Such differences are biologically supported by the reproductive physiology of cherry, whereby the floral buds achieve anthesis around 710 days after the bud swelling, and the stigma is receptive up to 23 days and optimal temperatures (around 18 °C) (Ravi 2023; Fadón et al. 2020; Hedhly et al. 2009). Fruit set and fruit quality are different processes, as one effective visit by a pollinator can trigger fertilization, the initiation of fruit is a binary reaction, whereas the increase in fruit growth and quality is highly dependent on pollen load and pollen competition (Garratt et al. 2014). The high pollen deposition increases pollen tube competition, where the most active pollen grain ensures fertilisation. Pollen germination takes place between 1-4 hours, and fertilisation is achieved between 24-48 hours (Herrero and Hormaza 1996). It leads to better embryo development and better production of growth-regulating hormones (auxins and gibberellins) to enhance the fruit size, weight, and quality, in general (Fadón et al. 2020; Baral et al. 2025). In general, the results clearly indicate that the frequency of pollination as well as compatibility of sources of pollen is a clear and complementary factor that influences reproductive success, yield and fruit quality of cherry.

3.22.1. Effect of different pollination regimes by Native insect pollinator species on cherry fruit set and development.

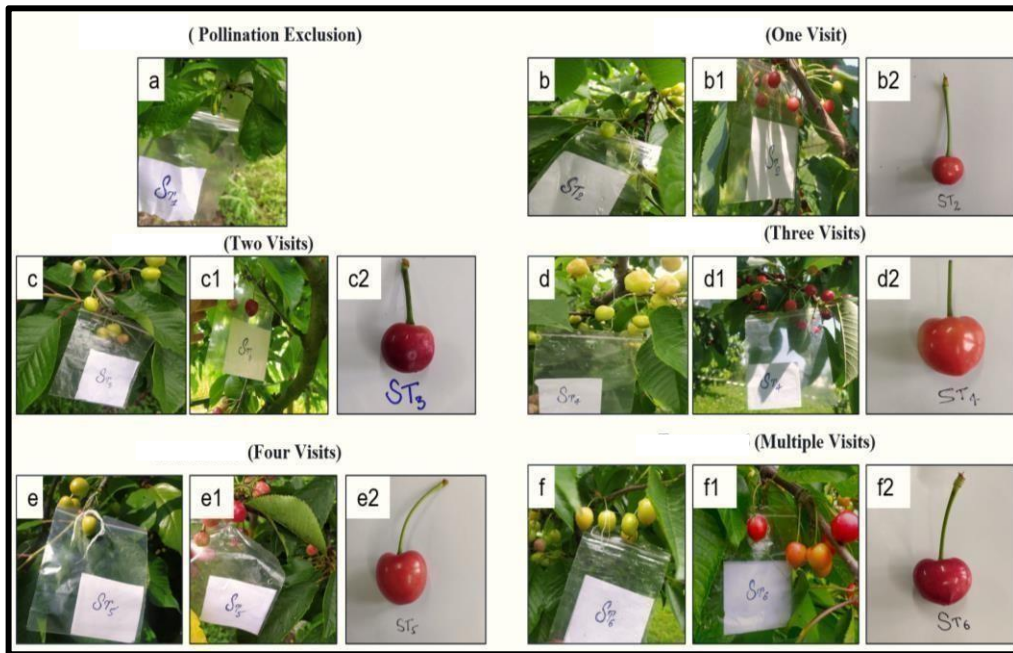


Figure 79: Photographs (a-f) from cherry orchards depicting regimes with Native insect pollinators, including pollination exclusion, single visit, two visits, three visits, four visits, and multiple visits, along with the corresponding fruit set and quality.

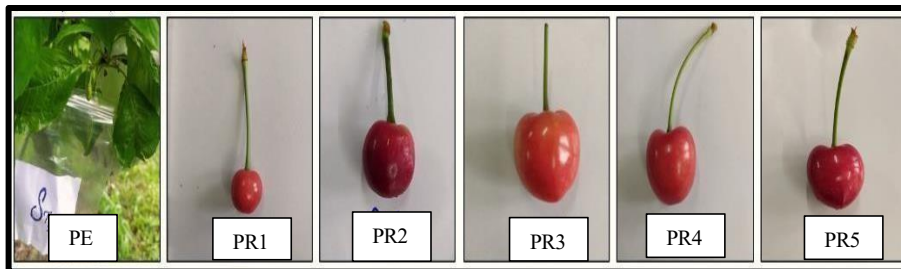


Figure 80: Effect of Native insect pollinator visitation on cherry fruit development and quality. Pollination exclusion (PE) shows no fruit formation, whereas one to multiple visits (PR1-5) depict progressive improvement in fruit set, size, and quality with increasing pollinator visits.

Table 19: Quantitative parameters of cherry fruit, viz., Fruit set, fruit weight, fruit size, TSS, and Acidity with Pollination Regimes by other native insect pollinator species

Pollination Regimes	Fruit Set (%)	Fruit Size (mm)	Fruit Weight (g)	TSS (°Brix)	Acidity (pH)
Pollinator Exclusion	0.000±0.000	0.000±0.000	0.000±0.000	0.000±0.000	0.000±0.000
One visit by other native insect pollinators	0.010±0.000	16.657±0.633	3.423±0.402	11.400±0.611	1.240±0.021
Two Visits by other native insect pollinators	0.010±0.000	16.860±0.421	3.837±0.018	12.233±0.088	1.670±0.015
Three Visits by other native insect pollinators	0.010±0.000	16.850±0.252	4.257±0.009	13.333±0.088	2.297±0.029
Four Visits by other native insect pollinators	0.010±0.000	17.103±0.180	4.497±0.009	14.400±0.208	2.440±0.038
Multiple Visits by Other native insect pollinators	0.010±0.000	17.927±0.015	5.220±0.012	15.567±0.285	2.903±0.064
		SD: 0.50 CV: 0.03 CD: 0.45	SD: 0.68 CV: 0.16 CD: 0.61	SD: 1.66 CV: 0.12 CD: 1.49	SD: 1.04 CV: 0.31 CD: 0.66

3.22.2. Effect of different pollination regimes by *Apis cerana* on cherry fruit set and development.

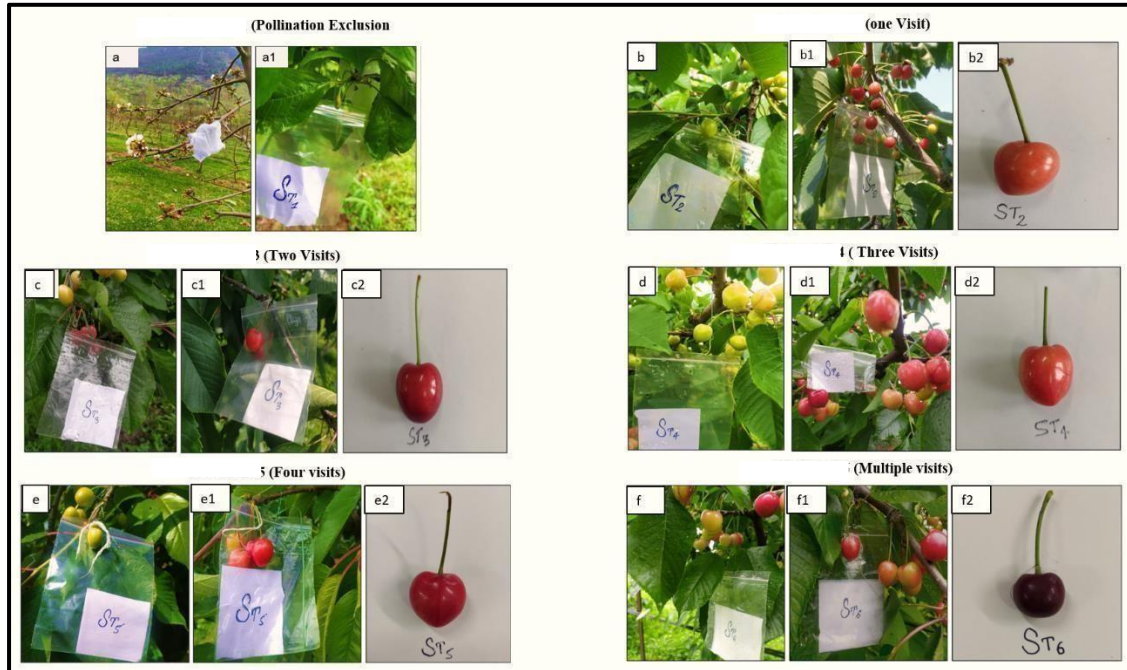


Figure 81: Photographs (a-f) from cherry orchards depicting regimes with *Apis cerana*, including pollination exclusion, single visit, two visits, three visits, four visits, and multiple visits, along with the corresponding fruit set and quality.

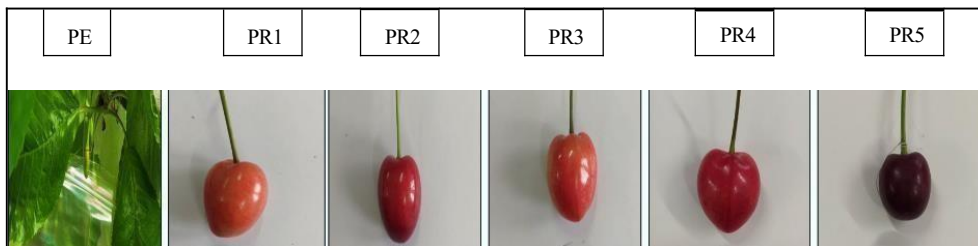


Figure 82: Effect of *Apis cerana* visitation on cherry fruit development and quality. Pollination exclusion (PE) shows no fruit formation, whereas one to multiple visits (PR1-5) depict progressive improvement in fruit set, size, and quality with increasing pollinator

Table 20: Quantitative parameters of cherry fruit, viz., Fruit set, fruit weight, fruit size, TSS, and Acidity with Pollination Regimes by *Apis cerana*

Pollination Regimes	Fruit Set (%)	Fruit Size (mm)	Fruit Weight (g)	TSS (°Brix)	Acidity (pH)
Pollinator Exclusion	0.000±0.000	0.000±0.000	0.000±0.000	0.000±0.000	0.000±0.000
One visit by <i>Apis Cerana</i>	0.010±0.000	16.820±0.500	4.120±0.300	12.600±0.550	1.520±0.018
Two visits by <i>Apis Cerana</i>	0.010±0.000	17.020±0.400	4.520±0.020	13.500±0.080	2.150±0.014
Three visits by <i>Apis Cerana</i>	0.010±0.000	17.100±0.250	5.650±0.010	14.700±0.085	2.380±0.026
Four visits by <i>Apis Cerana</i>	0.010±0.000	17.250±0.200	5.700±0.010	15.800±0.200	3.220±0.035
Multiple Visits by <i>Apis cerana</i>	0.010±0.000	18.000±0.010	6.820±0.011	16.900±0.270	3.720±0.062
		SD: 0.45 CD: 0.41 CV: 0.34	SD: 1.07 CD: 0.96 CV: 0.20	SD: 1.31 CD: 1.54 CV: 0.12	SD: 0.87 CD: 0.78 CV: 0.34

3.22.3. Effect of *Apis mellifera* pollination on cherry fruit set and development under different regimes.

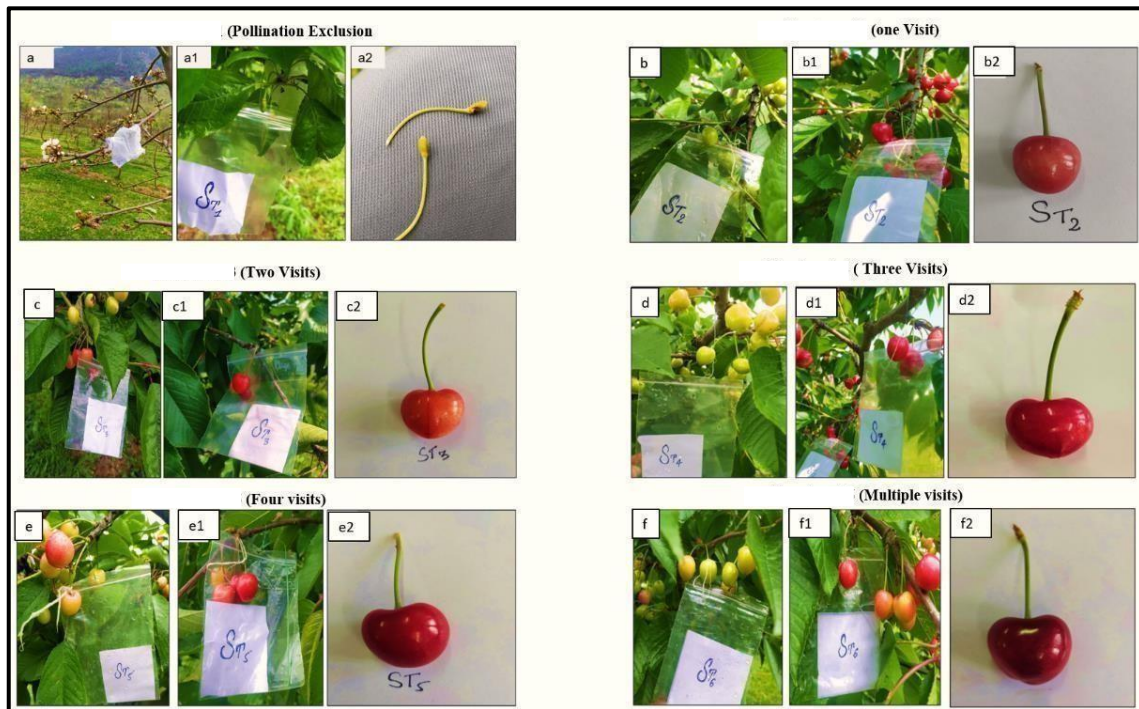


Figure 83: Photographs (a–f) from cherry orchards depicting regimes with *Apis mellifera*, including pollination exclusion, single visit, two visits, three visits, four visits, and multiple visits, along with the corresponding fruit set and quality.

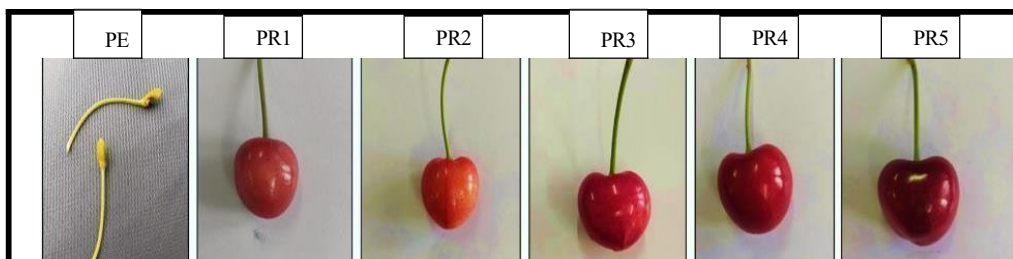


Figure 84: Effect of *Apis mellifera* visitation on cherry fruit development and quality. Pollination exclusion (PE) shows no fruit formation, whereas one to multiple visits (PR1-5) depict progressive improvement in fruit set, size, and quality with increasing pollinator visits.

Table 21: Quantitative parameters of cherry fruit, viz., Fruit set, fruit weight, fruit size, TSS, and Acidity with Pollination Regimes by *Apis mellifera*

Pollination Regimes	Fruit Set (%)	Fruit Size (mm)	Fruit Weight (g)	TSS (°Brix)	Acidity (pH)
Pollination Exclusion	0.000±0.000	0.000±0.000	0.000±0.000	0.000±0.000	0.000±0.000
One visit by <i>Apis mellifera</i>	0.010±0.000	17.327±0.042	5.290±0.036	13.467±0.088	2.070±0.012
Two visits by <i>Apis mellifera</i>	0.010±0.000	18.260±0.089	6.337±0.018	14.600±0.115	2.957±0.020
Three visits by an <i>Apis mellifera</i>	0.010±0.000	18.283±0.088	6.357±0.009	15.433±0.186	3.873±0.039
Four visits by an <i>Apis mellifera</i>	0.010±0.000	18.333±0.109	6.403±0.012	16.400±0.153	3.960±0.006
Multiple visits by <i>Apis mellifera</i>	0.010±0.000	19.697±0.044	7.430±0.006	17.667±0.088	4.270±0.009
		SD: 0.85 CD: 0.76 CV: 0.05	SD: 0.76 CD: 0.68 CV: 0.12	SD: 1.60 CD: 1.45 CV: 0.10	SD:0.90 CD: 0.81 CV: 0.26

When compared across regimes, a clear gradient was observed in the quantitative parameters of cherry fruit. In the case of Native insect pollinators (**Table 19**), fruit set remained uniformly low (0.01), but fruit size improved gradually from 16.657 mm (one visit) to 17.927 mm (multiple visits), fruit weight increased from 3.423 g to 5.220 g, and TSS rose from 11.400 °Brix to 15.567 °Brix, while acidity increased from 1.240 to 2.903. However, relatively higher variability (e.g., SD for fruit size = 0.50; CV = 0.03; SD for fruit weight = 1.66; CV = 0.12) indicated inconsistent efficiency of these random visitors. With *Apis cerana* (**Table 20**), improvements were more pronounced and consistent. Fruit size increased from 16.820 mm to 18.000 mm, fruit weight from 4.120 g to 6.820 g, and TSS from 12.600 °Brix to 16.900 °Brix, while acidity rose from 1.520 to 3.720. The relatively lower variation (SD for fruit size = 0.45, CV = 0.34; SD for fruit weight = 1.31, CV = 0.12) reflected more reliable pollination compared to random insect visitors. The best result was recorded with *A. mellifera* (**Table 21**), where fruit size improved from 17.327 mm to 19.697 mm, fruit weight from 5.290 g to 7.430 g, and TSS

from 13.467 °Brix to 17.667 °Brix, with acidity rising from 2.070 to 4.270. Importantly, the lowest variability (SD for fruit size = 0.85, CV = 0.05; SD for fruit weight = 1.60, CV = 0.10) confirmed the superior and consistent pollination efficiency of *A. mellifera* compared with *A. cerana* and wild visitors. The comparative analysis of pollination treatments, therefore, highlights a distinct gradient in cherry fruit improvement (**Figure 85-88**). The other native insect pollinators contributed to fruit set and quality, but with higher variability and limited gains. *A. mellifera* proved to be more efficient, ensuring better fruit weight, size, sweetness (TSS), and moderate acidity with relatively less variability.

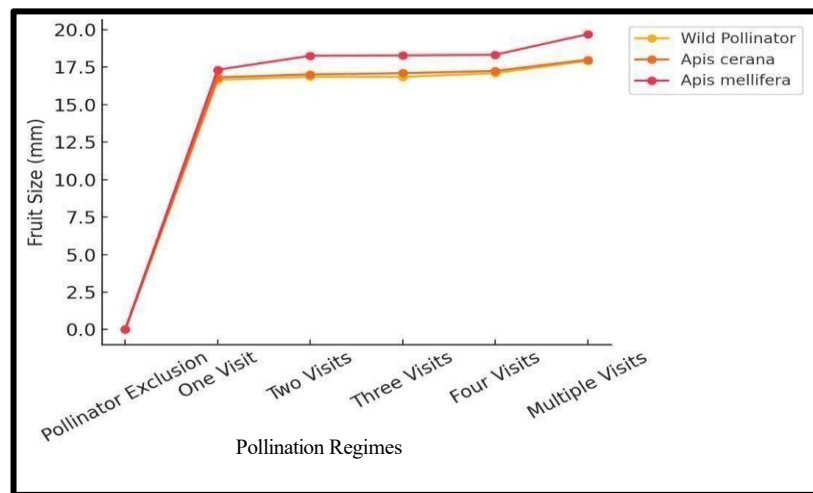


Figure 85: The line graph shows the variation in fruit size (mm) of cherry fruits under different pollination regimes. Pollinator exclusion resulted in no fruit development, confirming the essential role of pollinators. Fruit size increased markedly from one visit to multiple visits across all pollinator groups. *A. mellifera* consistently produced the largest fruits across treatments, followed by *A. cerana* and wild pollinators. Maximum fruit size was recorded under multiple visits, highlighting the positive impact of repeated pollinator activity on fruit development.

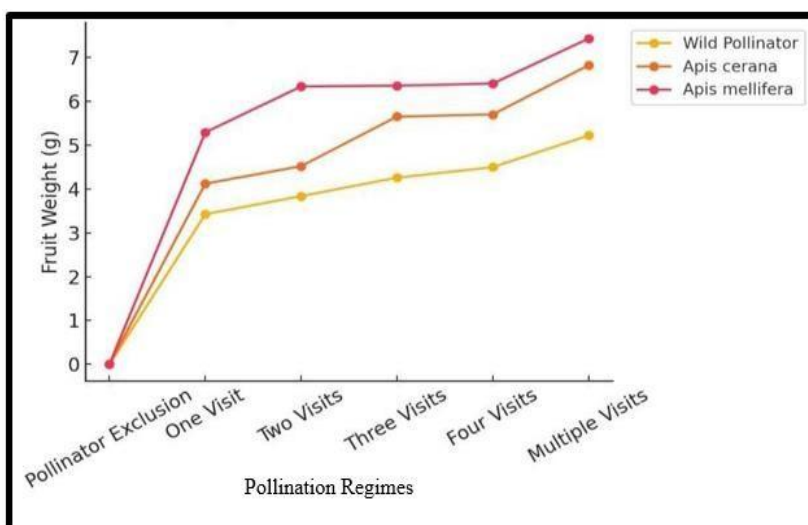


Figure 86: The line graph illustrates variation in fruit weight (g) under different pollination regimes. No fruit development was observed under pollinator exclusion, resulting in negligible fruit weight. Fruit weight increased progressively from one visit to multiple visits across all pollinator groups. Fruits pollinated by *Apis mellifera* exhibited the highest fruit weight at all visitation levels, followed by *Apis cerana* and wild pollinators. Maximum fruit weight was recorded under multiple visits, indicating that increased pollinator activity enhances fruit development and overall yield.

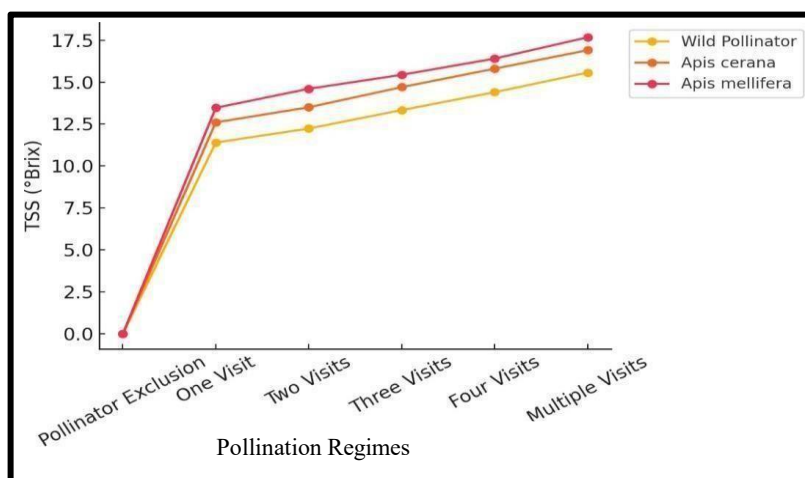


Figure 87: The line graph shows the variation in TSS (°Brix) of cherry fruits under different pollination regimes. Pollinator exclusion resulted in no fruit formation and, therefore, no measurable TSS. TSS increased sharply from the first visit onward across all pollinator groups. *A. mellifera* produced fruits with the highest TSS values across all visitation levels, followed by *A. cerana* and wild pollinators. The maximum TSS was recorded during multiple visits, indicating that repeated pollinator activity enhances fruit sweetness and overall quality.

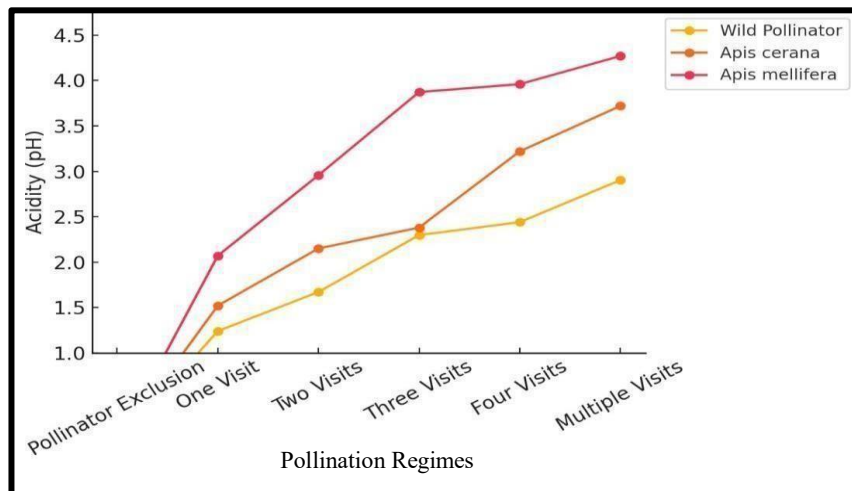


Figure 88: The line graph illustrates changes in fruit acidity (pH) under different pollination regimes. No fruit developed under pollinator exclusion, resulting in no measurable acidity. Acidity increased progressively from one visit to multiple visits for all pollinator groups. Fruits pollinated by *A. mellifera* exhibited the highest acidity across all visitation levels, followed by *A. cerana* and wild pollinators. Maximum acidity occurred under multiple visits, indicating that repeated pollinator activity influences fruit biochemical properties, including acidity.

3.23. Discussion

In this study, a total of 30 insect pollinator species were recorded from cherry orchards distributed across the ecologically heterogeneous and climatically diverse landscapes of the Kashmir Valley. The documented fauna encompassed representatives from 03 major insect orders, Hymenoptera, Diptera, and Lepidoptera, comprising 08 taxonomically distinct families. Within Hymenoptera, four families were represented: Apidae, Halictidae, Andrenidae, and Vespidae. Dipteran pollinators belonged exclusively to the family Syrphidae, whereas lepidopteran representatives were distributed across three families, namely Nymphalidae, Pieridae, and Lycaenidae (**Table 5**). This taxonomic composition highlights the complex nature of the cherry pollinator community in the region. The observed diversity reflects the strong pollinator potential and ecological significance of temperate orchard ecosystems. Similar patterns of pollinator richness have been reported in other temperate agroecosystems, such as those in Europe and the Mediterranean region, where habitat heterogeneity and floral abundance support high diversity of visiting insects (Paray et al. 2014). Among the Hymenoptera, 10 species were identified, exhibiting a range of morphometric adaptations and family-specific traits. The Apidae family comprised *Bombus albopleurialis*, *Apis mellifera*, and *A. cerana*. Among all identified insect pollinators, *B. albopleurialis* showed the largest body size (24.41 mm) and the longest forewing and hind tibia lengths of any of these, suggesting a strong ability to forage over long distances and strong flight mechanics. Such characteristics are essential for improving pollen transport and navigating fragmented orchard landscapes, especially in climates with fluctuating temperatures (Mir et al. 2021; Pull et al. 2022). With their compact body forms and narrower thoraxes, *Lasioglossum rugifrons*, *L. matianense*, and *L. marginatum* were representative of the Halictidae family. As efficient pollinators of small and dense floral structures, these characteristics probably make it easier for them to reach densely packed cherry blossoms and floral crevices (Gibbs 2009). Similarly, members of the family Andrenidae (*Andrena fucata*, *A. pilipes*, and *A. agilissima*) are distinguished by their thorax size and relatively longer antennae. Polidori et al. (2020) report that such morphological features are documented to facilitate thermoregulation and foraging in early spring, and, therefore, make these solitary bees remain active in colder seasons when cherry trees typically start flowering. *Vespula vulgaris* is the only species of the family Vespidae with strong mandibular and head development. Although it is not a specialist pollinator, its random visits to flowers, mainly to obtain nectar or to hunt prey, have a dual purpose in agroecosystems as a predator and pollinator (Borchardt et al. 2024). As shown in Tables 6-12, non-*Apis* hymenopterans, particularly *Bombus albopleurialis*, exhibited larger

body size, including greater body length, head width, thorax dimensions, wingspan, and compound eye size compared to other species. These larger bees not only possess enhanced pollen-carrying capacity due to their well-developed hind tibiae and basitarsi, but also demonstrate superior sensory and flight capabilities. For instance, larger bees tend to have longer compound eyes and antennae, which are associated with improved visual and olfactory orientation in diverse habitats (Reynolds et al. 2022). Conversely, species such as *Lasioglossum rugifrons* and *Apis mellifera* exhibited shorter body lengths and narrower basitarsi, suggesting a greater degree of specialization for targeted pollination, particularly within structurally complex floral environments such as orchard systems. The family Syrphidae (Diptera) also exhibited notable morphometric variation. A total of six species were recorded, with *Sphaerophoria scripta* being the smallest (5.33 mm) and *Eristalis tenax* the largest (14.55 mm). The well-developed thoracic musculature and larger compound eyes observed in larger syrphid species indicate enhanced flight capability and visual acuity, enabling efficient foraging of floral resources (Tables 13 and 14). Notably, *E. tenax* possessed a wider abdomen and longer forewings, which facilitate sustained flight and effective pollen transport (Reynolds et al. 2022). In contrast, smaller syrphids such as *S. scripta* demonstrated greater agility, allowing them to forage effectively within compact floral structures. These morphometric differences highlight the diverse ecological roles and foraging strategies of syrphid flies as pollinators.

The lepidopteran assemblage, comprising 14 butterfly species, exhibited considerable morphological and ecological diversity. Representatives of the families Pieridae (e.g., *Gonepteryx rhamni*, *Colias electo*, *C. erate*, *Pieris brassicae*, and *P. canidia*), Nymphalidae (e.g., *Vanessa cardui* and *Nymphalis canace*), and Lycaenidae (e.g., *Lycaena phlaeas* and *Polyommatus eros*) displayed notable variation in wing structure, body morphology, and genital characteristics (Tables 15 and 16). Larger species, such as *Aulocera saraswati*, possessed well-developed compound eyes and a robust thorax, facilitating strong flight performance and precise floral localization. In contrast, smaller species, including *L. phlaeas*, exhibited more delicate and sensitive morphological features, enabling efficient exploitation of niche habitats and low-lying vegetation. In Lepidoptera, reliance solely on external morphology for species identification can be problematic due to phenotypic plasticity, sexual dimorphism, and seasonal variation in wing coloration (Common 1990). Consequently, more reliable taxonomic characters, such as genitalia and wing venation, are widely employed. Wing venation provides stable, environmentally insensitive features that are highly useful for distinguishing taxa at both genus and species levels (Scoble 1995; Kristensen et al. 2006).

Similarly, genital structures are highly species-specific and evolutionarily conserved, making them essential for differentiating closely related or cryptic species. In particular, male genital components such as the uncus, tegumen, and valvae serve as critical diagnostic features (Klots 1970; Carvalho et al. 2017). Moreover, external characters such as bifid or specialized tarsal claws observed in certain families also contribute to taxonomic differentiation and may play functional roles in flower attachment and pollination (Khyade et al. 2018). Such as Pieridae and Lycaenidae, is helpful in flower binding and pollination, and it also helps in taxonomic differentiation (Khyade et al. 2018). The combination of these characters provides a powerful and integrative system of correct species assignment in Lepidoptera, especially where morphological intermingling is intense.

Wing venation in butterflies is a highly conserved yet variable expressed morphological feature and a fundamental component of lepidopteran taxonomy, phylogeny and morphometric analysis. The differentiation of species, genera, and higher taxonomic ranks presented by the standard nomenclature of wing veins, identified includes the costa (C), Subcosta (Sc), radius (R), media (M), cubitus (Cu) and anal veins (A), and their branching and points of fusion (Kristensen et al. 2006). The wing venation patterns of each of the 14 butterfly species that were examined during the study were species-specific arrangements, which are shown to be related to the taxonomic groups. A similar report given by Braby et al. (2006) demonstrated radial sectors (Rs-R5) as uniformly distributed and closely clumped as in the genus *Colias electo*, *C. philodice*, etc., which he observed as proof of the homogeneity of the genus Pieridae at the genus level. The diagnostic features of the elongated discal cells and strong precostal veins (PV) in *Pieris canidia* and *P. brassicae* are valid reasons to classify the two species as part of the *Pieris* clade. *Pontia daplidice* and *Gonepteryx rhamni*, however, have a characteristic Rs configuration (R-sector fusion, stalking) and angled forewing margins, which help them to stand out among other pierids (according to the standard venation references (Kristensen et al. 2006) and at the family level (molecular systematics) (Braby et al. 2006). The more multifaceted (Wing venation) discocellular system (UDC, MDC, LDC) and highly cystiform discal cells that are present in species like *Nymphalis polychloros*, *N. canace*, *Argynnis hyperbius*, and *Vanessa cardui* in the Nymphalidae have been employed to differentiate tribes within the subfamily Nymphalinae (Wahlberg et al. 2005). *Aulocera saraswati* showed a clear case of discocellular branching and margin demarcation (e.g., tornus, termen), a feature in support of the species belonging to a separate lineage of evolution (Wahlberg et al. 2003). Moreover, the wing structures of the Lycaenidae butterflies *Polyommatus eros* and *Lycaena phlaeas* were found to be highly compact with a tight cluster

of radial series and narrow vein spacing, which are features of small body size and stable flight (Vila et al. 2011; Pengliang et al. 2025). The present research thus confirms that wing venation is a multifunctional characteristic influenced by ecological, biomechanical, and evolutionary factors rather than just being a morphological relic. It is still a crucial tool in lepidopteran systematics, especially when combined with ecological and molecular data to validate morphological identification and provide a comprehensive understanding of species diversity and evolutionary relationships.

In this study, the mitochondrial COX1 gene was applied as the primary genetic marker for molecular identification of insect pollinators associated with cherry orchards of the Kashmir Valley. High-quality DNA barcodes were generated through PCR amplification and sequencing, and the obtained sequences were edited and aligned using BioEdit software. Phylogenetic analyses were conducted in MEGA version 6 using the Maximum Likelihood method under the General Time Reversible (GTR) substitution model, which yielded well-supported clades and strongly corroborated the morphological identification of the pollinator species (Tamura et al. 2013). Furthermore, nucleotide sequences were compared with reference sequences available in the NCBI database using BLAST (Table 17), and validated sequences were submitted to GenBank, where accession numbers were obtained. This ensured that species identification was accurate, transparent, and reproducible, providing a reliable molecular framework for future pollinator biodiversity and taxonomic studies (Chen et al. 2022). In addition to COX-I barcoding, several other genetic markers have been employed for insect species identification to overcome the limitations associated with mitochondrial DNA, particularly in closely related and cryptic taxa. Nuclear ribosomal markers such as ITS2 have been shown to provide reliable species-level resolution in insects, especially in Hymenoptera and Diptera, where mitochondrial introgression and low interspecific divergence can reduce the effectiveness of COX-I (Beebe and Saul 1995; Lv et al. 2014). Previous studies have demonstrated that ITS2 successfully discriminates morphologically similar insect species and serves as an effective complementary barcode to COX-I, thereby improving taxonomic resolution and identification accuracy (Tan et al. 2020). Similarly, the mitochondrial 16S rRNA gene has been widely used as an alternative or supplementary marker for insect identification, particularly when COX-I amplification fails or when degraded DNA samples are encountered, as reported for Diptera and Hymenoptera in several molecular identification studies (Sarri et al. 2014). Further insights were drawn from the calculation of diversity indices across cherry orchards in different districts. The Dominance index remained low (0.03408-0.03552), indicating no single species dominated any

orchard. The Simpson Index values (~ 0.965) suggested highly diverse communities with even species distributions. Shannon-Weiner Index (H') values (3.352-3.372) highlighted high pollinator diversity across all sites. Evenness indices, ranging from 0.9853 to 1.005, further confirmed the relatively balanced representation of different species. Margalef's Index values (4.405-4.559) pointed toward high species richness throughout the orchards (**Table 18**). Together, these indices suggest that the cherry orchards of Kashmir Valley provide stable and resource-rich habitats conducive to sustaining diverse pollinator communities, consistent with findings in well-managed agroecosystems (Paray et al. 2014).

This study also highlighted the crucial role of insect pollinators in cherry production. In pollination regimes, where pollinators were excluded, no fruit set was observed, confirming that insect-mediated pollination is essential for fruit development in cherries (Osterman et al. 2024). When regimed with *A. mellifera*, significant improvement was seen in fruit set, fruit size, weight, sweetness (TSS), and acidity, which resulted in higher-quality fruits. These findings indicate that the frequency of pollinator visits is directly correlated with fruit quality, emphasising the importance of sustained and efficient pollination (Wang et al. 2022). Among the insect pollinators, *A. mellifera* was found to be the most effective, producing the largest and sweetest fruits with the lowest acidity. Its superior performance is likely due to its larger colony size, broader foraging range, and high flower fidelity, which together enhance pollen transfer efficiency. *A. cerana*, on the other hand, also contributed positively to fruit set and quality, particularly after repeated visits, but its efficiency was slightly lower, possibly due to a smaller colony size and shorter foraging range. These results were consistent with previous studies reporting that both *A. mellifera* and *A. cerana* improve fruit yield and quality in temperate fruit crops, with managed honeybees generally being more consistent and reliable (Paray et al. 2014). Wild insect pollinators contributed to fruit development; however, their pollination efficiency showed greater variability and was generally lower than that of managed honeybees. This pattern has been consistently reported in temperate fruit orchards, where unmanaged pollinators provide valuable but less predictable pollination services due to fluctuating population densities and foraging behaviour (Klein et al. 2007; Garibaldi et al. 2013). The activity of wild pollinators is strongly influenced by environmental factors such as temperature, wind speed, rainfall, humidity, and temporal availability of floral resources. Low temperatures and high wind speeds significantly reduce flight activity in solitary bees, bumble bees, and syrphid flies, particularly during early spring flowering of cherry and other stone fruits (Brittain et al. 2013; Vicens and Bosch 2000). Rainfall during bloom further restricts foraging duration and pollen transfer efficiency, resulting in reduced fruit set (Free 1993).

Although wild pollinators such as bumble bees, halictid bees, and syrphid flies play a crucial role in maintaining pollination diversity and long-term ecosystem stability, they cannot be practically managed under orchard conditions. Unlike managed honeybees, wild pollinators cannot be confined to specific plots, their nest densities cannot be manipulated, and their visitation frequency cannot be standardised for experimental pollination regimes (Potts et al. 2010; Rader et al. 2016). This makes it difficult to quantify their individual contribution under controlled visitation treatments. Managed honeybees were therefore preferred in the present study because colonies could be deliberately introduced into orchards, allowing controlled and repeatable pollination treatments. The use of managed colonies enables precise regulation of flower visitation and ensures adequate pollinator density during peak bloom, which is essential for reliable fruit set in self-incompatible crops such as cherry (Free 1993; Holzschuh et al. 2012). Previous studies in cherry and other fruit orchards have demonstrated that managed honeybees provide consistent and effective pollen transfer, resulting in higher fruit set, increased fruit size, and improved uniformity compared to orchards relying solely on wild pollinators (Bosch and Blas 1994; Garratt et al. 2014). Honeybee foraging behaviour, including repeated flower visits and high pollen carryover, enhances cross-pollination efficiency in mass-flowering crops (Delaplane and Mayer 2000). Importantly, managed honeybees do not replace wild pollinators but rather complement their activity. Large-scale global analyses have shown that crop yield stability is highest when managed pollinators operate alongside diverse wild pollinator communities (Garibaldi et al. 2013). Wild pollinators contribute to resilience under variable environmental conditions, while managed honeybees ensure baseline pollination when wild pollinator activity is reduced (Rader et al. 2016). In the present study, improved fruit quality parameters were most strongly associated with managed honeybee activity, particularly under controlled visitation regimes. Similar findings have been reported in cherry orchards, where honeybee pollination significantly enhanced fruit weight, diameter, and marketable yield compared to unmanaged pollination systems (Holzschuh et al. 2012; Osterman et al. 2024). These results confirm that while wild pollinators are ecologically indispensable, managed honeybees remain critical for achieving consistent yield and quality in commercial cherry production systems. At the same time, conservation of native pollinators, including *A. cerana* and other native insects, supports ecosystem resilience and safeguards pollination services under changing environmental conditions. Thus, sustainable orchard management practices such as habitat preservation, floral resource enhancement, and reduced pesticide use are essential to maintain both ecological balance and long-term productivity in cherry agroecosystems.

Chapter 5

Summary and Conclusion

With a multidisciplinary approach, this study offers the first thorough and integrative assessment of insect pollinator diversity in cherry orchards of the Kashmir Valley. The region's great ecological variability and abundant floral resources are reflected in the 30 species that were documented from three main insect orders: Hymenoptera (10 spp.), Diptera (6 spp.), and Lepidoptera (14 spp.). This study provides the first DNA-based (COX-I) confirmations of *Lasioglossum matianense*, *Lasioglossum marginatum*, *Lasioglossum rugifrons*, and *Nymphalis canace* from the Kashmir Valley, India. Until now, these species were known only through morphological reports from other regions of the country, with no molecular evidence available from India. From small native pollinators like *Lasioglossum matianense*, *Lasioglossum marginatum*, *Lasioglossum rugifrons*, *A. mellifera*, *A. cerana*, etc, that were capable of pollinating densely crowded cherry blossoms to the large-bodied *Bombus albopleuralis* that was fit for long-distance foraging, hymenopterans demonstrated a variety of adaptations. The syrphid flies ranged from small, quick foragers like *Sphaerophoria scripta*, powerful fliers like *Eristalis tenax*. The morphological identification of insect pollinator species was validated by molecular analysis, which also produced GenBank accessions for reference and well-supported phylogenetic clades. A stable and well-balanced pollinator community was indicated by diversity indices that showed low dominance, equal dispersion, and high species richness. Insect-mediated pollination is essential for cherry fruit set and quality, according to pollination efficiency trials. In comparison to other pollination regimes, *A. mellifera* emerged as the most effective pollinator, resulting in a significant increase in fruit size, weight, sweetness, and a reduction in acidity. This superior performance can be attributed to its wider foraging range, high floral fidelity, and dense body hairs that enable efficient collection and transfer of pollen grains. Multiple floral visits by *A. mellifera* (max. 5-6 visits per flower) produced the best fruit set and quality because cherry is predominantly an entomophilous and self-incompatible crop, requiring repeated pollen deposition from genetically compatible flowers to ensure complete and successful fertilisation. With each additional visit, more pollen grains are transferred to the stigma, improving pollen tube growth, enhancing ovule fertilisation, and ultimately leading to healthier fruit development and better yield. Overall, the findings demonstrate that the cherry orchards of the Kashmir Valley harbor a rich, diverse, and ecologically resilient pollinator community. The integration of morphological, morphometric, molecular, and ecological approaches not only ensured accurate species identification but also provided insights into functional roles within the ecosystem. The study highlights the urgent need to conserve pollinator diversity through habitat preservation, pollinator-friendly orchard management, and

reduced pesticide use. Such measures are essential to safeguard both biodiversity and agricultural productivity, offering a replicable model for pollinator studies in other temperate agroecosystems worldwide.

Future Scope of the Study

By describing the variety, taxonomy, and molecular identification of insect pollinators connected to Kashmir Valley cherry orchards, the current study has established a strong foundation. The complexity of pollinator relationships and the diversity of this agroecosystem, however, suggest that there is still considerable room for further study. The future research may focus on other commercially significant fruit crops grown in the area, such as apples, pears, apricots, and almonds, which together make up Kashmir's temperate horticulture. Long-term monitoring would help identify trends in population dynamics, phenological changes, and community turnover since pollinator abundance and composition are extremely susceptible to environmental fluctuation. To build prediction models and adaptive conservation methods that protect pollinator populations under future climatic scenarios, multi-year information will be essential for understanding how climate change affects pollinator assemblages. Upcoming research should use other nuclear markers and next-generation sequencing (NGS) techniques, even though the current study effectively used the COXI gene barcoding for species-level identification at the molecular level.

Undertaking cryptic species complexes, evaluating genetic diversity among populations, and more accurately recreating evolutionary histories are all made possible by such sophisticated methods. Integrating these genomic findings with ecological features, morphology, and morphometrics will improve taxonomic resolution and pave the way for more comprehensive evaluations of biodiversity. Beyond species inventories, future studies should investigate the functional roles of pollinators in agricultural yield.

To ensure consistent fruit set, production, and quality in cherry orchards, the most efficient pollinators will be identified, and evidence-based recommendations for their focused conservation and management will be provided. Examining how agricultural activities affect pollinator diversity and health is equally essential. Monocropping, habitat change, and the extensive use of pesticides provide serious dangers that need to be carefully considered. To create sustainable orchard systems, research on pollinator-friendly management techniques will be essential. These techniques include integrated pest control, organic farming, blooming strip maintenance, and nesting habitat supply.

Predictive modeling under different climate change scenarios may also be able to identify pollinator species that are at risk and foresee future obstacles to their continued existence in the valley. The results of this study can potentially be used as a starting point for farmer-focused projects and conservation legislation. Researchers, legislators, and agricultural communities

must work together to develop solutions that combine horticulture production with biodiversity protection to bridge the gap between knowledge and practice. In the end, this data will encourage more investment in pollinator conservation across temperate agroecosystems by highlighting their ecological significance and underscoring their role in maintaining farmer livelihoods.

Appendices

List of Publications

Sr. No.	Title of the Paper	Journal Name	Article Type	Published	Indexing
1	Morphometric Profiling of Hymenopteran Pollinators from Cherry Orchards in the Kashmir Valley, India	Plant Protection	Research	August, 2025	Scopus Indexed
2	Effect of pollination on fruit set and quality of sweet cherry (<i>Prunus avium</i> L.) in Kashmir Valley, India	Journal of Applied and Natural Sciences	Research	September 2025	Scopus Indexed
3	Adapting to climate extremes: Implications for insect populations and sustainable solutions	Journal for Nature Conservation	Review	March 2024	Scopus Indexed



Available Online at EScience Press

Plant Protection

ISSN: 2617-1287 (Online), 2617-1279 (Print)
<http://esciencepress.net/journals/PP>

Research Article

Morphometric Profiling of Hymenopteran Pollinators from Cherry Orchards in the Kashmir Valley, India

^{a,b}Arjumand John, ^bSajad Ahmad Ganie, ^cKaisar Ahmad Bhat, ^aAmaninder Kaur Riat^a School of Bioengineering and Bioscience, Lovely Professional University, Phagwara, Jalandhar, Punjab-144402, India.^b Department of Entomology, Sher-e-Kashmir University of Agricultural Science and Technology, Srinagar, Jammu and Kashmir-190025, India.^c Department of Biotechnology, Baba Ghulam Shah Badshah University, Rajouri, Jammu and Kashmir-185234, India.

ARTICLE INFO

Article history

Received: 13th May, 2025Revised: 1st August, 2025Accepted: 3rd August, 2025

Keywords

Cherry

Hymenoptera

Morphological measurements

Pollination

ABSTRACT

Hymenoptera, a diverse and ecologically important insect order, plays a vital role in enhancing fruit crop productivity through pollination. Despite their significance, morphometric data on pollinators from the temperate cherry orchards of the Kashmir Valley are limited. The present study, therefore, assessed interspecific and intraspecific morphological variation among 10 hymenopteran species belonging to four families: Apidae (*Apis mellifera*, *A. cerana*, *Bombus albopoleuralis*), Halictidae (*Lasioglossum rugifrons*, *L. matianense*, *L. marginatum*), Andrenidae (*Andrena fucata*, *A. pilipes*, *A. agilissima*), and Vespidae (*Vespula vulgaris*). A total of 38 morphometric traits were recorded from the head, thorax, abdomen, and wings. Multivariate analysis, including Principal Component Analysis and Hierarchical Cluster Analysis using Python, revealed clear patterns of morphometric divergence and genus-level clustering. Closely related species such as *A. mellifera* and *A. cerana*, and the *Lasioglossum* group, formed tight clusters. In contrast, distinct species like *B. albopoleuralis* and *V. vulgaris* were separated due to larger body sizes and unique structural adaptations. Morphological diversity among species has ecological relevance, influencing pollination efficiency, foraging behavior, and floral specialization. Robust bees like *B. albopoleuralis*, with strong tibiae and long wings, are suited for long-distance foraging and pollinating deep flowers. In contrast, *L. matianense* is adapted to localized foraging and shallow blooms. These functional differences highlight the complementary roles of diverse pollinators in supporting stable and efficient pollination services. The integration of morphometric and ecological analyses emphasizes the value of both *Apis* and non-*Apis* bees in cherry orchard ecosystems.

Corresponding Author: Amaninder Kaur Riat

Email: amaninder.21097@lpu.co.in

© 2025 EScience Press. All rights reserved.

Introduction

The order *Hymenoptera* is one of the largest and most diverse insect groups. Members typically possess two pairs of membranous wings (with smaller hindwings),

well-developed compound eyes, and chewing or chewing-lapping mouthparts adapted to varied feeding behaviors (Papa et al., 2022). A distinctive trait in many species, especially bees, ants, and wasps, is the narrow

Research Article

Effect of pollination on fruit set and quality of sweet cherry (*Prunus avium* L.) in Kashmir Valley, India

Arjumand John

School of Bioengineering and Bioscience, Lovely Professional University, Phagwara, Jalandhar-144402 (Punjab), India; Department of Entomology, Sher-e-Kashmir University of agricultural science and Technology, Srinagar- 190025 (J&K), India

Sajad A. Ganie

Department of Entomology, Sher-e-Kashmir University of agricultural science and Technology, Srinagar- 190025 (J&K), India

Kaisar A. Bhat

Department of Biotechnology, Baba Ghulam Shah Badshah University Rajouri – 165234 (J&K), India

Amaninder Kaur

School of Bioengineering and Bioscience, Lovely Professional University, Phagwara, Jalandhar-144402 (Punjab), India

Corresponding author: E-mail: amaninder.21097@lpu.co.in

Article Info

<https://doi.org/10.31018/jans.v17i3.6628>

jans.v17i3.6628

Received: March 10, 2025

Revised: July 29, 2025

Accepted: August 15, 2025

How to Cite

John, A. et al. (2025). Effect of pollination on fruit set and quality of sweet cherry (*Prunus avium* L.) in Kashmir Valley, India. *Journal of Applied and Natural Science*, 17(3), 1137 - 1145. <https://doi.org/10.31018/jans.v17i3.6628>

Abstract

Pollinators play a crucial role in the reproduction of cherries, ensuring successful fruit set and enhancing the quality and yield of cherries. The study aimed to highlight the crucial role of insect pollinators in enhancing the fruit set and quality of sweet cherries (*Prunus avium* L.) in orchards of the Kashmir Valley, with significant implications for sustainable horticultural practices. Utilizing a Randomized Block Design (RBD) with six treatments and three replications, the contributions of three key pollinators *Apis mellifera*, *Apis cerana*, and *Eristalis tenax* were systematically evaluated. While all pollination treatments resulted in 100% fruit set, notable differences in fruit quality were observed based on pollinator species and visit frequency. *A. mellifera* emerged as the most effective pollinator, attributed to its high foraging rate (1.65 flowers per second) and strong fidelity. It produced the largest fruits (18.00 mm), highest fruit weight (8.82 g), lowest acidity (1.12% citric acid), and highest TSS (17.90°Brix). *A. cerana* also contributed significantly, particularly under multiple visit scenarios, yielding fruit size of 17.10 mm, weight of 7.22 g, acidity of 1.44%, and total soluble solids (TSS) of 16.57°Brix. Though *E. tenax* exhibited lower efficiency, it still played a supplemental role, improving fruit characteristics moderately with repeated visits. Foraging efficiency, measured as time spent per flower, further reinforced the dominance of *A. mellifera* (8.34 seconds/minute/flower) over *A. cerana* (9.38 seconds/minute/flower) and *E. tenax* (11.34 seconds/flower).

Keywords: Acidity, Cherry, Fruit set, Foraging time, Fruit size, Fruit weight, Foraging speed, Total soluble solids (TSS)

INTRODUCTION

Pollination is pivotal in agricultural productivity, especially for crops such as cherry (*Prunus avium* L.), where fruit set and quality largely depend on effective cross-pollination. While cherries possess some self-fertility, cross-pollination, particularly by insect pollinators, is crucial for optimal fruit production (Osterman et al., 2024). The global cherry industry is highly reliant on insect pollinators to ensure the success of its yields, with several studies demonstrating the positive impact of pollinator activity on both fruit quantity and quality

(Hünicken et al., 2021). Among the insect pollinators, bees, including honeybees (*Apis mellifera*), bumblebees (*Bombus* spp.), and solitary bees, are recognised as the most efficient agents of cherry pollination. These insects facilitate the transfer of pollen between flowers, thereby enhancing fertilisation and ultimately increasing fruit set (Khalifa et al., 2021). In many parts of the world, particularly in Europe and North America, extensive research has been conducted to evaluate the role of these pollinators in cherry orchards (Rosas-Ramos, Baños-Picón, Tormos and Asís, 2020). For instance, honeybees are known to be highly effective due to their



ELSEVIER

Contents lists available at ScienceDirect

Journal for Nature Conservation

journal homepage: www.elsevier.com/locate/jnc

Adapting to climate extremes: Implications for insect populations and sustainable solutions

Arjumand John^a, Amaninder Kaur Riat^a, Kaisar Ahmad Bhat^b, Sajad A. Ganie^c, Otto endarto^d, Cipto Nugroho^e, Handoko Handoko^d, Atif Khurshid Wani^{a,*}

^a School of Bioengineering and Biosciences, Lovely Professional University, Jalandhar, 144411, Punjab, India

^b Department of Biotechnology, School of Biosciences and Biotechnology, Baba Ghulam Shah Badkhal University, Rajouri 185234, India

^c Division of Entomology, Sher-e-Kashmir University of Agricultural Science and Technology, Srinagar 190025, India

^d Research Center for Horticulture, National Research and Innovation Agency, Bogor 16911, Indonesia

^e Research Center for Food Crops, National Research and Innovation Agency, Bogor 16911, Indonesia

ARTICLE INFO

Keywords:

Extreme climate
Insects
Mitigation
Population Dynamics
Temperature
Agriculture
Food security

ABSTRACT

Climate change emerges as the most dynamic and pervasive environmental challenge of the contemporary era. Its consequences, including the greenhouse effect resulting in elevated temperatures, increasingly frequent droughts, and unpredictable rainfall patterns, are already evident. The effects of climate change and extreme weather phenomena encompass insects, plants, and various taxonomic categories. Heightened temperatures, increased CO₂ levels, and sudden shifts in rainfall patterns hold the potential to significantly alter the biochemical processes within insects and thus alter their survival pattern. These dynamic alterations in climate have a notable effect on multiple aspects of insect life, including fertility, feeding patterns, survival rates, population dynamics, and patterns of dispersal. As a result, their abundance, distribution, and life cycles undergo modifications in response to these evolving environmental conditions. This review explores the varied impacts of extreme climate changes on insect populations, explaining the complex relationships between climatic variables and insect ecology. Such changes can have cascading effects on ecosystems leading to disruptions in pollination with indirect implications on food security. Recognizing the urgency of addressing these challenges, this review also delves into sustainable approaches to reduce the risks posed by extreme climate changes on insect populations. Thus, integrated pest management strategies, organic farming, conservation of natural habitats, and the promotion of resilient agricultural practices emerge as key components of a comprehensive framework. This review advocates for a complete and adaptive approach to reduce the effect of extreme climate changes on insect populations, ensuring the long-term ecological balance and the resilience of ecosystems in the face of a varying climate.

1. Introduction

Over the last few decades, there has been a growing body of evidence indicating a persistent decline in the earth's insect population. Despite insects comprising three-quarters of all animal and plant species worldwide, they have received limited attention in scientific research, nature conservation initiatives, and environmental policymaking (van der Sluis, 2020). Insects play a key role in shaping the future of our planet as these contribute to pest control, facilitate the decomposition of organic matter, and release vital nutrients into the soil. Additionally, flying insects serve as crucial pollinators for numerous essential food

crops, including fruits and spices (Jankielsohn, 2018). As environmental changes unfold, insect populations have become highly responsive indicators, with extreme climate conditions witnessing notable shifts, resulting in heightened frequencies and intensities of extreme weather events. The decrease in insect populations poses a significant threat to human health due to its impact on essential micronutrients sourced from insect-pollinated crops. Additionally, the availability of phytopharmaceuticals and nutritional supplements is reliant on pollinators, further underscoring the importance of insect populations for human well-being. An analysis revealed that the complete eradication of pollinators may result in a yearly rise of roughly 1.4 million deaths worldwide

* Corresponding author.

E-mail addresses: atifkhurshid61200216@gmail.com, atif.12009032@lpu.in (A.K. Wani).

<https://doi.org/10.1016/j.jnc.2024.126602>

Received 8 January 2024; Received in revised form 9 March 2024; Accepted 15 March 2024

Available online 16 March 2024

1617-1381/© 2024 Elsevier GmbH. All rights reserved.

List of Conferences

- 1) Presented a poster at the 3-day International Conference (AI-CIAS) on “**AgriTech Intelligence and Beyond: Cutting Edge Innovations in Agriculture and Allied Sciences**” held at the Faculty of Veterinary Sciences & Animal Husbandry, SKUAST-K, Shuhama Campus (**24-06-2024**).
- 2) Presented an oral paper at the International Conference on “**Recent Advances in Smart and Sustainable Agriculture for Food and Nutritional Security (SSAFNS)**” held at Lovely Professional University, Punjab, and secured **First Position (23-11-2023)**.
- 3) Presented paper (Oral) at 5th International Conference on “**Climate Change and its Impact (CCI 2023)**” Held at Sheir Kashmir University of Agricultural Science and Technology, Shalimar SKUAST-K (**9-11-2023**).



C.No. AFTEFS/SKUAST/24/06

International Conference on

AGRITECH INTELLIGENCE AND BEYOND: CUTTING EDGE INNOVATIONS IN AGRICULTURE AND ALLIED SCIENCES

15-17 OCTOBER, 2024

DIVISION OF VETERINARY BIOCHEMISTRY, FACULTY OF VETERINARY SCIENCES & AH, SKUAST-KASHMIR SRINAGAR INDIA

AGRICULTURE FORUM FOR TECHNICAL EDUCATION OF FARMING SOCIETY (AFTEFS)

CERTIFICATE OF PARTICIPATION



This is to certify that Prof./Dr./Mr./Ms. Arjumand John(Ph.D. Scholar) Zoology, Lovely Professional University participated in the three-day International

Conference on "Agritech Intelligence and Beyond: Cutting Edge Innovations in Agriculture and Allied Sciences"

He/She contributed as a distinguished Delegate, and also presented a scholarly Paper/Poster entitled

Morphometric and Molecular Analysis of Orders; Hymenoptera and Diptera in Cherry Orchards of Kashmir Valley

during the conference.

Dr. Shahzada Mudasir Rashid
ORGANIZING SECRETARY
AI-CIAS 2024
(VETERINARY BIOCHEMISTRY)
SKUAST-KASHMIR

Prof. Z.A. Pampori
CONVENER
AI-CIAS 2024
(VETERINARY BIOCHEMISTRY)
SKUAST-KASHMIR

Dr. K.S. Nama
PRODUCT MANAGER
VITAL BIOTECH
VICE PRESIDENT, AFTEFS

Dr. Jitendra Mehta
PRESIDENT, AFTEFS
VITAL BIOTECH
KOTA, RAJASTHAN, INDIA



SCHOOL OF
AGRICULTURE



Dhanu Certificate No. 303146



Certificate of Merit

This is to certify that **Prof./Dr./Mr./Ms. Arjumand John** stood **First Prize** in the International conference
“**Recent Advances in Smart and Sustainable Agriculture for Food and Nutritional Security-2023**” held from **22nd to 23rd November, 2023** organized by School of Agriculture, Lovely Professional University, Punjab.

Date of Issue: 02-01-2024
Place: Phagwara (Punjab), India

Prepared by
(Administrative Officer-Records)

Organizing Secretary

Head of School

Think BIG



5th International Conference

Climate Change and Its Impact (CCI-2023)

CERTIFICATE



This is to certify that Prof./Dr./Mr./Ms. **ARJOMAND JOHN** of **LOVELY PROFESSIONAL UNIVERSITY, JHALANDHAR - PUNJAB - 144402** Actively participated/presented a paper (Oral/Poster) entitled **Effects Of Extreme Climate Changes on Insects**

As a Delegate/Scholar in the "5th International Conference on "Climate Change and Its Impact (CCI 2023)" jointly organized by Sher-e-Kashmir University of Agricultural Sciences and Technology (SKUAST-K) Srinagar, J&K., India; Agricultural & Environmental Technology Development Society (AETDS), U.S. Nagar, Uttarakhand, India; University of Agricultural Sciences Raichur, Karnataka, India; Vasant Rao Naik Marathwada Krishi Vidyapeeth Parbhani, M.H., India Sher-e-Bangla Agricultural University, Dhaka, Bangladesh and Mid-West University, Surkhet, Nepal at Sher-e-Kashmir University of Agricultural Sciences and Technology (SKUAST-K) Srinagar, J&K., India on June 9-11, 2023.

Prof. (Dr.) C. P. Singh

Conference Director
President, AETDS
Former Professor
GBPUAT, Pantnagar, India

Prof. Mirza Hasanuzzaman

Conference Director
Sher-e-Bangla Agri. University
Bangladesh

Prof. (Dr.) Gururaj Sunkad

Conference Chairman
Dean Postgraduate Studies
University of Agricultural Sciences
Raichur, Karnataka, India

Prof. (Dr.) F. A. Khan

Organizing Secretary
Head, Faculty of Horticulture
SKUAST, Srinagar (J&K), India

Dr. Karan Singh Dhami

Conference Associate Director
Mid-West University, Nepal

Dr. Wajid Khan

Organizing Convener
Secretary, AETDS
KVK, Jehanabad
BAU Sabour, Bihar, India

RECIPIENT'S NAME
ARJOMAND JOHN



AETDS/PC/CCI/2023

Chapter 6

References

- Abrol DP. 2011. *Pollination biology: biodiversity conservation and agricultural production*. Dordrecht: Springer. p. 1-792.
- Ačanski J, Vujić A, Djan M, Obreht D. 2023. Geometric morphometrics of wing shape variation in hoverflies (Diptera: Syrphidae). *Zool Anz.* 302:45-53.
- AgriFarming. 2024. Cherry farming: cultivation practices, production statistics, and profitability. AgriFarming. in. Available from: <https://www.agrifarming.in>
- Ahmed M, Babayola M, Bake I. 2024. Role of horticultural crops in food and nutritional security: a review. *Nutr Food Process.* 7(8):7-29.
- Alam M, Abbas K, Usmani N, Mustafa M, Husain A. 2024. A comprehensive review of DNA barcoding for species identification across diverse taxa. *Munis Entomol Zool J.* 19(2):1057-1072.
- Aytekin AM, Terzo M, Rasmont P, Çağatay N. 2007. Landmark based geometric morphometric analysis of wing shape in bumblebees (*Bombus* spp.). *Ann Zool Fenn.* 44(5):345-356.
- Bali D, Barwal P, Sharma R, Deep A, Kashyap P. 2022. Trend analysis of cherry cultivation. *Agro-Economist Int J.* 9(2):127-131.
- Banyal HS, Sharma S, Kumar N, Kumari D. 2024. Insect pollinators diversity, distribution, ecological function and conservation status in the Himalayan region. In: *Insect pollinators diversity: distribution*, 2024. Wildflower strips in polytunnel cherry orchard alleyways support pest regulation services but do not counteract edge effects on pollination services. *Front Sustain Food Syst.* 8:142-171.
- Bare N, Jadhav P, Ponnuchamy M. 2024. DNA barcoding for species identification and phylogenetic investigation employing five genetic markers of *Withania coagulans*. *J Appl Biol Biotechnol.* 12(1):69-76.
- Bare VV, Sharma A, Singh R, Thakur M. 2023. Multi-gene DNA barcoding (COI and rRNA) improves pollinator identification in Himalayan fruit orchards. *Sci Rep.* 13(1):102-134.
- Barrios B, Pena SR, Salas A, Koptur S. 2016. Butterflies visit flowers but contribute little to pollination: a case study in a tropical system. *Am J*

- Bot.* 103(3):1-8.
- Bartholomée O, Aullo A, Becquet J, Vannier C, Lavorel S. 2020. Pollinator presence in orchards depends on landscape-scale habitats more than in-field flower resources. *Agric Ecosyst Environ.* 293:106-126.
- Beasley DE, Bonisoli-Alquati A, Mousseau TA. 2019. Wing shape variation in a solitary bee (*Andrena barbara*) across urban environments using geometric morphometrics. *Urban Ecosyst.* 22(3):451-460.
- Beasley DE, Fitzgerald JL, Fowler A, Keleher K, Lopez-Urbe MM, Dunn Beebe NW, Saul A. 1995. Discrimination of all members of the *Anopheles punctulatus* complex by polymerase chain reaction-restriction fragment length polymorphism analysis. *Am J Trop Med Hyg.* 53(5):478-481.
- Beebe NW, Saul A. 1995. Discrimination of all members of the *Anopheles punctulatus* complex by polymerase chain reaction–restriction fragment length polymorphism analysis. *Am J Trop Med Hyg.* 53(5):478-481.
- Bell KL, Loeffler VM, Brosi BJ. 2022. An rbcL and ITS2 metabarcoding approach to pollen identification: overcoming limitations of morphology. *Apple Plant Sci.* 10(3):114-130.
- Bihaly AD, Piross IS, Pellaton R, Szigeti V, Somay L, Vajna F, Soltész Z, Báldi A, Sáróspataki M, Kovács-Hostyánszki A. 2024. Landscape-wide floral resource deficit enhances the importance of diverse wildflower plantings for pollinators in farmlands. *Agric Ecosyst Environ.* 367:108-140.
- Borchardt N, Klein AM, Scherber C. 2024. Ecological roles of *Vespula vulgaris* in agroecosystems: predator and incidental pollinator. *Agric Ecosyst Environ.* 361:108-155.
- Bosch J, Blas M. 1994. Foraging behaviour and pollination efficiency of *Osmia cornuta* in almond orchards. *Apidologie.* 25(6):593-602.
- Braby MF, Vila R, Pierce NE. 2006. Molecular phylogeny and systematics of the Pieridae (Lepidoptera: Papilionoidea). *Syst Entomol.* 31(4):646-671.
- Brannoch S, Wieland F, Rivera J, Klass KD, Béthoux O, Svenson G. 2017. Manual of praying mantis morphology, nomenclature, and practices

- (Insecta: Mantodea). *ZooKeys*. 696:1-100.
- Brittain C, Williams N, Kremen C, Klein AM. 2013. Synergistic effects of non-Apis bees and honey bees for pollination services. *Proc R Soc B*. 280(1754):201-237.
- Carvalho APS, Duarte M, Marconato G, Casagrande MM. 2017. Comparative morphology of genitalia in Lepidoptera and its taxonomic significance. *Zool Anz*. 268:1-10.
- Chen C, Compton A, Nikolouli K, Wang A, Aryan A, Sharma A, Qi Y, Dellinger C, Hempel M, Potters M, Augustinos A, Severson DW, Bourtzis K, Tu Z. 2022. Marker-assisted mapping enables forward genetic analysis in *Aedes aegypti*. *Genetics*. 22(3):187-201.
- Chen G, Cong Q, Feng Y, Ren L. 2003. Study on the wettability and self-cleaning of butterfly wing surfaces. *Inst Phys Conf Ser*. 18(2):245-251.
- Chen X, Li Y, Zhang Z, Wang H. 2022. DNA barcoding and molecular identification of insect species using COI sequences. *Mitochondrial DNA B*. 7(3):567-575.
- Cho S, Lee S, Park HC. 2016. Preservation and drying techniques for maintaining insect specimen integrity in morphological studies. *J Asia Pac Entomol*. 19(4):1105-1110.
- Choi SW, Jung C. 2015. Diversity of insect pollinators in agricultural crops and wild flowering plants in Korea: literature review. *J Apic*. 30(3):191-205.
- Common IFB. 1990. *Moths of Australia*. Melbourne: Melbourne University Press.
- Connor EF, Courtney AC, Yoder JM. 2019. Sampling techniques and specimen preservation methods in entomological studies. *J Insect Conserv*. 23(2):321-330.
- Cornalba M, Biella P, Galimberti A. 2020. DNA barcoding unveils the first record of *Andrena allosa* for Italy and unexpected genetic diversity in *Andrena praecox*. *Fragm Entomol*. 52(1):1-6.
- Dar S, Wani A, Sofi M. 2018. Diversity and abundance of insect pollinators of sweet cherry (*Prunus avium*) in Kashmir Valley. *Indian J Entomol*. 80(3):725-730.

- Dar SA, Wani AA, Ahmad SB, Bhat FA. 2018. Insect pollinator diversity in temperate fruit orchards of Kashmir Himalaya. *J Entomol Zool Stud.* 6(5):234-239.
- Delaplane KS, Mayer DF. 2000. *Crop pollination by bees*. Wallingford: CABI Publishing.
- Dhokane VS, Chavan SP. 2025. Morphological characterization of insect pollinators in fruit crops of Aurangabad district, Maharashtra. *J Entomol Zool Stud.* 13(1):45-52.
- Dincă V, Wiklund C, Lukhtanov VA, Kodandaramaiah U, Norén K, Dapporto L, Wahlberg N, Vila R. 2021. Reproductive isolation and morphological divergence in cryptic butterfly species. *Mol Ecol.* 30(5):1122-1136.
- Directorate of Horticulture, Jammu and Kashmir. 2023. Area and production diversity. *Ecol Environ Conserv.* 20: S471-S477.
- Dunn L, Lequerica M, Reid CR, Latty T. 2020. Dual ecosystem services of syrphid flies (Diptera: Syrphidae): pollination and biological control. *Insects.* 11(5):1-12.
- Eeraerts M, Smagghe G, Meeus I. 2019. Pollinator diversity, floral resources and semi-natural habitat, instead of honey bees and intensive agriculture, enhance pollination service to sweet cherry. *Agric Ecosyst Environ.* 22(4):106-136.
- Eeraerts M, Vanderhaegen R, Smagghe G, Meeus I. 2020. Pollination efficiency and foraging behaviour of honey bees and non-*Apis* bees to sweet cherry. *Agric For Entomol.* 22(1):75-82.
- Erogul D. 2018. An overview of sweet cherry fruit cultivation in Turkey. extraction from preserved stoneflies (Insecta: Plecoptera). *J Entomol Res Soc.* 11(3):1-9.
- FAOSTAT. 2024. FAOSTAT statistical database: crops and livestock products – cherries. Rome (Italy): Food and Agriculture Organization of the United Nations. Available from: <https://www.fao.org/faostat>
- Faraz A, Jamali M, Kumar G, Mir S. 2023. Importance of hymenopteran insects in pollination. In: *Advances in entomology and zoology*. Chap. 8. India: AkiNik Publications. p. 140.

- Fliszkiewicz M, Giejdasz K. 2023. Effect of pollination by *Osmia bicornis* (syn. *O. rufa*) on fruit set, seed set, and yield in three apple cultivars. *J Apic Sci.* 67(1):125-134.
- Folmer O, Black M, Hoeh W, Lutz R, Vrijenhoek R. 1994. DNA primers for amplification of mitochondrial cytochrome c oxidase subunit I from diverse metazoan invertebrates. *Mol Mar Biol Biotechnol.* 3(5):294-299.
- Free JB. 1993. *Insect pollination of crops*. London: Academic Press.
- Gamboa D, Arrivillaga J. 2009. Preservation of insect specimens in ethanol for molecular and genetic analysis. *J Med Entomol.* 46(3):589-593.
- Garibaldi LA, Steffan-Dewenter I, Winfree R. 2013. Wild pollinators enhance fruit set of crops regardless of honey bee abundance. *Science.* 339(6127):1608-1611.
- Garner BH, Needleman HM, Young JH. 2011. Standard insect pinning techniques and specimen preservation for taxonomic studies. *J Insect Conserv.* 15(3):457-463.
- Garratt MPD, Breeze TD, Jenner N, Polce C, Biesmeijer JC, Potts SG. 2014. Avoiding a bad apple: insect pollination enhances fruit quality. *Agric Ecosyst Environ.* 184:34-40.
- Gautam RD, Kumar S, Singh B, Khan ZH. 2024. Taxonomic revision of genus *Andrena* (Hymenoptera: Andrenidae) with description of new species from India. *Zootaxa.* 5400(2):201-230.
- Gibbs J. 2009. Integrative taxonomy identifies new cryptic species of *Lasioglossum* (Dialictus) in North America. *Zootaxa.* 2032(1):1-38.
- Gibbs J. 2018. Bees of the genus *Lasioglossum* (Hymenoptera: Halictidae) from Greater Puerto Rico, West Indies. *Eur J Taxon.* 400:1-125.
- Gogala A. 2019. Diversity and distribution of Andrenid bees (Hymenoptera: Andrenidae) in Slovenia. *Acta Entomol Slov.* 27(1):5-30.
- Hardwick DF. 1950. Preparation of slide mounts of lepidopterous genitalia. *Can Entomol.* 82(11):231-235.
- Hazir C, Bock CH. 2019. Success of DNA extraction and PCR amplification from dry pinned sand bees (*Andrena* spp.) using newly designed primers. *Turk J Entomol.* 43(1):79-96.
- Hebert PDN, Cywinska A, Ball SL, deWaard JR. 2003. Biological

- identifications through DNA barcodes. *Proc R Soc B*. 270(1512):313-321.
- Hederström V, Lundin O, Smith HG, Rundlöf M. 2025. Pollinator diversity is shaped by landscape complexity, floral resources, and pesticide exposure. *Agric Ecosyst Environ*. 365:108-134.
- Holzschuh A, Dudenhöffer JH, Tschardt T. 2012. Landscapes with wild pollinators enhance crop yield. *Ecol Lett*. 15(3):251–259.
- Huang X, Zhang Q, Sheikh UAA, Wang Y, Zheng L. 2024. Bumblebee foraging dynamics and pollination outcomes for cherry tomato and pear varieties in northern China. *Insects*. 15(4):216-247.
- Huemer P, Mutanen M, Sefc KM, Hebert PDN. 2020. DNA barcode library for European Lepidoptera and its taxonomic implications. *Genome*. 63(2):123-134.
- Ian F. B. Common. 1990. *Moths of Australia*. Melbourne: Melbourne University Press. *Int Acad J Sci Eng*. 5(1):87-110
- Iler A, Goodell K. 2014. Relative floral density of an invasive plant affects pollinator foraging behavior on a native plant. *J Pollinat Ecol*. 13:173-183.
- Inouye DW, Larson B, Symank A, Kevan P. 2015. Flies and flowers III: ecology of foraging and pollination. *J Pollinat Ecol*. 16:115-133.
- John A, Ganie S, Bhat K, Riat A. 2025. Morphometric profiling of hymenopteran pollinators from cherry orchards in the Kashmir Valley, India. *Plant Protect*. 9(3):527-548.
- Kachhawa S. 2023. DNA barcoding and its applications in insect taxonomy using COI gene. *J Genet Eng Biotechnol*. 21(1):65-85.
- Kashyap A, Jaiswal DK. 2024. Optimized DNA extraction from insect tissues using spin-column based DNase kits for molecular applications. *J Genet Eng Biotechnol*. 22(1):115-145.
- Katumo DM, Liang H, Ochola AC, Lv M, Wang QF, Yang CF. 2022. Pollinator diversity benefits natural and agricultural ecosystems, environmental health, and human welfare. *Plant Divers*. 44(5):429-435.
- Katumo DM, Ngatia RM, Muli E, Mueke J. 2022. Insect pollinator visitation and foraging behaviour in temperate fruit orchards. *J Pollinat*

- Ecol.* 30(12):215-225.
- Katumo DM, Ngatia RM, Muli E, Mueke J. 2022. Insect pollinators enhance fruit set and yield in flowering plants. *J Pollinat Ecol.* 30(12):215-225.
- Kaya M, Demir H, Demirbağ Z. 2015. Taxonomic keys and morphological identification of insect species based on diagnostic characters. *Turk J Zool.* 39(2):245-256.
- Khan KA, Liu Z. 2022. Scanning electron microscopy reveals structural adaptations of body hairs in *Apis mellifera* related to pollination efficiency. *Microsc Res Tech.* 85(6):2150-2158.
- Khanna R, Singhal K, Mohanty S. 2016. Quantification of single *Drosophila* fly genomic DNA using UV spectrophotometry, NanoDrop and Qubit fluorometry. *Pranikee.* 28:65-76.
- Khyade VB, Tikar SN, Kalyankar SV. 2018. Morphological adaptations in Lepidoptera and their role in pollination and taxonomy. *J Entomol Zool Stud.* 6(2):145-150.
- Kitnya N, Brockmann A, Otis G. 2024. Taxonomic revision and identification keys for the giant honey bees. *Front Bee Sci.* 2:137-162.
- Klein AM, Vaissière BE, Cane JH, Steffan-Dewenter I, Cunningham SA, Kremen C, Tscharntke T. 2007. Importance of pollinators in changing landscapes for world crops. *Proc R Soc B.* 274(1608):303-313.
- Kline KL, Msangi S, Dale VH. 2022. Agricultural landscapes as biodiversity hotspots: the role of orchards in pollinator conservation. *Biol Conserv.* 268:109-125.
- Klots AB. 1970. Lepidoptera. In: Tuxen SL, editor. *Taxonomist's glossary of genitalia in insects*. Copenhagen: Munksgaard. p. 115-130.
- Kratochwil A, Paxton R, Schwabe A, Aguiar A, Husemann M. 2021. Morphological and genetic data suggest a complex pattern of inter-island colonisation and differentiation for mining bees (*Andrena*) on the Macaronesian Islands. *Mol Phylogenet Evol.* 155:106-134.
- Krishna S, Keasar T. 2018. Morphological complexity as a floral signal: from perception by insect pollinators to co-evolutionary implications. *Int J Mol Sci.* 19(6):16-83.
- Kristensen NP, Scoble MJ, Karsholt O. 2006. Lepidoptera phylogeny and

- systematics: the state of inventorying moth and butterfly diversity. *Zootaxa*. 1668:699-747.
- Krogmann L, Holstein J. 2010. Preserving and mounting techniques for entomological specimens to retain morphological characters. *J Hymenopt Res*. 19(2):200-210.
- Lafontaine JD. 2004. *Noctuoidea, Noctuidae (part): Noctuinae (part – Agrotini)*. Ottawa: NRC Research Press.
- Lanyon SM, Sanson GD. 2006. Sampling requirements for quantitative studies of insect morphology and functional traits. *Biol J Linn Soc*. 89(2):197-210.
- Liakou C, Mamuris Z. 2014. A new set of 16S rRNA universal primers for the identification of animal species. *Food Control*. 43:35-41.
- Liu Y, Zhang L, Li Q, Chen X. 2023. Integrating ecological surveys with DNA barcoding reveals pollinator diversity in orchard ecosystems. *Insects*. 14(3):245-258.
- Lopez VA, Ramirez MJ, Torres PJ. 2020. Standard practices for labeling and curation of entomological specimens. *J Insect Conserv*. 24(4):567-575.
- Lv J, Wu S, Zhang Y, Chen Y, Feng C, Yuan X, Jia L, He L. 2014. Assessment of four DNA fragments (COI, 16S rDNA, ITS2, and 28S rDNA) for species identification of Diptera. *Parasites Vectors*. 27(2):318-331
- Maggi T, Pardo L. 2024. Insect pollinators: a key to ecosystem resilience and food security. In: *Pollination biology: advances and applications*. London (UK): Academic Press. p. 35-50.
- Makkar G, Dey D, Chhuneja P. 2016. Mining bee *Andrena (Agandrena) agilissima* (Hymenoptera: Andrenidae): a new record from India with morphological and molecular notes. *J Appl Nat Sci*. 8(4):1775-1778.
- Malcolm J. Scoble. 1995. *The Lepidoptera: form, function and diversity*. Oxford: Oxford University Press.
- Meena LK, Lokesh C, Meena K, Dey D. 2018. A review of Indian subgenera *Agandrena* and *Oreomelissa* of *Andrena*. *J Entomol Zool Stud*. 6(3):1182-1185.

- Michener CD. 2007. *The bees of the world*. 2nd ed. Baltimore (MD): Johns Hopkins University Press.
- Mielczarek LE, Tofilski A. 2018. Semiautomated identification of a large number of hoverfly (Diptera: Syrphidae) species based on wing measurements. *Orient Insects*. 52(3):245-258.
- Mir GM, Dar SA, Ahmad SB, Bhat FA. 2021. Morphometric analysis of insect pollinators in temperate fruit orchards of Kashmir Valley. *J Insect Sci*. 21(5):1-9.
- Mir M, Mir M, Waida UI, Mushtaq I, Rehman M, Iqbal R, et al. 2025. The impact of pollination requirements in sweet cherry: a systematic review. *J Plant Growth Regul*. 28(2):1-19.
- Mir S, Jamali M, Majeed D. 2021. Studies on hymenopteran insect pollinators in District Baramulla of Jammu and Kashmir. *Int J Entomol Res*. 6(1):1-5.
- Mitra S, Ahmad SB, Bhat FA, Dar SA. 2025. DNA barcoding (COI gene) reveals pollinator diversity and cryptic species in cherry orchards of Kashmir Valley. *Mitochondrial DNA B*. 10(1):120-128.
- Molin AD, Menard K. 2018. Non-destructive DNA extraction protocol for minute insects. *Protocols.io*. 152:45-52.
- Montiel J, Bosch J, Retana J. 2010. Foraging behaviour and pollination efficiency of honey bees and wild pollinators in fruit orchards. *Apidologie*. 41(4):531-542.
- Müller CJ, Schmidt BC, Wahlberg N. 2025. Reliability of genital morphology and wing venation in Lepidoptera species identification. *Syst Entomol*. 50(1):85–98.
- Mutanen M, Kaila L, Tabell J. 2016. Wide-scale morphometric analysis of Lepidoptera using standard measurement techniques. *Syst Entomol*. 41(3):567-578.
- Mutanen M, Wahlberg N, Kaila L. 2010. Comprehensive gene and taxon coverage elucidates radiation patterns in moths and butterflies. *Proc R Soc B*. 277(1695):2839-2848.
- Niels P. Kristensen. 2003. Skeleton and muscles: adults. In: Kristensen NP, editor. *Lepidoptera, moths and butterflies, Vol. 2: Morphology*,

- physiology, and development. Berlin: Walter de Gruyter. p. 39-131.*
- Nyarko G. 2012. Diurnal activity patterns of insect pollinators and their influence on pollination efficiency. *J Pollinat Ecol.* 8(3):45-52.
- O'Connor R, Kunin W, Garratt M, Potts SG, Roy H, Andrews C, et al. 2019. Monitoring insect pollinators and flower visitation: the UK Pollinator Monitoring Scheme. *Methods Ecol Evol.* 10(7):1252-1264.
- Ortego J, Noguerales V, Tonzo V, Gonzalez-Serna MJ, Cordero PJ. 2021. Broadly distributed but genetically fragmented: demographic consequences of Pleistocene climatic oscillations in a common Iberian grasshopper. *Insect Syst Divers.* 5(5):24-36.
- Osterman J, Aizen MA, Biesmeijer JC, Bosch J, Howlett BG, Inouye DW. 2021. Global trends in the number and diversity of managed pollinator species. *Agric Ecosyst Environ.* 322:107-143.
- Osterman J, Mateos-Fierro Z, Siopa C, Castro H, Castro S, Eeraerts M. 2024. The impact of pollination requirements, pollinators, landscape and management practices on pollination in sweet and sour cherry: a systematic review. *Agric Ecosyst Environ.* 374:109-143.
- Osterman J, Theodorou P, Radzeviciute R, Schnitker P, Paxton RJ. 2021. Apple pollination is ensured by wild bees when honey bees are drawn away from orchards by a mass co-flowering crop, oilseed rape. *Agric Ecosyst Environ.* 315:107-153.
- Osterman J, Theodorou P, Radzevičiūtė R, Schnitker P, Paxton RJ. 2021. Bumblebees and honey bees differ in their pollination efficiency and behavior. *Sci Rep.* 11(1):1-10.
- Osterman J, Theodorou P, Radzevičiūtė R, Schnitker P, Paxton RJ. 2024. Pollinator exclusion and its impact on fruit set and yield in orchard crops. *Sci Rep.* 14(1):112-134.
- Padial JM, Miralles A, De la Riva I, Vences M. 2014. The integrative future of taxonomy: combining morphological and molecular approaches. *Front Zool.* 11(1):1-14.
- Papa R, Lepore E, Spina F, Grimaldi D. 2022. Morphological diversity and functional adaptations in Hymenoptera. *Insects.* 13(4):305-345.
- Paray BA, Kumari I, Sharma N, Kumar D. 2014. Pollinator diversity and

- abundance in temperate agroecosystems of Kashmir Himalaya. *J Entomol Zool Stud.* 2(4):85-89.
- Pardo A, Borges P. 2020. Worldwide importance of insect pollination in apple orchards: a review. *Agric Ecosyst Environ.* 293:106-129.
- Parey SH, Ahmad H, Khan AA, Mir SA. 2024. Morphometric differentiation of *Bombus* species (Hymenoptera: Apidae) in Kashmir Valley. *J Insect Sci.* 24(2):1–10.
- Parrey H, Raina R, Khan S, Parrey M, Choudhary P. 2024. Morphometric studies of subgenus *Megabombus* (Hymenoptera: Apidae) from Jammu and Kashmir, India. *Rec Zool Surv India.* 123(3):275-282.
- Patzold F, Vences M, Steinke D, Hanner R. 2020. DNA barcoding of insect pollinators using mitochondrial COI gene for species identification. *Mol Ecol Resour.* 20(3):789-800.
- Pengliang L, Zhang Y, Chen X. 2025. Wing morphology and flight adaptations in Lycaenidae butterflies. *Zool Anz.* 310:1-10.
- Perveen F. 2016. A contribution key for identification of butterflies (Lepidoptera) of Tehsil Tangi, Khyber Pakhtunkhwa, Pakistan. *J Entomol Zool Stud.* 4(4):1088-1098.
- Pisanty G, Richter R, Martin T, Cardinal S. 2022. Phylogeny, classification, and historical biogeography of the bee subfamily Andreninae (Hymenoptera: Andrenidae). *Mol Phylogenet Evol.* 166:107-127.
- Polidori C, Jorge A, Ormosa C. 2020. Morphological adaptations and thermoregulation in solitary bees under varying climatic conditions. *J Therm Biol.* 90:102-138.
- Potts SG, Biesmeijer JC, Kremen C, Neumann P, Schweiger O, Kunin WE. 2010. Global pollinator declines: trends, impacts and drivers. *Trends Ecol Evol.* 25(6):345-353.
- Potts SG, Vulliamy B, Dafni A, Ne'eman G, Willmer P. 2005. Role of nesting resources in organising diverse bee communities in a Mediterranean landscape. *Ecol Entomol.* 30(1):78–85.
- Praz C, Müller A, Genoud D. 2019. Hidden diversity in European bees: production under temperate conditions. *Sarhad J Agric.* 36(4):1265-1273.

- Pull CD, McMahon DP, Woodcock BA, et al. 2022. Body size and flight performance influence foraging range in bee pollinators. *Funct Ecol.* 36(3):678-689.
- Queiros F, Carvalho R, Sousa R, Sanchez C. 2024. Insect pollination improves fruit set, yield and fruit quality of commercial sweet cherry. *Acta Hortic.* 14(8):267-274.
- Quicke DLJ, Lopez-Vaamonde C, Belshaw R. 1999. Preservation of hymenopteran specimens for subsequent molecular and morphological study. *Zool Scr.* 28(2):261-267.
- Rader R, Bartomeus I, Garibaldi LA, Garratt MPD, Howlett BG, Winfree R, et al. 2016. Non-bee insects as pollinators of crops. *Proc Natl Acad Sci USA.* 113(1):146-151.
- Ramzan M, Khan KA, Shah M, Bhat AH. 2019. Effect of insect pollination on fruit set and quality of cherry (*Prunus avium* L.) in Kashmir valley. *J Entomol Zool Stud.* 7(3):1120-1124.
- Rommel T, Davison J, Tammaru T. 2024. Cryptic diversity and limitations of morphology-based species identification in insects. *Ecol Evol.* 14(2):118-146.
- Reynolds AM, Smith AD, Menzel R, Greggers U. 2022. Body size, sensory capacity and foraging performance in insect pollinators. *Funct Ecol.* 36(7):1652-1663.
- Robinson GS. 1976. *The preparation of slides of Lepidoptera genitalia with special reference to the Microlepidoptera.* *Entomologist's Gazette.* 27(2):127-132.
- Rohlf FJ. 1990. Morphometrics. *Annu Rev Ecol Syst.* 21:299-316.
- Rosas-Ramos N, Baños-Picón L, Tormos J, Asís JD. 2020. Morphological identification of pollinators and its limitations in diverse ecosystems. *J Hymenopt Res.* 75(1):1-15.
- Santos BF, Wahl DB, Rousse P. 2017. Morphological diversity and species delimitation in Ichneumonidae (Hymenoptera). *Syst Entomol.* 42(1):1-15.
- Sarri C, Stamatis C, Sarafidou T, et al. 2014. A new set of 16S rRNA universal primers for identification of animal species. *Food Control.*

43:35-41.

- Schmidt S, Schmid-Egger C, Morinière J, Haszprunar G, Hebert PDN. 2015. DNA barcoding largely supports 250 years of classical taxonomy: identifications for Central European bees (Hymenoptera: Apoidea partim). *Mol Ecol Resour.* 15(4):985-1000.
- Scoble MJ. 1995. *The Lepidoptera: form, function and diversity*. Oxford: Oxford University Press.
- Sharma H, Bakshi N, Thakur RK, Devi M. 2016. Diversity and density of insect pollinators on sweet cherry (*Prunus avium* L.) in the temperate region of Kullu Valley of Himachal Pradesh. *J Entomol Zool Stud.* 4(6):123-128.
- Sharma R, Singh D, Kumar S. 2025. Standardized entomological collection and preservation techniques for morphological studies. *J Entomol Zool Stud.* 13(2):210-215.
- Shashank PR, Meshram NM, Sreedevi K. 2022. DNA barcoding of insect fauna in India: integrating molecular and morphological approaches. *Curr Sci.* 122(5):567-575.
- Sheffield CS, Heron J, Gibbs J, Onuferko TM, Oram R, Best L, de Silva N, Dumesh S, Pindar A, Rowe G. 2017. Contribution of DNA barcoding to the study of the bees (Hymenoptera: Apoidea) of Canada: progress to date. *Can Entomol.* 149(6):736-754.
- Simonsen TJ, Wahlberg N, Brower AVZ. 2021. Morphology and evolution of Lepidoptera: insights from modern imaging techniques. *Syst Entomol.* 46(2):300-315.
- Sourakov A, Zakharov EV. 2019. Morphological variation and measurement techniques in Lepidoptera using microscopy. *J Insect Sci.* 19(4):1-10. *Southeast Nat.* 18(2):183-191.
- Speight M, Castella E, Sarthou JP, Vujić C. 2021. StN key for the identification of the genera of European Syrphidae 2020. *Syrph the Net Publ.* 20(1):118-129.
- Steiner FM, Schlick-Steiner BC, Seifert B, Christian E, Crozier RH, Stauffer C. 2007. Combined molecular and morphological approaches reveal cryptic diversity in European ants. *Mol Phylogenet Evol.* 45(2):629-636.

- Stern R, Sapir G, Shafir S, Dag A, Goldway M. 2007. The appropriate management of honey bee colonies for pollination of Rosaceae fruit trees in warm climates. *Middle East Russ J Plant Sci Biotechnol.* 1(1):13-89.
- Tamura K, Stecher G, Peterson D, Filipiski A, Kumar S. 2013. MEGA6: molecular evolutionary genetics analysis version 6.0. *Mol Biol Evol.* 30(12):12-29.
- Tan DS, Ang Y, Lim GS, Ismail MRB, Meier R. 2020. From ‘cryptic species’ to integrative taxonomy: using ITS2 as a complementary marker for insect identification. *Syst Entomol.* 45(3):1-12.
- Techer MA, Clémencet J, Simiand C, Turpin P. 2025. Ecological roles of Hymenoptera in pollination, parasitism, and ecosystem functioning. *Annu Rev Entomol.* 70:211-230.
- Todisco V, Gratton P, Cesaroni D, Sbordoni V. 2022. Integrative taxonomy and morphometric approaches in Lepidoptera systematics. *Zool J Linn Soc.* 194(2):456-472.
- Vicens N, Bosch J. 2000. Weather-dependent pollinator activity in fruit orchards. *Environ Entomol.* 29(3):413-420.
- Vila R, Bell CD, Macniven R, et al. 2011. Phylogeny and diversification of Lycaenidae butterflies. *Mol Phylogenet Evol.* 61(2):237-251.
- Villalta I, Dufrière M, Castro L, Rasmont P. 2021. DNA barcoding reveals hidden diversity of wild bees in urban ecosystems. *Ecol Evol.* 11(15):10547-10560.
- Wahlberg N, Braby MF, Brower AVZ. 2005. Synergistic effects of combining morphological and molecular data in resolving butterfly phylogeny. *Proc R Soc B.* 272(1572):1577-1586.
- Wahlberg N, Zimmermann M, Nylin S. 2003. Phylogenetic relationships and historical biogeography of butterflies. *Evolution.* 57(6):1369-1383.
- Wang H, Ran N, Jiang HQ, Wang QQ, Ye M, Bowler PA, Jin XF, Ye ZM. 2024. Complex floral traits shape pollinator attraction to flowering plants in urban greenspaces. *Urban For Urban Green.* 91:128-165.
- Wang L, Feng Y, Wang Y, Zhang J, Chen Q, Liu Z, Liu C, He W, Wang H, Yang S, Zhang Y, Luo Y, Tang H, Wang X. 2022. Accurate chromosome identification in the *Prunus* subgenus *Cerasus* (*Prunus pseudocerasus*)

- and its relatives by oligo-FISH. *Int J Mol Sci.* 23(21):132-154.
- Wang X, Chen J, Li Y, Zhang Z. 2022. Pollinator visitation frequency influences fruit quality and yield in fruit crops. *Agric Ecosyst Environ.* 330:107-132.
- Watanabe ME, Takahashi J, Sato Y. 2024. DNA barcoding using mitochondrial COI gene improves insect species identification. *Mol Ecol Resour.* 24(1):45-56.
- Weekers T, De Meulemeester T, Michez D, Smagghe G. 2022. Landscape connectivity shapes genetic structure of pollinators in agricultural ecosystems. *Landsc Ecol.* 37(6):1501-1514.
- Wiemers M, Balletto E, Dincă V, Fric ZF, Lamas G, Lukhtanov V, Munguira ML, van Swaay CAM, Vila R, Vliegenthart A, Wahlberg N, Verovnik R. 2018. An updated checklist of the European butterflies (Lepidoptera: Papilionoidea). *ZooKeys.* 811:9-45.
- Winter WD. 2000. Basic techniques for observing and studying moths and butterflies. *Lepid Soc.* 54(1):1-10.
- Wood TJ, Cross I, Baldock D. 2020. Updates to the bee fauna of Portugal with the description of three new Iberian *Andrena* species (Hymenoptera: Apoidea: Anthophila). *Zootaxa.* 4790(2):201-226.
- Wood TJ, Ghisbain G, Michez D, Praz CJ. 2021. Revisions to the faunas of *Andrena* of the Iberian Peninsula and Morocco with the descriptions of four new species (Hymenoptera: Andrenidae). *Eur J Taxon.* 758:147-193.
- Yokoi K, Hatakeyama M, Kuwazaki S, Maeda T, Yoshiyama M, Horigane-Ogihara M, Matsuyama S, Jouraku A, Bono H, Kimura K. 2025. Comprehensive expression data for two honey bee species, *Apis mellifera* and *Apis cerana japonica*. *Sci Data.* 12(1):926-938.